Molecular characterization of defensin-like proteins in the fertilization process of *Nicotiana tabacum*

Molekulare Charakterisierung Defensin-ähnlicher Proteine beim Befruchtungsvorgang in *Nicotiana tabacum*

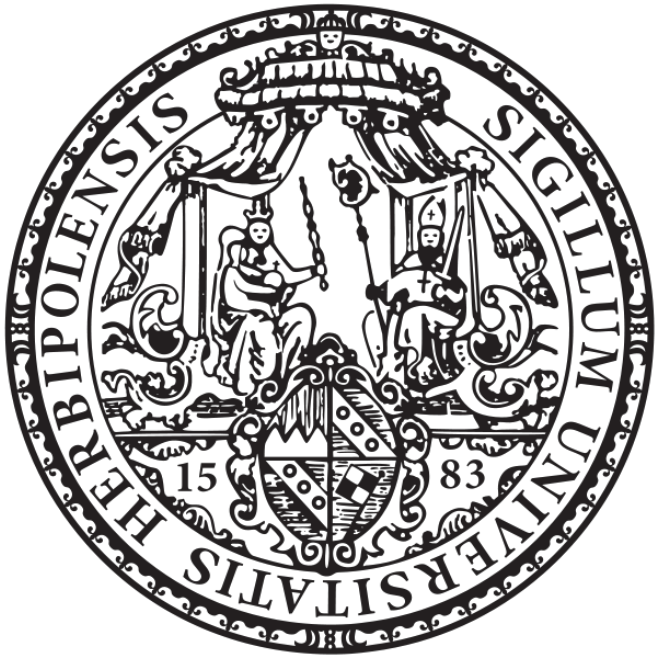

Dissertation zur Erlangung des
naturwissenschaftlichen Doktorgrades
der Julius-Maximilians-Universität Würzburg

vorgelegt von

Katharina von Meyer

aus Hamburg

Würzburg, 2019

Eingereicht am: ……..

Mitglieder der Promotionskommission:

Vorsitzender:……..……..

Gutachter: Prof. Dr. Dirk Becker

Gutachter: Prof. Dr. Jörg Schultz

Tag des Promotionskolloquiums: ……..…

Doktorurkunde ausgehändigt am:……..…

Acknowledgement

I would like to thank everyone who supported me during the process of this work. Special thanks belongs to

Prof. Dr. Dirk Becker for enabling me to do this thesis in his group, his support and the suggestions on how to develop the topic, for letting me work independently and all the good discussions.

Prof. Dr. Jörg Schultz for being my second supervisor in reviewing this thesis and for the great support on bioinformatic topics.

Prof. Dr. Rainer Hedrich for allowing me to work in his group at the Julius-von-Sachs Institute at the University of Würzburg.

The people who contributed to this work, especially Niklas Terhoeven for performing the bioinformatics analyses, Kevin Bongers for dissecting countless tobacco flowers and tirelessly continuing to perform experiments on this topic and Joachim Rothenhöfer for providing me with the plants for the experiments.

The current and former employees of the institute for supporting me in any kind of situations and who made me feel at home in this institute.

And of course my family who always loved and patiently supported me along this (long) way.

Summary

Flowering plants or angiosperms have developed a fertilization mechanism that involves a female egg and central cell, as well as two male sperm cells. A male gametophyte carries the two non-mobile sperm cells, as they need to be delivered to the female gametophyte, the embryo sac. This transport is initiated by a pollen grain that is transmitted onto the stigma of the angiosperm flower. Here it hydrates, germinates, and forms a pollen tube, which navigates through the female plant tissue towards the ovary. The pollen tube grows into an ovule through the funiculus and into one of the two synergid cells. There, growth arrests and the pollen tube bursts, releasing the two sperm cells. One of the sperm cells fuses with the egg cell, giving rise to the embryo, the other one fuses with the central cell, developing into the endosperm, which nourishes the embryo during its development. After a successful fertilization, each ovule develops into a seed and a fruit is formed. This usually consists of several fertilized ovules.

The directional growth of the pollen tube through the maternal tissues towards the ovule, as well as sperm cell release, requires a complex communication between the male and the female gametophyte to achieve reproductive success. Over the last years many studies have been performed, contributing to the understanding of cell-cell communication events between the two gametophytes, nevertheless still many aspects remain to be elucidated.

This work focused on two topics: i.) Analysis of biological processes affected by pollination and fertilization in the *Nicotiana tabacum* flower and identification of cysteine rich proteins (CRPs) expressed via isolating and sequencing RNA from the tissue and analyzing the resulting data. ii.) Identification of the defensin-like protein (DEFL) responsible for pollen tube attraction towards the ovule in tobacco.

First, tissue samples of pollen tubes and mature ovules were taken at different stages of the fertilization process (unpollinated ovules, after pollination, and after fertilization of the flower). RNA was then isolated and a transcriptome was created. The resulting reads were assembled and transcriptome data analysis was performed. Results showed that pollen tubes and mature ovules differ severely from each other, only sharing about 23 % of the transcripts, indicating that different biological processes are dominant in

the two gametophytes. A MapMan analysis revealed that in the pollen tube the most relevant biological processes are related to the cell wall, signaling, and transport, which supports the fact that the pollen tube grows fast to reach the ovule. On the other hand, in the ovule the values of highest significance were obtained for processes related to protein synthesis and regulation. Upon comparing the transcripts in the ovule before and after pollination, as well as after fertilization, it showed that pollination of the flower causes a bigger alteration in the ovule on the transcriptomic level compared to the step from pollination to fertilization.

A total of 953 CRPs were identified in *Nicotiana tabacum*, including 116 DEFLs. Among those, the peptide responsible for pollen tube attraction towards the ovule should be found. Based on *in-silico* analysis four candidate peptides were chosen for further analysis, two of which had increased expression levels upon pollination and fertilization and the other two displayed an opposite expression. Quantitative real time PCR experiments were performed for the candidates, confirming the *in-silico* data *in vivo*.

The candidate transcripts were then expressed in a cell free system and applied to pollen tubes in order to test their effect on the growing cells. Positive controls were used, where pollen tubes grew towards freshly dissected ovules. The four candidates did not provoke a pollen tube attraction towards the peptide, leaving open the chance to work on the 112 remaining DEFLs in the future.

Zusammenfassung

Für den Befruchtungsvorgang von Blütenpflanzen, bzw. Angiospermen werden je eine weibliche Eizelle und Zentralzelle, sowie zwei männliche Spermazellen benötigt. Da diese Spermazellen immobil sind, werden diese zum weiblichen Gametophyten, dem Embryosack, transportiert. Dieser Vorgang wird eingeleitet, indem ein Pollenkorn auf die Narbe des Blütenstempels gelangt. Dort hydriert es, keimt aus und bildet einen Pollenschlauch aus, welcher sich mittels Richtungswachstum durch den Griffel zum Fruchtknoten der Pflanze hin ausdehnt. Der Pollenschlauch wächst daraufhin durch den Funikulus zu den Samenanlagen hin, in eine der beiden Synergiden hinein, wo das Zellwachstum eingestellt wird. Der Pollenschlauch platzt und die zwei Spermazellen werden freigegeben. Eine dieser Spermazellen verschmilzt mit der Eizelle, woraus ein Embryo entsteht, während die andere Spermazelle mit der Zentralzelle verschmilzt, die sich zum Endosperm entwickelt und den Embryo während seiner Entwicklung mit Nährstoffen versorgt. Nach einer erfolgreichen Befruchtung bildet sich aus jeder Eizelle ein Samen aus, in der Regel bilden mehrere befruchtete Eizellen dann einen Fruchtkörper.

Eine erfolgreiche Fortpflanzung erfordert eine hochkomplexe Kommunikation zwischen männlichem und weiblichem Gametophyten, die sowohl beim Richtungswachstum des Pollenschlauchs durch das weibliche Pflanzengewebe hin zu den Samenanlagen eine essentielle Rolle spielt, als auch bei der Freisetzung der Spermazellen. Während der letzten Jahre wurden viele Studien durchgeführt, die zum Verstehen dieser Zell-Zell Kommunikation beigetragen haben, dennoch gibt es einige unbekannte Aspekte, die noch zu untersuchen sind.

Diese Arbeit konzentriert sich auf zwei Themen: i.) Die Analyse der biologischen Prozesse, die von der Bestäubung und Befruchtung der Blüte in *Nicotiana tabacum* beeinflusst werden, sowie die Identifizierung von cysteinreichen Proteinen (CRPs), die während dieses Prozesses exprimiert werden. Hierfür wurde RNA aus dem Gewebe isoliert, sequenziert und die resultierenden Daten analysiert. ii.) Die Identifizierung des Defensin-ähnliche Proteins (DEFL), welches für das Anlocken des Pollenschlauchs zu den Samenanlagen hin in Tabak verantwortlich ist.

Zunächst wurden Gewebeproben von Pollenschläuchen, sowie von reifen Samenanlagen in verschiedenen Stadien der Befruchtung entnommen (unbestäubte Samenanlagen, nach der Bestäubung und nach Befruchtung der Blüte). Von diesen Geweben wurde im Anschluss die RNA isoliert und ein Transkriptom erstellt. Die erhaltenen Sequenzfragmente wurden zusammengesetzt und die resultierenden Daten analysiert. Die Ergebnisse zeigten, dass sich Pollenschläuche und Samenanlagen stark voneinander unterscheiden; nur 23 % der Transkripte wurden in beiden Geweben gefunden. Eine Untersuchung mit MapMan hat gezeigt, dass die relevantesten biologischen Prozesse im Pollenschlauch mit Zellwand, Signalwegen und Transportvorgängen assoziiert sind. Diese Ergebnisse unterstützen die These, dass der Pollenschlauch schnell wachsen muss, um die Spermazellen zu den Samenanlagen zu transportieren. In den Samenanlagen haben hingegen die Prozesse den höchsten Signifikanzwert, welche mit Proteinsynthese und –regulation zusammenhängen. Wenn man die Transkripte in den Samenanlagen vor der Bestäubung, nach der Bestäubung, sowie nach der Befruchtung betrachtet, stellt man fest, dass die Bestäubung mit einer größeren Veränderung auf Transkriptomlevel einhergeht als der Schritt zwischen Bestäubung und Befruchtung.

Es konnten insgesamt 953 CRPs in *Nicotiana tabacum* identifiziert werden, wovon 116 DEFLs sind. Es sollte herausgefunden werden, welches dieser DEFLs für das Anlocken des Pollenschlauchs zu den Samenanlagen hin verantwortlich ist. Auf Basis von *in-silico* Analysen wurden vier Kandidatentranskripte ausgewählt, die näher untersucht wurden; bei zweien davon wurde ein ansteigendes Expressionsniveau bei Bestäubung und Befruchtung festgestellt; die anderen beiden Kandidaten zeigten ein gegensätzliches Expressionsmuster. Mittels quantitativer real-time PCR konnten die *in-silico* Daten *in-vivo* bestätigt werden. In einem zell-freien System wurden die Kandidatentranskripte exprimiert und auf Pollenschläuche gegeben, um ihren Effekt auf die wachsenden Zellen zu beobachten. Als Positivkontrollen wurden frisch präparierte Samenanlagen verwendet. Keines der vier Kandidatenproteine hat ein Anlocken der Pollenschläuche bewirkt, sodass noch die 112 verbleibenden DEFLs zur weiteren Untersuchung bereitstehen.

CONTENTS

1. Introduction

1.1 Morphology of the angiosperm flower

Flowers of angiosperms harbor the reproductive tissues of the plant. A flower is composed of two parts: a vegetative part, the perianth, and the reproductive tissues, the androecium and the gynoecium (Figure 1) (Weiler and Nover 2008).

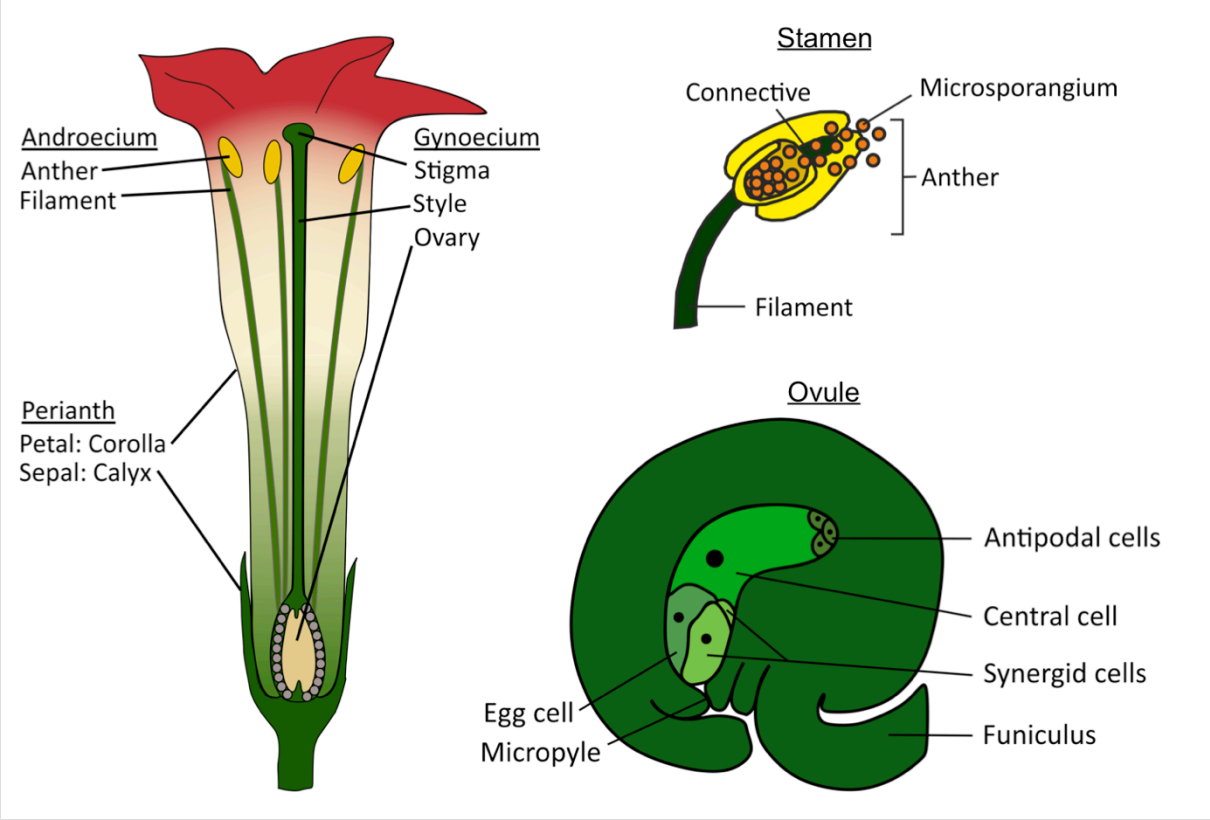

Figure 1: Morphology of the angiosperm flower

The perianth represents the non-sexual part of the flower and envelops the reproductive tissue. Sepals and petals build it up. Sepals form the outer most whorl of the flower and they are collectively called calyx. Sepals are usually green and protect the flower bud and support petals during blossom. Petals surround the reproductive organs of the plant and are often brightly colored. They are unusually shaped in order to attract pollinators, if the plant is animal-pollinated. The soft leaves of the petal

whorl can show a variety of patterns and are of bilateral or radial symmetry (Weiler and Nover 2008).

The androecium contains the male sexual reproductive organs of the flower. It is built up by a collection of stamina. A stamen is usually composed of a filament and an anther. The anther is bilobed and connected to the filament either at the base or in the middle of the anther via the connective. It contains the pollen, which develops from microspores in the microsporangium and contains the male gametophyte (Weiler and Nover 2008).

The gynoecium is the innermost whorl of the flower and contains one or more pistils, which are composed of a stigma, style and ovary. The stigma is located at the tip of the style and receives the pollen. It often has a sticky and/or enlarged surface to promote attachment of the pollen. Between stigma and ovary, the style is located. It is a stalk-like structure that can be hollow or contain a transmitting tissue where the pollen tubes can grow through in order to reach the ovary. The ovary consists of the placenta and the ovules (Weiler and Nover 2008).

1.2 The female and the male gametophyte

Angiosperms, or flowering plants, undergo a life cycle that alternates between a haploid gametophytic stage and a diploid sporophytic stage. The fertilization process is initiated with the sporogenesis, in which specialized mother cells undergo meiosis within the sporophyte and produce haploid spores. These spores undergo cell proliferation and differentiation; a process called gametogenesis, where multicellular gametophytes are developed and which then produce the gametes (sperm cell and egg cell) in specialized reproductive organs, female archegonia and male antheridia. A fusion of the two gametes gives rise to a diploid zygote and develops into the sporophyte, which completes the lifecycle (Gifford and Foster 1989).

1.2.1 The female gametophyte

Alike about 70 % of all angiosperm plants *Nicotiana tabacum* as well as *Arabidopsis thaliana* exhibit the *Polygonum*-type pattern during gametophyte development. Many other economically important plants like tomato, bean, soybean, cotton, maize, wheat

and rice also exhibit the *Polygonum*-type (Maheshwari 1950, Willemse and van Went 1984, Huang and Russell 1992). The development of the female gametophyte takes place in the developing ovule and consists of two phases: megasporogenesis followed by megagametogenesis (Yadegari and Drews 2004).

During megasporogenesis the mother cell is formed and meiosis takes place in order to produce four haploid megaspores. During megaspore selection, one of the four megaspores will be determined to develop into the female gametophyte (Webb and Gunning 1994, Schneitz, Hülskamp et al. 1995, Christensen, Subramanian et al. 1998, Bajon, Horlow et al. 1999). In megagametogenesis the megaspore expands and two cycles of mitosis take place without cytokinesis, thereby creating a four-nucleate coenocyte with two nuclei at each pole. Afterwards a third mitosis occurs and phragmoplasts and cell plates form between sister and non-sister nuclei. The cellularization process is initiated and cell walls of the female gametophyte are formed. One nucleus from each polar end migrates towards the center of the female gametophyte, resulting in a seven-celled structure: one egg cell, one central cell, two synergid cells and three antipodal cells (Sundaresan and Alandete-Saez 2010). The central cell is homodiploid, containing two identical haploid nuclei (Schneitz, Hülskamp et al. 1995, Christensen, Subramanian et al. 1998, Sprunck and Gross-Hardt 2011).

The cells of the female gametophyte possess several structure specifications (Mansfield, Briarty et al. 1991, Murgia, Huang et al. 1993, Kasahara, Portereiko et al. 2005, Kägi, Baumann et al. 2010). It has been shown that the nuclei of egg and central cell are very close to each other, which is beneficial as they are being targeted by the two sperm cells. In addition to that, the cell walls where egg, synergid and central cells meet, are discontinuous or absent and the plasma membranes are in direct contact with each other (Mansfield, Briarty et al. 1991, Kasahara, Portereiko et al. 2005). The cell wall of the synergid cells is largely invaginated at their micropylar end, building the filiform apparatus. The filiform apparatus extensively increases the surface area of the synergid cell plasma membrane. It contains a high number of secretory organelles and is composed of different substances as cellulose, hemicellulose, pectin, callose and protein. The filiform apparatus is important for pollen tube attraction as the attractant

molecules are secreted by it (Higashiyama and Hamamura 2008, Higashiyama and Takeuchi 2015, Dresselhaus, Sprunck et al. 2016) and it also serves as entry point for the approaching pollen tube (Maheshwari 1950, Willemse and van Went 1984, Huang and Russell 1992, Higashiyama 2002, Punwani and Drews 2008, Leshem, Johnson et al. 2013).

1.2.2 The male gametophyte

The development of the male gametophyte takes place in the anther loculi and leads to the release of mature pollen from the anther. During this process two cell types arise, vegetative cells and sperm cells (Borg, Brownfield et al. 2009, McCue, Cresti et al. 2011, Hafidh, Fila et al. 2016). The sperm cells form the male gametophyte and together with the vegetative cell, they represent the male germline (Berger and Twell 2011). Pollen development is characterized by two cell divisions that lead to a morphological and physiological differentiation into the two cell types, including formation of pollen cell wall and storage of metabolites and protective substances (Hafidh, Fila et al. 2016).

Male gametophyte development starts with microsporocytes or pollen mother cells that are generated within the anther loculi. During the first of two meiosis steps dyads are produced, while the second meiosis leads to tetrads of microspores. Meiotic divisions are highly synchronized, suggesting communication between the microspore mother cells via cytoplasmic bridges (Brett and Waldron 1996). Following second meiosis, a callose wall is formed around the tetrad and each microspore within the tetrad. This process of callose wall formation not necessarily takes place throughout all plant species at the same time point (Chen and Kim 2009, De Storme and Geelen 2013, Lu, Chai et al. 2014).

A specialized nutritive cell layer is found in the sporangium, the tapetum. It is located between the sporangenous tissue and the anther wall (Furness and Rudall 2001) (see Figure 2) and is important for nutrition and development of the pollen grains (Polowick and Sawhney 1993). Tapetal cells contain mitochondria, ribosomes, endoplasmatic reticulum, golgi apparatus and specialized lipid-rich organelles, the tapetosomes (Bedinger 1992, Ting, Wu et al. 1998, Hsieh and Huang 2005).

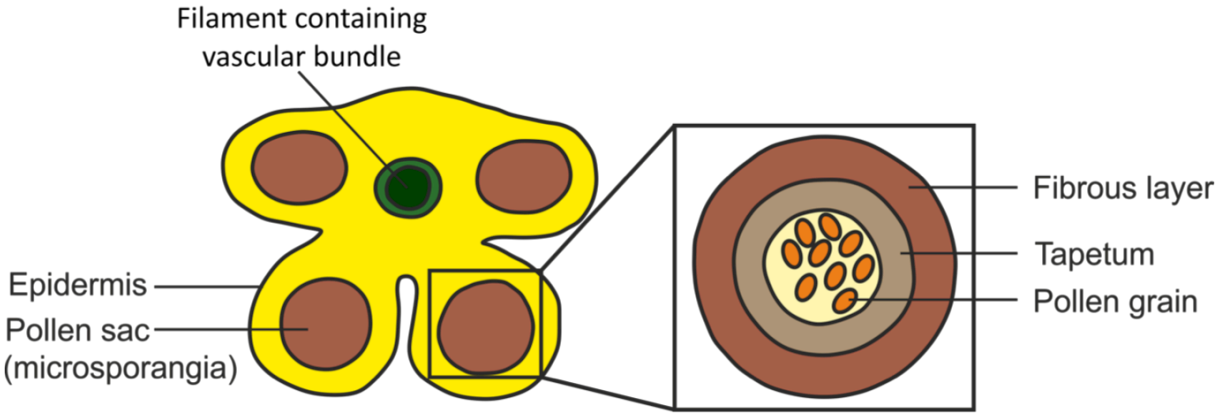

Figure 2: Section and structure of anther and pollen sac.

After the second meiosis the microspores inside the tetrads quickly develop and a cell wall consisting of an inner intine and an outer exine is synthesized around the spores. After cell wall formation the microspores are released from the tetrads. This process is facilitated by secretion of an enzyme mix containing callase (β-1,3-glucanase) by the tapetal cells in order to digest the callose wall around the microspores (Scott, Spielman et al. 2004, Lu, Chai et al. 2014). The secretion of callase is crucial for microsporogenesis, a dissolution of the callose wall leads to male sterility (Worrall, Hird et al. 1992). *quartet* mutants occur in *Arabidopsis thaliana* if the microspores do not separate during pollen development. This could be caused by a failure of pectin degradation in the pollen mother cell (Rhee and Somerville 1998).

After release from the tetrads the microspore enlarges and changes its shape. Numerous small vacuoles merge to a large one, pushing the nucleus from a central position towards the cell periphery. During pollen mitosis I the polarized microspores undergo an unequal division that results in the formation of two asymmetric daughter cells, which develop into vegetative and generative cell. The generative cell moves into the vegetative cell and builds a unique “cell-within-a-cell” structure (Russell, Strout et al. 1996, Russell and Jones 2015). Pollen mitosis I is another important process during microsporogenesis as it has been shown through various transcriptomic (Honys and Twell 2004, Wei, Xu et al. 2010, Bokvaj, Hafidh et al. 2015) and proteomic (Holmes-Davis, Tanaka et al. 2005, Noir, Bräutigam et al. 2005, Sheoran, Sproule et al. 2006,

Grobei, Qeli et al. 2009, Chaturvedi, Ischebeck et al. 2013, Ischebeck, Valledor et al. 2014) studies. During pollen mitosis II the generative cell undergoes a second mitosis, thereby resulting in two sperm cells. Depending on plant species pollen mitosis II can occur before pollen maturation or after. In the latter case the generative cell undergoes second mitosis during pollen tube growth through the style.

The pollen cell wall is of unique composition and not only protects the pollen but also facilitates communication with the stigma surface (Scott, Spielman et al. 2004). It is composed of three main layers: The inner strata, the intine, is of gametophytic origin, while the outer layer, the exine, is largely of sporopytic descent. The major component of the exine is sporopollenin, a compound of yet unknown composition containing fatty acids and phenylpropanoids. The production of sporopollenin requires a tight communication between microspores and tapetal cells (Dobritsa, Shrestha et al. 2009, Dobritsa, Lei et al. 2010, Ariizumi and Toriyama 2011, Quilichini, Grienenberger et al. 2015) and it is one of the toughest known polymers, being resistant to enzyme degradation and chemicals and is therefore ideal for pollen protection. The exine is not spread evenly on the pollen surface, it is e.g. completely absent or diminished where the pollen tube emerges (Furness and Rudall 2004). The decayed areas of the exine are filled with a pollen coat, which consists of lipids, proteins, pigments and aromatic compounds (Edlund, Swanson et al. 2004, Zheng, Lin et al. 2018). The properties and composition of the pollen cell wall are highly species-specific. The composition influences the pollen adhesiveness, color and is crucial for the interaction of pollen and papillary cells on the stigma. Plants that are animal-pollinated produce pollen that promote recognition by pollinators and that possess highly complex surface structures (Fellenberg and Vogt 2015).

1.3 The fertilization process in flowering plants

After pollen is produced and released from the anthers, it lands on the stigma of an angiosperm plant and undergoes adhesion and hydration processes before pollen tube growth occurs. The vegetative cell forms a pollen tube, which carries the two immobile sperm cells through the maternal tissue towards the ovule via polar tip growth (Weterings and Russell 2004). During its long way through the maternal tissues, the

pollen tubes gets in contacts with seven different pistil cell types before accomplishing double fertilization (stigma, style, transmitting tract, septum, funiculus, integument and synergid cells) (Sogo and Tobe 2006). The pollen tube grows through the funiculus towards the ovule and enters the ovule through the micropyle. The pollen tube grows into one of the two synergid cells, where it bursts, thereby releasing the two sperm cells allowing double fertilization (Berger, Hamamura et al. 2008). During this process one sperm cell fertilizes the egg cell to give rise to the diploid zygote and the other one fuses with the central cell that develops into the triploid endosperm that nourishes the growing embryo during its development (Weiler and Nover 2008). After fertilization, every ovule develops into a seed and the plant pistil including several fertilized ovules matures into a fruit.

During the fertilization process of angiosperm plants, a complex and tightly regulated communication between the male and the female gametophyte is essential. The journey of the pollen tube towards the embryo sac can be divided into five phases (Dresselhaus and Franklin-Tong 2013). Phase I includes pollen adhesion on the stigma of the female carpel, its hydration and germination. During phase II the pollen tube grows into the stigma via intercellular spaces between the papillar cells towards the transmitting tract. Along a nutrient-rich extracellular matrix, the pollen tube grows through the transmitting tract, which connects stigma, style and ovary during phase III. In phase IV the pollen tube leaves the transmitting tract close to the ovules and grows along the funiculus towards the micropylar end of the ovule. Completion of the fertilization process occurs in phase V where the pollen tube enters the ovule and grows into one of the synergid cells, growth arrest and bursting of the pollen tube occurs, thereby releasing the two sperm cells, allowing double fertilization.

1.3.1 Pollen hydration and germination

After maturation, the pollen is released from the anthers and undergoes different processes of interaction with the flower's pistil: adhesion, hydration and germination (Chapman and Goring 2010). Adhesion of pollen to the papillar cells of the stigma displays a first level of species specificity, as has been shown by cross-species pollination between *Arabidopsis thaliana* and *Brassica* ssp., where a low rate of pollen

adhesion was detected (Zinkl, Zwiebel et al. 1999). On the other hand high levels of adhesion could be shown after cross-pollination between different Brassicaceae species (Luu, Passelègue et al. 1998). Different studies have shown that pollen coat proteins are of high importance during pollen adhesion (Luu, Marty-Mazars et al. 1999, Zinkl, Zwiebel et al. 1999, Takayama, Shiba et al. 2000).

To remain viable, mature pollen is dehydrated until it lands on the stigma of a flower. After adhesion it undergoes hydration, where water is taken up from the stigma (Firon, Nepi et al. 2012). It could be shown that the pollen ER-localized aquaporin SIP2;1 is involved in pollen germination and pollen tube elongation (Sato and Maeshima 2019). It has also been revealed that pollen coat lipids are not only important for pollen adhesion, the also play a significant role is the hydration process in plants with dry stigmas like *Arabidopsis thaliana* (Preuss, Lemieux et al. 1993, Lush, Grieser et al. 1998, Wolters-Arts, Lush et al. 1998, Mayfield and Preuss 2000, Mayfield, Fiebig et al. 2001). In plants possessing wet stigmas, like tobacco, components of the secreted fluids support pollen germination as well as pollen tube growth into the stigma (Kandasamy and Kristen 1987, J B Nasrallah, T Nishio et al. 1991).

Plants with wet stigmas are quite unspecific in accepting pollen on its surface. Plants with dry stigmas, on the other hand, are more restricted when it comes to capturing pollen, as pathogen infection and self-pollination should be avoided (Dickinson 1995, Swanson, Edlund et al. 2004). It is important for plants to prevent in-breeding for a broad genetic diversity. Self-incompatibility can be distinguished in a homomorphic and heteromorphic type. In the heteromorphic type pollination is allowed only between flowers of a different morphologic type, while in the homomorphic type flowers of the corresponding flower type are allowed (de Nettancourt 2001). The homomorphic self-incompatibility can be further divided by genetic control into gametophytic self-incompatibility and sporophytic self-incompatibility. In the gametophytic type, self-incompatibility is regulated by the genotype of the pollen or pollen tube and in the sporophytic type, self-incompatibility is imposed by the producing plant (sporophyte) (Nasrallah 2002, Hiscock and Tabah 2003, Sehgal and Singh 2018).

In more recent studies a stigmatic protein localized at the plasma membrane, Exo70A1, has been identified to be necessary for pollen hydration in *Arabidopsis thaliana* as well as in *Brassica napus.* It was also shown that Exo70A1 plays a role in self-incompatibility (Samuel, Chong et al. 2009). Furthermore, it could be discovered that the phosphoinositide PI4P (phosphatidylinositol-4-phosphate) is involved in the response of the pistil towards pollen, as mutants display a decreased pollen hydration rate on the stigma (Chapman and Goring 2011).

After hydration, a tube protrudes from the pollen grain; the pollen germinates and grows into the stigma. Pollen on the stigma germinates relatively quick, e.g. *Arabidopsis thaliana* pollen takes less than 30 min to germinate (Fiebig, Kimport et al. 2004). As *in-vivo* applied pollen germinated quicker than pollen germinated *in-vitro*, it was suggested that pistil factors influence pollen recognition as well as germination on the stigma. Mass spectrometry experiments of *Arabidopsis thaliana* stigma samples, identified small molecules called sulfinylated azedecalins that stimulated pollen germination *in-vitro* (Qin, Wysocki et al. 2011). Also the glycosyl transferase AtOFT1 seems to play a role in pollen- pistil interaction (Smith, Harper et al. 2018). Further studies have shown that cytosolic calcium levels increase in the pollen after hydration at the future pollen tube emergence site and stays elevated until after germination (Holdaway-Clarke and Hepler 2003, Iwano, Shiba et al. 2004). This physiological activation is accompanied by cytoplasmic reorganization and formation of a calcium gradient underneath the site where the pollen tube grows (Heslop-Harrison and Heslop-Harrison 1992).

1.3.2 Pollen tube growth through the style towards the ovule

1.3.2.1 Pollen tube growth

On its way to the ovary, the pollen tube grows through the style via the transmitting tissue. This polar tip growth is facilitated via different mechanisms that have been studied over many years. Callose plugs divide the growing pollen tube into the viable streaming zone and the distal region. The viable streaming zone is separated into the shank region, which contains the vegetative nucleus as well as the two sperm cells, the

subapical organelle-rich zone and the apical zone, which comprises exocytotic vesicles (Yang 1998).

During pollen tube growth F-actin plays an important role in the structural organization (Cheung and Wu 2008) and is differently structured in each sub-region. The F-actin cable network supports cytoplasmic streaming, which transports vesicles and organelles between shank, apical and subapical region (de Graaf, Cheung et al. 2005, Ye, Zheng et al. 2009, Onelli, Scali et al. 2018). After being transported towards the apical and subapical region, vesicles are caught by the actin fringe as well as microfilaments and are transported towards the apical dome in a membrane-targeted way (Fu, Wu et al. 2001, Gu, Fu et al. 2005, Lee and Yang 2008, Qin and Yang 2011). The vesicles contain cell wall materials and proteins like ion transporters as well as enzymes for cell wall modifications and signaling. Exocytosis of the vesicles contributes to pollen tube elongation (Chen, Wong et al. 2002, Lee and Yang 2008, Cheung, Niroomand et al. 2010). During growth, regulation of the pollen tube cell wall properties is crucial, as it has to keep its integrity under high turgor pressure while maintaining its plasticity in order to allow tip growth. Loosening and biosynthesis of the cell wall therefore needs to be strictly balanced, which leads to differences in the cell wall composition in the pollen tube sub-regions (Guan, Guo et al. 2013).

Tip growth of pollen tubes is highly regulated by signaling networks. ROP (RHO-RELATED PROTEIN FROM PLANTS) GTPases have been established as a critical component in pollen tube growth as they are localized in the apical region and display spatiotemporal dynamics in their activity (Yang 1998, Zheng and Yang 2000, Qin and Yang 2011, Craddock, Lavagi et al. 2012, Yang and Lavagi 2012). They act like molecular switches as they can cycle between their inactive GDP-bound and their active GTP-bound form. This makes ROP GTPases critical for regulation of cell elongation (Kost, Lemichez et al. 1999, Li, Lin et al. 1999, Vernoud, Horton et al. 2003, Hwang, Vernoud et al. 2008, Hwang, Wu et al. 2010). It has been shown that ROP1 plays a key role in the pollen tube's self-organizing system and is highly controlled by positive and negative feedback mechanisms (Hwang, Wu et al. 2010).

Another important component in the signaling network of growing pollen tubes is calcium (Steinhorst and Kudla 2013, Zheng, Su et al. 2019). In the elongating pollen

tube, an apical-focused calcium gradient can be detected, which oscillates in a delayed phase correlated to pollen tube growth (Jaffe, Weisenseel et al. 1975, Holdaway-Clarke, Feijo et al. 1997, Messerli, Creton et al. 2000). It has been shown that calcium is taken up into the pollen tube from the stigma surface and its papillae, and in the transmitting tract, calcium is stored in the intercellular matrix, as well as in the call wall (Bednarska 1991, Tirlapur, Van Went et al. 1993, Zhang, Yang et al. 1995, Zhang, Yang et al. 1997). Because calcium is taken up from storages in the female pistil tissue during *in-vivo* growth, *in-vitro* growth is increased by external calcium (Brewbaker and Kwack 1963, Franklin-Tong 1999). ROP GTPases and calcium work together in order to regulate pollen tube tip growth. ROP1 activity has been shown to oscillate as well in the apical region, ahead of calcium and the elongation (Gu, Fu et al. 2005, Hwang, Gu et al. 2005). Thereby ROP1 activates ROP-INTERACTIVE CRIB MOTIF-CONTAINING PROTEIN 3 (RIC3), a downstream effector, which activates calcium signaling (Li, Lin et al. 1999, Gu, Fu et al. 2005). The increased calcium then induces dismantling of F-actin in the apical region, which in turn increases vesicle exocytosis and thus cell elongation. Calcium influx regulates F-actin-mediated ROP1 activation (Gu, Fu et al. 2005, Yan, Xu et al. 2009, Hwang, Wu et al. 2010).

Calcium plays an important role in many signaling processes and can by perceived by several sensor proteins like CALCIUM-DEPENDENT PROTEIN KINASES (CDPKs), CALCINEURIN B-LIKE PROTEINS (CBLs), CALMODULIN (CaM) and CALMODULIN-LIKE (CML) (Cheng, Willmann et al. 2002, Zhou, Fu et al. 2009, Hashimoto and Kudla 2011, Steinhorst and Kudla 2013). The influx of calcium into the pollen tube is mediated by plasma membrane-localized channels like CYCLIC NUCLEOTIDE-GATED CHANNELS (CNGCs) and GLUTAMATE RECEPTOR-LIKE (GLR) channels (Chang, Yan et al. 2007, Frietsch, Wang et al. 2007, Michard, Lima et al. 2011, Moeder and Yoshioka 2017, Pan, Chai et al. 2019). CNGC13 and CNGC18 seem to be ion channels for calcium influx into the pollen tube and therefore important components in the tip-focused gradient in the apical region (Chang, Yan et al. 2007, Frietsch, Wang et al. 2007, Moeder and Yoshioka 2017, Pan, Chai et al. 2019).

1.3.2.2 Pollen tube growth through the style

A comparison between pollen tubes of *Arabidopsis thaliana* and *Torenia fournieri* grown *in-vitro* and in a semi *in-vivo* condition, shows that an interaction with the pistil tissue is necessary for pollen tube maturation or activation. This suggests that pollen tubes are primed by the female tissue to react to secreted attraction signals (Higashiyama, Kuroiwa et al. 1998, Palanivelu and Preuss 2006). When pollen tubes of these two plant species were grown through cut-off styles in presence of excised ovules, attraction of the pollen tubes by the ovules could be observed as well as double fertilization. When pollen was germinated on pollen germination medium, attraction towards excised ovules could either not be detected at all or very rarely (Higashiyama, Kuroiwa et al. 1998, Palanivelu and Preuss 2006). These observations lead to the conclusion that in these plants some signals by the female tissue induce pollen tube competence.

In angiosperm plants, there are two types of transmitting tracts, the open hollow type, which can be found e.g. in lily and the solid type style, as found in e.g. in *Arabidopsis thaliana* (Lennon, Roy et al. 1998, Erbar 2003). Programmed cell death is of crucial importance for transmitting tract development and therefore pollen tube growth. Cell death of septum tissue generates the intercellular space and several proteins have been identified in this process. This includes the bHLH-type transcription factors HECATE 1 (HEC1), HEC2, HEC3 and HALF-FILLED (HAF), as well as the C2H2/C2HC zinc finger transcription factor NO TRANSMITTING TRACT (NTT) (Crawford, Ditta et al. 2007, Gremski, Ditta et al. 2007, Crawford and Yanofsky 2011, Boex-Fontvieille, Rustgi et al. 2015).

Several studies point out the important role of the pistil for competency control, directional and rapid growth, as well as self- and non-self recognition in different plant species (Crawford, Ditta et al. 2007, Palanivelu and Tsukamoto 2012, Takeuchi and Higashiyama 2012, Dresselhaus and Franklin-Tong 2013, Smith, Eberle et al. 2013). Significant progress in figuring out signals involved in the communication between male and female gametophyte was achieved in the last decade. In *Arabidopsis thaliana* transcriptome studies of the growing pollen tube have been performed (Qin, Leydon et al. 2009), as well as whole genome studies of pistils and ovules before and after

pollination (Boavida, Borges et al. 2011). In *Torenia fournieri* transcriptome studies in pollen tubes have been done (Okuda, Suzuki et al. 2013) and these studies revealed a multitude of genes involved in metabolism and intracellular signaling. A comparison between pollen tubes grown *in-vitro* and semi *in-vivo* revealed *de novo* gene expression in pollen tubes that achieved competence, i. e. had been in contact with the female tissue. Amongst other data, a set of 383 genes was identified that were uniquely expressed in pollen tubes grown through the pistil (Qin, Leydon et al. 2009). Analysis of expression profiles of *Arabidopsis thaliana* pistils at different time points after pollination identified more than 1000 genes that were regulated differentially (Boavida, Borges et al. 2011).

Many female molecules have been identified that stimulate pollen tube growth and/or maturation, including molecules like plant hormones, sugars and small peptides. One compound that might be involved in ovular guidance is the stress metabolite gamma-aminobutyric acid (GABA), which is distributed unequally across the pistil. Studies have shown that a low GABA-concentration, as found in the stigma, promotes pollen tube elongation. Higher concentrations, as occurring in the micropyle, however, inhibit pollen tube growth (Palanivelu, Brass et al. 2003, Ling, Chen et al. 2013). Research showed that GABA caused an increase in calcium influx in the pollen tube (Yu, Zou et al. 2014). Meanwhile it was also discovered that GABA regulates pollen tube growth via aluminium-activated malate transporters (ALMTs) (Ramesh, Tyerman et al. 2015).

Another component of the female-derived male-female communication system in plants are peptides/proteins and glycoproteins (Higashiyama 2010). In the extracellular matrix of the transmitting tract arabinogalactan proteins can be found, which affect trafficking and signaling processes (Coimbra, Almeida et al. 2007, Suarez, Zienkiewicz et al. 2013, Pereira, Pereira et al. 2015). The arabinogalactan TRANSMITTING TRACT SPECIFIC (TTS) gene found in tobacco has been shown to be involved in stimulating pollen tube growth *in-vitro* (Cheung, Wang et al. 1995, Wu, Wong et al. 2000). It could also be shown that TTS is glycosylated over a gradient in the transmitting tract, in the same direction as the pollen tubes grow, indicating an incorporation of TTS into the pollen tube where deglycosylation occurs (Wu, Wang et al. 1995).

Over the last years several molecules have been identified that are secreted by female plant tissues and belong to the group of secreted polypeptides. These proteins with less than 150 amino acids and an N-terminal signal peptide can be divided into two groups, the post-translationally modified small peptides and the cysteine-rich proteins (CRPs) (Kanaoka and Higashiyama 2015). CRPs possess more than four cysteines and can be divided into many classes (Broekaert, Cammue et al. 1997, Garcia-Olmedo, Molina et al. 1998, Boman 2003, Bulet, Stocklin et al. 2004, Theis and Stahl 2004). The number as well as the arrangement of the cysteines is characteristic for each class and every pair of cysteines forms a disulfide bond that leads to a distinctive tertiary structure (Broekaert, Cammue et al. 1997). In plants, CRPs are not only involved in the fertilization process, they also play a role in the immune answer. In *Arabidopsis thaliana* more than 800 CRPs were found (Silverstein, Moskal et al. 2007). STIGMA/STYLE CYSTEINE-RICH ADHESIN (SCA) - a member of the LIPID TRANSFER PROTEIN (LTP) subgroup of CRPs - interacts with pectin (Mollet, Park et al. 2000) and plays a role in forming the adhesive matrix inside the transmitting tract that is necessary for pollen tube guidance (Mollet, Park et al. 2000, Park, Jauh et al. 2000, Chae, Zhang et al. 2007).

In tomato the pollen CRP LAT52, was shown to be essential during pollen hydration and pollen tube growth. LAT52 interacts with the receptor like kinase SERINE/THREONINE PROTEIN KINASE 2 (LePRK2) which exists in a complex with LePRK1 at the pollen tube plasma membrane (Wengier, Valsecchi et al. 2003) (Tang, Kelley et al. 2004). Further, the CRP STIGMA-SPECIFIC PROTEIN 1 (STIG1), that is found in stigma exudates, interacts with phosphatidylinositol 3-phosphate and LePRK2. This interaction dissociates the LePRK1 LePRK2 complex, which in turn promotes pollen tube growth (Huang, Liu et al. 2014).

1.3.2.3 Pollen tube guidance in the ovary

Once the pollen tube has completed its growth through the transmitting tract, it grows on the surface of the septum where it is eventually being attracted by an ovule. Changing growth direction the pollen tube now grows along the funiculus and enters an ovule through the micropyle. After growing into the filiform apparatus of one of the two synergid cells, the pollen tube stops growing, bursts and thereby releases the two

immobile sperm cells. The synergid cell degrades and one of the sperm cells fuses with the egg cell, while the other one fuses with the central cell.

Over the past years intensive research on pollen tube guidance in the ovary was carried out, improving knowledge on this fascinating process continuously. Several mutants exhibiting unsuccessful fertilization phenotypes were discovered. Knock-out of transcription factor (TF) CENTRAL CELL GUIDANCE (CCG) and its interacting partner CCG-BINDING PROTEIN 1 (CBP1), the AAA+ ATPase MAGATAMA (MAA3), the SUMO E3 LIGASE (SIZ1), the membrane protein GAMETE-EXPRESSED 3 (GEX3) and the TF MYB98 leads to impaired pollen tube targeting towards the ovule (Shimizu and Okada 2000, Kasahara, Portereiko et al. 2005, Chen, Li et al. 2007, Alandete-Saez, Ron et al. 2008, Ling, Zhang et al. 2012, Li, Zhu et al. 2015). Recent studies have shown that MYB98 expression in the synergid cells is controlled by CCG and CBP1 expressed in the central cell (Higashiyama and Yang 2017).

It was discovered that synergid cells secrete a variety of signals via the filiform apparatus, including a chemical signal attracting pollen tubes (Higashiyama and Hamamura 2008, Higashiyama and Takeuchi 2015, Dresselhaus, Sprunck et al. 2016). In the monocotyledonous plant *Zea mays*, the secreted peptide EGG APPARATUS 1 (EA1) was identified to attract pollen tubes in a species-specific manner (Marton, Cordts et al. 2005, Marton, Fastner et al. 2012, Uebler, Dresselhaus et al. 2013).

In dicots, CRPs are secreted by the synergid cells, which are involved in the fertilization process (Jones-Rhoades, Borevitz et al. 2007, Silverstein, Moskal et al. 2007, Okuda, Tsutsui et al. 2009). They are divided in many classes and contain an N-terminal signal peptide (Silverstein, Moskal et al. 2007). The number and arrangement of cysteines defines the tertiary structure of the peptides by forming disulfide bonds (Broekaert, Cammue et al. 1997, Boman 2003, Theis and Stahl 2004, Silverstein, Moskal et al. 2007). LURE peptides belong to the defensin-like CRPs and can be found in several eukaryotic taxa (Mygind, Fischer et al. 2005), comprise six cysteine residues and attract pollen tubes in *Torenia fournieri* (TfLURE1 and TfLURE2) (Higashiyama, Yabe et al. 2001, Okuda, Tsutsui et al. 2009). First identified in *Torenia fournieri*, LUREs are found in other species like *Torenia concolor* (TcCRP1), *Arabidopsis thaliana* (AtLUREs) and *Arabidopsis lyrata* (AlLUREs) and act in a species preferential manner

(Kanaoka, Kawano et al. 2011, Marton, Fastner et al. 2012, Takeuchi and Higashiyama 2012). *Arabidopsis thaliana* comprises six LURE genes, AtLURE1.1 to AtLURE1.6 (Marton, Fastner et al. 2012, Kanaoka and Higashiyama 2015, Higashiyama and Yang 2017). Species specificity is possibly based on pronounced sequence diversity, even in closely related species (Higashiyama, Inatsugi et al. 2006). Arabinogalactan proteins have also been identified to play a critical role in many steps of the fertilization process in *Torenia fournieri*, including ovule and pollen development, pollen germination and tube growth, degradation of the synergid cell, transfer of female self-incompatibility factors and block of polytubey (Pereira, Pereira et al. 2015, Dresselhaus and Coimbra 2016, Hou, Guo et al. 2016, Pereira, Lopes et al. 2016).

Receptor-like kinases such as POLLEN RECEPTOR-LIKE KINASE 6 (PRK6), MALE DISCOVERER 1 (MDIS1), MDIS-INTERACTING RECEPTOR-LIKE KINASE 1 (MIK1) and MIK2 seem to function as receptors for AtLURE1 and are localized at the pollen tube tip plasma membrane (Takeuchi and Higashiyama 2016, Wang, Liang et al. 2016). According to current models AtLURE1 leads to a heterodimerization of the leucine-rich repeats receptor-like kinases MDIS1 and the two MIKs and activates their kinase activity. Respective knock-out mutants display defective micropylar pollen tube guidance and transformation of AtMDIS1 to the sister species *Capsella rubella* partially breaks down the reproductive isolation barrier (Wang, Liang et al. 2016). In *Arabidopsis thaliana* eight PRKs seem to be involved in pollen germination and pollen tube growth (Miyawaki and Yang 2014). One of these PRKs, PRK6, is specifically localized to the plasma membrane at the pollen tube tip and interacts with PRK6 pollen-expressed ROPGEFs. More importantly, PRK6 was shown to accumulate asymmetrically in response to an externally applied AtLURE1 just before reorientation of pollen tube tip growth (Qin, Leydon et al. 2009, Chang, Gu et al. 2013, Takeuchi and Higashiyama 2016).

Knock-out mutants of the cytosolic RLCK-VII-type receptor-like protein kinases LOST IN POLLEN TUBE GUIDANCE AtLIP1 and AtLIP2 represent further components and also show defects in pollen tube guidance (Liu, Zhong et al. 2013). Palmitoylation-based anchoring of LIP1 and LIP2 to the pollen tube tip region seems crucial for their role in guidance control. Thus, although they do not represent bona fide receptors for

LUREs, LIP receptor kinases may act as cytosolic co-receptors in LURE-signaling (Liu, Zhong et al. 2013).

It was further stated that the ER-localized membrane protein POLLEN DEFECTIVE IN GUIDANCE 1 (POD1) plays a role in pollen tube guidance, too, as it regulates the response of the pollen tube towards the female signaling (Li, Xue et al. 2011). POD1 cooperates with CALRETICULIN 3 (CRT3), which is a chaperone controlling folding of membrane proteins and binds calcium (Li, Xue et al. 2011). ABNORMAL POLLEN TUBE GUIDANCE 1 (APTG1) is part of the vegetative and reproductive development by playing a role in processing of glycosylphosphatidylinositol (GPI)- anchored proteins. Mutants are defective in micropylar guidance and display embryo lethality (Dai, Gao et al. 2014). APTG1 is part of the GPI- anchor synthesis of the tip-localized COBRA-LIKE PROTEIN 1 (COBL10) (Li, Ge et al. 2013). A correct localization in the pollen tube tip is essential for COBL10 and relies on GPI-anchor targeting and C-terminal hydrophobic residues. COBL10 plays a role in deposition of pectin and cellulose microfibrils at the pollen tube cap. Mutation of COBL10 displays a decrease in pollen tube growth and affected guidance in the female tissue and causes thereby male sterility (Li, Ge et al. 2013). Other proteins involved in pollen tube guidance are MITOGEN-ACTIVATED PROTEIN KINASE 3 (MPK3) and MPK6, which play a role in controlling pollen tube competence for signaling. Mutation of MPK3 and MPK6 shows a dimished funicular pollen tube guidance, which leads to embryo lethality (Guan, Lu et al. 2014).

Fertilization reaches its final phase when the pollen tube arrives at the micropyle and grows into one of the synergid cells via the filiform apparatus. It was shown that upon tube arrival in one of the two synergid cells, the receptive cell, the cytosolic calcium concentration increased more than in the other (Hamamura, Nishimaki et al. 2014). Synergid cell death occurs simultaneously with pollen tube rupture, resulting in sperm cell release into the space between central cell and egg cell allowing double fertilization to take place (Boisson-Dernier, Lituiev et al. 2013, Leshem, Johnson et al. 2013, Denninger, Bleckmann et al. 2014, Hamamura, Nishimaki et al. 2014, Ngo, Vogler et al. 2014). The receptor-like kinase FERONIA (FER) which acts as a sensor of cell wall integrity (Richter, Ploderer et al. 2017, Feng, Kita et al. 2018) in the synergid cell has been suggested to play a role in pollen tube rupture (Huck, Moore et al. 2003, Escobar-

Restrepo, Huck et al. 2007). It was also indicated that the CRP LORELEI (LRE), together with LORELEI-LIKE GPI-ANCHORED PROTEIN 1 (LLG1) and LLG3 act as co-receptors for directing the *Catharanthus roseus* RECEPTOR-LIKE KINASE 1-LIKE (CrRLK1L) FER to the cell surface of the filiform apparatus or play a role in the stabilization of the FER-receptor complex at the plasma membrane (Capron, Gourgues et al. 2008, Tsukamoto, Qin et al. 2010, Li, Yeh et al. 2015, Hafidh, Potesil et al. 2016, Liu, Castro et al. 2016). When the pollen tube arrives, the FER-LRE complex regulates the production of reactive oxygen species (ROS), which seem to cause pollen tube burst in a calcium-dependent manner (Iwano, Ngo et al. 2012, Denninger, Bleckmann et al. 2014, Duan, Kita et al. 2014).

In the pollen tube, the CrRLK1L-type receptor-like protein kinase proteins ANXURE 1 (ANX1) and ANX2, as well as BUDDHA's PAPER SEAL 1 (BUPS1) and BUPS2 play important roles in maintaining cell integrity during growth by building heterodimers with their extracellular peptide ligands of the RAPID ALKALINIZATION FACTOR (RALF) family RALF4 and RALF19 (Boisson-Dernier, Roy et al. 2009, Miyazaki, Murata et al. 2009, Boisson-Dernier, Lituiev et al. 2013, Ge, Bergonci et al. 2017). Possibly RALF4 and RALF19 are replaced with the female-derived RALF34 upon contact of the pollen tube with the female gametophyte. This could deregulate BUPS-ANX signaling and thereby lead to pollen tube rupture (Boisson-Dernier, Roy et al. 2009, Miyazaki, Murata et al. 2009, Boisson-Dernier, Lituiev et al. 2013, Zhu, Chu et al. 2018).

In maize, the DEFLs *Zea mays* EBRYO SAC 1-4 (ZmES1-4) are expressed in the embryo sac. ZmES4 provokes pollen tube rupture in a species-specific way. It targets the potassium channel KZM1, which leads to an opening of KZM1. K^+-influx and water uptake may lead to pollen tube bursting (Amien, Kliwer et al. 2010). Pollen tube rupture in maize also seems to be provoked by PECTINMETHYLESTERASE INHIBITOR (PMEI) (Okuda, Tsutsui et al. 2009, Leydon, Beale et al. 2013, Woriedh, Wolf et al. 2013).

1.3.2.4 Avoidance of polytubey and polyspermy

A characteristic feature of the fertilization process in flowering plants is that each ovule receives one pollen tube only. In plants with multiple ovules, like *Arabidopsis thaliana* or *Nicotiana tabacum,* precise pollen tube guidance is a key controlling

component in the fertilization process (Beale, Leydon et al. 2012, Kasahara, Maruyama et al. 2012, Maruyama, Hamamura et al. 2013, Maruyama, Volz et al. 2015). An attraction of multiple pollen tubes towards one ovule (polytubey) and the resulting polyspermy, which is the fusion of multiple sperm cells with one female gamete, should be avoided (Dresselhaus, Sprunck et al. 2016). On the other hand, in case of an unsuccessful fertilization, a rescue system is activated and another pollen tube is attracted to the second synergid cell (Kasahara, Maruyama et al. 2012, Nagahara, Takeuchi et al. 2015). This rescue system takes several hours to initiate, indicating the existence of a chemical block, which inhibits attraction of more than one pollen tube towards and ovule and degrades the secreted attractants (Shimizu and Okada 2000, von Besser, Frank et al. 2006, Kasahara, Maruyama et al. 2012). Possibly, the vacuolar acidification, mediated by ADAPTER PROTEIN 1 GAMMA SUBUNIT (AP1G) and VACUOLAR ATP SYNTHASE SUBUNIT A (VHA-A), leads to cell death of the synergid cell, which may function as the pollen tube blocking signal (Wang, Feng et al. 2017).

1.4 Plant model systems for fertilization research

In this work the fertilization mechanism of flowering plants should be investigated on a molecular level. In plant research several species could be chosen for this purpose. The most widely used species is *Arabidopsis thaliana*. It has a short generation time, a diploid genome, which facilitates research on recessive genes, it self-fertilizes and possesses a relatively small genome of around 140 Mb, that has been thoroughly investigated (Koornneef and Meinke 2010). Also in regards to fertilization processes, significant progress has been achieved using *Arabidopsis thaliana*.

Another model plant often used is the monocotyledonous plant *Zea mays* (Strable and Scanlon 2009). Being a crop plant, research on maize is of high common and economic interest and with the identification and characterization of ZmES4, important research on fertilization has been carried out in maize (Amien, Kliwer et al. 2010). *Zea mays* is picky with its growth conditions, requiring specific temperatures, humidity etc, which makes working with maize a little challenging. Also the big plant size has to be considered when selecting maize as a model plant.

For this work *Nicotiana tabacum* was chosen as the model plant to work with, as its characteristics are offering suitable conditions for research. Tobacco is a dicotyledonous crop plant belonging to the family of Solanaceae, same as e.g. tomato and potato. Tobacco is easily transformable and to cross, has a short life cycle of three to four months and is often used in tissue culture (Ganapathi, Penna et al. 2004). It is especially suitable for research in fertilization, because plants are sufficiently big to dissect ovule, collect pollen etc. without need of a microscope. Easy performance of semi *in-vivo* fertilization experiments are another advantage, as tobacco pollen tubes do not require growing through the stigma in order to become competent for attraction to the ovule.

1.5 Aim of this work

The fertilization process of flowering plants requires the fusion of a non-mobile male gametophyte, the sperm cells, with the female gametophyte, the embryo sac. The sperm cells are transported to the egg cell and the central cell via a growing pollen tube that germinates on the surface of the flower stigma and then navigates through the female pistil tissue towards the ovary via polar cell growth. This directional growth requires a close communication between male and female gametophyte.

Aim of this work was to investigate the fertilization process of the model plant *Nicotiana tabacum*. We wanted to obtain insights about relevant processes occurring in the male and the female gametophyte on a molecular level. Therefore we aimed to determine important biological processes in both the male and female gametophyte and to get a closer look at the impact of pollination and fertilization in the ovule on a transcriptional level. Tissue samples from tobacco plants were taken during different steps of the fertilization process and made subject to RNA sequencing experiments. The obtained data was analyzed and the expression counts of the pollen tubes and ovules were mapped to biological process pathways in order to receive insights into relevant processes in the tissues. Differential gene expression analysis was used to broaden our understanding about biological processes in the ovule during reproduction of tobacco plants.

For the navigation of the growing pollen tube towards the ovule a precise communication between male and female gametophyte is crucial. We wanted to identify the peptide, which provokes attraction of the pollen tube towards the ovule. Therefore the obtained transcriptome data was analyzed to find the expressed defensin like proteins among the cysteine rich proteins. We selected candidate transcripts and verified their expression *in vivo* using quantitative real time PCR. Subsequently these candidates were expressed in a cell free environment and applied to growing pollen tubes in attraction assays in order to investigate their impact on the pollen tube growth.

2. Material and Methods

2.1 Plant growth conditions

Nicotiana tabacum SR1 plants were grown at 22°C and 60 % rh. The plants were exposed to 40 kLux of light from sodium-vapor lamps for 14 h/day. For transcriptome and expression analysis plant material was harvested from flowering, about 12 week old plants.

2.1.1 Sample preparation

For transcriptome and expression analysis plant tissue for four different samples were harvested.

2.1.1.1 Pollen tubes (PT)

Pollen from flowering *Nicotiana tabacum* SR 1 plants was harvested. 50 µg of pollen were germinated *in-vitro* in liquid tobacco pollen germination medium (NtPGM) for four hours. Using a microscope successful pollen tube growth was verified. To separate non-germinated pollen from pollen tubes, the medium was passed through a 40 µm filter. The non-germinated pollen was discarded with the flow through. Pollen tubes were homogenized in liquid nitrogen using mortar and pestle and stored at -80°C.

2.1.1.2 Ovules from unpollinated flowers (OV)

Anthers from *Nicotiana tabacum* flower stage 9 were detached in order to avoid pollination of the pistil. Ovules from flower stage 12 plants were dissected. Per sample two ovules were harvested and immediately stored at -80°C.

2.1.1.3 Ovules from pollinated flowers (OVP)

Anthers from *Nicotiana tabacum* flower stage 9 were detached in order to avoid pollination of the pistil. Ovules from flower stage 12 plants were pollinated by hand with Lelat::YFP pollen. Pollen tube growth through the stigma and the style was tracked under a microscope observing the emitted fluorescence. The ovules were harvested after the pollen tubes had grown about half way through the style, about

20 hours after pollination. Per sample two ovules were harvested and immediately stored at -80°C.

2.1.1.4 Ovules from fertilized flowers (OVF)

Anthers from *Nicotiana tabacum* flower stage 9 were detached in order to avoid pollination of the pistil. Ovules from flower stage 12 plants were pollinated by hand with Lelat::YFP pollen. Pollen tube growth through the stigma and the style was tracked under a microscope observing the emitted fluorescence. The ovules were harvested after the pollen tubes had grown completely through the style and into the ovary to make sure fertilization had taken place. Sample preparation occurred after about 48 hours after pollination. Per sample two ovules were harvested and immediately stored at -80°C.

Pollen tube growth through the stigma and the style for OVP and OVF samples was tracked using Lelat::YFP pollen, monitoring its growth through the style via an inverted Zeiss microscope AxioObserver (Carl Zeiss AG). The YFP was excited with a VisiChrome High-Speed Polychromator System (Visitron Systems) (λ_{ex}= 505 nm, λ_{em}= 535/30 nm).

2.1.2 mRNA isolation

For extracting RNA from *Nicotiana tabacum* pollen tubes and ovaries, the plant material was homogenized. The samples were ground with liquid N_2 using mortar and pistil. After homogenization 50- 100 µg of plant material was transferred into a 1.5 ml Eppendorf tube and 1 ml of TRI Reagent (Sigma-Aldrich, St. Louis, MO, USA) was added per sample. To ensure complete dissociation of nucleoprotein complexes, the solutions were incubated at room temperature for 5 minutes. Then 0.1 ml of 1-bromo-3-chloropropan was added, the samples were shaken vigorously for 1 min and incubated at room temperature for 10 minutes. Afterwards the samples were centrifuged at 12.000 g for 15 minutes at 4°C , which separated the solutions into three phases: a red organic phase containing the proteins, an interphase which contained the DNA and an upper aqueous phase that contained the RNA. The upper phase was transferred to a new 1.5 ml Eppendorf tube and 0.5 ml isopropanol was added. The samples were then

incubated at room temperature for 10 minutes. Afterwards they were centrifuged again at 12,000 g for 10 minutes at 4°C. The supernatant was discarded and the pellet containing the RNA was washed with 1 ml 70 % Ethanol. Therefore the samples were shaken vigorously for 1 minute and centrifuged at 7,500 g for 5 minutes. The supernatant was discarded and the pellets were dried at 37°C for 10 minutes to remove the Ethanol completely. The RNA was solved in 40 µl DEPC (Diethyl pyrocarbonate)-water and incubated at 65°C for 10 minutes. DEPC inactivates RNases in the water. The water is treated with 0.1% v/v DEPC for at least 2 hours at 37°C and then autoclaved to inactivate traces. During autoclaving the DEPC dismounts into carbon dioxide and ethanol.

2.1.3 Quality and quantity control of isolated RNA

To test the quality and determine the quantity of the isolated RNA, the samples were examined with a bioanalyzer (Experion™ Automated Electrophoresis Station, Biorad, Hercules, CA, USA). The bioanalyzer uses the lab-on-a-chip technology to perform a gel electrophoresis. The RNA is separated by its length via a high voltage using a capillary system. Fluorescence measurements ware performed from 670-700 nm to measure the quantity of the RNA. The results can be displayed as electropherograms or virtual gels. The samples were treated according to the manufacturers specifications.

2.1.4 DNase digestion

After determination of the quality and the quantity of the isolated RNA, 1 µg of RNA was digested using an RNase free DNase to eliminate remaining DNA contaminations. The quantity of RNA measured by the experion was used to calculate the volume of RNA for 1 µg.

$$Volume\ RNA[\mu l] = \frac{Amount\ RNA\ [ng]}{Concentration\ \left[\frac{ng}{\mu l}\right]}$$ Formula 1

For a 10 µl reaction:

10x DNase Buffer	6 µl
RNase freie DNase I (1U/µl)	1 µl
RiboLock RNase Inhibitor (40 U/µl)	0.5 µl
isolierte RNA	1 µg
DEPC-H_2O	to 10 µl

The samples were incubated for 30 min at 37°C.

2.1.5 RNA precipitation

For further experiments (qPCR) the DNase digested RNA needs to be precipitated. Per sample 90 µl DEPC-water, 10 µl 5M NH_4Ac in 100 mM in EDTA, 1 µl Glycogen (20 mg/ml) (Thermo Scientific) and 75 µl Isopropanol were added to the 10 µl of RNA. The samples were centrifuged at 12.000 g for 20 min at 4°C. The supernatant was discarded and the pellet was washed with 500 µl of 70% Ethanol (in DEPC-water) and centrifuged at 7.500 g for 15 min at 4°C. The supernatant was discarded and the samples were dried at 37°C for 10 min. The RNA was solved in 10 µl of DEPC-water.

2.1.6 Reverse transcription: RNA to cDNA

Because in qPCR double-stranded cDNA is amplified, the RNA needed to be transcribed into cDNA. Therefore an RNA-dependent DNA-polymerase formed a double-stranded RNA-DNA hybrid-strand from the single-stranded RNA. Afterwards the RNA was degraded and a DNA-dependent DNA-polymerase completed the double-strand.

Each reaction contained the following ingredients:

mRNA	6.7 µl
RT-Primer (oligo dT 100 µM)	0.4 µl
10 µM dNTPs [10 mM]	0.5 µl
5x RT-Puffer (Promega)	2.0 µl

The samples were incubated at 70°C for 2 min and afterwards immediately placed on ice. 0.4 µl MMLV-RT (Promega) were added and the reaction was incubated for 1 h at 42°C.

2.2 Amplification via Polymerase Chain Reaction (PCR)

The polymerase chain reaction (PCR) is a widely used molecular biological method to amplify DNA *in-vitro* established by Kary Banks Mullis in 1986 (Mullis, Erlich et al. 1987). A heat-stable enzyme DNA-polymerase is used to amplify the DNA. Because the amplified DNA from the previous cycle are used as templates in the next cycle, an exponential amplification of DNA is theoretically possible.

A PCR consists of 12-50 cycles; each one is divided into three steps:

1. Melting

The double-stranded DNA is heated to 95°C, in order to separate the strands. During this process, the hydrogen bonds between the strands are broken. In the first cycle the melting step is often prolonged to ensure that the template-DNA as well as the primers are presented in a single-stranded form.

2. Annealing

During the second step the primers anneal to the single-stranded template DNA. The primers frame the region of DNA that should be amplified and serve as starting point for the polymerase. The temperature for the annealing step is chosen for optimal annealing of the primers to the DNA. If the temperature is too low, unspecific binding is possible, while a high temperature leads to inefficient binding, due to thermic movement.

3. Elongation

The heat-stable polymerase synthesizes a new strand of DNA complementary to the DNA template by adding dNTPs (desoxy nucleoside triphosphates) from the reaction solution in 5'-to-3' direction. Which polymerase is used depends on the experiment, as the polymerases possess different characteristics. The Phusion CX polymerase e.g. does contain a proofreading activity, but is mutated in a way that it doesn't identify uracils as errors. This makes this polymerase suitable for USER-cloning. The optimal temperature for the Phusion CX polymerase is 72°C and the elongation time is 30 s/kb.

Example reaction for a PCR:

Buffer	2.5 µl
Polymerase	0.75 µl
forward Primer [10 µM]	0.5 µl
reverse Primer [10 µM]	0.5 µl
dNTPs [10 mM]	1 µl
cDNA/gDNA	1 µl
PCR-Wasser	18.8 µl
	25 µl

Table 1: Example PCR-program

	Phusion CX			Advantage		
Step	Temperature	Time		Temperature	Time	
Initial denaturation	98°C	2 min		94°C	2 min	
Denaturation	98°C	30 sec	35x	94°C	30 sec	35x
Annealing	55°C	30 sec		52°C	30 sec	
Elongation	72°C	1:10 min		72°C	3 min	
Final elongation	72°C	15 min		72°C	15 min	
Hold	4°C	∞		4°C	∞	

2.2.1 Expression analysis via quantitative Real-Time PCR (qPCR)

The qPCR uses the principle of PCR but incorporates a method of quantifying the PCR product after each cycle. It therefore uses a DNA-dye, e.g. SYBR Green (Absolute Capillary Mix, Thermo Scientific), which intercalates into the DNA. The emitted fluorescence is measured by the machine (Realplex, Eppendorf/ Lightcycler, Roche). Because the emitted fluorescence is proportional to the DNA, it is possible to calculate the amount of DNA, which increases after each amplification step.

A disadvantage of this system is the low specificity, as it can't be distinguished between different PCR products. On the other hand, a melting curve analysis can be performed, where the temperature is increased slowly and the DNA strands separate abruptly at a certain temperature. At time point the fluorescence decreases as well. As DNA

products of different size mostly possess a different melting temperature, the melting curve analysis increases the specificity in the qPCR method.

The process of a qPCR can be divided into three phases. In the first phase of amplification, the fluorescence of the DNA product is overlaid by the background fluorescence, because with the small amount of template DNA the probability of DNA, primers and polymerase meeting each other, is quite low. The cycle at which the emitted fluorescence rises above the background fluorescence the first time is called threshold cycle. This is followed by a logarithmic increase of fluorescence (log-phase). The last phase of amplification is the plateau phase, where the amount of PCR product has increased at a level that it inhibits itself and the substrates are slowly used up or are damaged by the heat.

If external gene specific standards with defined DNA-concentrations are used, a software can determine amounts of DNA in each sample from the emitted fluorescence. In order to compare expressions of different genes, a constitutively expressed gene is needed as a housekeeping gene. In this work the tobacco actin (NtActin) was chosen for this purpose, so that the expression values as calculated as x molecules of gene of interest per 10,000 actin molecules. With this it is not necessary that all samples contain the exact same amount of template DNA from the beginning.

2.2.1.1 qPCR: Experimental procedure

In this work the cDNA was diluted 1:20 in tRNA (transfer-RNA)-water. For tRNA-water 1 µl of tRNA [10 µg/µl] is diluted in 1 µl HPLC-water (Roth). The expression of seven genes (Nt136007, Nt46443, Nt47038, Nt79003, Nt54117, Nt22095, NtActin) was investigated in different tissues (pollen tubes, unpollinated ovules, pollinated ovules, fertilized ovules).

For each gene a primer mix (400 µl) was prepared:

forward primer [100 µM] (TIB MOLBIOL)	6 µl
revers primer [100 µM] (TIB MOLBIOL)	6 µl
tRNA-water	388 µl
	400 µl

Each reaction contained the following ingredients:

cDNA (1:20)	2 µl
Primer Mix	8 µl
SYBR Green	10 µl
	20 µl

For the qPCR 96-well plates (Eppendorf) were used. Each reaction, including the standards and a negative control (water), was pipetted into a well. The plate was sealed with a transparent adhesive tape and placed into the machine (Mastercycler ep realplex, Eppendorf/ Lightcycler, Roche).

Table 2: PCR program in qPCR analysis

	Temperature	Time	
Initial denaturation	95°C	15 min	
Denaturation	95°C	15 sec	40x
Annealing	Tm	30 sec	
Elongation	72°C	20 sec	
Excitation SYBR Green	79°C	20 sec	
Melting Curve	95°C	15 sec	
	60-95°C	0.3°C/sec	
Hold	40°C	∞	

For NtActin an annealing temperature of 53°C was chosen, for the other genes (Nt136007, Nt46443, Nt47038, Nt79003, Nt65117, Nt22095) 59°C was used. The annealing temperature for each primer pair was determined with a temperature gradient. For this special qPCR the same sample was pipetted in ten wells and for each sample a different annealing temperature between 48-64°C was used. After the qPCR 1 µl of each reaction was used for an agarose gel electrophoresis. If one distinct band with the correct size could be identified on the gel and the melting curve showed one single peak, the annealing temperature could be used for further qPCR analysis.

Table 3: Standards with according DNA concentration used in qPCR analysis

Standard	DNA concentration
7	20 fg/2µl
8	2 fg/2µl
9	0,2 fg/2µl
10	0,02 fg/2µl

2.2.1.2 qPCR: Data analysis

After performing the qPCR reaction, the data was analyzed in order to calculate the expression levels of the genes in the different tissues. Therefore the emitted fluorescence was used to first calculate the number of molecules and then the number of molecules per 10,000 actin molecules.

$$number\ of\ molecules = \frac{910}{length\ of\ fragment\ [kb]} \cdot fluorescence\ [fg] \qquad \text{Formula 2}$$

This equation uses the correlation that a DNA fragment of 1000 bp has an average weight of 910 femtograms (Giulietti, Overbergh et al. 2001). The expressed number of molecules was calculated for each gene. Afterwards the number of transcripts per

10,000 actin molecules was calculated to be able to compare the expression levels of the genes of interest.

$$rel.trancsription = \frac{molecules\ gene\ of\ interest}{molecules\ NtActin} \cdot 10{,}000 \qquad \text{Formula 3}$$

In order to analyze the expression levels of the genes of interest in the plant tissues involved in the fertilization process, two technical replicates were performed. The two obtained data sets were analyzed as described above and normalized for comparison. For each gene the data was normalized to the mean value of unpollinated ovules (OV). Afterwards the two data sets were combined and the mean value, standard deviation and standard error was determined for each tissue (Pollen tubes, unpollinated ovules, pollinated ovules and fertilized ovules).

For statistical analysis a Student's t-test (Student 1908) was done to determine whether there was a statistically significant different expression of the genes between unpollinated and pollinated ovules and between unpollinated and fertilized ovules. In order to avoid type I errors, a multiple testing correction according to Bonferroni (Bonferroni 1936) was performed. In statistical analysis the relationship between two groups is studied. The null hypothesis is a general statement that there is no correlation between the two groups, therefore the null hypothesis is rejected if there is a statistical difference between the analyzed groups. If a p-value of 0.05 is defined as significant, there is a probability of 5 % that this significance between the two values detected is a false positive. If multiple comparisons are carried out, the probability of discovering false positives (type I errors, falsely rejecting the null hypothesis) increases.

$$\text{P(min. one significant result)} = 1 - \text{P(no significant result)}$$

$$= 1-(1- 0.05)^{60}$$

$$\approx 0.95$$

In our case, where 60 experiments were carried out, there is a 95 % chance of detecting a false positive.

The Bonferroni correction sets a significance cut-off at α/n, with α being the significance cut-off and n the total number of hypotheses tested This procedure minimizes the probability of false positives. In our experiment, where α is set to 0.05 and the total number of experiments performed was n= 60, a null hypothesis would only be rejected if the p-value is less than $8.3*10^{-4}$. Using the Bonferroni correction, the probability of observing minimum one false positive would be around 0.05.

$$P(\text{min. one significant result}) = 1 - P(\text{no significant result})$$

$$= 1-(1- 8.3*10^{-4})^{60}$$

$$\approx 0.049$$

Using this calculation, the p-value at which a correlation between two experiments would be considered significant would be $8.3*10^{-4}$. To make our results more comparable to published results, the p-value obtained by the t-test was multiplied with the n of experiments (n= 60). This resulted in a Bonferroni corrected p-value and makes our p-values assignable to the standard significance values of p= 0.05 (*), p= 0.005 (**) and p= 0.0005 (***) were maintained.

2.3 Agarose gel electrophoresis

DNA fragments can be separated by their size in an electrical field with an agarose gel electrophoresis. Due to the negative charge of the DNA caused by the sugar-phosphate backbone, the DNA fragments move along an electric field towards the positive charge (anode) in the gel. Smaller and therefore less positively charged fragments move faster through the agarose matrix. For DNA fragments over 1000 bp a 1 % agarose gel is used, for smaller fragments a 2 or 3 % gel is required in order to separate the molecules. For visualization of the fragments in the gel, the DNA-intercalating fluorescent dye GelGreen (GelGreen Nucleic Acid Stain, Biotium, Hayward, California, USA) is added to the gel. The separated DNA fragments emit light when being exposed to UV light of

254-366 nm. If a ladder containing DNA fragments of specific sizes is applied with the samples of interest, the DNA fragment size can be determined after the electrophoresis.

2.3.1 Experimental procedure and analysis of agarose gels

For performing an agarose gel electrophoresis 1 to 3 % of agarose in 1x TAE-buffer is heated until the agarose dissolves and GelGreen is added to the solution (5 µl/100 ml). The gel is poured in a cast and a comb is placed in the liquid gel. After the gel is completely set, the comb is removed. A 5x loading buffer is added to 500- 100 ng of DNA and the sample is loaded into the wells. A voltage of 80 to100 V is applied to move the DNA towards the anode. After 20 to 40 min the gel is removed from the cast and exposed to UV light of 254-366 nm in a gel imager. For fragments up to 1000 bp a 100 bp-marker and for fragments up to 10,000 bp a λ-PST marker is used as reference to identify the fragment size of the DNA samples.

2.4 Purification of DNA-fragments

2.4.1 Extraction of DNA-fragments from agarose gels

For extracting DNA fragments from agarose gels, the gel was placed on a UV-imager. The fluorophore GelGel visualizes the DNA and a razor blade was used to cut the desired DNA fragment from the gel. The gel fragment was placed in a 1.5 ml Eppendorf tube for extraction of the DNA.

2.4.1.1 Gel extraction kit

For extraction of the DNA from a cut agarose gel fragment, the QIAquick Gel Extraction Kit (Qiagen) was used and the extraction was performed according to the manufacturer's specifications. The extracted DNA was stored at -20°C until further usage.

2.4.1.2 The squeezing method

The cut agarose gel fragment was frozen at -20°C for about 30 min. Afterwards the fragment was wrapped in a piece of parafilm and carefully squeezed until a drop

drained from the gel. The liquid including the DNA fragment was collected in a 1.5 ml Eppendorf tube and stored at -20°C until further usage.

2.4.2 Purification of PCR reactions

To purify DNA from a PCR reaction the QIAquick PCR-Purification Kit (Qiagen) was used. The purification was performed according to the manufacturer's specifications. The extracted DNA was stored at -20°C until further usage.

2.5 Molecular cloning

Molecular cloning is an experimental procedure that is used to insert a DNA fragment (e.g. a coding sequence of a gene of interest) into a destination vector. This construct can then be transformed into a host organism. In this work *Escherichia coli* was used as host.

The circular plasmid vectors can be cleaved using a restriction endonuclease at the site where the DNA fragment is be inserted. DNA and vector should have a compatible configuration at the cleavage site, e.g. by using the same restriction enzyme. Vectors usually contain an antibiotic resistance in order to select positively transformed cells.

2.5.1 USER cloning

The USER (uracil-specific excision reagent) cloning technique offers an efficient way of cloning a cDNA fragment into a vector without needing a ligation step (Nour-Eldin, Hansen et al. 2006). The method is based on the generation of an 8 bp overlap at the 5' and 3' end of the insert and the destination vector. These overlaps are complementary to each other and result in a stable hybrid product without a ligation step.

USER vectors contain a 38 bp PacI cassette that is cleaved by a PacI restriction enzyme (New England Biolabs Inc) which leads to a linearization of the vector. The nicking enzyme NtBbvCI (New England Biolabs) generates the 8 bp overlaps that are non complementary to each other, avoiding a re-hybridization of the vector and allows the incorporation of the cDNA fragment.

The PCR product that should be inserted into the USER vector needs to possess the overlap at its 3' end that is complementary to the 5' overlap of the vector. These

overlaps are created with special primers that contain not only the sequence for annealing to the gene of interest but also the sequence for creating the overlap. The sense primer comprises the nucleotides 5'- GGCTTAAU- 3' and the antisense primer 5' –GGTTTAAU- 3'. During the PCR these nucleotides are attached to the fragment. Afterwards the PCR product is treated with a USER enzyme mix that consists of a uracil DNA glycosylase and a DNA glycosylase-lyase endo VIII (New England Biolabs Inc.). The enzymes catalyze the detachment of the primer-uracil and cleavage of the phoshodiester backbone in order to generate single-stranded overlaps. It is important to use a polymerase for the PCR that possesses a proofreading activity but does not recognize uracils as errors. In this case the Phusion CX polymerase was used for that purpose.

2.5.2 Vectors

The vector used in this work was the pIVEX2.6 vector, which was modified for our purposes. The contained His-Tag was replaced with a 3xFLAG-Tag and a USER-cassette was incorporated. The existing ampicillin resistance was kept for selection. cDNA of three genes of interest were amplified and cloned into the vector: *Nicotiana tabacum* SR1 Nt136007 and Nt46443 and *Arabidopsis thaliana* Col-0 AtLURE1.2.

2.5.3 Molecular biological methods using *E.coli*

2.5.3.1 Bacteria transformation through heat shock

Plasmid DNA can be brought into chemically competent bacteria cells via transformation through a heat shock. Therefore 50 µl of bacteria cells (*E.coli* MRF') were thawed on ice. 100 to 500 ng of plasmid DNA was added to the cells and sored on ice for 20 min. The reaction was heat shocked at 42°C for 42 sec and afterwards immediately stored on ice. If the plasmid DNA contains an ampicillin resistance, the transformed bacteria can directly be streaked on antibiotic containing agar plates for selection. The plates are incubated at 37°C for 12 to 16 h.

2.5.3.2 Cultivation of *E.coli*

For cultivation of selected *E.coli* colonies, single colonies were picked from agar plates (2.5.3.1) and grown in 3-5 ml on LB-Amp medium in 15 ml falcon tubes. The samples for

incubated at 37°C and continuously shaken (Shaker Model G25“, New Brunswick scientific co. Inc.). In order to generate large amounts of plasmid DNA, approximately 0.5 ml of the cultivated bacteria culture was diluted in 100 ml of LB-Amp medium and incubated at 37°C for 12-16 h in a 500 ml flask while being continuously shaken.

2.5.3.3 Isolation of plasmid DNA from *E.coli*

Plasmid DNA from a bacteria culture (3-5 ml) was isolated using the QIAprep Spin Miniprep Kit (QIAGEN) according to the manufacturer's specifications. Plsamid DNA from bacteria culture (100 ml) was isolated using the QIAprep Spin Midiprep Kit (QIAGEN). The yielded DNA concentration was determined using a spectrophotometer (Nanodrop 2000c Spectrophotometer, Thermo Fisher Scientific). The isolated DNA was stored at -20°C.

2.5.3.4 DNA sequencing and sequencing analysis

In order to verify the sequence of PCR products and cloning constructs, selected samples were sent to being sequenced at GATC Biotech (GATC Biotech AG, Konstanz) using the Sanger sequencing method (Sanger, Nicklen et al. 1977). The samples were prepared according to GATC's requirements and gene or vector specific primers were used. Sequence analysis was performed with the software Geneious 9 (http://www.geneious.com), (Kearse, Moir et al. 2012).

2.6 RNA-sequencing

For RNA-sequencing 1 µg of DNase-digested RNA was used. The libraries were prepped according to “TruSeq® RNA Sample Preparation v2 Guide” (Illumina). The samples were sequenced on a HiSeq 3000 Sequencer (Illumina).

2.7 Localization analysis

2.7.1 *In-vivo* pollen tube staining

For RNA-sequencing experiments PT, OV, OVP and OVF samples were prepared. To visualize pollen tube growth in stigma and style of the OVP and OVF samples, aniline staining was performed. Therefore the pants were treated as described in 2.1.1. Afterwards the samples were transferred into 3:1 ethanol: acetic acid and incubated for

48 h, while changing the solution after 24 h in order to destain the tissue. The styles were washed three times with 70 % ethanol, followed by an incubation in 8 M NaOH for 24 h to soften the tissue for later staining. The samples were washed in50 mM KH_2PO_4 buffer, pH= 7.4 and incubated in 0.01% aniline blue solution (in phosphate buffer) for 24 h. The stained samples were stored in phosphate buffer. For observation the samples were transferred to phosphate buffer containing 50 % glycerine and observed under a laser scanning microscope. The samples were analyzed with a 25 x magnification, using a UV laser diode with an excitation wavelength of 405 nm and the emitted fluorescence was detected between 505- 520 nm. The obtained images were assembles in Fiji (Schindelin, Arganda-Carreras et al. 2012) with the plugin Mosaic J in order to reconstruct the whole stigma and style.

2.8 Expression of defensin-like proteins and *in-vivo* attraction assay

2.8.1 *In-vitro* expression of defensin-like proteins

Candidate genes Nt136007, Nt46443 and AtLURE1.2 were expressed *in-vitro* using the PURExpress *In-Vitro* Protein Synthesis Kit (New England Biolabs) system. This method uses a cell-free transcription and translation system reconstituted from the purified components necessary for *E. coli* translation.

The coding region of three genes of interest were cloned into a modified pIVEX2.6 vector (2.5.1, 2.5.2) and transformed into chemically competent *E.coli* (2.5.3.1) for amplification. 250 ng of isolated plasmid DNA (2.5.3.3) from each of the three constructs was used as template for *in-vitro* protein synthesis. The expression was carried out according to the manufacturer's specifications.

Each reaction contained the following ingredients:

Solution A	10 µl
Solution B	7.5 µl
RNase Inhibitor (40 U/µl)	0.4 µl
Template DNA	250 ng
Nuclease-free H_2O	to 25 µl
	25 µl

2.8.2 Purification of expressed proteins

The expressed peptides (2.8.1) were purified using anti-FLAG magnetic beads (Sigma-Aldrich) according to the manufacturer's specifications using 20 µl as packed gel volume and 3x FLAG peptide for elution.

2.8.3 Quality control of expressed proteins: Dot blot

A dot blot is a technique to detect and identify proteins using specific antibodies. In this study it was tested whether the expression of Nt136007 and Nt46443 using the PURExpress system was successful. With a dot blot it can be verified if the FLAG tag, and therefore most probably the whole peptide, was expressed but it cannot give information about folding of the peptides.

For the dot blot 2 µl of the expressed (2.8.1) and purified (2.8.2) peptides Nt136007 and Nt46443 were blotted on a nitrocellulose membrane together with a 3x FLAG tag as a control using a narrow-mouthed pipet. The spot where the peptides were applied was marked with a pencil. After the membrane dried, the non-specific sites were blocked with 5 % BSA in TBS-T for 1 h at room temperature. Afterwards the membrane was incubated for 30 min with the primary antibody that binds to the FLAG tag of the peptides and the control (Mouse Anti-DYKDDDDK (FLAG) tag,1 µg/ml, Epitope Biotech Inc., Vancuver, Canada). The sample was then washed 3 times for 5 min with TBS-T and incubated with the second antibody for 30 min (anti-mouse IgG, HRP-linked antibody, 1:1000, Cell Signaling Technology, Cambridge, UK). After that the sample was washed 3 times with TBS-T (one time for 15 min and then twice for 5 min) and once with TBS for 5 min. The membrane was then incubated with ECL reagent for

1 min, which luminesces when exposed to the horseradish peroxidase reporter of the secondary antibody. The membrane was covered with saran wrap and a CCD camera (BioRad) detected the chemiluminescent signal in the dark.

2.8.4 *In-vitro* attraction assay

2.8.4.1 *In-vitro* attraction assay of Nt pollen tubes and ovules

For the attraction assay 1 ml of liquid NtPGM containing 1 % low-melt agarose was poured into 3.5 cm petri dishes. After solidification of the agar NtSR1 pollen was applied and the samples were incubated at room temperature for 3 to 4 h. Ovules from a non-pollinated flower were excised using a gauge needle and placed close to the pollen tubes. To ensure that the ovule was not pollinated, the anthers were dissected from stage 9 flowers. Pollen tube growth was monitored with an inverted light microscope using a 4x magnification for 210 min. Pictures were taken every 15 min.

2.8.4.2 *In-vitro* attraction assay of Nt pollen tubes and peptide

After the expression (2.8.1) and purification (2.8.2) of the tobacco defensins, the peptides were tested *in planta* with an attraction assay. As a positive control whole NtSR1 ovules were used.

For the attraction assay with the expressed peptides, 15 % bovine gelatin was diluted in liquid NtPGM and heated at 40°C. 3 µl of the gelatin solution was mixed with 2 µl of the peptide, that was also preheated to 40°C. After solidification of the gelatin, small pieces were cut off using sharp forceps and placed close to the pollen tubes that were grown as described in 2.8.4.1. Pollen tube growth was monitored with an inverted microscope using a 20x magnification for 30 min. Pictures were taken every 5 min.

2.8.4.3 *In-vitro* attraction assay of Nt YFP-pollen tubes and WT ovules

Pollen tubes were germinated and grown as described in 2.8.4.1, with the difference that Lelat::YFP-tagged pollen of *Nicotiana tabacum* SR1 were used and the pollen was germinated and grown in the dark due to photosensitivity of the fluorophore. After placement of the dissected ovule, pollen tube growth was monitored with an inverted Zeiss microscope AxioObserver (Carl Zeiss AG) using a 40x magnification. The YFP was excited with a VisiChrome High-Speed Polychromator System (Visitron Systems)

(λ_{ex}= 505 nm, λ_{em}= 535/30 nm). Pollen tube growth was monitored over a time period of 80 min. Pictures were taken every 10 sec in which the emitted fluorescence as well as bright flied images were detected. Image data analysis was performed using Fiji software (Schindelin, Arganda-Carreras et al. 2012).

2.9 Bioinformatic analyses

Niklas Terhoeven performed bioinformatic analysis of the transcriptome data as described below.

For data preparation a quality and adapter trimming of the sequencing libraries was performed using trimmomatic 0.33 (`trimmomatic-first-set.sh` and `trimmomatic-second-set.sh`) and quality of the RNA was analyzed with fastqc (`fastqc-first-set.sh` and `fastqc-second-set.sh`). For assembly of the transcriptome Trinity (Grabherr, Haas et al. 2011) (Version v2.2.0) was used in the genome guided mode (`run_trinity.sh`). The reads were mapped to the *Nicotiana tabacum* TN90 genome (Sierro, Battey et al. 2014) with tophat v2.0.11 (`run_mapping.sh`).

In order to annotate the assembled transcripts, peptides were predicted using Trapid via its webinterface (http://bioinformatics.psb.ugent.be/webtools/trapid/) and plaza 2.5 as reference database. A functional annotation was performed on peptides with 10 amino acids or more using the mercator web interface (http://www.plabipd.de/portal/mercator-sequence-annotation) to assign mapman categories to the peptides. For annotation of features like Pfam domains and GO-terms an interproscan Version 5.25-64.0 was done (`chunk-input-data.sh`,`run_Interproscan.sh`,`start-jobs.sh`). DESeq was used for the differential expression analysis and quantification of the transcripts was performed with salmon version 0.7.2 (`run_salmon-index.sh` and `run_salmon-quant.sh`) (Patro, Duggal et al. 2016). The annotated transcriptome and expression data was uploaded into TBro (Transcriptome Browser) (Ankenbrand, Weber et al. 2016).

Prof. Dirk Becker mainly performed identification and analysis of cysteine-rich proteins (CRPs). For identification of CRPs Hidden-Markov-Models (HMMs) were created for the different CRP classes based the results from (Silverstein, Moskal et al.

2007) and (Huang, Dresselhaus et al. 2015) using the tools hmmbuild, hmmscan and hmmsearch from http://hmmer.org/.

For the table containing all identified CRP transcripts, Niklas Terhoeven added the CRP description with the R tidyverse package (needed for ggplot) and used `convert_table_for_plots.pl` for converting the differential DEFL expression into the bar plot.

2.9.1 Principal Component Analysis

In order to get an general idea about the obtained transcriptome data, PCA plots were created by Niklas Terhoeven with the plotPCA() analysis from the R-package DESeq2 (Love, Huber et al. 2014).

2.9.2 Venn diagram

To get further insides about differentially expressed or shared transcripts in the sequenced and analyzed transcriptome data, first an expression search was performed on the TBro interface. With this tool genes can be filtered depending on their expression in the different analyzed samples. For each tissue that had been sequenced (PT, OV, OVP and OVF) all genes with a mean expression equal to or higher than 500 were extracted. Venn diagrams were than created using InteractiVenn (Heberle, Meirelles et al. 2015) for comparing OV vs. PT and OV vs OVP vs OVF.

2.9.3 Differential gene expression

2.9.3.1 Preparation

The reads generated by transcriptome sequencing were assembled using Trinity, guided by *Nicotiana tabacum* TN90 genome. 522,736 transcripts could be assembled. Because there can exist more than one isoform for a gene, the longest isoform was selected. This was performed using a perl script 'extract_longest_isoform.pl', written by Niklas Terhoeven (see in 5.6) and resulted in 358,767 transcripts.

In order to perform a MapMan analysis a so-called 'Mapping file' needs to be generated, which enables MapMan to associate each transcript of a .fasta file with one ore more MapMan bins. For creating the list of identifiers, first the transcript IDs were

shortened to only contain the unigene ID using grep. TransDecoder (https://test.galaxyproject.org) was used to identify coding regions and the amino acid length was set to minimum 70. The conducted assembly post processing resulted in 90,240 sequences. Cleaning was done with OrthoFinder (Emms and Kelly 2015), which allows identification of orthologous protein sequence families. The resulting remaining 90,240 transcript IDs were used for generating the mapping file, which was created using Mercator sequence annotation tool (http://www.plabipd.de/portal/mercator-sequence-annotation).

2.9.3.2 Expression analysis

An expression analysis was performed to examine the processes occurring in mature ovules and in growing pollen tubes. Therefore the expressed transcripts were extracted from Tbro with a mean minimum expression of 500. The data was imported in Excel and the mean expression level was determined. The table with transcript identifier and mean expression level was used for visualization in MapMan.

To obtain insights about fertilization processes on a cellular level, differential gene expression analysis was performed in Tbro.

Table 4: Conditions for expression analysis pollen tubes (PT) vs. mature ovules (OV):

Condition	Log2FoldChange	Adjusted p-value
Upregulated in PT	≥ 4	≤ 1e-5
Upregulated in OV	≤ -4	≤ 1e-5

Table 5: Conditions for expression analysis mature ovules (OV) vs. ovules from pollinated flowers (OVP)

Condition	Log2FoldChange	Adjusted p-value
Upregulated in OV	≥ 1	≤ 1e-5
Upregulated in OVP	≤ -1	≤ 1e-5

Table 6: Conditions for expression analysis ovules from pollinated flowers (OVP) vs. ovules from fertilized flowers (OVF)

Condition	Log2FoldChange	Adjusted p-value
Upregulated in OVP	≥ 1	≤ 1e-5
Upregulated in OVF	≤ -1	≤ 1e-5

Table 7: Conditions for expression analysis mature ovules (OV) vs. ovules from fertilized flowers (OVF):

Condition	Log2FoldChange	Adjusted p-value
Upregulated in OV	≥ 1	≤ 1e-5
Upregulated in OVF	≤ -1	≤ 1e-5

The obtained data was imported in Excel and the log2foldChange was converted into foldChange for each comparison. A table was created with the transcript ID and fold change and used for import into MapMan.

2.9.3.3 Visualization in MapMan

In MapMan Version 3.6.0 the tables generated in 2.9.3.2 were imported and associated with the mapping file created in 2.9.3.1. For visualization of mapping the 'overview' pathway was selected. The WilcoxRank sum test, corrected according to Benjamini Hochberg was used for further analysis.

3. Results

3.1 *In-vivo* pollen tube staining

Aim of this work was to provide a comprehensive overview of the transcriptomic profiles of pollen tubes and ovules at defined stages of the fertilization process in tobacco (*Nicotiana tabacum* SR1). For this purpose, we planned to harvest tissue samples from mature, non-pollinated ovules (OV), from pollinated ovules (OVP) and from ovules where fertilization was accomplished (OVF). In order to determine representative time points for sampling, pollen tube growth was monitored by means of *in-vivo* pollen tube staining experiments. Therefore, tobacco plants were grown on soil in the greenhouse until flowering and anthers were detached right before pollen maturation/release in order to avoid self-pollination. Tobacco flowers were then manually pollinated with wild type pollen. Tissue samples consisting of stigma and style were taken after 20 h for OVP samples or after 48 h for OVF samples. Samples were stained using the aniline blue method as described in 2.7.1 and subsequently mounted on glass slides for observation using a confocal laser scanning microscope (cLSM). Following UV-excitation (λ_{ex}= 405 nm, λ_{em}= 505/10 nm) Z-stacks were taken at 25x magnification. Images were reassembled using the Mosaic J plugin of the Fiji software (Schindelin, Arganda-Carreras et al. 2012).

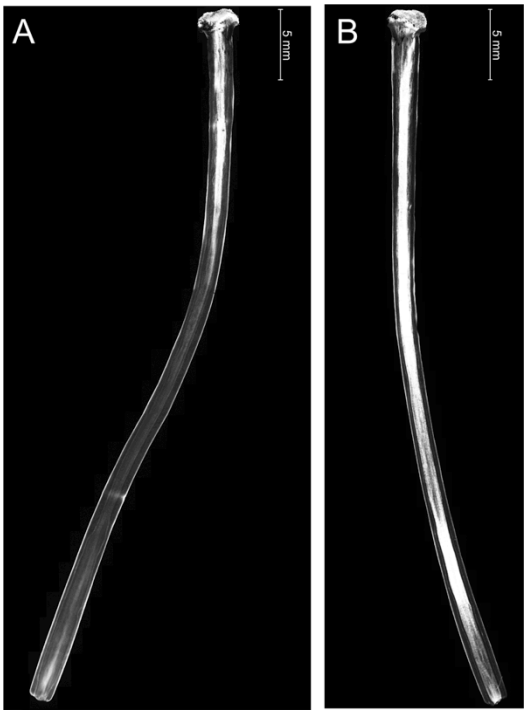

Figure 3: *in-vivo* pollen tube staining. Aniline blue staining of *Nicotiana tabacum* styles. The imagines were taken using a 25 x magnification and were excited with UV light.
(A) 20 h after pollination with wild type pollen. The pollen tubes have grown almost half way through the style
(B) 48 h after pollination with wild type pollen. The pollen tubes have grown completely through the style.

In Figure 3 the pollen tube growth through the transmitting tract is shown. The callose plugs in the pollen tubes are stained by aniline blue, thereby allowing to track their growth through the style towards the ovary. In (A) the pollen tubes of the OVP samples have grown about 20 mm through the style, showing that pollination has occurred but that fertilization has not yet happened. In (B) it is visible that the stained pollen tubes have grown completely through the stigma and the style, which indicated that fertilization was completed in the OVF sample.

3.2 Transcriptome analysis

3.2.1 Quality control on isolated RNAs for sequencing

For RNA-sequencing, RNA from different *Nicotiana tabacum* tissue samples was isolated from harvested and homogenized plant material: *in-vitro* grown pollen tubes (PT), ovules from non-pollinated flowers (OV), ovules from pollinated flowers (OVP) and ovules from fertilized flowers (OVF).

Quality and quantity of the isolated RNA was analyzed employing an Experion device (Bio-Rad) using 'lab-on-a-chip' technology. RNA is separated by its size via high voltage. For quantification fluorescence measurements at 600-700 nm were performed. The results are displayed as electropherograms (Figure 18) and virtual gels (Figure 4).

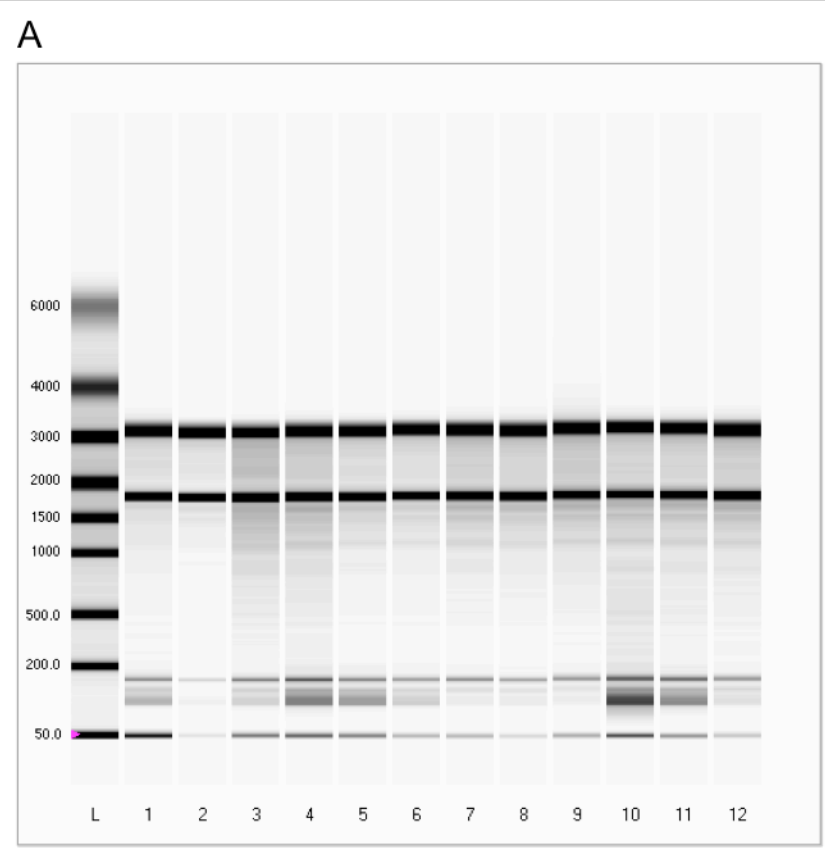

B

Nr.	Sample	c [ng/µl]
1	PT1	231,66
2	PT2	1404,37
3	PT3	512,70
4	OV1	465,14
5	OV2	451,79
6	OV3	676,18
7	OVP1	747,97
8	OVP2	1251,81
9	OVP3	410,45
10	OVF1	390,35
11	OVF2	526,36
12	OVF3	1147,74

Figure 4: Results from quality and quantity analysis of isolated RNAs for RNA-sequencing.
(A) Virtual gel displaying a ladder for scale (L) and the bands obtained from electrophoresis in the RNA samples (1-12). (B) Number of sample on the chip, sample name and concentration measured. The number indicates the lane in the electrophoresis in which the RNAs were analyzed. The concentration is displayed in ng per µl. All samples contain a high concentration of RNA. For further analysis 1 µg of RNA per sample were used.

In Figure 4 the results from quality and quantity analysis of isolated RNAs for sequencing is displayed. (A) Using molecular size ladder, which contains RNAs of specified length, the fragment lengths of the isolated RNAs could be determined. All samples (1-12) display a band at 50 bp, which is the lower marker. It serves the Experion device for sample recognition. Weak bands between 100 and 200 bp containing miRNAs could be detected in all samples. Two very prominent bands of about 1900 and 3700 bp referring to 18S and 25S rRNAs, respectively are found in all samples. Peaks for the rRNAs of prokaryotic descent (16S and 23S rRNA) were not detected, because RNA was only isolated from non-photosynthetic tissue. All RNA

samples appeared non-degraded, of high quality and sufficient quantity (Figure 2B) to be able to subjected to subsequent RNA Sequencing.

3.2.2 RNA Sequencing and differential expression analyses

A transcriptome reveals information about active processes in the analyzed cells or tissues. A transcriptome represents an accumulation of all gene readouts present at the moment the sample is harvested. Counting the number of sequenced transcripts offers the opportunity to determine fold changes in gene expression. In this work the 'Sequencing-by-Synthesis' technology (Illumina) was used, which performs the sequencing process in the following steps (Illumina 2015). The samples were sequenced on a HiSeq 3000 Sequencer (Illumina).

Addition of adaptors

In this first step a transposase cuts the RNA randomly into smaller fragments. Afterwards adaptors are added at both ends of the fragments. During reduced cycle amplification indices, terminal sequences and sites for primer binding are attached. The indices are used for identifying different samples, therefore up to 96 different samples can be sequenced at the same time and can be separated again during data analysis (Feng, Liu et al. 2016). Sequencing is carried out on glass flow cells, which are covered with two types of oligos that are complementary to the terminal sequences attached to the RNA fragments (Quail, Smith et al. 2012).

Cluster amplification

The RNA hybridizes to one of the oligos on the flow cell and a polymerase complements the single strand. The original RNA strand is washed away and the newly synthesized strand bends over and its terminal sequence on the other end hybridizes with the second type of oligo sequence on the glass cell. A polymerase then generates a complementary strand, resulting in a double-stranded bridge. Denaturation of the two strands leads to two single stranded copies, each comprising a terminal sequence at the unbound end, which next hybridizes with another free complementary oligo on the flow cell surface. Repetition of this bridge amplification allows a cluster generation of clonal fragments. After completing the amplification, the reverse strands are washed away and a sequencing primer binds to the primer sequence of the fragment adapter,

initiating the first round of sequencing. During each cycle of the sequencing, a fluorescently labeled nucleotide is attached to the growing complementary strand. A reversible terminal sequence at each nucleotide makes sure that during each cycle only one nucleotide is incorporated. After attachment of a nucleotide, the unbound nucleotides are washed off and a light source excites the fluorophore. The characteristic fluorescence signal of each one of the four different nucleotides allows the sequencer to identify which nucleotide was added. The number of repition of this cycle determines the length of the read. In this work a read length of 150 bp was used. After the first round of sequencing the generated read is washed away. In order to then sequence the reverse strand of the fragment, the previously sequenced forward strand bends over and hybridizes to the second type of oligo of the flow cell surface. A polymerase complements the forward strand during bridge amplification, leading to a double strand. The two strands are separated and the forward strand is washed away. Similar to the first round of sequencing, a primer binds to the corresponding site of the adapter, which is attached to the flow cell and one cycle after the other, fluorescently labeled nucleotides are incorporated. This sequencing by synthesis occurs simultaneously at all fragment clusters and is repeated until, in this study, a sequence depth of 35 million paired end reads is achieved.

Data analysis

During sequence data analysis, samples can be separated due to their unique indices, which were attached in the beginning. The overlapping fragments of forward and reverse sequencing are aligned, resulting in contigs. For this work, the genome of *Nicotiana tabacum* TN90 was known, which is closely related to *Nicotiana tabacum* SR1 that was used for sequencing the transcriptome. Even though there are differences between the genomes, the TN90 sequence was used as a template for assembling the SR1 transcriptome. For differential expression analysis Niklas Terhoeven used DESeq and quantification of the transcripts was performed with version 0.7.2 (`run_salmon-index.sh` and `run_salmon-quant.sh`) (Patro, Duggal et al. 2016). The annotated transcriptome and expression data was uploaded into TBro (Transcriptome Browser) (Ankenbrand, Weber et al. 2016).

3.2.3 Principal Component Analysis (PCA)

A principal component analysis (PCA) (Pearson 1901) is a method that visualizes and analyses genetic distances between individual samples and how related they are to each other. In order to visualize the results, the dimensionality between the samples is reduced, while the variations in the dataset are maintained. Therefore, principal components are identified where the variations between the data sets are the greatest. The PCA plots shown in Figure 5 and Figure 6 are kindly provided by Niklas Terhoeven.

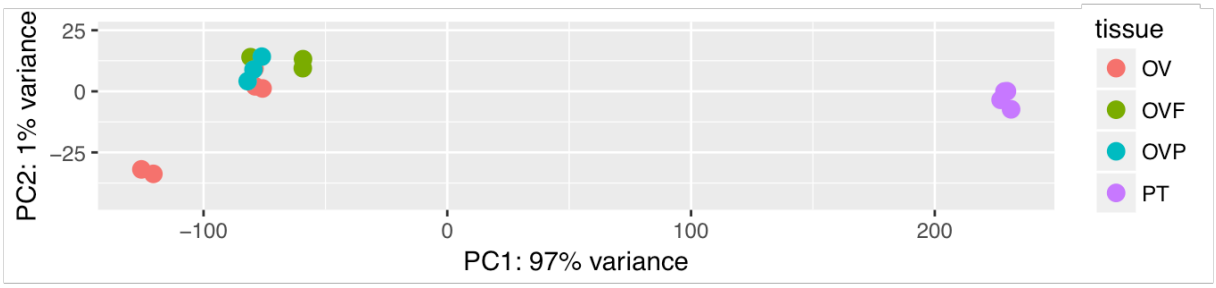

Figure 5: Principal component analysis of the samples analyzed in the RNA-sequencing experiments. Shown are all samples analyzed: Mature ovules (OV), ovules of fertilized flowers (OVF), ovules of pollinated flowers (OVP) and *in-vitro* grown WT pollen tubes; OVF; OVP: n=3, PT: n= 4 OV: n= 5 (DESeq2)

The data shown in Figure 5 display the variance between the expression analysis samples analyzed based on differential expression analysis (DESeq2). Figure 5 shows that the three pollen tube (PT) samples cluster together and are clearly separated from ovule samples (OV, OVP, OVF). This shows that the top 500 differentially expressed genes (DEGs) exhibit similar expression in all ovule samples and all pollen tube samples, but that the pollen tube samples seem to be very different from ovules in terms of gene expression. Since the pollen tube samples are significantly different from the ovule samples, it is hard to distinguish the differences between the individual ovule samples in this PCA-plot. It should be noted that genes underlying PC1 accounted for 97 % of the observed variance.

In order to obtain further insights in the genetic differences between these samples, a second principal component analysis was performed in which the pollen tube samples were excluded and only the ovule samples (OV, OVP, OVF) were plotted (Figure 6).

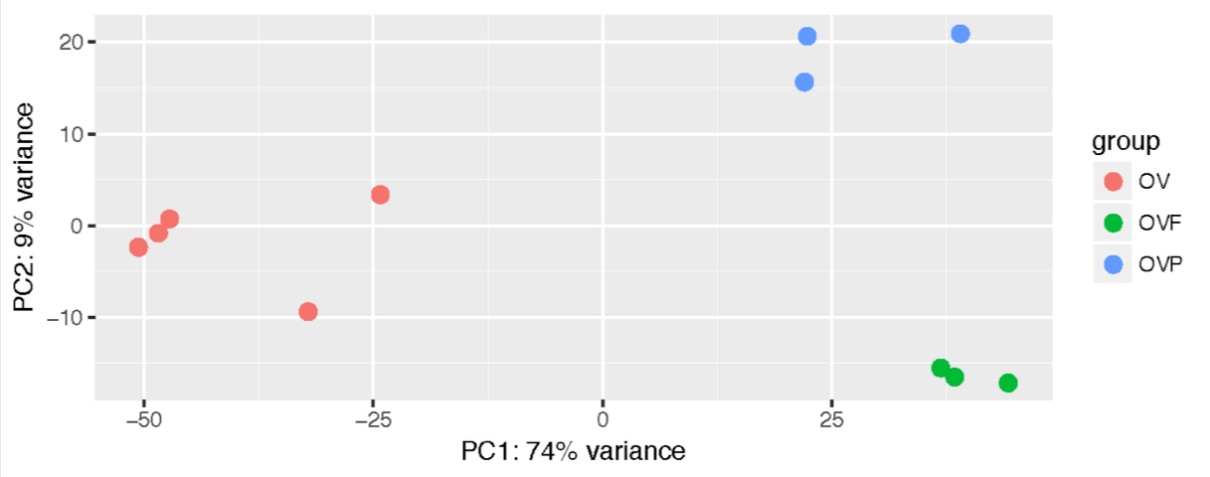

Figure 6: Principal component analysis of selected samples analyzed in the RNA-sequencing experiments.
Shown are the following samples analyzed: Mature ovules (OV), ovules of fertilized flowers (OVF) and ovules of pollinated flowers (OVP); OVF; OVP: n=3, OV: n=5.

Omitting pollen tube samples, the differences in gene expression patterns between mature ovules, ovules from pollinated flowers and ovules from fertilized flowers become visible. Figure 6 shows at first that all samples/replicates of the same treatment cluster together and that treatments are clearly separated from each other. Further, mature ovules are separated from pollinated or fertilized ovules and the corresponding genes of PC1 account for 74 % of the observed variance. Fertilized ovules, however, can be separated from pollinated ovules by a second principal component. This component though accounts for 9 % of the observed variance, only.

3.2.4 Tissue specific transcripts

In order to reveal further insides into the transcriptome profiles, Venn diagrams were created, in which genes expressed predominantly and specifically in the different tissues and under different conditions were compared. Therefore, RNAseq data were mapped and quantified using salmon (Patro, Duggal et al. 2016) and data were

subsequently imported into TBro (Ankenbrand, Weber et al. 2016). Using the 'expression search' function of TBro transcripts with a mean expression level equal to or higher than 500 were extracted for each tissue analyzed (PT, OV, OVP and OVF). The obtained lists were uploaded on the InteractiVenn (Heberle, Meirelles et al. 2015) homepage, where Venn diagrams of OV vs PT and OV vs OVP vs OVF were created (Figure 7).

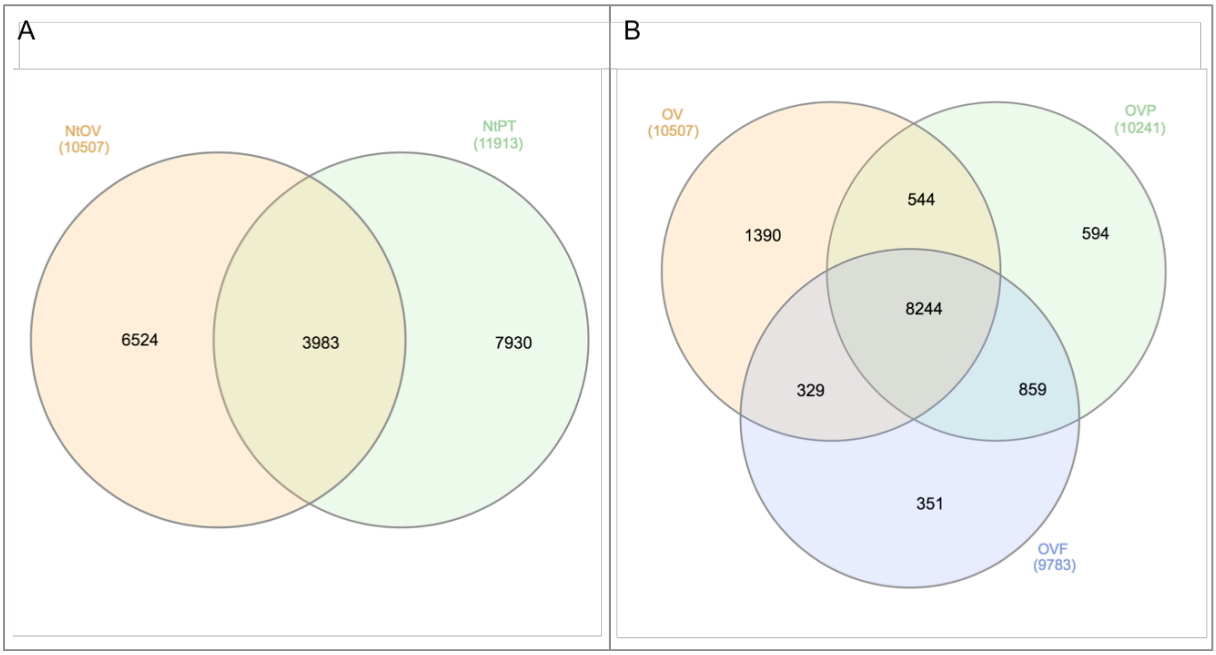

Figure 7: Venn diagram of differentially expressed and shared transcripts

(A) Differentially expressed and shared transcripts of *Nicotiana tabacum* pollen tubes (PT) and mature ovules of non-pollinated flowers (OV). (B) Differentially expressed and shared transcripts of *Nicotiana tabacum* mature ovules of non-pollinated flowers (OV), ovules of pollinated flowers (OVP) and ovules of flowers, in which fertilization had occurred (OVF)

'Expression searches' for transcripts exhibiting a mean expression level equal to or higher than 500 revealed 11,913 transcripts for in *in-vitro* grown pollen tubes, 10,507 transcripts in mature ovules from flowers that had not been pollinated (OV), 10,241 transcripts in ovules from pollinated flowers (OVP) and 9,783 transcripts in ovules, in which fertilization had occurred (OVF). The Venn diagram in Figure 7A shows that only 21.6 % (3,983) of all transcripts were shared between OV and PT, while 35.4 % (6,524) were OV-specific and 43 % (7,930) PT-specific.

When comparing the transcriptional changes in ovules during pollination and fertilization, the majority of genes were commonly expressed in all three samples, i.e. 8244 genes (67 %; Fig. 6B). Only 11.3 % (1,390) of the genes were OV-specific, 4.8 % (594) OVP-specific and 2.9 % (351) OVF-specific. The OV sample shares a higher number of genes with the OVP sample than to the OVF sample. Between OV and OVP 4.4 % (544) of the genes are shared, in comparison to 2.9 % (351) of the genes, which can be found in OV and OVF. 7 % (859) of the transcripts could be found in OVP and OVF samples.

3.2.5 Functional analysis of transcriptome data

After identifying the number of genes that are either expressed in a tissue-specific manner or which could be found in several tissues, it was of interest to figure out their underlying biological function.

The first goal was to obtain insights about relevant processes, which occur in pollen tubes and ovules based on the transcripts enriched/specific in these samples, previously described in the Venn diagrams. Subsequently differential expression analysis was performed to identify genes regulated during fertilization in ovules and to find genes, which are up or down regulated between pollen tubes and unpollinated, mature ovules. These identified genes were then subjected to a functional mapping in order to obtain insights on relevant processes governing fertilization.

Functional analysis of specifically expressed genes

MapMan Version 3.6.0 tool was used to assign functional categories (MapMan bins) to these transcripts, which allows putting the transcripts into a biological context. The first tissue analyzed was the pollen tubes samples. For visualization the 'overview' pathway was selected (Table 8).

Table 8: Association of transcripts expressed in pollen tubes (PT) to MapMan bins. The table displays the top 15 results of the 'overview' pathway sorted by p-value. Shown are the bin number and its name, the number of elements mapped to the bin and its p-value. The WilcoxRank sum test, corrected according to Benjamini Hochberg was used for further analysis. Colored in greys are the bins with a p-value < 1E-2.

Bin	Name	Elements	P-Value
10	Cell Wall	212	0,00E+00
30	Signaling	581	0,00E+00
34	Transport	514	0,00E+00
27	RNA	809	1,82E-12
31	Cell	487	5,47E-09
11	Lipid Metabolism	236	2,09E-05
20	Stress	281	1,10E-04
13	Amino Acid Metabolism	151	2,26E-04
35	Not Assigned	2813	6,43E-04
22	Polyamine Metabolism	16	2,98E-03
8	TCA / Org Transformation	71	3,78E-03
26	Misc	258	8,02E-03
28	DNA	193	2,04E-02
25	C1-Metabolism	30	2,58E-02
3	Minor CHO Metabolism	83	7,09E-02

The above shown table presents the most significant MapMan bins enriched in pollen tubes with its p-value and the number of transcripts, assigned to the regarding bin. According to their p-value, the most significant bins are cell wall with 212 transcripts, signaling, containing 581 transcripts and transport with 514 transcripts. The small p-value indicates that these biological processes play a dominant role in the pollen tube. 809 transcripts cluster in bin 27 (RNA) and are involved e.g. in RNA processing or transcription. Regarding cell functions there were 487 transcripts assigned and 236 of which biological function involved lipid metabolism. With a p-value of 2,26E-04 there were 281 stress-related transcripts and there were 151 transcripts assigned to the amino acid metabolism. For most transcripts (2813) a biological function could not be

assigned. With a p-value in the E-03 range, 16 transcripts belong to the TCA (tricarboxylic acid) bin and 258 transcripts cluster in bin 26, which groups miscellaneous biological functions. The transcripts clustered in bins DNA, C1 metabolism and minor CHO metabolism display p-values < 1E-2.

In contrast to pollen tubes, mature, non-pollinated ovules were characterized by biological processes differing from the processes relevant in the pollen tubes, as described in Table 9.

Table 9: Association of transcripts expressed in mature ovules (OV) to MapMan bins. The table displays the top 15 results of the 'overview' pathway sorted by p-value. Shown are bin number and name, the number of elements mapped to the bin and its p-value. The WilcoxRank sum test, corrected according to Benjamini Hochberg was used for further analysis. Colored in greys are the bins with a p-value < 1E-2.

Bin	Name	Elements	p-value
29	Protein	1904	0,00E+00
35	Not Assigned	2164	1,52E-19
15	Metal Handling	27	3,68E-05
28	DNA	288	7,00E-04
4	Glycolysis	69	3,35E-03
13	Amino Acid Metabolism	192	4,70E-03
22	Polyamine Metabolism	16	8,39E-03
16	Secondary Metabolism	153	2,75E-02
19	Tetrapyrrole Synthesis	15	2,84E-02
11	Lipid Metabolism	178	7,91E-02
34	Transport	394	7,91E-02
14	S-Assimilation	12	8,59E-02
20	Stress	263	1,36E-01
8	TCA / Org Transformation	69	1,65E-01
7	OPP	24	1,81E-01

Table 9 shows the results for the ovule samples with the most relevant MapMan bins and the number of transcripts assigned to these bins, as well as its p-value. The bin

with the most relevant p-value is the protein bin (29). Is contains 1904 transcripts that are related to protein synthesis and regulation. Bin 35 contains all transcripts (2164) not assigned to any other bin and displays a p-value of 1,52E-19. Slightly less significant are the bins containing transcripts involved in metal handling (27 transcripts), DNA (288 transcripts), glycolysis (69 transcripts), amino acid metabolism (192 transcripts) and polyamine metabolism (16 transcripts) with p-values.

The bins containing transcripts related to secondary metabolism, tetrapyrrole synthesis, lipid metabolism, transport, S-assimilation, stress, TCA / organic acid transformation and OPP are less significant than 1E-2. There are a total of 936 transcripts assigned to these bins.

Functional analysis of differentially expressed genes

After identifying transcripts expressed in the mature ovule and in the growing pollen tube and mapping them to biological processes, it should be further investigated, which biological processes are involved in the fertilization process. Therefore, differential gene expression analysis was performed and the resulting genes were assigned to MapMan bins, in order to map them to different biological processes.

First differential gene expression analysis was performed between mature ovules and pollen tubes according 2.9.3. Transcripts higher expressed in pollen tubes than in ovules were considered to be differentially expressed if the Log2FoldChange was ≥ 4.

Table 10: Association of differentially expressed transcripts higher expressed in pollen tubes (PT) than in mature ovules (OV) to MapMan bins. The table displays the top 15 results of the 'overview' pathway sorted by p-value. Shown are bin number and name, the number of elements mapped to the bin and its p-value. The WilcoxRank sum test, corrected according to Benjamini Hochberg was used for further analysis. Colored in greys are the bins with a p-value < 1E-2.

Bin	Name	Elements	P-Value
10	Cell Wall	185	0,00E+00
35	Not Assigned	2974	6,83E-07
20	Stress	148	8,94E-06
25	C1-Metabolism	14	7,90E-04
26	Misc	188	1,22E-03
9	Mitochondrial Electron Transport / ATP Synthesis	17	1,26E-03
30	Signaling	349	1,55E-03
31	Cell	201	1,82E-03
33	Development	125	5,18E-03
34	Transport	321	5,20E-03
23	Nucleotide Metabolism	38	5,82E-02
4	Glycolysis	19	1,18E-01
8	TCA / Org Transformation	14	1,57E-01
29	Protein	423	1,92E-01
7	OPP	2	2,08E-01

The above shown table Table 10) shows the most relevant MapMan bins of the 'overview' pathway. The bin with the highest significance contains 185 transcripts, which play a role in the plant cell wall. There are 2974 transcripts not assigned to any other biological function, summarized in bin 35. With a p-value of 8,94E-06, there are 148 stress-related transcripts and 14 transcripts, which are involved in the C1 metabolism with a p-value of 7,90E-04. During MapMan analysis a total of 1088 transcripts were assigned to six bins (Miscellaneous, Mitochondrial Electron Transport/ ATP Synthesis, Signaling, Cell, Development and Transport) that all display significance in the 1E-3 range. The remaining five results of the top 15 of the overview

pathway, Nucleotide Metabolism, Glycolysis, TCA / Org Transformation, Protein and OPP) show a significance less than 1E-2.

Not only were the transcripts analyzed, which displayed a higher expression in pollen tubes than in ovules, also the transcripts found with a higher expression in ovules than in pollen tubes were analyzed with the MapMan. The differentially expressed genes were assigned to different bins and the top 15 results of the overview pathway are shown in Table 11:

Table 11: Association of differentially expressed transcripts higher expressed in mature ovules (OV) than in pollen tubes (PT) to MapMan bins. The table displays the top 15 results of the 'overview' pathway sorted by p-value. Shown are bin number and name, the number of elements mapped to the bin and its p-value. The WilcoxRank sum test, corrected according to Benjamini Hochberg was used for further analysis. Colored in greys are the bins with a p-value < 1E-2.

Bin	Name	Elements	P-Value
34	Transport	573	1,77E-17
16	Secondary Metabolism	312	5,49E-13
30	Signaling	890	2,06E-10
26	Misc	670	4,07E-10
33	Development	398	5,80E-10
1	PS	148	1,92E-08
27	RNA	1406	9,15E-08
10	Cell Wall	254	1,12E-06
17	Hormone Metabolism	352	1,04E-05
28	DNA	255	1,08E-02
15	Metal Handling	33	3,15E-02
20	Stress	393	3,34E-02
35	Not Assigned	4922	5,46E-02
11	Lipid Metabolism	206	2,07E-01
12	N-Metabolism	9	2,14E-01

When identifying the transcripts differentially expressed between mature ovules and pollen tubes and focus on the transcripts upregulated in the ovules, there are 573 transcripts assigned to the transport bin. This bin shows the highest significance with a p-value of 1,77E-17 (Table 11). The bin with the second highest significance is the bin, which contains all transcripts playing a role in secondary metabolism (312 transcripts). There are 890 transcripts involved in signaling, 670 transcripts assigned to bin 26, which contains miscellaneous biological functions and 398 transcripts assigned to the development bin. All three bins show a p-value in the 1E-10 range. 148 transcripts are involved in photosynthesis (p= 1,92E-08) and 1406 in RNA-related biological functions (p= 9,15E-08). There are 254 transcripts that play a role in cell wall and 352 transcripts being assigned to hormone metabolism. Bins containing transcripts involved in DNA, Metal Handling, Stress, are not assigned to any other biological function, lipid metabolism and N-metabolism display a p-value higher than 1E-2.

After comparing the transcripts in mature ovules and pollen tubes, it should be investigated, which transcripts are effected in the ovule during the course of fertilization. Therefore, the tissues mature ovule and ovules of flowers, which have been pollinated were compared and a differential gene analysis was performed. The resulting transcripts (Log2FoldChange was ≥ 1) were assigned to MapMan bins. First the transcripts upregulated in the mature ovule (non-pollinated) were analyzed.

Table 12: Association of differentially expressed transcripts higher expressed in mature ovules (OV) than in ovules of pollinated flowers (OVP) to MapMan bins. The table displays the top 15 results of the 'overview' pathway sorted by p-value. Shown are bin number and name, the number of elements mapped to the bin and its p-value. The WilcoxRank sum test, corrected according to Benjamini Hochberg was used for further analysis. Colored in greys are the bins with a p-value < 1E-2.

Bin	Name	Elements	P-Value
31	Cell	82	1,24E-03
17	Hormone Metabolism	73	9,43E-02
26	Misc	100	1,98E-01
9	Mitochondrial Electron Transport / ATP Synthesis	3	3,77E-01
14	S-Assimilation	3	3,77E-01
35	Not Assigned	646	3,77E-01
29	Protein	162	3,88E-01
30	Signaling	81	5,15E-01
22	Polyamine Metabolism	3	5,83E-01
24	Biodegradation Of Xenobiotics	4	5,83E-01
4	Glycolysis	3	6,35E-01
7	OPP	1	6,35E-01
16	Secondary Metabolism	50	6,52E-01
6	Gluconeogenesis / Glyoxylate Cycle	1	6,66E-01
3	Minor CHO Metabolism	20	7,15E-01

Table 12 shows the top 15 results of the 'overview' pathway in MapMan analysis. The only bin with a p-value smaller than 1E-2 contains the 82 transcripts and is involved in cellular biological functions. All the other bins are less significant. There are 73 transcripts involved in hormone metabolism, 100 transcripts playing a role in miscellaneous biological functions, 3 transcripts related to mitochondrial electron transport and ATP synthesis, 3 transcripts for S assimilation and 646 transcripts that could not be assigned to any other bin. With a p-value less than or equal to 3,88E-01 are protein, signaling, polyamine metabolism, biodegradation of xenobiotics, glycolysis, OPP, secondary metabolism, gluconeogenesis / glyoxylate cycle and minor CHO metabolism.

When comparing the transcripts differentially expressed between mature ovules and ovules of flowers, which have been pollinated, it was then focused on the transcripts upregulated in the pollinated plants (Table 13). The transcripts of the differential expression analysis with a significance of Log2FoldChange of ≥ 1 were assigned to MapMan bins.

Table 13: Association of differentially expressed transcripts higher expressed in ovules of pollinated flowers (OVP) than in mature ovules (OV) to MapMan bins. The table displays the top 15 results of the 'overview' pathway sorted by p-value. Shown are bin number and name, the number of elements mapped to the bin and its p-value. The WilcoxRank sum test, corrected according to Benjamini Hochberg was used for further analysis. Colored in greys are the bins with a p-value < 1E-2.

Bin	Name	Elements	P-Value
20	Stress	44	1,15E-08
1	PS	23	3,38E-06
13	Amino Acid Metabolism	20	5,98E-06
26	Misc	78	6,33E-06
34	Transport	55	9,23E-06
16	Secondary Metabolism	45	2,39E-05
17	Hormone Metabolism	48	3,20E-05
10	Cell Wall	50	1,84E-04
31	Cell	18	7,81E-04
11	Lipid Metabolism	25	4,39E-03
27	RNA	123	4,47E-03
21	Redox	10	4,95E-03
4	Glycolysis	7	6,40E-03
33	Development	27	1,00E-02
30	Signaling	85	1,11E-01

The above shown table displays the top 15 results of the 'overview' pathway, when performing a MapMan analysis. The results are sorted by p-value and it could be shown that the bin with the highest significance is bin 20, containing stress-related transcripts (44). Four bins (biological functions related to photosynthesis, amino acid

metabolism, miscellaneous functions and transport) show a p-value in the 1E-6 range and contain combined 176 transcripts. There are 45 transcripts assigned to secondary metabolism and 48 transcripts to hormone metabolism. With a p-value in the 1E-4 range there were 50 transcripts assigned to biological functions regarding the cell wall and 18 regarding the cell. 25 transcripts are lipid metabolism related, 123 transcripts RNA related, 10 transcripts redox related and 7 transcripts related to glycolysis. Bins 33 and 30 for biological functions regarding development and signaling show a p-value of 1E-2 or higher.

After pollination of the flower, fertilization takes place. In order to continue identifying processes involved in the fertilization process, it was of interest, which transcripts are upregulated in this last step. Therefore, a differential expression analysis was performed and the resulting transcripts with a Log2FoldChange of ≥ 1 were assigned to MapMan bins (Table 14).

Table 14: Association of differentially expressed transcripts higher expressed in ovules of fertilized flowers (OVF) than in ovules of pollinated flowers (OVP) to MapMan bins. The table displays the top 15 results of the 'overview' pathway sorted by p-value. Shown are bin number and name, the number of elements mapped to the bin and its p-value. The WilcoxRank sum test, corrected according to Benjamini Hochberg was used for further analysis. Colored in greys are the bins with a p-value < 1E-2.

Bin	Name	Elements	P-Value
29	Protein	30	2,94E-01
16	Secondary Metabolism	10	2,94E-01
10	Cell Wall	14	3,06E-01
13	Amino Acid Metabolism	4	3,44E-01
26	Misc	43	4,94E-01
2	Major CHO Metabolism	3	4,94E-01
5	Fermentation	1	4,94E-01
20	Stress	20	5,97E-01
30	Signaling	15	6,17E-01
33	Development	8	7,28E-01
28	DNA	1	7,36E-01
17	Hormone Metabolism	24	8,02E-01
34	Transport	21	8,35E-01
24	Biodegradation Of Xenobiotics	1	8,96E-01
23	Nucleotide Metabolism	1	9,42E-01

Table 14 displays the results of the 'overview' pathway and the 15 MapMan bins with the highest significance. All bins show a p-value higher than 1E-2. There are 30 transcripts assigned to the protein bin, 10 transcripts assigned to secondary metabolism, 14 transcripts assigned to the cell wall bin and 4 transcripts assigned to secondary metabolism. 43 transcripts are related to miscellaneous biological functions, 3 to major CHO metabolism, 1 to related to fermentation and 20 to stress. With a p-value of 6,17E-01 15 transcripts play a role in signaling, while 8 are related to development and 1 related to DNA. 24 transcripts were assigned to bin 17, which contains the transcripts related to hormone metabolism and 21 transcripts assigned to

bin 34 containing transport related transcript. Each 1 transcript was assigned to biodegradation of xenobiotics and nucleotide metabolism.

3.2.6 Identification of CRPs

Recent work on pollen-tube guidance revealed that DEFLs, a subgroup of the cysteine-rich proteins (CRPs), play a prominent role in attracting the growing pollen towards the ovule (micropylar guidance). Having the transcriptomic data in our hand, we aimed to identify the CRPs expressed in tobacco during the different stages of the fertilization process. We based our data analyses on previously performed research (Silverstein, Moskal et al. 2007, Huang, Dresselhaus et al. 2015), in which Hidden Markov Models were built to identify CRPs in plants (Silverstein, Moskal et al. 2007) and used to identify CRPs in rice (Huang, Dresselhaus et al. 2015).

In order to analyze the obtained data from the transcriptome analysis, Hidden Markov Models were used to identify the CRP classes and tools hmmbuild, hmmscan and hmmsearch from http://hmmer.org/ were used in order to further analyze the data for retrieving CRPs. A total number of 953 CRPs were identified and sorted to the CRP class they belong (see Table 19). The classes were then gathered into groups depending on their characteristic cysteine motifs and matched to previously known proteins.

An aim of this work was to identify the CRP, which provokes pollen tube attraction towards the ovule in *Nicotiana tabacum*. Because the pollen tube attractant in *Arabidopsis thaliana*, AtLURE1.2, belongs to the DEFLs, this work focuses on the DEFLs found in the transcriptome data. A subset of Table 19, is displayed in Table 15, where only the Defensins/ DEFLs are listed. It could be shown that a total number of 116 Defensins/ DEFLs were found, which belong to 36 CRP classes.

Table 15: Overview about identified Defensin/ DEFL transcripts from transcriptome data

Transcript ID	CRP class	CRP description
TRINITY_GG_49624_c0_g1	CRP0020	Defensin/DEFL
TRINITY_GG_96432_c0_g1	CRP0020	Defensin/DEFL
TRINITY_GG_74342_c0_g1	CRP0020	Defensin/DEFL
TRINITY_GG_107409_c0_g1	CRP0030	Defensin/DEFL
TRINITY_GG_144472_c0_g2	CRP0030	Defensin/DEFL
TRINITY_GG_53571_c2_g1	CRP0030	Defensin/DEFL
TRINITY_GG_61150_c0_g1	CRP0030	Defensin/DEFL
TRINITY_GG_75926_c0_g1	CRP0040	Defensin/DEFL
TRINITY_GG_94414_c1_g1	CRP0050	Defensin/DEFL
TRINITY_GG_70101_c0_g2	CRP0050	Defensin/DEFL
TRINITY_GG_140127_c0_g1	CRP0050	Defensin/DEFL
TRINITY_GG_102990_c6_g1	CRP0050	Defensin/DEFL
TRINITY_GG_29284_c0_g1	CRP0060	Defensin/DEFL
TRINITY_GG_29284_c0_g2	CRP0060	Defensin/DEFL
TRINITY_GG_6520_c0_g1	CRP0080	Defensin/DEFL

TRINITY_GG_23841_c0_g1	CRP0080	Defensin/DEFL
TRINITY_GG_6519_c0_g1	CRP0080	Defensin/DEFL
TRINITY_GG_9018_c1_g1	CRP0080	Defensin/DEFL
TRINITY_GG_5432_c0_g1	CRP0080	Defensin/DEFL
TRINITY_GG_50531_c2_g1	CRP0080	Defensin/DEFL
TRINITY_GG_96436_c0_g1	CRP0080	Defensin/DEFL
TRINITY_GG_2075_c1_g1	CRP0080	Defensin/DEFL
TRINITY_GG_6516_c2_g1	CRP0080	Defensin/DEFL
TRINITY_GG_46443_c4_g1	CRP0090	Defensin/DEFL
TRINITY_GG_102990_c6_g2	CRP0090	Defensin/DEFL
TRINITY_GG_43051_c0_g1	CRP0120	Defensin/DEFL
TRINITY_GG_135525_c2_g1	CRP0120	Defensin/DEFL
TRINITY_GG_9476_c0_g2	CRP0130	Defensin/DEFL
TRINITY_GG_78671_c1_g1	CRP0130	Defensin/DEFL
TRINITY_GG_71617_c0_g2	CRP0130	Defensin/DEFL
TRINITY_GG_9476_c0_g1	CRP0130	Defensin/DEFL
TRINITY_GG_49437_c0_g1	CRP0130	Defensin/DEFL
TRINITY_GG_49437_c0_g2	CRP0130	Defensin/DEFL
TRINITY_GG_71617_c0_g1	CRP0130	Defensin/DEFL
TRINITY_GG_47031_c0_g1	CRP0220	Defensin/DEFL
TRINITY_GG_104337_c0_g1	CRP0220	Defensin/DEFL
TRINITY_GG_140477_c0_g1	CRP0220	Defensin/DEFL
TRINITY_GG_135373_c0_g2	CRP0220	Defensin/DEFL
TRINITY_GG_79593_c0_g1	CRP0300	Defensin/DEFL
TRINITY_GG_69155_c0_g1	CRP0300	Defensin/DEFL
TRINITY_GG_46996_c3_g1	CRP0300	Defensin/DEFL
TRINITY_GG_46996_c0_g1	CRP0300	Defensin/DEFL
TRINITY_GG_18954_c0_g2	CRP0300	Defensin/DEFL
TRINITY_GG_92727_c0_g1	CRP0300	Defensin/DEFL
TRINITY_GG_18954_c0_g1	CRP0300	Defensin/DEFL
TRINITY_GG_32707_c3_g1	CRP0300	Defensin/DEFL
TRINITY_GG_136007_c0_g1	CRP0300	Defensin/DEFL
TRINITY_GG_136007_c0_g2	CRP0300	Defensin/DEFL
TRINITY_GG_107419_c12_g1	CRP0310	Defensin/DEFL
TRINITY_GG_117309_c0_g1	CRP0320	Defensin/DEFL
TRINITY_GG_45480_c0_g2	CRP0360	Defensin/DEFL
TRINITY_GG_110558_c0_g1	CRP0360	Defensin/DEFL
TRINITY_GG_6516_c1_g1	CRP0460	Defensin/DEFL
TRINITY_GG_1955_c1_g1	CRP0460	Defensin/DEFL
TRINITY_GG_119879_c0_g1	CRP0560	Defensin/DEFL
TRINITY_GG_134027_c0_g1	CRP0560	Defensin/DEFL
TRINITY_GG_104312_c0_g3	CRP0560	Defensin/DEFL
TRINITY_GG_104312_c0_g2	CRP0560	Defensin/DEFL
TRINITY_GG_104312_c0_g1	CRP0560	Defensin/DEFL
TRINITY_GG_62342_c0_g1	CRP0570	Defensin/DEFL
TRINITY_GG_127378_c9_g1	CRP0620	Defensin/DEFL
TRINITY_GG_101737_c0_g1	CRP0620	Defensin/DEFL
TRINITY_GG_101727_c0_g1	CRP0620	Defensin/DEFL
TRINITY_GG_101734_c0_g1	CRP0620	Defensin/DEFL
TRINITY_GG_129413_c0_g1	CRP0620	Defensin/DEFL
TRINITY_GG_126102_c0_g1	CRP0670	Defensin/DEFL
TRINITY_GG_118340_c7_g1	CRP0670	Defensin/DEFL
TRINITY_GG_118340_c7_g2	CRP0675	Defensin/DEFL
TRINITY_GG_145706_c0_g2	CRP0730	Defensin/DEFL
TRINITY_GG_133550_c0_g1	CRP0860	Defensin/DEFL
TRINITY_GG_4530_c0_g1	CRP0860	Defensin/DEFL
TRINITY_GG_143817_c0_g1	CRP0880	Defensin/DEFL
TRINITY_GG_16251_c0_g1	CRP0960	Defensin/DEFL
TRINITY_GG_73835_c0_g3	CRP1004	Defensin/DEFL
TRINITY_GG_73835_c0_g2	CRP1004	Defensin/DEFL
TRINITY_GG_97807_c0_g1	CRP1004	Defensin/DEFL
TRINITY_GG_127546_c0_g1	CRP1006	Defensin/DEFL
TRINITY_GG_144717_c0_g1	CRP1006	Defensin/DEFL
TRINITY_GG_139821_c0_g1	CRP1006	Defensin/DEFL
TRINITY_GG_134979_c0_g1	CRP1006	Defensin/DEFL
TRINITY_GG_40208_c4_g1	CRP1006	Defensin/DEFL
TRINITY_GG_35829_c0_g1	CRP1006	Defensin/DEFL
TRINITY_GG_82958_c0_g1	CRP1006	Defensin/DEFL
TRINITY_GG_29436_c0_g1	CRP1008	Defensin/DEFL
TRINITY_GG_29464_c31_g1	CRP1008	Defensin/DEFL
TRINITY_GG_117316_c0_g1	CRP1010	Defensin/DEFL
TRINITY_GG_46064_c2_g1	CRP1010	Defensin/DEFL
TRINITY_GG_102202_c0_g1	CRP1010	Defensin/DEFL
TRINITY_GG_102202_c0_g2	CRP1010	Defensin/DEFL
TRINITY_GG_47038_c1_g2	CRP1010	Defensin/DEFL
TRINITY_GG_117064_c16_g1	CRP1010	Defensin/DEFL
TRINITY_GG_38281_c0_g1	CRP1010	Defensin/DEFL
TRINITY_GG_52151_c0_g1	CRP1010	Defensin/DEFL
TRINITY_GG_47038_c1_g1	CRP1010	Defensin/DEFL
TRINITY_GG_40208_c6_g1	CRP1015	Defensin/DEFL
TRINITY_GG_39318_c0_g1	CRP1015	Defensin/DEFL
TRINITY_GG_122872_c0_g1	CRP1015	Defensin/DEFL
TRINITY_GG_55548_c0_g1	CRP1015	Defensin/DEFL
TRINITY_GG_50696_c10_g1	CRP1025	Defensin/DEFL
TRINITY_GG_127777_c3_g1	CRP1025	Defensin/DEFL
TRINITY_GG_31166_c0_g1	CRP1025	Defensin/DEFL
TRINITY_GG_44581_c0_g1	CRP1025	Defensin/DEFL
TRINITY_GG_81852_c0_g1	CRP1030	Defensin/DEFL
TRINITY_GG_29437_c0_g1	CRP1030	Defensin/DEFL
TRINITY_GG_79003_c21_g1	CRP1100	Defensin/DEFL
TRINITY_GG_79003_c19_g1	CRP1100	Defensin/DEFL
TRINITY_GG_76239_c0_g1	CRP1110	Defensin/DEFL
TRINITY_GG_76236_c0_g2	CRP1110	Defensin/DEFL
TRINITY_GG_118171_c2_g1	CRP1110	Defensin/DEFL
TRINITY_GG_76233_c1_g1	CRP1110	Defensin/DEFL
TRINITY_GG_76224_c0_g2	CRP1110	Defensin/DEFL
TRINITY_GG_142728_c0_g1	CRP1140	Defensin/DEFL
TRINITY_GG_92887_c12_g1	CRP1150	Defensin/DEFL
TRINITY_GG_79003_c32_g1	CRP1150	Defensin/DEFL
TRINITY_GG_65569_c1_g1	CRP1190	Defensin/DEFL
TRINITY_GG_79003_c4_g1	CRP1250	Defensin/DEFL

3.3 Expression analysis

3.3.1 Differential expression of DEFLs

After identification of CRPs and DEFLs from the sequenced data, a closer look was taken into the differential expression of the found DEFLs among the examined tissue samples. Therefore, it was analyzed whether the expression of a DEFL transcript was up regulated, down regulated or if there was no significant change in expression between two tissue samples. In Figure 8 these results are plotted. Niklas Terhoeven performed data analysis and designing of the plot.

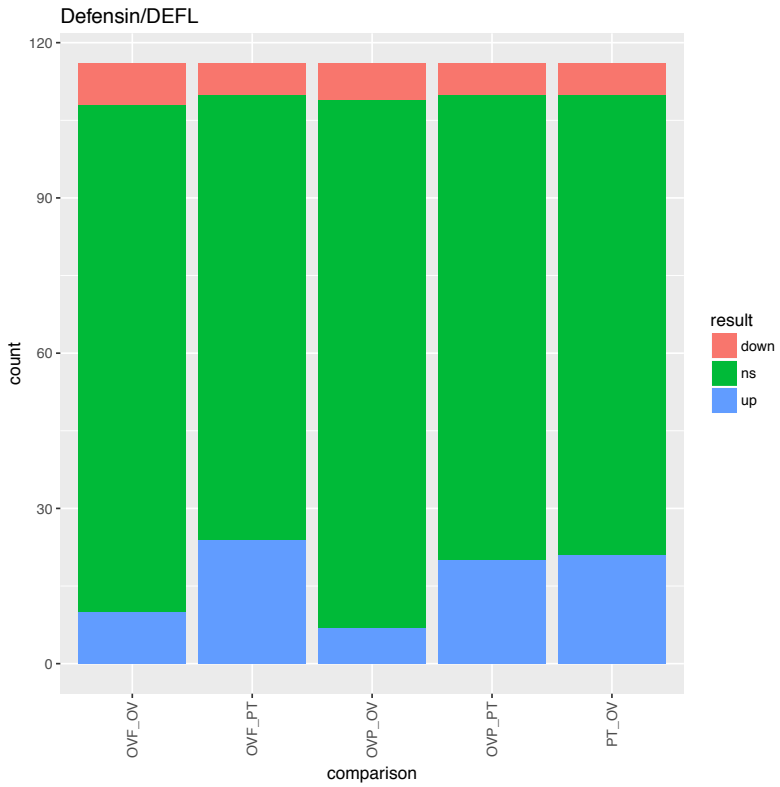

Figure 8: Change in DEFL expression in different tissues at several time points throughout the fertilization process in *Nicotiana tabacum*.
Comparison of number of DEFLs being up regulated, down regulated or with no significant change between two samples (OVF vs OV, OVF vs PT, OVP vs OV, OVP vs PT, PT vs OV).

In Figure 8 the relation between the samples taken during the fertilization process in *Nicotiana tabacum* is shown regarding the expression of DEFLs. It can be observed that between the samples the majority of DEFL transcripts are not significantly up- or downregulated. There is always a number of 5 to 10 DEFLs being down regulated between two samples, although the number of down regulated DEFLs is higher when comparing an ovule sample to the pollen tube sample than when comparing two ovule samples of different time points with each other.

A clearer difference in DEFL expression could be noticed when looking at the upregulated transcripts. A comparison between the DEFLs in OVP and OV reveals that around 5% of the transcripts are up regulated, while between OVF and OV around 9% are up regulated. When comparing an ovule sample to the pollen tube sample, the data displayed in Figure 8 shows that around 20% of the DEFL transcripts are significantly higher expressed in the ovule sample than in the pollen tube.

3.3.2 Identification and differential expression of candidate DEFLs

After the identification of *Nicotiana tabacum* SR1 CRPs and DEFLs, candidate genes for a further analysis were chosen. In order to take a closer look at a diverse group of genes, four ovule-specific genes were chosen, all of them DEFLs. Two of these candidates showed to be down regulated after pollination and fertilization: TRINITY_GG_136007_c0_g1 (Nt136007) and TRINITY_GG_46443_c1_g1 (Nt46443) and two genes that seem to be up regulated after pollination and fertilization: TRINITY_GG_47038_c1_g2 (Nt47038) and TRINITY_GG_79003_c21_g1 (Nt79003). Because the transcriptome data did not reveal any DEFLs, which were highly expressed in pollen tubes, two additional genes belonging to Pollen Ole e 1 allergen and extensin family were chosen to be analyzed in more detail: TRINITY_GG_54117_c1_g1 (Nt54117) and TRINITY_GG_22095_c1_g1 (Nt22095).

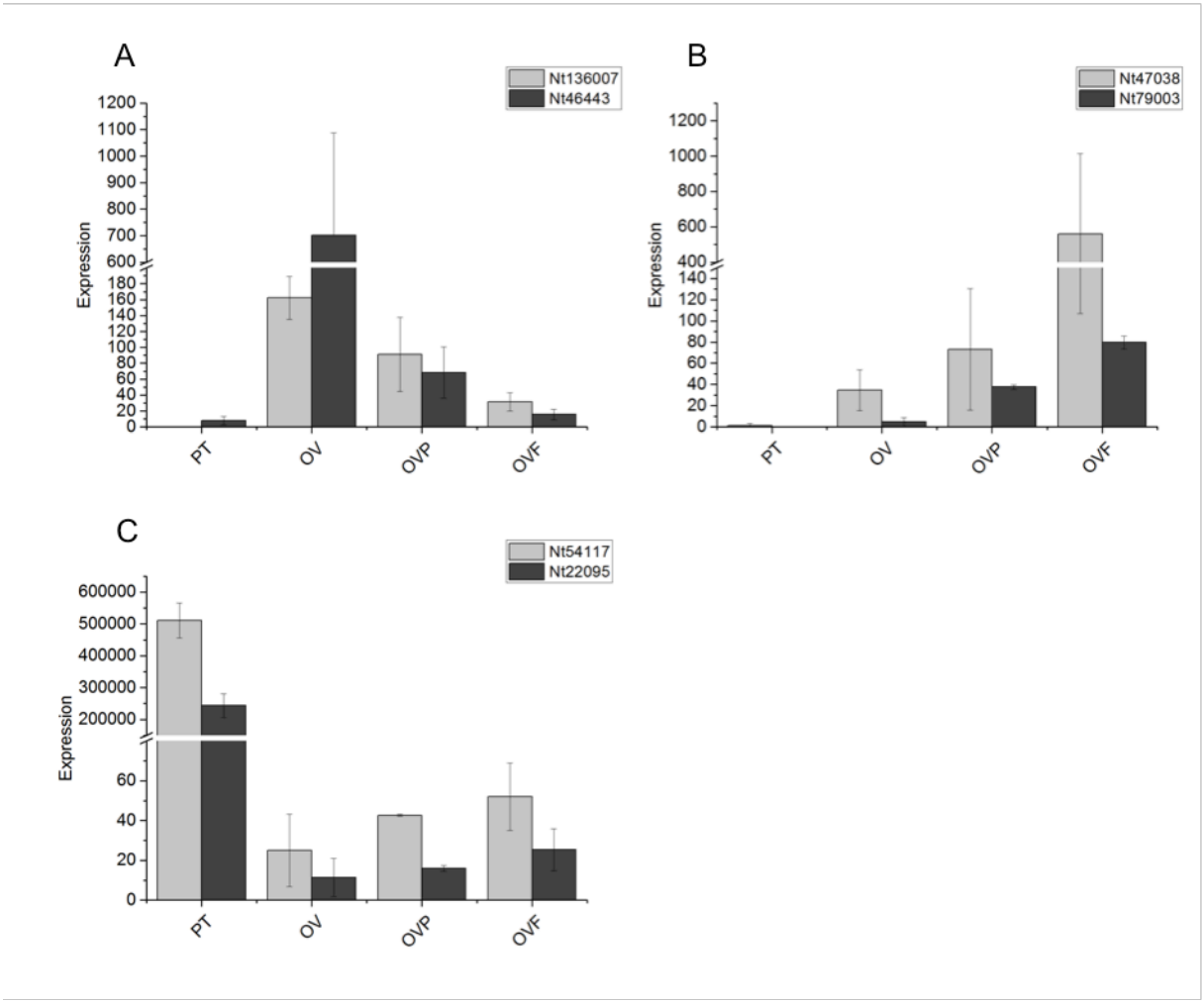

Figure 9: Expression levels of candidate genes from transcriptome data.

(A) Transcriptomic expression levels obtained from the transcriptome browser TBro (Ankenbrand, Weber et al. 2016) of the unigenes TRINITY_GG_136007_c0_g1 (Nt136007) and TRINITY_GG_46443_c1_g1 (Nt46443); (B) Transcriptomic expression of the unigenes TRINITY_GG_47038_c1_g2 (Nt47038) and TRINITY_GG_79003_c21_g1 (Nt79003); (C) Transcriptomic expression levels of the unigenes TRINITY_GG_54117_c1_g1 (Nt54117) and TRINITY_GG_22095_c1_g1 (Nt22095); n= 3

Figure 9 displays the expression data obtained from the RNA-sequencing experiment. Genes Nt136007, Nt46443, Nt47038 as well as Nt79003 show almost no expression in the pollen tubes. For Nt136007 and Nt46443 the highest expression could be detected in the non-pollinated ovule samples (162.2; 701.4) with a decrease in expression after pollination (91.3; 68.3) and fertilization (31.7; 15.7). A reverse trend in expression could be observed e.g. in Nt47038 and Nt79003. Both genes are relatively low expressed in mature ovules (34.6; 4.8) but strongly increase after pollination (73.0; 37.7) and

fertilization (560.3; 79.7). Between pollination and fertilization the expression of Nt47038 increases 7.6 times.

In contrast to the four genes displayed in Figure 9 (A) and (B) the expression of genes Nt54117 and Nt22095 is distributed almost exclusively in the pollen tube samples. Nt54117 shows an expression of 510,664, while Nt22095 displays an expression of 243,268. Both genes are almost not expressed in the ovule samples, maintaining about the same expression levels in mature ovules, after pollination and fertilization. The expression in the pollen tubes is 12,800 times higher in pollen tubes than in the averaged ovules samples for Nt54117 and 13,800 times higher for Nt22095.

3.3.3 Expression analysis in RNA-sequencing libraries

In order to confirm the results obtained from RNA-sequencing experiments, qPCR experiments were performed. Therefore six genes of interest were chosen and the *in-vivo* expression was compared to the *in-silico* obtained expression values from RNA-sequencing (Figure 9). The libraries from RNA-sequencing (2.6) were diluted 1:20 and specific primers (5.3) for the chosen genes (Nt136007, Nt46443, Nt47038, Nt79003, Nt54117, Nt22095) were used for qPCR.

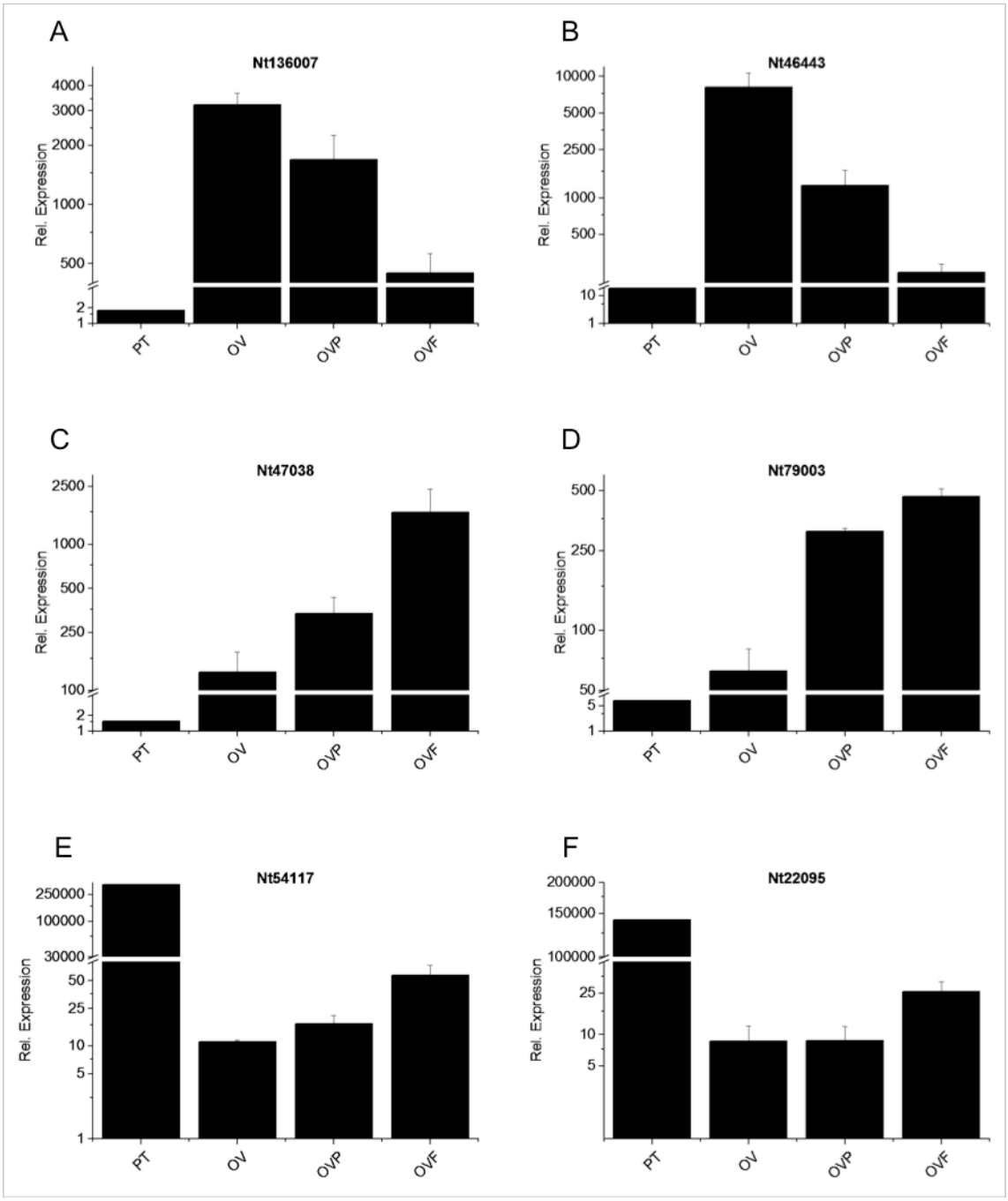

Figure 10: Relative expression levels of candidate genes in pollen tubes and ovules.
(A-F) shows the expression of candidate genes in relation to 10,000 molecules of NtActin in pollen tubes and ovules of mature (OV), pollinated (OVP) and fertilized (OVF) flowers. (A): Nt136007; (B): Nt46443; (C): Nt47038; (D): Nt79003; (E): Nt54117; (F): Nt22095; PT: n= 2, OV, OVP, OVF: n=3; ± SE

In Figure 10 the expression of candidate genes in relation to 10,000 molecules of NtActin is shown. The genes investigated in (A-D) (Nt136007, Nt46443, Nt47038 and Nt79003) have very little expression in the pollen tube samples (1.8; 18.1; 1.6; 6.9

molecules/ 10,000 NtActin). (A): Nt136007 showed the highest expression in mature ovules (OV; 3220.1). After pollination (OVP; 1694.6) and fertilization (OVF; 449.6) the expression decreases. The *in-vivo* expression shows the same trend as the RNA-sequencing data. In (B) the highest Nt46443 expression could be obtained in mature ovules (OV; 8179.5), while after pollination (OVP; 1260.8) and fertilization (OVF; 244.1) the expression decreases. This expression profile could also be observed in the RNA-sequencing data. In (C) and (D) the gene expression of Nt47038 and Nt79003 shows a different pattern, as the expression levels increase after pollination and fertilization. In Nt47038 the molecules/ 10,000 NtActin increase 12.4 times between mature ovules and fertilized ovules. In these tissues the expression in Nt79003 increases times 7.5. The expression levels of Nt47038 and Nt79003 showed the same pattern as in the RNA-sequencing data.

Figure 10 (E) and (F) display a completely different expression pattern than the genes investigated in Figure 10 (A-D). Nt54117 as well as Nt22095 show a very high expression in the pollen tube samples (346,108.0; 141,053.8 molecules/ 10,000 NtActin), while being very low expressed in the ovule samples. The expression of Nt54117 is 12,200 times higher in the pollen tubes than in the averaged ovule samples and in Nt22095 9,900 times higher. It can be concluded that the relative expression data obtained from qPCR experiments (Figure 10) verify the results from RNA-sequencing (Figure 9).

3.3.4 Tissue specific expression analysis

The expression analysis via qPCR verified the data obtained from RNA-sequencing in the pollen tube and ovule samples that were investigated. In order to get further insights on the fertilization process of *Nicotiana tabacum* we investigated the expression of our candidate genes (Nt136007, Nt46443, Nt47038, Nt79003, Nt54117 and Nt22095) more specifically in different tissues involved in the process. New tissue samples were harvested from *in-vitro* grown pollen tubes, mature, but unpollinated flowers (OV), from flowers that had been pollinated but not yet fertilized (OVP) and from flowers where fertilization was assured (OVF). From each fertilization stage (OV, OVP, OVF) six flowers were harvested and separated into five tissue samples: the stigma, upper part of the style (style 1), the lower part of the style (style 2), ovules and

the placenta. RNA from the tissue samples was isolated as described in 2.1.1 and the quality was checked. Good quality RNAs were transcribed into cDNA and qPCR experiments were performed as described in 2.2.1. In order to confirm the results, two technical replicated were prepared, the results were normalized to expression of mature ovules (OV) and their expression was set to one. Statistical analysis was performed as described in 2.2.1.2.

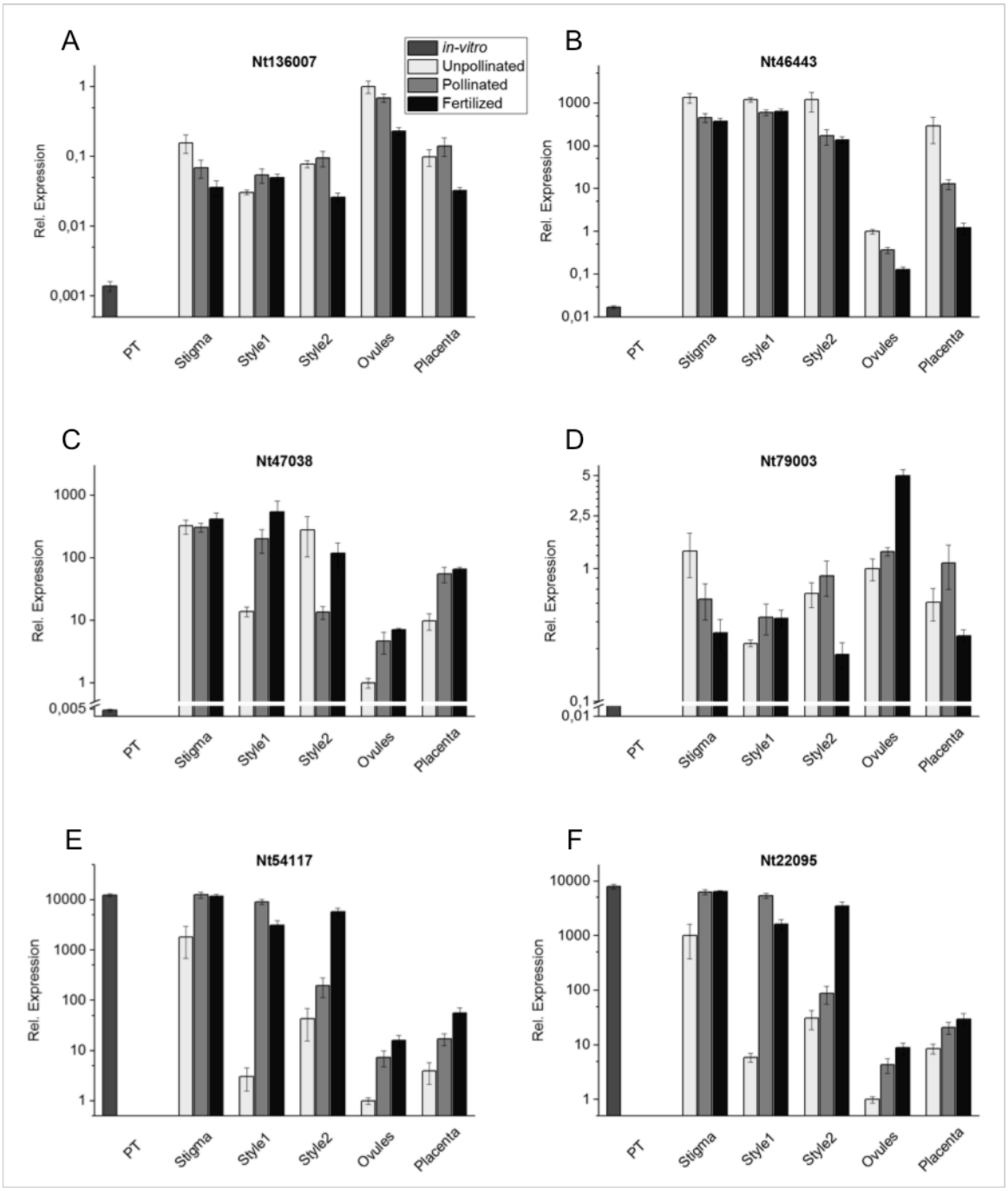

Figure 11: Relative expression levels of candidate genes in different tissues involved in the fertilization process.

(A-F) shows the expression of candidate genes in relation to 10,000 molecules of NtActin in stigma, style 1, style 2, ovules and placenta of mature flowers (OV) and flowers that had been pollinated (OVP) or fertilized (OVF). (A): Nt136007; (B): Nt46443; (C): Nt47038; (D): Nt79003; (E): Nt54117; (F): Nt22095; OV Style 2: n=6, OVF Stigma; OV Style 1; OVF Style 1; OVP Style 2; OV Placenta; OVP Placenta: n=8; OVP Stigma, OV Ovules; OVP Ovules; OVF Ovules; OVF Placenta: n=10; OV Stigma; OVP Style 1: n= 12; ± SE

Table 16: Overview about the significances obtained from qPCR experiments (Figure 11).
Significances obtained from qPCR data of stigma, style 1, style 2, ovules and placenta investigated for the expression of the following genes: Nt136007, Nt46443, Nt47038, Nt79003, Nt54117 and Nt22095 in pollinated (light grey) and fertilized (dark grey) flowers in comparison to mature ovules. A Student's t-test was performed on the data and a multiple testing correction was performed according to Bonferroni (Bonferroni 1936). (* = p ≤ 0.05; **= p ≤ 0.005; ***= p ≤ 0.0005)

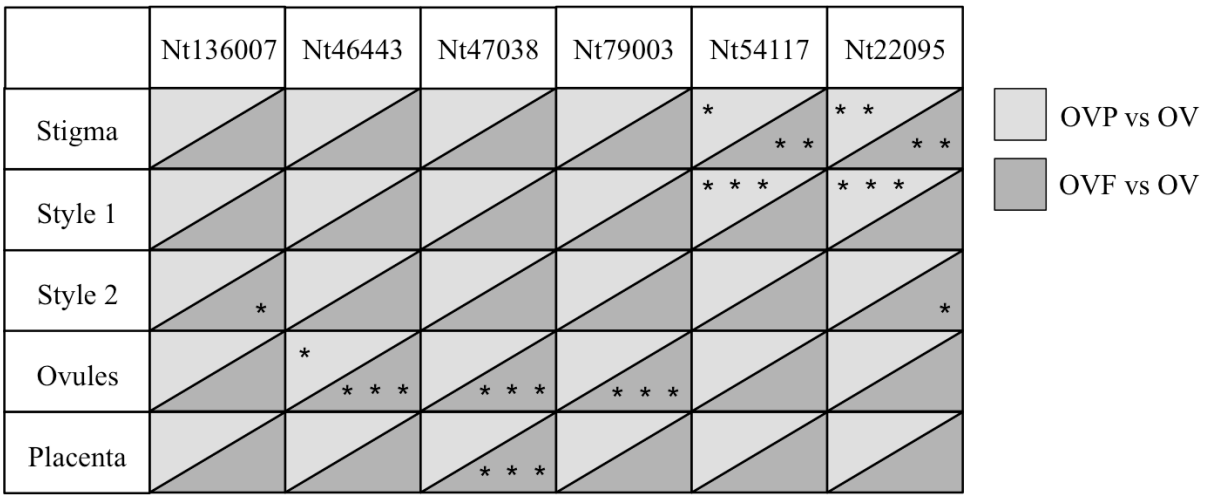

Figure 11 shows the expression of candidate genes (Nt136007, Nt46443, Nt47038, Nt79003, Nt54117 and Nt22095) in different tissues involved in the fertilization process of *Nicotiana tabacum*. The relative expression is plotted against the tissue investigated (pollen tubes, stigma, style 1, style 2, ovules and placenta). In order to analyze the obtained data statistically a Student's t-test was performed and to counteract the problem of multiple comparisons and the therefore resulting type I errors (false positives) a Bonferroni correction of the data was done. The results of the statistical analysis are displayed in Table 16.

In Figure 11 (A) the relative expression of Nt136007 in different tissues and three time points in fertilization is shown. The expression in pollen tubes is very low (0.014) in comparison to the Nt136007 expression in ovules. The highest expression could be detected in mature ovules of non-pollinated flowers (OV ovules) with an expression of 1. A non-significant decreasing expression level after pollination and fertilization could be shown in ovules, verifying the data obtained in RNA sequencing (Figure 9) and previous qPCR analysis (Figure 10). In all flower tissue samples the expression level of Nt136007 shows only a slight alteration between non-pollinated and pollinated plants.

Between non-pollinated and fertilized flowers a stronger change in expression level could be observed. In all flower tissue samples, except for style 1, a decrease in expression was detected, although a significant decrease could only be observed in style 2 (Bonferroni corrected p-value = 0.087).

In Figure 11 (B) the expression of Nt46443 in different tissues was investigated. In pollen tubes a clearly lower expression level was obtained in comparison to the expression in the female flower parts (stigma, style 1, style 2, ovules, placenta). In all female flower parts a decrease in Nt46443 expression after pollination and fertilization was observed. In stigma, style 1 and style 2 the strongest expression could be shown (1335.3; 1212.9; 1167.2). In the same tissues the expression decreased non-significantly after pollination and maintained about the same level between pollination and fertilization. In ovules and placenta a decreasing expression could be observed after pollination and fertilization, although the change in expression was not significant. A significant (p= 0.0321) decrease was detected in ovules after pollination and a highly significant decrease (p= 0.0003) after fertilization. This data shows the same tendency in Nt46443 expression as observed in the RNA-sequencing data (Figure 9) and the previous qPCR analysis (Figure 10).

The expression levels of Nt47038 in pollen tubes, stigma, style 1, style 2, ovules and placenta were investigated in Figure 11 (C). The expression in the pollen tube samples was very low in comparison to the expression in the other tissues. While in stigma, style 1 and style 2 no significant changes could be observed after pollination and fertilization of the tobacco plants, a stronger change was detected in ovules and placenta. After pollination the expression in the ovules showed a 4.6-fold increase and between non-pollinated and fertilized a 7-fold increase (p= 3.39 E-9), a trend also observed in the RNA-sequencing data (Figure 9) as well as in the previously performed qPCR analysis (Figure 10). In the placenta the expression of Nt47038 increased from non-pollinated to pollinated plants from 9.87 to 55.16 (5.6-fold increase) and from non-pollinated to fertilized up to 65.10 (6.6-fold increase, p= 0.0002).

In Figure 11 (D) the changes in expression of Nt79003 were analyzed. As also observed in Figure 11 (A-C) the expression of this gene is very low in the pollen tube samples. A higher expression could be shown in all female flower parts analyzed. No significant

changes in the expression level in stigma, style 1, style 2 and placenta were detected. The expression of Nt79003 in ovules on the other hand shows the same tendency as previously observed in RNA-sequencing (Figure 9) and qPCR (Figure 10). From non-pollinated to pollinated plants the expression shows a 1.35-fold increase and from non-pollinated to fertilized plants a significant (p= 0.0002) 5.01-fold expression change could be detected.

While in Figure 11 (A-D) genes mainly expressed in the female flower parts were investigated, Figure 11 (E) showed a different pattern. The highest expression of Nt54117 was detected in pollen tubes with a relative expression of 12,323. When the tissue samples of pollinated plants were collected, the flowers were pollinated and the samples were harvested after the pollen tubes had grown about half way through the style. Therefore it is plausible that an elevated Nt54117 expression would be detected in stigma and style 1 of pollinated plants as they contain growing pollen tubes. In the stigma the Nt54117 expression increased significantly (p= 0.0067) after pollination, as well as after fertilization (p= 0.0011). After pollination the expression increased significantly (p= 0.0003) 3000-fold. After fertilization the Nt54117 expression increased 1000-fold, although this increase was not significant. In the pollinated plants, the pollen tubes should have grown about half way through the style and should therefore be mainly contained in the style 1 but not in the style 2 samples. In the qPCR analysis an increase in expression in style 2 increased 5-fold after pollination. After fertilization the pollen tubes should have grown completely through the style. Therefore the strong increase of 135-fold was detected. In ovules and placenta a small increase in expression level of Nt54117 after pollination and a stronger increase after fertilization was shown. This data verifies the RNA-sequencing results (Figure 9) as well as the previously performed qPCR analysis (Figure 10).

Figure 11 (F) shows the relative expression of Nt22095 in pollen tubes and female tissue samples of the *Nicotiana tabacum* flower. The highest expression could be detected in pollen tubes (8040.3). In the stigma Nt22095 increased significantly after pollination (p= 0.0013) and fertilization (p= 0.0020), both 6.4-fold. The expression in style 1 increased 914-fold after pollination (p= 0.0001) and 273-fold after fertilization. As in the style 2 samples there would be only few pollen tubes expected after pollination, the

expression if Nt22095 only increased 3-fold. After fertilization the expression increases significantly (p= 0.042) 113-fold. In ovules and placenta the expression increases after fertilization, but not at a significant level and verifies the results obtained by RNA-sequencing (Figure 9) and previous qPCR analysis (Figure 10).

3.4 Expression of defensin-like proteins

An aim of this work was to identify the DEFL that provokes pollen tube attraction towards the ovule in *Nicotiana tabacum*. Using HMMER searches, 116 DEFLs were identified out of the sequenced transcriptome data. In order to find the attractant peptide, the expression levels of all identified DEFLs were analyzed at the different time points: mature ovules of non-pollinated plants (OV), ovules from pollinated flowers (OVP) and ovules from flowers in which double fertilization had occurred (OVF).

To narrow the number of candidate peptides down, the expression levels of all identified DEFLs were compared to the expression level of AtLURE1.2, the peptide that was identified to elicit pollen tube attraction in *Arabidopsis thaliana*. As shown by Huang et al. 2015 (Huang, Dresselhaus et al. 2015), high expression values of AtLURE1.2 were found in mature ovules, but with increasing time after pollination the expression decreases. In order to find the tobacco pollen tube attractant peptide, the total number of DEFLs was reduced to the peptides showing a similar expression pattern as AtLURE1.2. Finally, two candidate genes were selected: TRINITY_GG_136007_c0_g1 (Nt136007) and TRINITY_GG_46443_c4_g1 (Nt46443).

Both coding regions of the genes were amplified from NtOV cDNA, cloned into a modified pIVEX2.6 vector (5.5) and amplified in chemically competent *Escherichia coli* cells (MRF'). After DNA isolation, the constructs were expressed *in-vitro* with the PURExpress *In-Vitro* Protein Synthesis Kit. The synthesized peptides were purified according to the kit's manufacturers specification. Expression of the peptides (Nt136007 and Nt46443) was verified on a dot blot by detecting the FLAG-tag attached to the expressed peptides together with a negative control. The samples were applied on a nitrocellulose membrane. The primary antibody (mouse anti-FLAG) attached to the FLAG-tag of the expressed peptides, while the secondary antibody (anti-mouse

IgG, HRP-linked) bound the first antibody. Incubation with ECL reagent provoked a chemiluminescent signal, which was detected by a CCD camera (Figure 12).

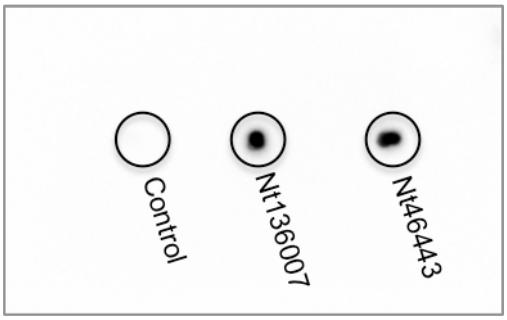

Figure 12: Dot Blot of peptides Nt136007, Nt46443 expressed *in-vitro* and negative control.

Figure 12 displays a dot blot of *in-vitro* expressed Nt136007 and Nt46443 peptides, as well as a negative control. The positive detection of Nt136007 and Nt46443 peptides indicates that *in-vitro* expression could have been successful. It proves that the attached FLAG-tag of the peptides was transcribed with the PURExpress system and therefore it is very probable that the attached peptides were also transcribed successfully. The positive dot blot signals do not give information about folding of the peptides and because of the small amount of expressed peptides a serial dilution for an estimation of quantity was also not possible. In order to test their biological role *in-vivo*, attraction assays were performed. Therefore the expressed peptides Nt136007 and Nt46443 were applied on *in-vitro* grown *Nicotiana tabacum* pollen tubes and growth performance was monitored.

3.5 *In-vitro* attraction assays

3.5.1 *In-vitro* attraction assay of Nt pollen tubes and ovules

Before the expressed peptides of Nt136007 and Nt46443 could be tested for their role *in-vivo*, the experimental setup had to be verified. Attraction assays with growing *Nicotiana tabacum* pollen tubes were performed with whole WT ovules to lure the pollen tubes.

Pollen of *Nicotiana tabacum* SR1 plants were applied on solid NtPGM (5.2) and grown in humid chambers for about 4 h at room temperature as described in 2.8.4.1. Whole

ovules were dissected from mature but unpollinated WT flowers using a gauge needle and immediately placed in front of the growing pollen tubes. Bright field images were taken every 15 min for 3 h. Example images taken after 0 min (A), 90 min (B) and 180 min (C) are shown.

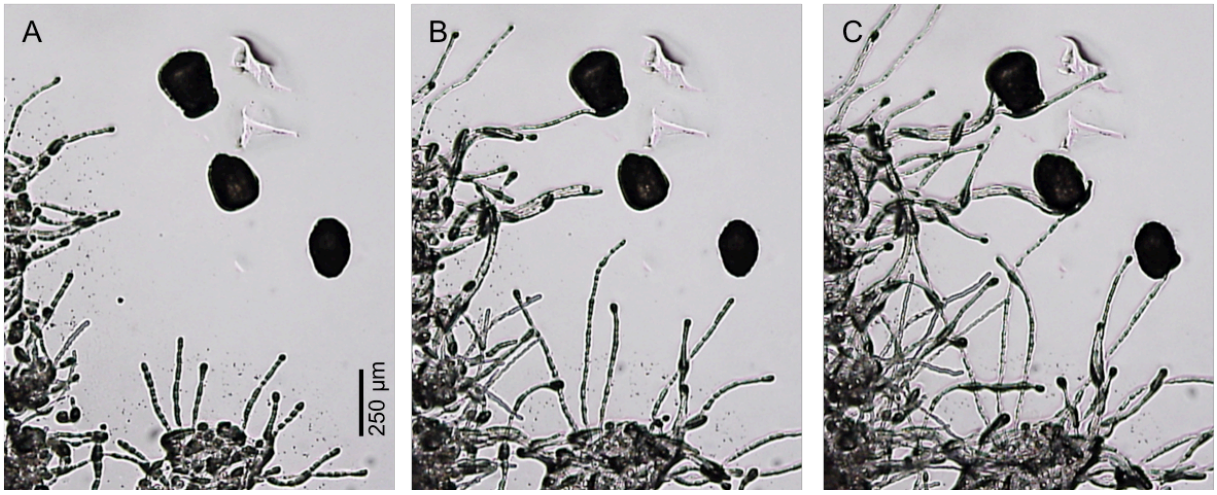

Figure 13: Attraction assay with *in-vitro* grown *Nicotiana tabacum* SR1 pollen tubes and WT mature ovules.
(A) Three mature whole ovules were placed in 200- 400 µm distance to *in-vitro* grown pollen tubes, which had been growing for about 4 h; 0 min after ovule placement. (B) 90 min after ovule placement. (C) 180 min after ovule placement; scale bar= 250 µm.

In Figure 13 an example attraction assay of *in-vitro* grown *Nicotiana tabacum* SR1 pollen tubes towards whole mature ovules is shown. (A) displays time point 0 min after placement of the ovules. Freshly dissected non-pollinated ovules from WT plants were placed in 200 to 400 µm distance to the pollen tubes. After 90 min (B) the pollen tubes have grown about 250 µm and many of the displayed pollen tubes appear to be growing towards one of the three the ovules. 180 min (C) after ovule placement several pollen tubes appear to be attracted by one of the ovules as they grow into close distance to it. Unfortunately it is not distinguishable whether a pollen tube only touches the ovule or whether it enters the ovule and may cause double fertilization to occur.

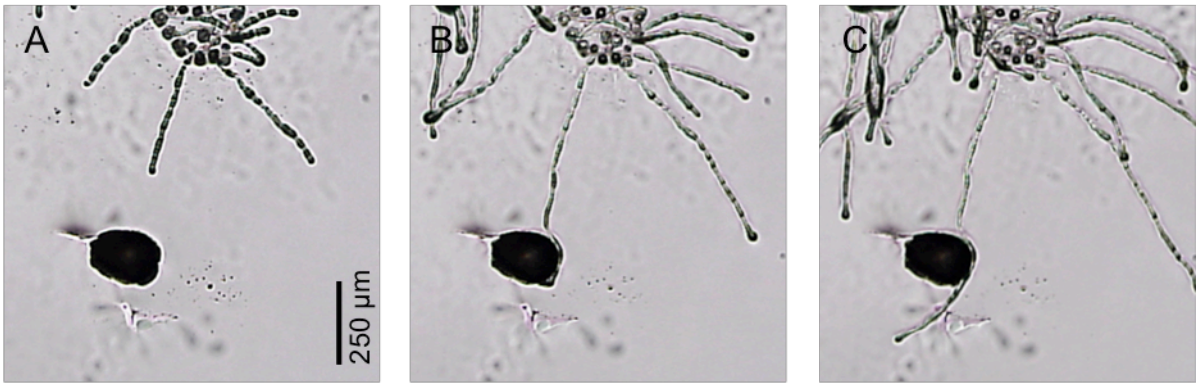

Figure 14: Attraction assay with *in-vitro* grown *Nicotiana tabacum* SR1 pollen tubes and WT mature ovules.

(A) A mature whole ovule was placed in 200- 400 µm distance to *in-vitro* grown pollen tubes, which had been growing for about 4 h; 0 min after ovule placement. (B) 90 min after ovule placement. (C) 180 min after ovule placement; scale bar= 250 µm.

Figure 14 shows another example attraction assay of *in-vitro* grown *Nicotiana tabacum* SR1 pollen tubes towards a whole mature ovule. As described above, *Nicotiana tabacum* pollen were germinated and grown for about 4 h before a freshly dissected ovule was placed in front of the pollen tubes. (A) shows the time point 0 min after placement of the ovule in 200- 400 µm distance to the growing pollen tubes. After 90 min (B) the pollen tubes have grown about 250 µm and the pollen tube in the middle of the image seems to be attracted by the ovule. It was growing straight towards the ovule, although it has to be considered that it did not have to change its direction for this purpose. In (B) it is growing around the ovule and possibly trying to enter the ovule. 180 min after ovule placement it is clear that the pollen tube did not enter the ovule but kept on growing after its interaction with the ovule.

3.5.2 *In-vitro* Attraction Assay of Nt YFP Pollen and WT Ovules

In order to allow a more detailed visualization of the pollen tubes in a close distance to the ovule, experiments with Lelat::YFP-tagged SR1 pollen tubes were performed. Pollen tubes were grown as described in 2.8.4.3. After growing for 3- 4 h in a humid chamber in the dark, freshly dissected ovules from a mature, but unpollinated flower were placed in 100- 150 µm distance to the growing pollen tubes. In contrast to previous experiments, several ovules were dissected together in order to secure intactness of the

ovules and its funiculus. By dissecting only one ovule from the ovary, the funiculus can easily be damaged, which showed to impair or diminish pollen tube growth into the ovule.

The pollen tube growth behavior was monitored over a time period of 80 min, taking a bright field picture and detecting the emitted YFP fluorescence every 10 sec. Example images of the time point 0 min, 40 min and 80 min are displayed in Figure 15.

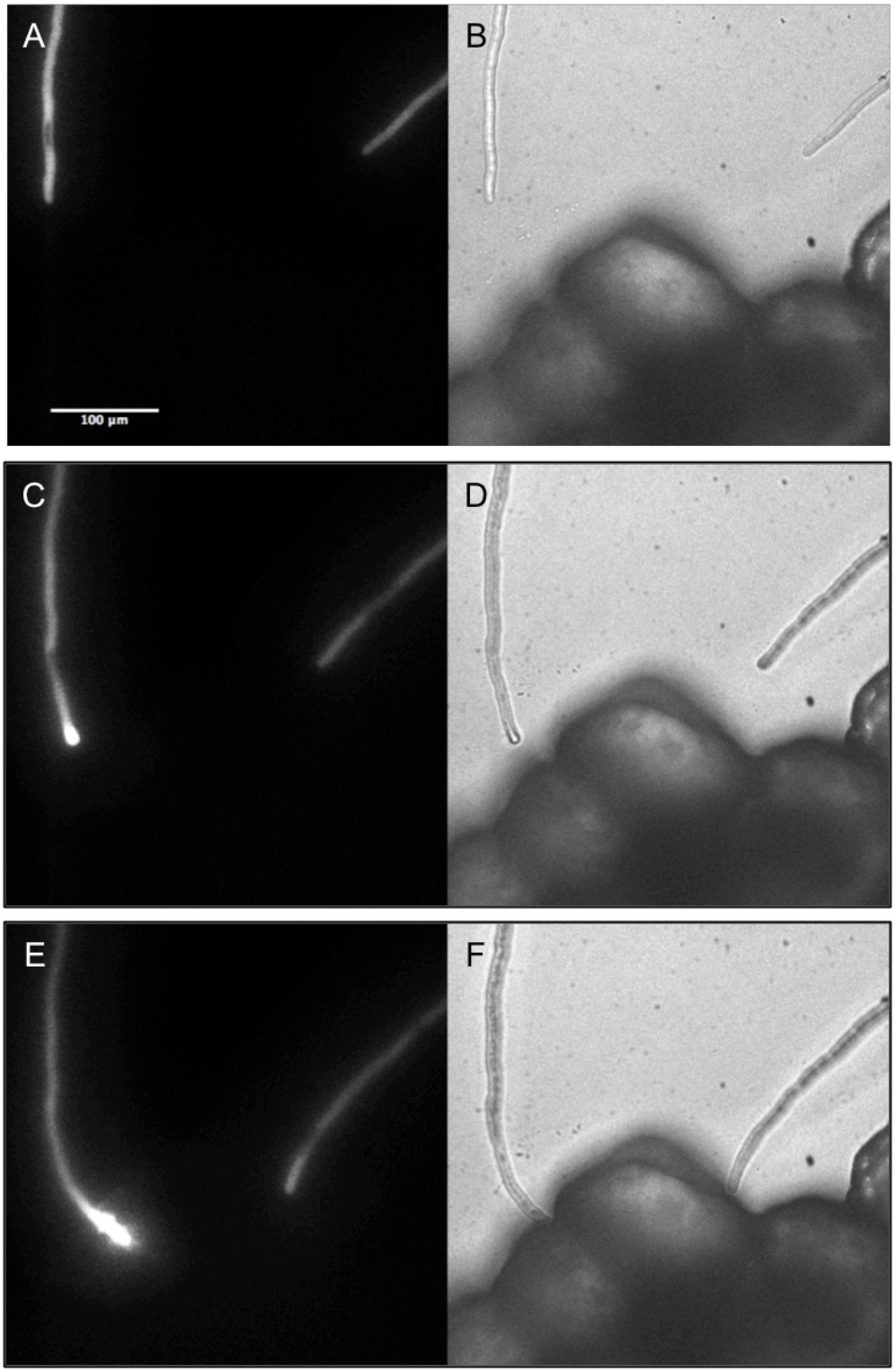

Figure 15: Attraction assay of *in-vitro* grown Lelat::YFP *Nicotiana tabacum* pollen tubes with WT ovules. Excitation wavelength: 505 nm, emission: 535/ 30 nm. (A, B): 0 min; (C, D): 40 min; (E, F): 80 min.

Figure 15 shows an attraction assay of *in-vitro* grown Lelat::YFP pollen tubes. (A) and (B) display time point 0 min after placement of the ovules. The ovules were placed in

about 100 µm distance to the pollen tube growing at the left side of the picture and about 150 µm to the right pollen tube. After 40 min ((C) and (D)) both visible pollen tubes have grown about 80 µm and both show a slight change in growth direction towards an ovule. 80 min after placement of the ovules ((E) and (F)), both pollen tubes have clearly changed their growth direction. While the right tube cell keeps growing towards an ovule, the left pollen tube seems to have grown into an ovule and probably pollen tube rupture has occurred. This is indicated by the sudden diffusion of the fluorescence signal in the tip area of the pollen tube.

3.5.3 *In-vitro* attraction assay of Nt pollen tubes and peptide

In-vitro attraction assay of Nt pollen tubes and Nt136007 peptide

Using an attraction assay, it was tested whether an effect on growing *Nicotiana tabacum* pollen tubes could be shown by Nt136007. The peptide was mixed with gelatin to enable a localized application. Pollen tubes were grown on solid NtPGM for 3-4 h before the peptide was applied and pollen tube growth behavior was monitored. Bright flied pictured were taken every 5 min over a time course of 60 min. Kevin Bongers, who performed the attraction assay, kindly provided the images shown in Figure 16.

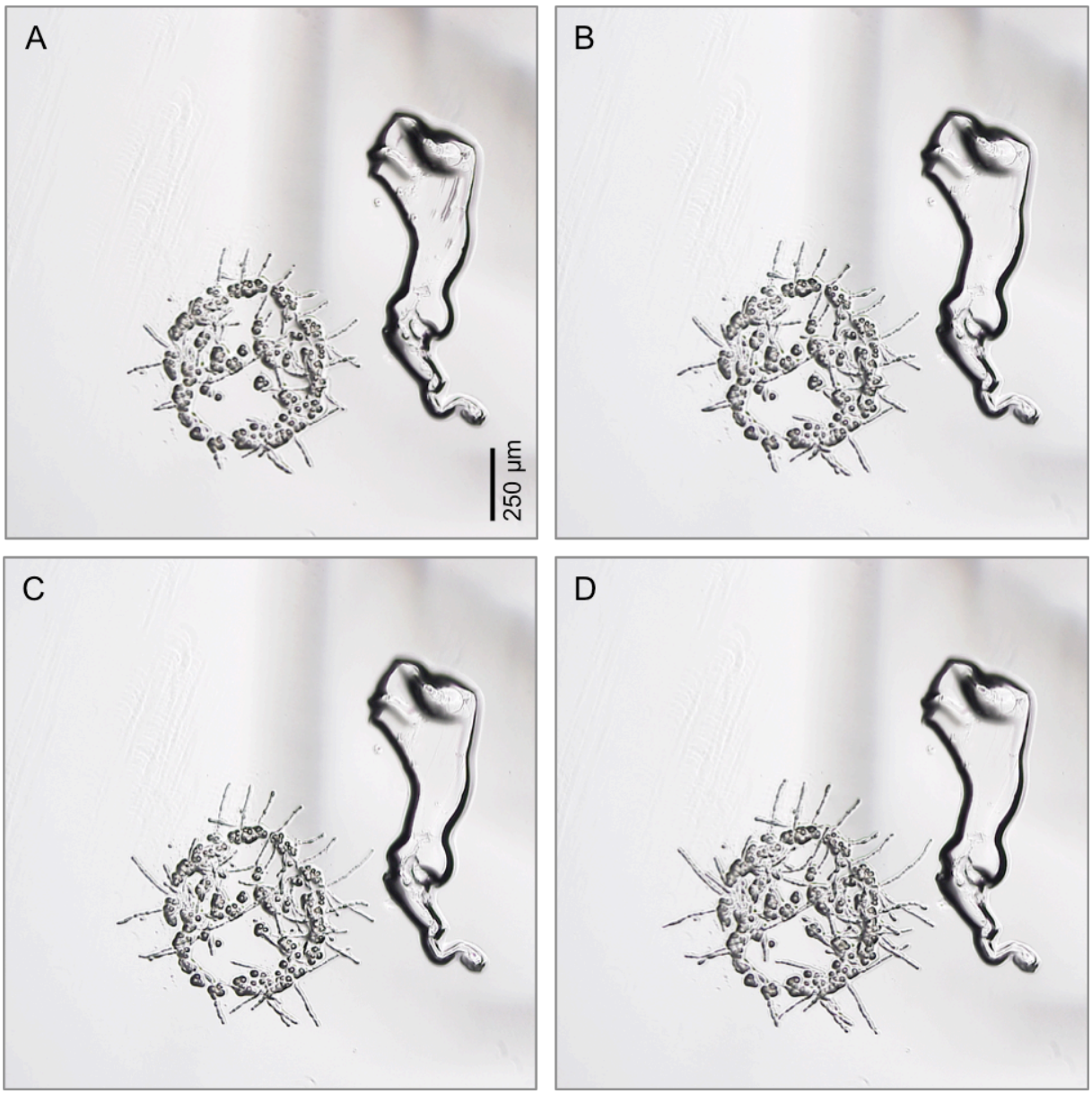

Figure 16: Attraction assay with *in-vitro* grown *Nicotiana tabacum* SR1 pollen tubes and *in-vitro* expressed Nt136007 peptide.

(A) A fragment of gelatin containing Nt136007 peptide was placed in 100- 250 µm distance of *in-vitro* grown pollen tubes, which had been growing for 3- 4 h; 0 min after peptide application. (B) 20 min after peptide application. (C) 40 min after peptide application. (D) 60 min after peptide application; scale bar= 250 µm.

Figure 16 shows example images of an attraction assay of *Nicotiana tabacum* pollen tubes towards Nt136007 peptide. (A) displays the time point immediately after placement of the gelatin fragment containing the Nt136007 peptide. The fragment was placed in a 100- 250 µm distance to the growing pollen tubes. 20 min after peptide

application the pollen tubes have grown approximately 40- 50 µm. A directional growth towards the gelatin fragment is not observed. (C) shows the time point 40 min after application of Nt136007. The pollen tubes have grown another 40- 50 µm, but a change in growth direction could not be detected. 60 min after application of the peptide (D) the pollen tubes have increased about 40- 50 µm and a growth behavior towards Nt136007 was not observed. Whether the pollen tube avoids the gelatin fragment or does not change its growth direction at all is difficult to distinguish, but it can be observed, that the pollen tubes do not grow towards the peptide.

In-vitro attraction assay of Nt pollen tubes and Nt46443 peptide

Attraction assays were also performed with *Nicotiana tabacum* pollen tubes and Nt46443 peptide. The peptide was applied in the same manner as Nt136007, mixed with gelatin to be placed in front of the growing pollen tubes. After growing for 3- 4 h, a fraction of Nt46443 peptide containing gelatin was applied to *in-vitro* growing pollen tubes and growth behavior was monitored. Bright flied images were taken every 5 min over a time course of 60 min. Kevin Bongers, who performed the displayed attraction assay, kindly provided the images shown in Figure 17.

Figure 17: Attraction assay with *in-vitro* grown *Nicotiana tabacum* SR1 pollen tubes and *in-vitro* expressed Nt46443 peptide.

(A) A fragment of gelatin containing Nt46443 peptide was placed in 100- 250 µm distance of *in-vitro* grown pollen tubes, which had been growing for 3- 4 h; 0 min after peptide application. (B) 20 min after peptide application. (C) 40 min after peptide application. (D) 60 min after peptide application; scale bar= 250 µm.

In Figure 17 example images of an attraction assay of *in-vitro* grown *Nicotiana tabacum* pollen tubes towards Nt46443 peptide is shown. A gelatin fragment containing Nt46443 peptide was placed in 50- 200 µm distance to pollen tubes, which had been growing for 3- 4 h. (A) displays the time point immediately after peptide application.

In (B), 20 min after placement of the gelatin fragment, the pollen tubes have grown 40-50 µm. Whether some pollen tubes are changing its growth direction towards the fragment can not be distinguished so far. 40 min after application of Nt46443 (C), the pollen tubes have grown another 40- 50 µm and it could be possible that one of the pollen tubes has changed its growth behavior and is growing towards the gelatin fragment, but the other cells do not seem to change their growth direction. (D) displays the time point 60 min after applying the peptide. The pollen tubes have grown about 40- 50 µm. It is not clearly distinguishable whether one or more pollen tubes have grown towards the gelatin fragment containing the Nt46443 peptide.

4. Discussion

In this work the fertilization process of the flowering plant *Nicotiana tabacum* was investigated on the basis of transcriptional profiling. In order to obtain insights into this process on a molecular level, tissue samples were taken at different time points throughout the fertilization process and the corresponding transcriptomic profiles of individual stages were determined. The following tissue samples from SR1 wild type plants were harvested: *in-vitro* grown pollen tubes (PT), mature ovules of flowers that had not been pollinated (OV), mature ovules of pollinated flowers (OVP) and mature ovules of flowers, in which fertilization had occurred (OVF). Following mRNA isolation, RNA-sequencing was performed and a transcriptome guided by the *Nicotiana tabacum* TN90 genome was assembled. Transcriptome data was analyzed with respect to enriched transcripts on the level of gene ontology. Further analyses aimed on the identification of cysteine-rich proteins and among those, defensin-like proteins. With regard to identifying the peptides, which are involved in pollen tube attraction in tobacco, candidate peptides were chosen, expressed *in-vitro* and attraction assays were performed.

4.1 RNA-sequencing and bioinformatics analyses

4.1.1 Prerequisites for RNA-sequencing

In order to harvest ovules from flowers, which had been pollinated and/or fertilized, it needed to be estimated, how much time the pollen tubes take to grow through the entire transmitting tract towards the ovary. Therefore, mature, non-pollinated flowers were pollinated with wild type pollen. Samples were taken and aniline blue staining experiments were carried out. The results displayed in Figure 3, demonstrate that 20 h after pollination (Figure 3 A), the pollen tubes have advanced about half way through the style and that they need about 48 h (Figure 3 B) to grow completely through the transmitting tract in order to reach the ovules. These results were used to ascertain taking the tissue samples for OVP and OVF at the correct time point. In *Arabidopsis thaliana* the degeneration of synergid cells could be observed 5 hours after pollination and karyogamy had taken place 7-8 hours after pollination (Faure, Rotman et al. 2002).

RNA was isolated from the plant tissue and to ensure a good quality of the samples for sequencing, experiments were performed to test quality and quantity of the extracted RNA. Figure 4 and Figure 18 the show the results of this analysis. In Figure 4 (A) the virtual gel is plotted. In all lanes, which contain the RNA samples, the lower marker of the kit is visible at 50 bp. Between 100 and 200 bp, traces of miRNA can be found. The two sharp bands at 1900 and 3700 bp display the 18S rRNA of the smaller subunit and 25S rRNA of the larger subunit of the cytoplasmic ribosome in the tissue samples. Because RNA was isolated only from non-green parts of the tobacco plant, no chloroplastic ribosomal rRNA is detected. The results are also displayed as electropherograms in Figure 18. The sharp peaks of the 18- and 25S rRNA confirm the good quality of the extracted RNAs and no degradation was detected. Figure 4 (B) displays the concentration of the isolated RNAs. Even though numbers varied between the samples, all were of high concentration and taken together with the quality analysis, all samples were well suited for RNA-sequencing.

4.1.2 Transcriptome assembly and bioinformatics analyses

4.1.2.1 General analysis of transcriptome data

In order to get a general idea about the quality of the sequenced samples, principal component analysis (PCA) was performed, which evaluates and visualized genetic distances between samples. To visualize the results, the dimensionality is reduced, while maintaining the variations in the dataset. Principal components are identified in which the differences between the datasets are the greatest. In Figure 5 the PCA of the sequenced RNA of PT, OV, OVP and OVF samples is plotted. The PCA plot nicely visualized the great genetic variance between the ovule samples (OV, OVP, OVF) and the PT samples. 97% of all genes investigated separate the pollen tubes from ovule tissues in the first dimension. This variance can be explained by the different origin of the samples. In further analyses the origin of this variances will be investigated using differential gene expression methods.

An indicator for good quality sequenced RNA samples is when the biological replicates of the same condition cluster closely together. This can be mostly observed in Figure 5. Because of the great genetic variance between the ovule and the pollen tube samples,

differences among the ovule samples (OV, OVP and OVF) are difficult to distinguish in the all versus all plot. Therefore, a second PCA, excluding the pollen tube sample, was performed displayed in Figure 6. In this PCA plot, a clear distinction between the ovule samples was possible. A variance of 74 % in component 1 demonstrates the difference between mature ovules and those from pollinated and fertilized flowers, which cluster more closely together. This indicates that after pollination biological processes are triggered that reprogram the ovules and thus lead to the considerable differentiation of OVP and OVF towards OV. The biological processes influenced by the fertilization process were analyzed in more detail with da differential gene expression analysis. Results were described in 3.2.5 and verify the results observed in the PCA plot. The difference in transcriptional activity is greater between mature, unpollinated ovules and ovules from pollinated flowers than between the samples of pollinated and fertilized flowers. The variation between OVP and OVF is mainly visualized in component 2, displaying a variance of 9 % between the samples. This variance could be provoked by the traces of pollen tubes included in the OVF samples, as well as the genetic proof of the fertilization having completed. On the other hand, similar as in the first PCA plot, the good qualities of the samples is verified by the fact that the biological replicates of each condition cluster closely together and are clearly separated from the other samples.

4.1.2.2 Overview about differentially expressed transcripts

As described above, a principal component analysis provides information about genetic variance between samples, nevertheless it does not give any details about the number of genes found in each sample. In order to get a closer look into the genes shared between the investigated tissues, but also at the number of genes, which can only be found in a specific sample, Venn diagrams were created. To assemble the Venn diagrams, all transcripts with an expression level equal to or higher 500 were extracted from the TBro instance. The minimum expression level of 500 was chosen to ensure only highly expressed transcripts were taken into account for comparison. For mature ovules a total number of 10,507 transcripts were exported from TBro, for pollinated ovules 10,241, for fertilized ovules 9,783 and for pollen tube samples 11,913 transcripts were exported.

Figure 7 (A) shows that mature ovules and pollen tubes only share about half of their expressed genes, confirming the data displayed in the PCA plot and indicating their distinct biological roles. A Venn diagram offers insights about absolute values of transcripts found in a tissue and compare this to other tissues, but it does not offer insights about the biological functions influenced. To also obtain insights regarding the biological processes involved in the fertilization process, a functional analysis of the transcriptome data was performed.

In Figure 7 (B) the Venn diagram displaying the comparison of expressed transcripts in mature ovule, pollinated ovules and fertilized ovules is shown. The analysis shows that the majority of transcripts (8244 transcripts) between the three tissue samples are shared among them and that only a small percentage of transcripts is expressed specifically under a given condition. 13 % of the transcripts expressed in mature ovules cannot be found in pollinated or fertilized ovules, 6 % are specifically found in pollinated ovules and only 3.6 % in fertilized ovules. It is not surprising that a high number of transcripts are shared between all samples, as all of them are ovules, even though the samples were taken at different time points throughout the fertilization process. The Venn diagram also shows that transcriptionally pollinated and fertilized ovule are more alike to each other than to mature ovules, which indicates that a number of processes are triggered in the ovule after pollination.

4.1.2.3 Functional analysis of transcriptome data

In 4.1.2.2 the number of transcripts expressed in each tissue was analyzed and based on the number of differentially expressed genes, it was suggested that different processes inside the pollen tube and the ovule are triggered by fertilization.

In order to obtain a closer look regarding these processes occurring at the distinct parts of the tobacco flower, an expression analysis was performed and the resulting transcripts were subjected to a MapMan analysis.

Functional analysis of expressed genes

First the transcripts expressed in the growing pollen tube and in ovule of the mature flower were analyzed to get an overview about the relevant processes taking place in the tissues.

As shown in 3.2.5 for growing pollen tubes, the bin for cell wall has the highest significance. It contains transcripts encoding different functions, including cell wall precursor synthesis, cellulose and hemicellulose synthesis, cell wall proteins like arabinogalactan proteins and leucine-rich proteins, transcripts involved in cell wall modification, as well as for cell wall degradation. Among the transcripts assigned to the cell wall bin, there are several genes known to be involved in the fertilization process of flowering plants. Among them, COBL10 (COBRA-LIKE 10), a GPI-anchored protein has been shown to facilitate pollen tube growth in a directional manner via deposing pectin and cellulose microfibrils at the pollen tube cap (Li, Ge et al. 2013).

The bin with second highest significance is signaling, which contains a total of 581 transcripts assigned to it. Among them are several receptor kinases, transcripts involved in calcium signaling, G-proteins, 14-3-3 proteins, phosphoinositides and proteins involved in sugar and nutrient physiology. PRK3 has been described to be essential for the fertilization process in *Arabidopsis thaliana*, as it works as a pollen tube tip-localized receptor sensing LURE peptides (Takeuchi and Higashiyama 2016, Chakraborty, Pan et al. 2018). Also other PRKs like PRK2 have been shown to be part of fertilization. PRK2 stimulates activation of ROP1 via RopGEFs to control polarized pollen tube growth (Chang, Gu et al. 2013, Zhao, Wang et al. 2013). CrRLK1L-receptor-like kinase ANX1 plays a role in maintaining cell wall integrity of the growing pollen tube (Boisson-Dernier, Roy et al. 2009, Boisson-Dernier, Lituiev et al. 2013, Kessler, Lindner et al. 2015, Mang, Feng et al. 2017, Du, Qu et al. 2018). Another CrRLK1L-receptor-like kinase is FER, which acts as a sensor for cell wall integrity and facilitates male female interactions during fertilization (Escobar-Restrepo, Huck et al. 2007, Richter, Ploderer et al. 2017, Feng, Kita et al. 2018).

There are 514 transcripts assigned to the transport bin, which are involved in different transport-related biological functions, e.g. P and V type ATPases, transcripts concerning transport of sugars, amino acids, peptides and polypeptides, nucleotides,

metabolites, ions and anions. Another bin containing transcripts assigned to a biological function is the RNA bin. It includes transcripts involved in RNA processing, e.g. splicing, helicases and ribonucleases and transcripts involved in transcription, regulation of transcription as well as RNA binding.

The cell bin contains 487 transcripts assigned to functions regarding the cell, which effect cell organization, including the cytoskeleton, microtubule and myosin, cell division and cell cycle as well as vesicle transport and cell death. There are 236 transcripts assigned to bin 11, which contains genes related to the lipid metabolism. The bin comprises transcripts involved in fatty acid synthesis, elongation and desaturation, as well as phospholipid and glycolipid synthesis, lipid transfer proteins and lipid degradation.

281 transcripts are assigned to the bin, which contains stress related biological functions. These contain genes involved in biological stress, like respiratory burst and pathogenesis related stress, but also abiotic stress, like heat, cold, drought/salt, touch/wounding and light. And there are 71 transcripts assigned to biological functions regarding the tricarboxylic acid cycle.

Next the transcripts found in the mature ovule samples were analyzed to identify the most significant biological functions. It could be shown that the relevant biological functions differ from the ones relevant in the growing pollen tube.

The bin with the most significant p-value for mature ovules is the protein bin. It contains 1904 transcripts assigned to protein-related biological functions. Among those are transcripts playing a role in amino acid activation and different functions in regards of protein synthesis, e.g. synthesis of prokaryotic and eukaryotic ribosomal proteins, ribosome biogenesis, and initiation, elongation and release of proteins. Other protein-related transcripts are involved in targeting of proteins to different places in the cell like the nucleus, mitochondria and chloroplast and to secretory pathways targeting the endoplasmatic reticulum, golgi apparatus, vacuole and plasma membrane. Other protein-related transcripts are involved in posttranslational modifications and degradation, e.g. cysteine proteases, aspartate proteases, serine

proteases and metaloproteases, while other transcripts play a role in protein folding, glycosylation and assembly and cofactor ligation.

There are 2164 transcripts assigned to the bin containing genes, which could not be assigned to a biological function. 27 transcripts play a role in metal handling and are involved in acquisition, binding and regulation of metals. 288 transcripts were assigned to the DNA bin, which incorporates transcripts involved in DNA synthesis, chromatin structure, DNA repair and other unspecified DNA-related functions. There are 69 transcripts assigned to the bin related to glycolysis. Among those are several transcripts involved on the cytosolic branch of glycolysis, e.g. phosphoglucomutases (PGM), pyrophostphate-fructose-6-P-phoshotransferases, pyruvatekinases and phospho-enol-pyruvat-carboxylases (PEPC). In the plastid branch of glycolysis are transcripts related to pyruvatkinases (PK) and phosphofructokinases (PFK). 192 transcripts are involved in biological functions related to the amino acid metabolism, in either synthesis or degradation of amino acids and 116 transcripts play a role in the polyamine metabolism, in the synthesis of e.g. decarboxylases, arginine decarboxylases and spermidine synthases.

Functional analysis of differentially expressed genes

During the fertilization process a diversity of biological processes are triggered in the female gametophyte. Differential gene expression analysis was used to identify transcripts, which are differentially regulated during the stages of fertilization.

It was identified that the biological function most affected by pollination is stress. There are 44 transcripts expressed higher in the ovules of pollinated flowers than in mature, unpollinated ones. The transcripts are involved either in biotic pathogenesis-related stress metabolism or abiotic stress metabolisms against heat or drought. Another biological function, which was higher expressed in the samples from pollinated flowers in comparison to unpollinated flowers is photosynthesis. From the 23 transcripts the majority is involved in light reaction, being part of the ATP synthase or in the cyclic electron flow, but one of them is also involved in the calvin cycle, interacting with RUBISCO.

Amino acid related biological functions are upregulated in pollinated flowers, too, being involved in the synthesis or degradation of amino acids. One transcript encodes for EDA 9 (EMBRYO SAC DEVELOPMENT ARREST 9), which amongst others regulates serine homeostasis by being part of serine biosynthesis and which plays an important role in pollen and embryo development (Toujani, Munoz-Bertomeu et al. 2013).

Upon pollination several transcripts playing a role in transport processes are upregulated. There are transcripts involved e.g. in transporting sugars, amino acids, nucleotides, anions and ions. KUP 3 (K+ UPTAKE TRANSPORTER 3) and HAK 5 (HIGH AFFINITY K+ TRANSPORTER) are examples of transcripts, which are involved in potassium transport and which are upregulated in the ovule upon pollination. Transcripts of the hormone metabolism are also subject of change of expression in the fertilization process. The affected transcripts are part of e.g. the auxin, ethylene or gibberellin metabolism. They encode e.g. for PIN 1 and 3 (PIN-FORMED) for auxin metabolism, EIN 4 (ETHYLENE INSENSITIVE 4) for ethylene metabolism and GASA 4 (GAST1 PROTEIN HOMOLOG 4) for giberrellin metabolism.

Other transcripts in the ovule affected by pollination are part of the cell wall biological processes and take part in the synthesis, modification and degradation of the cell wall. Involved in the degradation are e.g. CEL 3 (CELLULASE 3) and LRR (LEUCINE-RICH REPEAT) family proteins. Not only the cell wall is influenced by the fertilization process, upon pollination also cell functions like cell organization and division are impacted.

Pollination of the flower impacts the lipid signaling in the ovule, too. Fatty acid synthesis and lipid degradation are altered, but also the lipid transfer proteins are influenced, among them LTP 1 (LIPID TRANSFER PROTEIN 1). LTPs have been shown to be involved in many cell functions like development and plant growth and are part of metabolic pathways, as well as the fertilization process. Non-specific LTPs (nsLTPs) can transfer and bind different hydrophobic molecules like fatty acids and glycolipids (Carvalho Ade and Gomes 2007). In the fertilization process LTPs are secreted by the male gametophyte as well as by the female gametophyte and thereby playing an important role in plant reproduction (Mollet, Park et al. 2000, Park, Jauh et al. 2000,

Lord and Russell 2002, Chae, Zhang et al. 2007, Chae, Kieslich et al. 2009, Liu, Zhang et al. 2015).

4.1.2.4 Identification of cysteine rich proteins

After the general analysis of the transcriptome data, this work focused on identifying members of the superfamily of cysteine-rich proteins among the transcripts expressed in reproductive tissues. The majority of CRPs are known to be involved in plant-microbe interactions in the immune response of plants and have been isolated from several tissues (roots, leaves, stems, flowers, and seeds) (Nawrot, Barylski et al. 2014). CRPs have also been shown to play important roles in several steps in the fertilization process of flowering plants, like in plant development, pollen recognition and pollen tube guidance (Marshall, Costa et al. 2011, Qu, Li et al. 2015). It could be shown, that e.g. the LUREs in *Torenia fournieri* play a role in pollen tube attraction (Okuda, Tsutsui et al. 2009) and that ES4 causes pollen tube rupture in *Zea mays* (Amien, Kliwer et al. 2010). CRPs are characterized by being composed of less than 170 amino acids, containing an N-terminal signal peptide and possessing an even number of four or more cysteines (Broekaert, Cammue et al. 1997, Garcia-Olmedo, Molina et al. 1998, Boman 2003, Bulet, Stocklin et al. 2004, Theis and Stahl 2004, Silverstein, Moskal et al. 2007). Disulfide bonds between the thiol groups of two cysteines are crucial for the peptide's 3D structure and therefore its activity (Marshall, Costa et al. 2011, Haag, Kerscher et al. 2012, Vriens, Cammue et al. 2014). In previous studies 756 CRPs were found in *Arabidopsis thaliana* (Silverstein, Moskal et al. 2007, Huang, Dresselhaus et al. 2015).

In this work 953 CRPs could be identified in *Nicotiana tabacum* using Hidden Markov Models (Silverstein, Moskal et al. 2007) as shown in Table 19. According to characteristic cysteine motifs, disulfide bond pattern and tertiary structure, the CRPs were grouped into subgroups and assigned to previously known protein families. 669 of the identified total of 953 CRPs could be related to 14 known families (Antimicrobial peptide MBP-1, Defensin/DEFL, GASA/GAST/Snakin, Hevein, Kazal type inhibitor, Kunitz type inhibitor, LTP/2S Albumin/ECA 1, Maternally-expressed gene (MEG)/Ae1, Pollen Ole e I, Protease inhibitor II, RALF, Root cap/LEA, Stig1 and Thionin), while the

remaining 284 CRPs could not be matched to a protein family. A selection of these families and their main characteristics is described below.

The transcriptome data revealed 37 HEVEIN-like peptides in *Nicotiana tabacum*. Members of these CRPs contain six to ten cysteine residues, are built up by one alpha helix and an antiparallel beta sheet and are of a molecular mass of about 4 kD (Andersen, Cao et al. 1993, Xiang, Huang et al. 2004, Dubovskii, Vassilevski et al. 2011, R, V et al. 2012). It has been shown that they play a role in plant defense against fungal and oomycete pathogens (Broekaert, Marien et al. 1992, Lee, Lee et al. 2003, R, V et al. 2012, de Souza Cândido, e Silva Cardoso et al. 2014).

The biggest group of CRPs found in *Nicotiana tabacum* was the LIPID TRANSFER PROTEINS (LTPs) class encompassing 243 members. LTPs possess four alpha helices, which are stabilized by four disulfide bonds (Kader 1996). This characteristic tertiary structure leads to a hydrophobic cavity that allows binding and therefore transporting of lipids (Carvalho Ade and Gomes 2007, Tousheh, Miroliaei et al. 2013). LTPs are divided into two subfamilies by their molecular masses. LTP1 members are about 10 kD and LTP2 members about 7 kD (Douliez, Michon et al. 2000). Around 600 LTPs have been identified in different plant species (Wang, Lee et al. 2012), which were shown to play a role in response to abiotic stress, cutin synthesis, embryogenesis and reproduction (Blein, Coutos-Thevenot et al. 2002, Pii, Molesini et al. 2012, Nawrot, Barylski et al. 2014). It was shown that LTPs are expressed in the male and the female gametophyte and knockouts lead to partial sterility in male and female gametophyte, like a defective polar tip growth and an affected seed set (Chae, Kieslich et al. 2009).

RAPID ALKALINIZATION FACTOR (RALF) peptides, of which 44 were found in *Nicotiana tabacum*, contain four cysteines, forming two disulfide bonds (Pearce, Moura et al. 2001) and have been found in various plant species (Pearce, Moura et al. 2001, Haruta and Constabel 2003, Combier, Kuster et al. 2008, Mingossi, Matos et al. 2010, Cao and Shi 2012). They play a role in plant development by inhibition of root growth, decrease of nodulation and regulation of pollen tube growth (Pearce, Moura et al. 2001, Wu, Kurten et al. 2007, Combier, Kuster et al. 2008, Covey, Subbaiah et al. 2010, Murphy and De Smet 2014). RALF 4 and RALF 19 are pollen tube expressed and

interact with the receptors BUPS 1 and BUPS 2 (BUDDHA'S PAPER SEAL 1 AND 2) to maintain pollen tube integrity. This interaction between receptor and ligand is competing against the interaction with RALF 34, which is expressed by the female gametophyte and induces pollen tube burst (Ge, Bergonci et al. 2017, Peng, Li et al. 2018).

In the transcriptome data 44 SNAKIN/GIBBERELLIC ACID STIMULATED-LIKE (GASA) peptides were identified. They contain twelve cysteines and a molecular mass of about six kD. It was suggested that SNAKIN/GASA peptides are composed of two long alpha helices (Porto and Franco 2013, R., Sung - Hyun et al. 2014). They are antimicrobial and increase the plant's resistance against bacterial and fungal pathogens (Berrocal-Lobo, Segura et al. 2002, Almasia, Bazzini et al. 2008, Rong, Qi et al. 2013, García, Ayub et al. 2014) and are involved in plant development (Nahirnak, Almasia et al. 2012).

THIONINs, of which 37 were identified in *Nicotiana tabacum*, contain two parallel alpha helices, as well as a double-stranded beta sheet. Three or four disulfide bonds stabilize the tertiary structure and the peptides possess a molecular mass of around five kD (Stec 2006), although a 15 kD THIONIN was found in *Arabidopsis thaliana* (Asano, Miwa et al. 2013). THIONINs are involved in plant defense against fungi, yeast, bacteria, insect larvae, nematodes and mammalian cells (Epple, Apel et al. 1997, Shirasawa-Seo, Nakamura et al. 2002, Stec 2006, Muramoto, Tanaka et al. 2012, Ji, Gheysen et al. 2015).

The main focus of this work was on the DEFENSINs (DEF)/ DEFENSIN-LIKE (DEFL) proteins. DEFs/DEFLs contain four, six or eight cysteines and have a molecular mass of about five kD. They are composed of an alpha helice and a triple-stranded beta sheet, which is stabilized by up to four disulfide bonds (Tavormina, De Coninck et al. 2015) and belong to the pathogenesis-related protein family 12 (PR12 family) (van Loon, Rep et al. 2006). In *Arabidopsis thaliana* 317 DEFLs were identified (Silverstein, Moskal et al. 2007, Huang, Dresselhaus et al. 2015), of them 70 % have been shown to be

transcribed (Tesfaye, Silverstein et al. 2013). In the *Nicotiana tabacum* transcriptome there were 116 DEFLs identified, as displayed in Table 15.

DEFLs play a role in plant defense, as they show antifungal and antibacterial properties (Carvalho Ade and Gomes 2011, De Coninck, Cammue et al. 2013, Gaspar, McKenna et al. 2014). They find another purpose in abiotic stress tolerance and root growth (Koike, Okamoto et al. 2002, Mee Do, Chul Lee et al. 2004, van der Weerden, Bleackley et al. 2013), as well in the plant reproduction process (Li, Dai et al. 2014, Huang, Dresselhaus et al. 2015, Ingram and Gutierrez-Marcos 2015, Qu, Li et al. 2015). It could be shown that the DEFLs SCRs/SP11 plays a role as a pollen self incompatibility determinant in *Brassica* (Schopfer, Nasrallah et al. 1999), LUREs function as a pollen tube attractant in *Arabidopsis* (Takeuchi and Higashiyama 2012*)* and *Torenia* (Okuda, Tsutsui et al. 2009, Kanaoka, Kawano et al. 2011) and ES1-4 provoke pollen tube burst in maize (Amien, Kliwer et al. 2010, Woriedh, Merkl et al. 2015).

4.2 Expression analysis

4.2.1 Differential expression of tobacco CRPs

In Figure 8 the expression pattern of the DEFLs found in the transcriptome data was analyzed. It was plotted, how many of the 116 DEFLs were upregulated, downregulated or whether no significant change ($p > 0.05$) in expression level was detected between two compared tissue samples.

Interpretation of the data resulted in the conclusion that the expression level of the majority of DEFLs was not significantly altered and around 5 % of DEFLs were downregulated under all conditions (OVF vs OV, OVF vs PT, OVP vs OV, OVP vs PT, PT vs OV). The greatest difference in number of differentially expressed transcripts was found in the upregulated DEFLs. When comparing two ovule samples with each other, ovules of fertilized flowers against mature ovules and ovules of pollinated flowers against mature ovules, around 7 % of transcripts were identified as being upregulated. A comparison between an ovule sample and pollen tubes resulted in a higher number of up regulated DEFLs. This result of 20 % up regulated DEFLs can be explained by the greater difference between pollen tube and ovule samples in

comparison to ovule samples between each other, even if they were harvested at different time points during the fertilization process.

4.2.2 Expression analysis of selected DEFLs in transcriptome and *in-vivo*

A goal of this work was to identify those among these 116 DEFLs, that might cause pollen tube attraction in *Nicotiana tabacum*. In order to narrow down this number, the relative expression levels of these genes were investigated. It is known, that in *Arabidopsis thaliana* a member of the LURE family is responsible for attracting the pollen tube towards the ovule (Okuda, Tsutsui et al. 2009). In Solanaceae there are no LURES, therefore candidate genes were chosen, which either showed a similar expression pattern than AtLURE1.2, but also candidate genes, which showed the opposite expression pattern than AtLURE1.2. As attractants work in a species preferential manner, it cannot be secured that the tobacco attractant will possess a similar expression pattern than the *Arabidopsis thaliana* one. This is the reason why transcripts with different expression pattern were selected for a further analysis.

Two of them showed a high expression level in mature ovules and decreasing levels after pollination and fertilization (TRINITY_GG_136007_c0_g1 (Nt136007) and TRINITY_GG_46443_c1_g1 (Nt46443)) and the other two displayed a contrary expression pattern (TRINITY_GG_47038_c1_g2 (Nt47038) and TRINITY_GG_79003_c21_g1 (Nt79003)). In order to not only look at ovule-specific transcripts, two additional pollen tube-specific genes were picked for a more detailed analysis (TRINITY_GG_54117_c1_g1 (Nt54117) and TRINITY_GG_22095_c1_g1 (Nt22095)). Figure 9 visualizes the obtained data.

In order to test, whether the same tendencies could be found in *in-vivo*, quantitative real-time PCR experiments were performed on the transcriptome library samples with gene-specific primers as shown in Figure 10. To get more information about tissue-specific expression patterns, additional experiments were performed, displayed in Figure 11. For these, new tissue samples were harvested from different stages of the fertilization process and RNA isolation, cDNA transcription, as well as quantitative real-time PCR experiments were carried out. For harvesting the plant material, the tobacco flower was dissected into five parts: stigma, upper part of the style (style 1),

lower part of the style (style 2), ovule and placenta. The samples were harvested at the same time points during the fertilization process as described before: mature flower, pollinated and fertilized.

The carried-out qPCR experiments on the transcriptome libraries, as well as on the newly harvested ovule samples, reflect and verify the data obtained from RNA sequencing. Nt136007 and Nt46443 show the highest expression in mature, non-pollinated ovules. Their expression level decreases after pollination and fertilization significantly (p= 0.0321 after pollination, p= 0,0003 after fertilization for Nt46443). An inverse expression pattern was obtained for Nt79003 and Nt47038. The expression of these two transcripts increased after pollination and fertilization. The difference in expression level is highly significant between mature and fertilized ovules for both candidates (Nt79003 p= 1.8 E-4, Nt47038 p= 3.4 E-9).

As the previously tested transcripts are ovule-specific and are not expressed in the pollen tube, two additional transcripts were selected. Nt54117 and Nt22095 are pollen tube-specific genes according to the transcriptome data. This is confirmed by the *in-vivo* experiments. While the data in Figure 10 shows basically no expression of these two genes in any ovule sample, Figure 11 allows a more detailed look into their expression pattern along the flower during the fertilization process. For harvesting the tissue samples after pollination and fertilization, pollen was applied on the stigma of the flower. This explains the high expression levels of Nt54117 and Nt22095 on the stigma and in style 1 both genes. OVP samples were harvested after the pollen tubes had grown through the upper part of the style (style 1), while for the OVF samples, reflect pollen tubes that had grown through the whole style, into the ovules and fertilization had occurred. Therefore, an increased expression of Nt54117 and Nt22095 was found in ovules and placenta on ovules of fertilized flowers, but not in ovules of pollinated flowers.

The qPCR experiments could confirm the results obtained by transcriptome sequencing for the analyzed genes Nt136007, Nt46443, Nt47038, Nt79003, Nt54117 and Nt22095 and offer additional insights into the molecular processes occurring during the fertilization process in *Nicotiana tabacum*.

4.3 Pollen tube attraction assays

4.3.1 *In-vitro* expression of Nt136007 and Nt46443

Defensin-like proteins can contain six cysteines, which renders correct folding of the biochemically isolated peptide challenging. To cope with this difficulty, the cell-free *E.coli* based PURExpress system was chosen, which contains all necessary macromolecules for an *in-vitro* transcription and translation. Success of the transcription and translation of Nt136007 and Nt46443 was confirmed with a dot blot. As described in 3.4 and Figure 12 the attached FLAG-tag could be visualized on the blot, indicating that the transcription and translation worked properly. Even though the dot blot shows that the FLAG-tag was transcribed correctly, it does not give information about the folding of the expressed peptides. The precise 3D structure of a peptide is crucial for its biological function; the correct folding of Nt136007 and Nt46443 could not be tested and therefore not confirmed.

Due to the small amount of obtained peptide, its concentration could not be determined and thus the concentration of the peptides in further experiments was not known. The impact of peptide concentration was shown for TfCRP1 and AtLURE1.2, for which attraction assays with different concentrations were performed. It was shown that a maximal number attracted pollen tubes was achieved in *Torenia fournieri* at 40 nM TfCRP1 (Kanaoka, Kawano et al. 2011) and in *Arabidopsis thaliana* 5- 50 µM of (Takeuchi and Higashiyama 2012), while 50 µM AtLURE1.2 was used in further experiments. For both species the experiments displayed the importance of peptide concentration, as the rate of attracted pollen tubes decreased significantly when applying lower or higher concentrations. The fact that Nt136007 and Nt46443 concentration could not be investigated and was therefore not known, needs to be taken into consideration when analyzing the performed attraction assays in tobacco.

4.3.2 Pollen tubes are attracted by whole ovules

Before applying the expressed peptides Nt136007 and Nt46443 to growing pollen tubes, the experimental setup was optimized and a positive control was established. In order to optimize the setup for the attraction assay, previously performed experiments in other species were taken into consideration. In studies performed in *Arabidopsis*

thaliana (Palanivelu and Preuss 2006) and *Torenia fournieri* (Higashiyama, Yabe et al. 2001), it was shown that the attraction towards the ovule or a peptide is significantly higher when the pollen tube had previously grown through the stigma of the flower. Because of this, comparative experiments were conducted for *Nicotiana tabacum*, where attraction assays performed, in which the pollen tubes either first grew through a cut style or were directly grown *in-vitro* on solid NtPGM. These experiments revealed that no difference in attraction towards the ovules could be detected; successful attraction was observed in both settings. Thus, for simplicity, further experiments were performed with *in-vitro* grown pollen tubes, without previously growing through a cut style. The Higashiyama group pre-incubated their *Arabidopsis thaliana* growth medium for the pollen tubes with excised ovules for 20 h (Okuda, Tsutsui et al. 2009), while in Palanivelu et al. this procedure was not employed (Palanivelu and Preuss 2006). For tobacco pollen tubes both techniques were tested, showing no difference between pollen tube attraction either grown on medium that was pre-incubated with ovules, or not. In both cases a successful attraction was observed, therefore in further experiments, no pre-incubation was performed.

Before testing the role of the expressed Nt136007 and Nt46443, a positive control was established. Therefore, whole mature, unfertilized *Nicotiana tabacum* wild type ovules were applied in close distance (200- 400 µm) to pollen tubes, which had been growing for about 4 h (3.5.1). Pollen tube growth was observed for 3 h and bright field images were taken every 15 min. The example pictures displayed in Figure 13 show that several pollen tubes seem to be growing towards the ovules. Because of the high number of pollen tubes and the magnification at which the images were taken, it is not clearly distinguishable how many pollen tubes are really attracted to one of the ovules. Another factor that needs to be taken into account is the time of observation after application of the ovule. In Figure 14 (B) it seems like the pollen tube is attracted by the ovule as it grows directly towards it and then grows around the ovule. In Figure 14 (C) on the other hand, it shows that after growing along the ovule, the pollen tube continuous growing.

Figure 13 and Figure 14 also display the difficulty of determining the difference between pollen tubes that can be categorized as attracted or not attracted. The Higashiyama

group (University of Nagoya, Japan) defined “attracted” by a change of pollen tube growth direction of minimum 20° (Okuda, Tsutsui et al. 2009) or later 30° (Takeuchi and Higashiyama 2012). Defining a minimum angle of change in growth direction makes a differentiation between “attracted” and “not attracted” possible. In Figure 14 (B) the middle pollen tube seems to be growing directly towards the ovule, even though it does not change its direction. Even though this 20°-definition does not cover all scenarios and needs to be applied with precautions, it seems like a useful tool to analyze attraction assays. A revision of this definition should be considered for future experiments.

While performing the attraction assays with whole, unfertilized ovules, a characteristic was discovered. If the funiculus of the ovule was still intact, the attraction of pollen tubes was higher than with ovules, where the funiculus was detached during preparation from the plant. Palanivelu et al, (2006) who performed attraction assays with *Arabidopsis thaliana* pollen tubes and ovules, also observed this phenomenon (Palanivelu and Preuss 2006).

In order to allow a closer look on the pollen tube attraction towards ovules, further experiments were performed. For these, mature ovules were placed in front of Lelat::YFP pollen tubes and bright field, as well as fluorescence images were recorded every 10 seconds over a total time period of 80 minutes (Figure 15). The experiments were conducted using Lelat::YFP pollen, because pollen prefers to grow in the dark. This way, the growing cells were only exposed to light for a short period of time, which also minimized heating from a bright field lamp. As described above, it was observed, that attraction of pollen tubes towards an ovule was less when the funiculus was not intact or the ovule was damaged in another way. This can easily occur when excising a single ovule from the ovary with a gauge needle. To avoid this, several ovules were excised at once and placed at about 100- 150 µm distance to the growing pollen tubes in this experiment. Figure 15 (A) and (B) shows the time point directly after placement of the ovules. 40 minutes later (Figure 15 C and D) both pollen tubes have grown about 80 µm and the left pollen tube displayed a slight change of growth direction by 17° towards an ovule After 80 minutes (Figure 15 E and F) the right pollen tube seems to be

growing towards the ovules, as it changed its growth direction by 32°. The left pollen tube has performed a change in growth direction of 45° and entered one of the ovules. Pollen tube rupture has occurred, indicated by the blurry fluorescence, which is distributed around the ruptured pollen tube tip. By the attraction definition by Okuda et al, both pollen tubes were attracted by the ovule and probably fertilization took place with the left pollen tube. These experiments successfully serve as a positive control for attraction assays performed with tobacco pollen tubes and the two expressed candidate peptides Nt136007 and Nt46443.

4.3.3 Pollen tube attraction assays with Nt136007 and Nt46443

After establishing the positive control for the attraction assays using whole ovules, similar experiments were performed with the expressed candidate peptides Nt136007 and Nt46443 to investigate their role on growing tobacco pollen tubes.

In Figure 16 and Figure 17 example attraction assays of *Nicotiana tabacum* pollen tubes and applied Nt136007 or Nt46443 peptides are shown. The experimental setup is comparable to similar experiments performed in the Higashiyama group. Images were taken every 5 min over a total time period of 60 min after application of the peptide. The peptides were solved in 5 % gelatin. It could be observed that in Figure 16 the pollen tubes grow an average of 96 µm after application of Nt136007 and in Figure 17 a pollen tube growth of around 140 µm was observed after applying Nt46443 during the monitored time of 60 min, although the growth rate differed highly between the tube cells. It can be concluded that after 60 min pollen tubes grew faster in the presence of Nt46443 than when being exposed to whole ovules (see Figure 15). On the other hand a slower cell elongation could be observed when the pollen tubes were exposed to Nt136007 than when whole ovules were applied. It has to be taken into consideration that after application of Nt46443 pollen tubes grew faster, when they were in a bigger the distance to the gelatin bead. Neither with Nt46443, nor with Nt136007 it could clearly be determined, whether an attraction towards the peptide could be observed. In order to make a clear statement about the role of Nt136007 and Nt4633, a higher number of replicated would be necessary and the technique via which the peptides were applied, would need to be revised.

The applied gelatin fragments containing the peptides were too big in comparison to the growing pollen tubes. Therefore, it was hard to distinguish, whether a pollen tube grows towards the bead or not. In this work 2 µl of peptide were mixed with 3 µl of gelatin to form beads with 5 % gelatin. From these 5 µl beads, small fragments were separated with sharp forceps and placed in front of growing pollen tubes. With this procedure, the fragments ended up being too large for the experimental setup and the size of the fragments were not reproducible, too. For future experiments, production of the beads should be revised. Maybe the beads could be put in solution and sheared to a uniform, small size using ultrasound or vigorous shaking. On the other hand, diffusion of the peptide from the gelatin bead to the solution should be considered and avoided. Another option for applying the peptide could be the usage of an application pipet. If the liquid mixture of gelatin and peptide would be inserted into a narrow-mouthed pipet, the peptide could be applied in a more precise manner. Here, the pollen tubes would need to grow on solid PGM, covered by liquid PGM to allow diffusion of the peptide from the pipet towards the pollen tubes. It was tried to use the same approach as described by (Takeuchi and Higashiyama 2012) There, the pollen tubes were grown and then covered in hydrated silicone oil and the beads containing the peptide were also applied in the same oil. Unfortunately this experimental setup was not successful in this work, as the pollen tubes stopped growing after being covered by the silicone oil.

Apart from the technique via which the peptides were applied to the growing pollen tubes, the peptides themselves should be questioned. As described above, the attached FLAG-tag of the peptides was ensured, which indicates the transcription of the candidate peptides. Unfortunately, the transcription of the FLAG-tag offers no information about a correct folding of the expressed peptides. And due to the little amount of expressed peptide, a determination of concentration was also not possible. As the Higashiyama group described for TfCRP1 and AtLURE1.2, the concentration of the applied peptide is of significant importance for their role on the growing pollen tubes. When the concentration was too small or too high, no attraction or a decreased attraction was observed (Okuda, Tsutsui et al. 2009, Takeuchi and Higashiyama 2012).

Because determining the concentration of the peptides expressed in this work could not be performed, an estimated amount of 2 µl was used in the attraction assay.

The last source of error in the attraction assay was the selection of the candidate peptides themselves. RNA sequencing and assembly of a transcriptome revealed a total number of 116 defensin-like proteins. In order to avoid testing the role of each of these DEFLs *in-vivo* on pollen tubes, candidate peptides had to be selected. Peptides displaying a similar expression pattern as AtLURE1.2 were chosen. AtLURE1.2 is expressed highest in mature, but unpollinated ovules. After pollination its expression decreases (Huang, Dresselhaus et al. 2015). As described above, Nt136007 and Nt46443 show a similar expression pattern (Figure 10 and Figure 11). Although no other criteria for narrowing down the size of candidates were available, it needs to be questioned, whether this selection was sensible. It was shown that CRPs act in a species-preferential manner (Kanaoka, Kawano et al. 2011, Marton, Fastner et al. 2012, Takeuchi and Higashiyama 2012), which is at least partially caused by their high sequence diversity (Higashiyama, Inatsugi et al. 2006). AtLURE1.2 belongs to the CRP_810 class of CRPs (Silverstein, Moskal et al. 2007); a class which could not be found in *Nicotiana tabacum* in this work. This result underlines the high sequence diversity of CRPs and therefore questions using the expression pattern of AtLURE1.2 for narrowing down the number of tobacco DEFLs for finding the peptide, which causes pollen tube attraction towards the ovule in *Nicotiana tabacum*.

4.4 Outlook

In this work a transcriptome analysis was performed in order to reveal new insights into the fertilization mechanisms of the model plant *Nicotiana tabacum*. Even though our understanding of the molecular mechanisms underlying the fertilization process was increased, there remain some questions to be answered, which offer new research opportunities.

4.4.1 Molecular mechanisms in the fertilization process

One central aim was to identify the peptide that causes pollen tube attraction in tobacco. With assembly and analysis of a transcriptome, the number of candidates was narrowed down to 116 DEFLs. In order to continue searching for this peptide a reliable, cost-effective method would need to be established, which enables the large-scale expression of a high number of peptides. Finding a system with which a high number of different candidate peptides could be expressed in a reasonable quantity and correctly folded would be crucial for pursuing the identification of the peptide, which provoked pollen tube attraction in *Nicotiana tabacum*.

Another important aspects for continuing the work in this direction would be the optimization of the attraction assay. With this method it was investigated whether an expressed peptide had an impact on the pollen tube growth. Even though data was collected, the application of the peptide to the growing pollen tubes needs to be improved and the experimental setup as well as data analysis should be more standardized in order to offer more comparable and therefore significant results.

4.4.2 General analysis of transcriptome data

This work focused on the fertilization process of *Nicotiana tabacum*, this is why the transcriptome data was specifically analyzed for this purpose until now. On the other hand it does offer a great number of results, which were not taken a look at so far and which offer a variety of opportunities for future analysis.

An idea could be to identify all channels and transporters and from these select candidates to be investigated in more detail. These could be e.g. electrophysiologically

characterized in *Xenopus laevis* oocytes and their expression could be analyzed via qPCR and compared to the expression levels determined in transcriptome sequencing. Localization analysis of candidate genes could be performed with GUS staining or YFP.

5. Appendix

5.1 List of Abbreviations

The physical quantities used in this work are part of the International System of Units (SI) and are not explained in further detail. Additional abbreviations used are explained in more detail in the following list.

At	*Arabidopsis thaliana*
bp	base pair
cDNA	complementary DNA
CRP	cysteine-rich protein
D	Dalton
DEFL	defensin-like protein
DEPC	diethyl pyrocarbonate
DNA	desoxyribonucleic acid
DNase	desoxyribonuclease
dNTP	desoxy nucleoside triphosphate
E.coli	*Escherichia coli*
e.g.	exepli gratia (lat. for example)
et al.	et alteres (lat. and others)
f	femto (10^{-15})
HMM	Hidden-Markov-Model
k	kilo (10^{3})
µ	micro (10^{-6})
m	milli (10^{-3})
min	minute

miRNA	micro RNA
mRNA	messenger RNA
n	nano (10^{-9})
Nt	*Nicotiana tabacum*
OV	unpollinated ovules
OVF	fertilized ovules
OVP	pollinated ovules
PCA	Principal component analysis
PCR	polymerase chain reaction
PT	pollen tubes
qPCR	quantitative real-time polymerase chain reaction
RNA	ribonucleic acid
RNase	ribonuclease
Style 1	upper part of the *Nicotiana tabacum* style
Style 2	lower part of the *Nicotiana tabacum* style
TBro	Transcriptome Browser
TRINITY_GG_22095_c1_g1	Nt22095
TRINITY_GG_46443_c1_g1	Nt46443
TRINITY_GG_47038_c1_g2	Nt47038
TRINITY_GG_54117_c1_g1	Nt54117
TRINITY_GG_79003_c21_g1	Nt79003
TRINITY_GG_136007_c0_g1	Nt136007
tRNA	transfer ribonucleic acid
v/v	volume per volume
WT	Wild type

5.2 Solutions and Buffers

Tobacco Pollen Germination Medium (NtPGM):

MES	1 mM
H_3BO_3	1.6 mM
$CaCl_2$	0.2 mM
KH_2PO_4	50 µM
Sucrose	13 %
Low-melt agarose	1 %
pH= 5.6 (Tris)	

DNA-Agarose-Gel Electrophoresis

1x TAE-Puffer (Tris-Acetate-EDTA-Buffer)

Tris	40 mM
Acetic acid	40 mM
Na-EDTA	1 mM
in ddH2O	

5x DNA Loading Buffer

Glycerin	50 % (w/v)
EDTA	100 mM
Bromphenol blue	0,25 % (w/v)
Xylene Cyanol FF	0,25 % (w/v)
in ddH2O	

Media for Cloning

LB (Luria-Broth) Ampicillin Culture Medium

NaCl	10 g/l
Trypton	10 g/l
Yeast Extract	5 g/l
Ampicillin	50 µg/ml
in ddH2O	

LB-Ampicillin-Selection Agar Plates

Agar Agar (Applichem / Peqlab)	2 %
Autoclaved in LB Medium	
Ampicillin added 50 µg/ml	
Poured in 10 cm petri dishes	
Stored at 4°C	

Media for Dot Blot

TBS Medium:

Tris-HCl	20 mM
NaCl	150 mM
in ddH_2O	
pH 7.5	

TBS-T Medium:

Tween20 in TBS	0.05 %

BSA/TBS-T:

BSA in TBS-T	0.1 %

5.3 Primers

Primers for qPCR:

Table 17: List of primers used for qPCR and its properties:

Primer Name	Sequence 5'-3'	Product Length [bp]	Tm [°C]
NtAct fwd:	CCCAGAAGTCCTCTT	275	48- 54
NtAct rev:	CGGATGCGAGGAT		
Nt22095 fwd:	GCCGACATCCTGAAACTG	220	55- 64
Nt22095 rev:	TTTCCAGCCATGCCATTG		
Nt46443 fwd:	GACTATGGCTCGCTCCTT	200	55- 64
Nt46443 rev:	ACCGTCTGAGGAGTTTGC		
Nt47038 fwd:	AGTCGCTAGCAATCCAGT	200	55- 64
Nt47038 rev:	TCAACAGCGGCAGATTTT		
Nt54117 fwd:	TCCACTGCACACAACTCT	220	55- 64
Nt54117 rev:	TATCGAAGGTGCAACGGT		
Nt79003 fwd:	CTTTCCCGTCACCACATC	220	55- 64
Nt79003 rev:	TGGGTTTGCAACTTGTGT		
Nt136007 fwd:	AATGGCAATCTCACGGGT	200	55- 64
Nt136007 rev:	CTCAAATTGTTGCTGGCA		

Primers for user cloning:

Table 18: List of primers used for user cloning and its properties:

Primer Name	**Sequence 5'-3'**	**Product Length [bp]**	**Tm [°C]**
AtLURE1.2 user fwd:	GGCTTAAUACACTTATAAATGGATC TAGTGATG	216	
AtLURE1.2 user rev:	GGTTTAAUTTATTTAATATCACTAA TACTGCAACG		
Nt46443 user fwd:	GGCTTAAUAGAGAATGCAAAACAG AAAG	243	
Nt46443 user rev:	GGTTTAAUTTAGTTATCCATTATCT CTTCTTC		
Nt136007 user fwd:	GGCTTAAUAGAGTGTGCATCTCACA AAGCC	144	
Nt136007 user rev:	GGTTTAAUTTAGCAGAGCTTGGTGC AGAAAC		

5.4 Quality and Quantity on Isolated RNAs for Sequencing

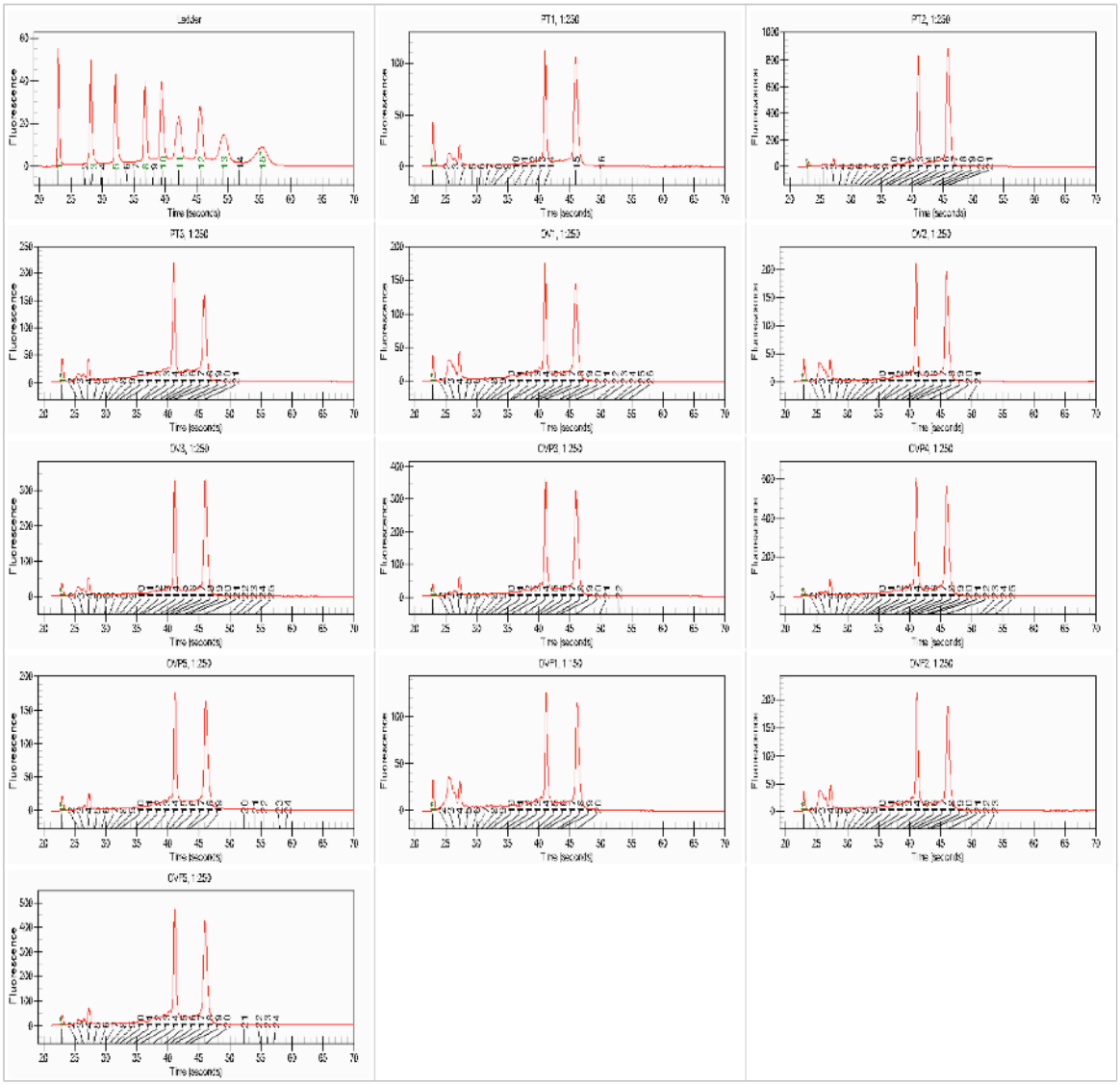

Figure 18: Electropherograms of RNA quality and quantity analysis.

The fluorescence intensity detected at 600- 700 nm is plotted against the time (s). For scale a ladder sample is analyzed in lane 1, samples PT1, PT2, PT3, OV1, OV2, OV3, OVP1, OVP2, OVP3, OVF1, OVF2 and OVF3 are displayed in lanes 2-12. All samples showa fluorescence peak for the lower marker at 22 s, fluorescence peaks displaying miRNA between 25 and 30 s, 18S rRNA at 41 s and 28S rRNA at 46 s.

5.5 Vectors

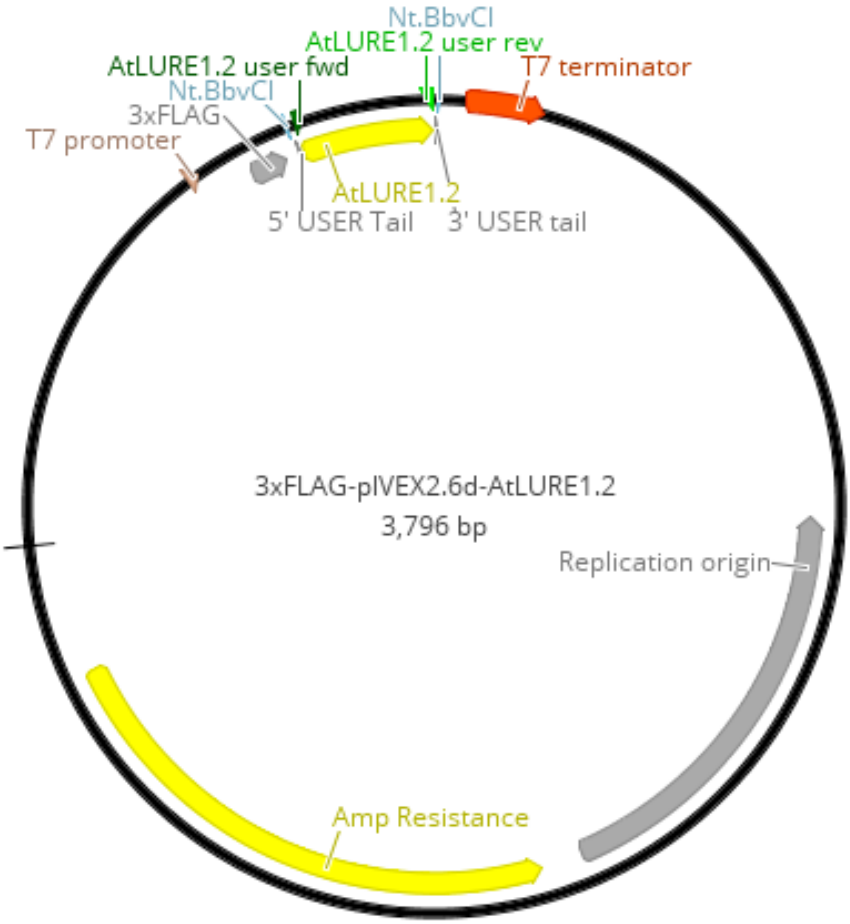

Supplementary figure 19: 3xFLAG-pIVEX2.6d-AtLURE1.2 expression vector.

Expression vector pIVEX2.6d containing a 3x FLAG tag, an ampicillin resistance and an AtLURE1.2 coding sequence without its signal peptide and without stop codon. The vector was used for heterologous expression in *E.coli*. AtLURE1.2 user fwd and AtLURE1.2 user rev: gene specific user primers for insertion of the AtLURE1.2 coding sequence into the user cassette (primer sequence: Table 18); Nt.BbvCI: restriction site for the nicking enzyme Nt.BbvCI; T7-promotor: specific promotor for the T7 RNA polymerase.

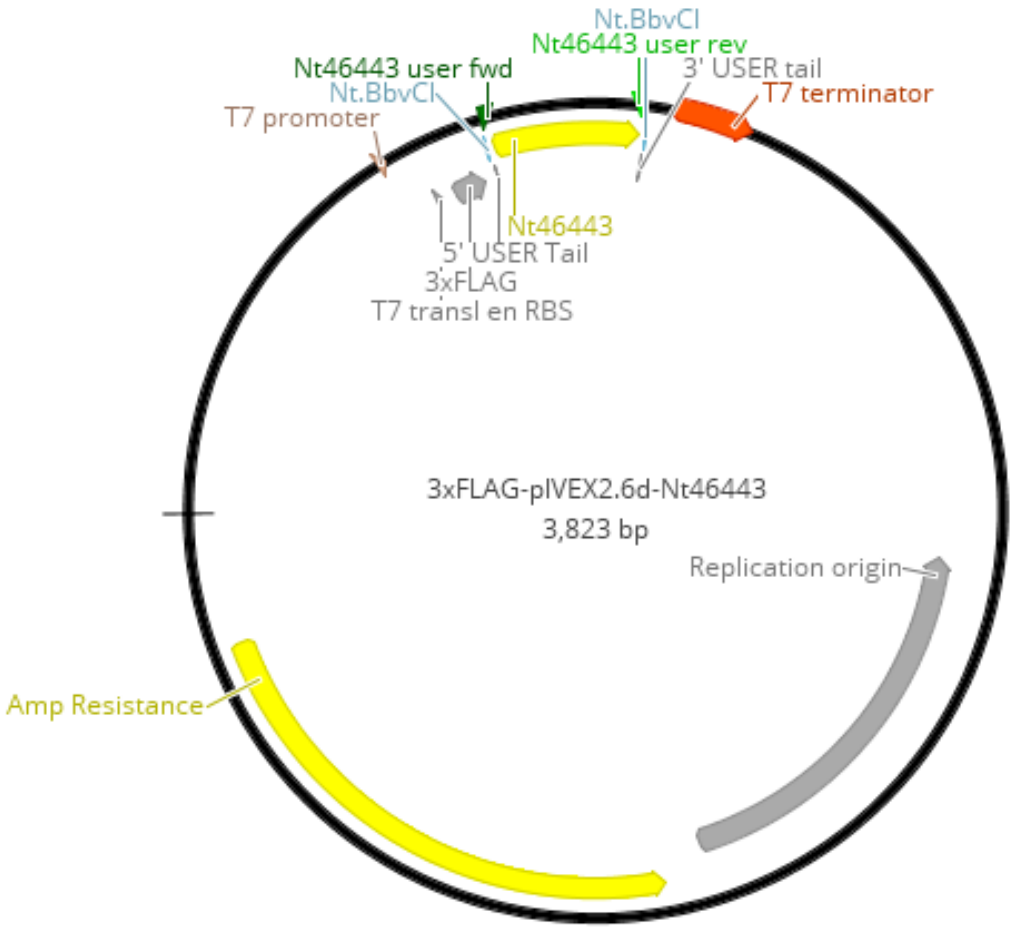

Supplementary figure 20: 3xFLAG-pIVEX2.6d-Nt46443 expression vector.

Expression vector pIVEX2.6d containing a 3x FLAG tag, an ampicillin resistance and an Nt46443 coding sequence without its signal peptide and without stop codon. The vector was used for heterologous expression in *E.coli*. Nt46443 user fwd and Nt46443user rev: gene specific user primers for insertion of the Nt46443 coding sequence into the user cassette (primer sequence: Table 18); Nt.BbvCI: restriction site for the nicking enzyme Nt.BbvCI; T7-promotor: specific promotor for the T7 RNA polymerase.

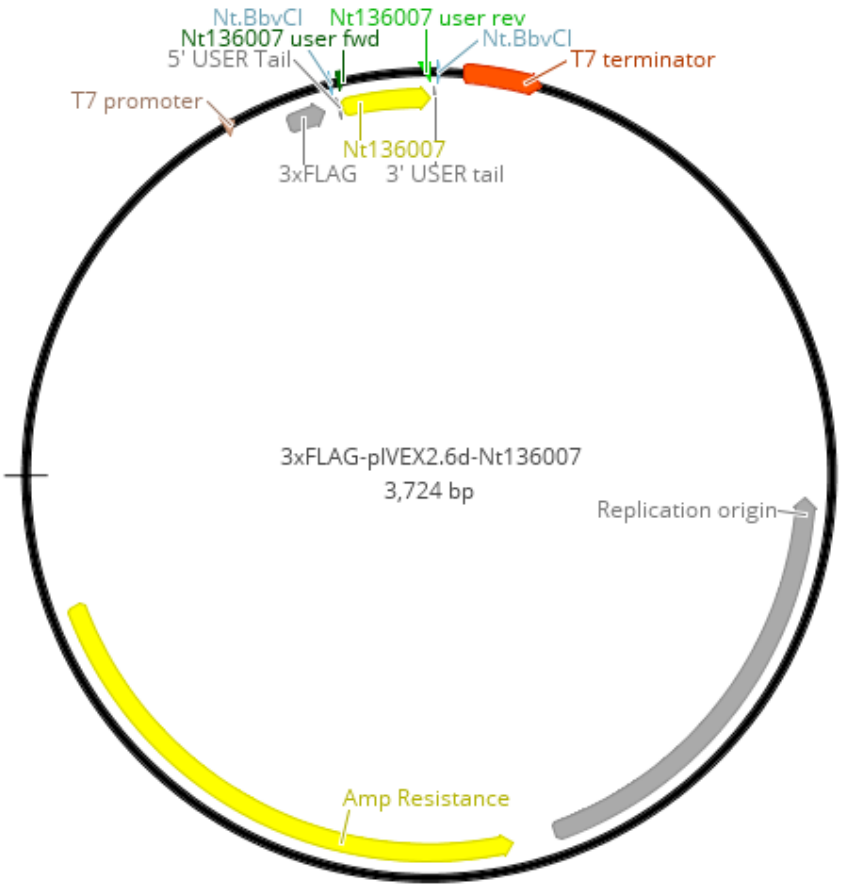

Supplementary Figure 21: 3xFLAG-pIVEX2.6d-Nt136007 expression vector.

Expression vector pIVEX2.6d containing a 3x FLAG tag, an ampicillin resistance and an Nt136007 coding sequence without its signal peptide and without stop codon. The vector was used for heterologous expression in *E.coli*. Nt136007user fwd and Nt136007user rev: gene specific user primers for insertion of

the Nt136007coding sequence into the user cassette (primer sequence: Table 18); Nt.BbvCI: restriction site for the nicking enzyme Nt.BbvCI; T7-promotor: specific promotor for the T7 RNA polymerase.

5.6 Identification of tobacco transcripts

In order to identify the longest isoform for each unigene, the following perl script was used:

```
#!/usr/bin/perl

use warnings;
use strict;


# This is a script written by Megan Morikawa in 2015 that takes an the output fasta file from Trinity and creates a new fasta with only the longest isoform.
# Usage perl LongestIsoformTrinity.pl file.fasta output.fasta

my ($input_file, $output_file) = @ARGV;

# Use dictionary to store key (isoform name) and values (contig length, sequence in same format as it was inputted)

# Read input file
# If it starts with >, extract what follows TRINITY_ [key], length of sequence [value[0]], header [value[1]], and sequence [value[2]]

# At end of file, sort keys, and print header then sequence (positions 1 and 2 of value array)

# Format of header
# >TRINITY_DN118274_c0_g1_i1 len=536 path=[7200:0-91 7201:92-535] [-1, 7200, 7201, -2]

my %fasta;

# Get length of file to be able to store last sequence of that file
my $filelength;
open(my $CHECK, "<", $input_file);
$filelength++ while <$CHECK>;
close $CHECK;

open(my $INPUT, "<", $input_file) or die "Cannot open $input_file\n";
open(my $OUTPUT, ">", $output_file) or die "Cannot create $output_file\n";
# Pop first character of line, check to see if it is >, if so, then extract information from header
```

```
# Extract information by split, substring first element to unique identifier,
substring length
# Check to see if in dictionary
# If not, read sequence, store, and move to next header

# Binary for knowing when to store sequence
my $storeseq = 0;
# Empty array of sequence
my @sequence;
# Empty string of identifier
my $identifier = '';


while(defined(my $readline = <$INPUT>)){
  my $test = substr $readline, 0, 1;
  if ($. == $filelength){
       # Store last sequence of file
         my @temp = @{$fasta{$identifier}};
         push @temp, [@sequence];
         $fasta{$identifier} = \@temp;
  }
  if ($test eq ">"){
       # We're in a header, end store sequence
       $storeseq = 0;
       if(length $identifier > 0){
              #Store sequence to most recent key
              my @temp = @{$fasta{$identifier}}; # check expansion
              push @temp, [@sequence];
  #           print join("\n", @temp), "\n";
              $fasta{$identifier} = \@temp;
       }
       @sequence = (); # reset sequence
       chomp $readline;
       # Evaluate header line
       my @row = split(/\s/,$readline);
       my $length = substr $row[1], 4, (length $row[1])-4;
       my @temp = split(/_/, $row[0]);
       # Identifier is DN]d+_c\d_g\d
       $identifier = $temp[1] . "_" . $temp[2] . "_" . $temp[3];
       if (defined $fasta{$identifier}){
              # Check to see if isoform is longer;
              if($length > $fasta{$identifier}[0]){
                     # Store sequence
                     $storeseq = 1;
                     # Replace length & header
                     $fasta{$identifier} = [$length, $readline];
```

```
                }
        }else{
                # Enter new key into dictionary & store sequence
                $fasta{$identifier} = [$length, $readline];
                # Store sequence
                $storeseq = 1;
        }
  }elsif($storeseq = 1){
        # Store sequence to preceeding header
        # Build @sequence
        push @sequence, $readline;
    }
}

foreach my $ids (sort keys %fasta){
        my $header = $fasta{$ids}[1];
        my @fasta = @{$fasta{$ids}[2]};
        print $OUTPUT $header, "\n", join('', @fasta);
  # For short name fasta
#  print $OUTPUT ">" , $ids, "\n", join('', @fasta);
}
```

5.7 Overview about Identified CRP Transcripts

Table 19: Overview of all identified CRP transcripts and their according CRP class as well as description

Transcript ID	CRP Class	CRP Description
TRINITY_GG_49624_c0_g1	CRP0020	Defensin/DEFL
TRINITY_GG_74342_c0_g1	CRP0020	Defensin/DEFL
TRINITY_GG_96432_c0_g1	CRP0020	Defensin/DEFL
TRINITY_GG_107409_c0_g1	CRP0030	Defensin/DEFL
TRINITY_GG_144472_c0_g2	CRP0030	Defensin/DEFL
TRINITY_GG_53571_c2_g1	CRP0030	Defensin/DEFL
TRINITY_GG_61150_c0_g1	CRP0030	Defensin/DEFL
TRINITY_GG_75926_c0_g1	CRP0040	Defensin/DEFL
TRINITY_GG_102990_c6_g1	CRP0050	Defensin/DEFL
TRINITY_GG_140127_c0_g1	CRP0050	Defensin/DEFL
TRINITY_GG_70101_c0_g2	CRP0050	Defensin/DEFL
TRINITY_GG_94414_c1_g1	CRP0050	Defensin/DEFL
TRINITY_GG_29284_c0_g1	CRP0060	Defensin/DEFL
TRINITY_GG_29284_c0_g2	CRP0060	Defensin/DEFL
TRINITY_GG_2075_c1_g1	CRP0080	Defensin/DEFL
TRINITY_GG_23841_c0_g1	CRP0080	Defensin/DEFL
TRINITY_GG_50531_c2_g1	CRP0080	Defensin/DEFL
TRINITY_GG_5432_c0_g1	CRP0080	Defensin/DEFL
TRINITY_GG_6516_c2_g1	CRP0080	Defensin/DEFL
TRINITY_GG_6519_c0_g1	CRP0080	Defensin/DEFL
TRINITY_GG_6520_c0_g1	CRP0080	Defensin/DEFL
TRINITY_GG_9018_c1_g1	CRP0080	Defensin/DEFL
TRINITY_GG_96436_c0_g1	CRP0080	Defensin/DEFL
TRINITY_GG_102990_c6_g2	CRP0090	Defensin/DEFL
TRINITY_GG_46443_c4_g1	CRP0090	Defensin/DEFL
TRINITY_GG_135525_c2_g1	CRP0120	Defensin/DEFL
TRINITY_GG_43051_c0_g1	CRP0120	Defensin/DEFL
TRINITY_GG_49437_c0_g1	CRP0130	Defensin/DEFL
TRINITY_GG_49437_c0_g2	CRP0130	Defensin/DEFL
TRINITY_GG_71617_c0_g1	CRP0130	Defensin/DEFL
TRINITY_GG_71617_c0_g2	CRP0130	Defensin/DEFL
TRINITY_GG_78671_c1_g1	CRP0130	Defensin/DEFL
TRINITY_GG_9476_c0_g1	CRP0130	Defensin/DEFL
TRINITY_GG_9476_c0_g2	CRP0130	Defensin/DEFL
TRINITY_GG_104337_c0_g1	CRP0220	Defensin/DEFL
TRINITY_GG_135373_c0_g2	CRP0220	Defensin/DEFL
TRINITY_GG_140477_c0_g1	CRP0220	Defensin/DEFL
TRINITY_GG_47031_c0_g1	CRP0220	Defensin/DEFL
TRINITY_GG_136007_c0_g1	CRP0300	Defensin/DEFL
TRINITY_GG_136007_c0_g2	CRP0300	Defensin/DEFL
TRINITY_GG_18954_c0_g1	CRP0300	Defensin/DEFL
TRINITY_GG_18954_c0_g2	CRP0300	Defensin/DEFL
TRINITY_GG_32707_c3_g1	CRP0300	Defensin/DEFL
TRINITY_GG_46996_c0_g1	CRP0300	Defensin/DEFL
TRINITY_GG_46996_c3_g1	CRP0300	Defensin/DEFL
TRINITY_GG_69155_c0_g1	CRP0300	Defensin/DEFL
TRINITY_GG_79593_c0_g1	CRP0300	Defensin/DEFL
TRINITY_GG_92727_c0_g1	CRP0300	Defensin/DEFL
TRINITY_GG_107419_c12_g1	CRP0310	Defensin/DEFL
TRINITY_GG_117309_c0_g1	CRP0320	Defensin/DEFL

Transcript ID	CRP Class	CRP Description
TRINITY_GG_110558_c0_g1	CRP0360	Defensin/DEFL
TRINITY_GG_45480_c0_g2	CRP0360	Defensin/DEFL
TRINITY_GG_1955_c1_g1	CRP0460	Defensin/DEFL
TRINITY_GG_6516_c1_g1	CRP0460	Defensin/DEFL
TRINITY_GG_104312_c0_g1	CRP0560	Defensin/DEFL
TRINITY_GG_104312_c0_g2	CRP0560	Defensin/DEFL
TRINITY_GG_104312_c0_g3	CRP0560	Defensin/DEFL
TRINITY_GG_119879_c0_g1	CRP0560	Defensin/DEFL
TRINITY_GG_134027_c0_g1	CRP0560	Defensin/DEFL
TRINITY_GG_62342_c0_g1	CRP0570	Defensin/DEFL
TRINITY_GG_101727_c0_g1	CRP0620	Defensin/DEFL
TRINITY_GG_101734_c0_g1	CRP0620	Defensin/DEFL
TRINITY_GG_101737_c0_g1	CRP0620	Defensin/DEFL
TRINITY_GG_127378_c9_g1	CRP0620	Defensin/DEFL
TRINITY_GG_129413_c0_g1	CRP0620	Defensin/DEFL
TRINITY_GG_118340_c7_g1	CRP0670	Defensin/DEFL
TRINITY_GG_126102_c0_g1	CRP0670	Defensin/DEFL
TRINITY_GG_118340_c7_g2	CRP0675	Defensin/DEFL
TRINITY_GG_145706_c0_g2	CRP0730	Defensin/DEFL
TRINITY_GG_133550_c0_g1	CRP0860	Defensin/DEFL
TRINITY_GG_4530_c0_g1	CRP0860	Defensin/DEFL
TRINITY_GG_143817_c0_g1	CRP0880	Defensin/DEFL
TRINITY_GG_16251_c0_g1	CRP0960	Defensin/DEFL
TRINITY_GG_73835_c0_g2	CRP1004	Defensin/DEFL
TRINITY_GG_73835_c0_g3	CRP1004	Defensin/DEFL
TRINITY_GG_97807_c0_g1	CRP1004	Defensin/DEFL
TRINITY_GG_127546_c0_g1	CRP1006	Defensin/DEFL
TRINITY_GG_134979_c0_g1	CRP1006	Defensin/DEFL
TRINITY_GG_139821_c0_g1	CRP1006	Defensin/DEFL
TRINITY_GG_144717_c0_g1	CRP1006	Defensin/DEFL
TRINITY_GG_35829_c0_g1	CRP1006	Defensin/DEFL
TRINITY_GG_40208_c4_g1	CRP1006	Defensin/DEFL
TRINITY_GG_82958_c0_g1	CRP1006	Defensin/DEFL
TRINITY_GG_29436_c0_g1	CRP1008	Defensin/DEFL
TRINITY_GG_29464_c31_g1	CRP1008	Defensin/DEFL
TRINITY_GG_102202_c0_g1	CRP1010	Defensin/DEFL
TRINITY_GG_102202_c0_g2	CRP1010	Defensin/DEFL
TRINITY_GG_117064_c16_g1	CRP1010	Defensin/DEFL
TRINITY_GG_117316_c0_g1	CRP1010	Defensin/DEFL
TRINITY_GG_38281_c0_g1	CRP1010	Defensin/DEFL
TRINITY_GG_46064_c2_g1	CRP1010	Defensin/DEFL
TRINITY_GG_47038_c1_g1	CRP1010	Defensin/DEFL
TRINITY_GG_47038_c1_g2	CRP1010	Defensin/DEFL
TRINITY_GG_52151_c0_g1	CRP1010	Defensin/DEFL
TRINITY_GG_122872_c0_g1	CRP1015	Defensin/DEFL
TRINITY_GG_39318_c0_g1	CRP1015	Defensin/DEFL
TRINITY_GG_40208_c6_g1	CRP1015	Defensin/DEFL
TRINITY_GG_55548_c0_g1	CRP1015	Defensin/DEFL
TRINITY_GG_127777_c3_g1	CRP1025	Defensin/DEFL
TRINITY_GG_31166_c0_g1	CRP1025	Defensin/DEFL
TRINITY_GG_44581_c0_g1	CRP1025	Defensin/DEFL
TRINITY_GG_50696_c10_g1	CRP1025	Defensin/DEFL
TRINITY_GG_29437_c0_g1	CRP1030	Defensin/DEFL
TRINITY_GG_81852_c0_g1	CRP1030	Defensin/DEFL
TRINITY_GG_79003_c19_g1	CRP1100	Defensin/DEFL

Appendix

Transcript ID	CRP Class	CRP Description
TRINITY_GG_79003_c21_g1	CRP1100	Defensin/DEFL
TRINITY_GG_118171_c2_g1	CRP1110	Defensin/DEFL
TRINITY_GG_76224_c0_g2	CRP1110	Defensin/DEFL
TRINITY_GG_76233_c1_g1	CRP1110	Defensin/DEFL
TRINITY_GG_76236_c0_g2	CRP1110	Defensin/DEFL
TRINITY_GG_76239_c0_g1	CRP1110	Defensin/DEFL
TRINITY_GG_142728_c0_g1	CRP1140	Defensin/DEFL
TRINITY_GG_79003_c32_g1	CRP1150	Defensin/DEFL
TRINITY_GG_92887_c12_g1	CRP1150	Defensin/DEFL
TRINITY_GG_65569_c1_g1	CRP1190	Defensin/DEFL
TRINITY_GG_79003_c4_g1	CRP1250	Defensin/DEFL
TRINITY_GG_17116_c0_g1	CRP1600	no-name
TRINITY_GG_17118_c0_g1	CRP1600	no-name
TRINITY_GG_9494_c0_g1	CRP1600	no-name
TRINITY_GG_19334_c0_g1	CRP1603	no-name
TRINITY_GG_78131_c0_g1	CRP1603	no-name
TRINITY_GG_93755_c2_g1	CRP1603	no-name
TRINITY_GG_94824_c0_g1	CRP1603	no-name
TRINITY_GG_9495_c0_g1	CRP1603	no-name
TRINITY_GG_9495_c0_g2	CRP1603	no-name
TRINITY_GG_5837_c16_g1	CRP1605	no-name
TRINITY_GG_61539_c0_g1	CRP1605	no-name
TRINITY_GG_61549_c0_g1	CRP1605	no-name
TRINITY_GG_133272_c6_g1	CRP1770	RALF
TRINITY_GG_130069_c0_g1	CRP1780	RALF
TRINITY_GG_126557_c0_g1	CRP1820	RALF
TRINITY_GG_126557_c0_g2	CRP1820	RALF
TRINITY_GG_135432_c0_g1	CRP1820	RALF
TRINITY_GG_135432_c0_g2	CRP1820	RALF
TRINITY_GG_137790_c0_g1	CRP1820	RALF
TRINITY_GG_137790_c0_g2	CRP1820	RALF
TRINITY_GG_60927_c0_g1	CRP1820	RALF
TRINITY_GG_97098_c0_g1	CRP1820	RALF
TRINITY_GG_141010_c0_g1	CRP1830	RALF
TRINITY_GG_29453_c0_g1	CRP1830	RALF
TRINITY_GG_51086_c0_g1	CRP1830	RALF
TRINITY_GG_51086_c0_g2	CRP1830	RALF
TRINITY_GG_32158_c0_g1	CRP1840	RALF
TRINITY_GG_79315_c0_g1	CRP1840	RALF
TRINITY_GG_79457_c0_g1	CRP1840	RALF
TRINITY_GG_10692_c0_g1	CRP1855	RALF
TRINITY_GG_10692_c0_g2	CRP1855	RALF
TRINITY_GG_44915_c0_g1	CRP1855	RALF
TRINITY_GG_49243_c0_g1	CRP1855	RALF
TRINITY_GG_6829_c0_g1	CRP1855	RALF
TRINITY_GG_6829_c0_g2	CRP1855	RALF
TRINITY_GG_70516_c0_g1	CRP1855	RALF
TRINITY_GG_73373_c0_g1	CRP1855	RALF
TRINITY_GG_79464_c0_g1	CRP1855	RALF
TRINITY_GG_128768_c0_g1	CRP1860	RALF
TRINITY_GG_128768_c0_g2	CRP1860	RALF
TRINITY_GG_131689_c0_g2	CRP1860	RALF
TRINITY_GG_136996_c0_g1	CRP1885	RALF
TRINITY_GG_30894_c0_g1	CRP1915	RALF
TRINITY_GG_32538_c3_g1	CRP1915	RALF

Transcript ID	CRP Class	CRP Description
TRINITY_GG_123358_c1_g1	CRP1920	RALF
TRINITY_GG_13554_c0_g1	CRP1920	RALF
TRINITY_GG_4798_c0_g1	CRP1920	RALF
TRINITY_GG_97869_c3_g1	CRP1920	RALF
TRINITY_GG_102725_c0_g1	CRP1935	RALF
TRINITY_GG_92192_c0_g1	CRP1935	RALF
TRINITY_GG_131689_c0_g1	CRP1950	RALF
TRINITY_GG_14587_c0_g1	CRP1985	RALF
TRINITY_GG_78366_c21_g1	CRP1985	RALF
TRINITY_GG_122545_c0_g1	CRP2030	RALF
TRINITY_GG_47067_c1_g1	CRP2030	RALF
TRINITY_GG_58322_c0_g1	CRP2030	RALF
TRINITY_GG_27599_c0_g1	CRP2210	Thionin
TRINITY_GG_42697_c0_g2	CRP2210	Thionin
TRINITY_GG_86826_c0_g1	CRP2210	Thionin
TRINITY_GG_42697_c0_g3	CRP2220	Thionin
TRINITY_GG_76064_c0_g1	CRP2220	Thionin
TRINITY_GG_112168_c0_g1	CRP2335	Thionin
TRINITY_GG_123888_c0_g1	CRP2340	Thionin
TRINITY_GG_96492_c0_g1	CRP2340	Thionin
TRINITY_GG_96492_c0_g2	CRP2340	Thionin
TRINITY_GG_110623_c0_g1	CRP2350	Thionin
TRINITY_GG_111159_c4_g1	CRP2350	Thionin
TRINITY_GG_111193_c0_g1	CRP2350	Thionin
TRINITY_GG_16386_c0_g1	CRP2350	Thionin
TRINITY_GG_61571_c0_g1	CRP2350	Thionin
TRINITY_GG_129697_c3_g1	CRP2420	Thionin
TRINITY_GG_57910_c0_g1	CRP2420	Thionin
TRINITY_GG_57910_c0_g2	CRP2420	Thionin
TRINITY_GG_67655_c4_g1	CRP2420	Thionin
TRINITY_GG_120730_c0_g1	CRP2480	Thionin
TRINITY_GG_9756_c0_g1	CRP2480	Thionin
TRINITY_GG_103356_c1_g1	CRP2490	Thionin
TRINITY_GG_134693_c0_g2	CRP2490	Thionin
TRINITY_GG_55646_c1_g1	CRP2490	Thionin
TRINITY_GG_104321_c2_g2	CRP2510	Thionin
TRINITY_GG_104321_c2_g3	CRP2510	Thionin
TRINITY_GG_119877_c1_g1	CRP2510	Thionin
TRINITY_GG_24943_c0_g1	CRP2510	Thionin
TRINITY_GG_24943_c0_g2	CRP2510	Thionin
TRINITY_GG_25483_c1_g1	CRP2510	Thionin
TRINITY_GG_31423_c0_g1	CRP2510	Thionin
TRINITY_GG_35048_c0_g1	CRP2510	Thionin
TRINITY_GG_35048_c0_g2	CRP2510	Thionin
TRINITY_GG_59790_c0_g2	CRP2510	Thionin
TRINITY_GG_104560_c2_g1	CRP2700	GASA/GAST/Snakin
TRINITY_GG_104560_c9_g1	CRP2700	GASA/GAST/Snakin
TRINITY_GG_105489_c0_g1	CRP2700	GASA/GAST/Snakin
TRINITY_GG_108379_c0_g1	CRP2700	GASA/GAST/Snakin
TRINITY_GG_110258_c5_g1	CRP2700	GASA/GAST/Snakin
TRINITY_GG_114939_c0_g1	CRP2700	GASA/GAST/Snakin
TRINITY_GG_114939_c0_g2	CRP2700	GASA/GAST/Snakin
TRINITY_GG_11858_c1_g1	CRP2700	GASA/GAST/Snakin
TRINITY_GG_121584_c0_g1	CRP2700	GASA/GAST/Snakin
TRINITY_GG_121953_c0_g2	CRP2700	GASA/GAST/Snakin

Transcript ID	CRP Class	CRP Description
TRINITY_GG_121953_c0_g4	CRP2700	GASA/GAST/Snakin
TRINITY_GG_125286_c5_g1	CRP2700	GASA/GAST/Snakin
TRINITY_GG_128146_c19_g1	CRP2700	GASA/GAST/Snakin
TRINITY_GG_128796_c0_g1	CRP2700	GASA/GAST/Snakin
TRINITY_GG_13137_c1_g1	CRP2700	GASA/GAST/Snakin
TRINITY_GG_134437_c1_g1	CRP2700	GASA/GAST/Snakin
TRINITY_GG_13479_c0_g3	CRP2700	GASA/GAST/Snakin
TRINITY_GG_13479_c0_g4	CRP2700	GASA/GAST/Snakin
TRINITY_GG_138709_c0_g1	CRP2700	GASA/GAST/Snakin
TRINITY_GG_144671_c1_g1	CRP2700	GASA/GAST/Snakin
TRINITY_GG_23743_c0_g2	CRP2700	GASA/GAST/Snakin
TRINITY_GG_24184_c0_g1	CRP2700	GASA/GAST/Snakin
TRINITY_GG_24184_c0_g2	CRP2700	GASA/GAST/Snakin
TRINITY_GG_24184_c0_g3	CRP2700	GASA/GAST/Snakin
TRINITY_GG_31271_c0_g1	CRP2700	GASA/GAST/Snakin
TRINITY_GG_31271_c0_g2	CRP2700	GASA/GAST/Snakin
TRINITY_GG_37212_c1_g1	CRP2700	GASA/GAST/Snakin
TRINITY_GG_37913_c0_g1	CRP2700	GASA/GAST/Snakin
TRINITY_GG_45820_c0_g1	CRP2700	GASA/GAST/Snakin
TRINITY_GG_46184_c1_g1	CRP2700	GASA/GAST/Snakin
TRINITY_GG_47540_c0_g1	CRP2700	GASA/GAST/Snakin
TRINITY_GG_53976_c0_g2	CRP2700	GASA/GAST/Snakin
TRINITY_GG_63540_c0_g1	CRP2700	GASA/GAST/Snakin
TRINITY_GG_63540_c0_g2	CRP2700	GASA/GAST/Snakin
TRINITY_GG_63540_c0_g3	CRP2700	GASA/GAST/Snakin
TRINITY_GG_65385_c0_g1	CRP2700	GASA/GAST/Snakin
TRINITY_GG_65615_c1_g1	CRP2700	GASA/GAST/Snakin
TRINITY_GG_68306_c0_g1	CRP2700	GASA/GAST/Snakin
TRINITY_GG_69462_c9_g1	CRP2700	GASA/GAST/Snakin
TRINITY_GG_70618_c0_g1	CRP2700	GASA/GAST/Snakin
TRINITY_GG_72799_c2_g1	CRP2700	GASA/GAST/Snakin
TRINITY_GG_77890_c1_g1	CRP2700	GASA/GAST/Snakin
TRINITY_GG_8728_c0_g1	CRP2700	GASA/GAST/Snakin
TRINITY_GG_9707_c0_g1	CRP2700	GASA/GAST/Snakin
TRINITY_GG_137955_c0_g1	CRP2820	Root cap/LEA
TRINITY_GG_49565_c0_g1	CRP2820	Root cap/LEA
TRINITY_GG_83352_c1_g1	CRP2820	Root cap/LEA
TRINITY_GG_85399_c2_g1	CRP2820	Root cap/LEA
TRINITY_GG_99379_c4_g1	CRP2820	Root cap/LEA
TRINITY_GG_132560_c0_g1	CRP2830	Root cap/LEA
TRINITY_GG_18486_c0_g1	CRP2830	Root cap/LEA
TRINITY_GG_85399_c3_g1	CRP2840	Root cap/LEA
TRINITY_GG_145382_c1_g1	CRP2850	Root cap/LEA
TRINITY_GG_49579_c0_g1	CRP2850	Root cap/LEA
TRINITY_GG_83348_c0_g1	CRP2850	Root cap/LEA
TRINITY_GG_117986_c0_g1	CRP2855	no-name
TRINITY_GG_59905_c0_g1	CRP2855	no-name
TRINITY_GG_116206_c6_g1	CRP2860	no-name
TRINITY_GG_29616_c0_g1	CRP2865	no-name
TRINITY_GG_58693_c0_g1	CRP2865	no-name
TRINITY_GG_65316_c0_g1	CRP2865	no-name
TRINITY_GG_50133_c0_g1	CRP2980	Antimicrobial peptide MBP-1
TRINITY_GG_106737_c0_g1	CRP3000	Antimicrobial peptide MBP-1
TRINITY_GG_106737_c0_g2	CRP3000	Antimicrobial peptide MBP-1
TRINITY_GG_132752_c0_g1	CRP3020	no-name

Transcript ID	CRP Class	CRP Description
TRINITY_GG_22546_c0_g1	CRP3020	no-name
TRINITY_GG_47107_c0_g1	CRP3020	no-name
TRINITY_GG_89837_c0_g1	CRP3020	no-name
TRINITY_GG_89841_c0_g1	CRP3020	no-name
TRINITY_GG_4069_c1_g3	CRP3040	no-name
TRINITY_GG_57100_c0_g1	CRP3040	no-name
TRINITY_GG_35387_c0_g1	CRP3080	Stig1
TRINITY_GG_56186_c0_g2	CRP3080	Stig1
TRINITY_GG_56198_c0_g1	CRP3080	Stig1
TRINITY_GG_56198_c0_g2	CRP3080	Stig1
TRINITY_GG_61188_c0_g1	CRP3080	Stig1
TRINITY_GG_78483_c0_g1	CRP3080	Stig1
TRINITY_GG_86369_c0_g2	CRP3210	no-name
TRINITY_GG_86369_c0_g4	CRP3210	no-name
TRINITY_GG_102795_c1_g1	CRP3330	Pollen Ole e I
TRINITY_GG_124241_c1_g2	CRP3330	Pollen Ole e I
TRINITY_GG_2730_c0_g1	CRP3330	Pollen Ole e I
TRINITY_GG_56981_c0_g1	CRP3330	Pollen Ole e I
TRINITY_GG_81458_c0_g1	CRP3330	Pollen Ole e I
TRINITY_GG_9017_c0_g1	CRP3330	Pollen Ole e I
TRINITY_GG_93131_c1_g1	CRP3330	Pollen Ole e I
TRINITY_GG_124121_c5_g1	CRP3340	Pollen Ole e I
TRINITY_GG_124241_c1_g1	CRP3340	Pollen Ole e I
TRINITY_GG_106608_c0_g1	CRP3360	Pollen Ole e I
TRINITY_GG_19632_c1_g1	CRP3360	Pollen Ole e I
TRINITY_GG_36589_c2_g1	CRP3360	Pollen Ole e I
TRINITY_GG_44775_c0_g1	CRP3360	Pollen Ole e I
TRINITY_GG_61770_c2_g1	CRP3360	Pollen Ole e I
TRINITY_GG_70266_c0_g1	CRP3360	Pollen Ole e I
TRINITY_GG_88540_c4_g1	CRP3360	Pollen Ole e I
TRINITY_GG_106609_c1_g1	CRP3370	Pollen Ole e I
TRINITY_GG_138900_c0_g1	CRP3370	Pollen Ole e I
TRINITY_GG_36589_c1_g1	CRP3370	Pollen Ole e I
TRINITY_GG_64603_c0_g1	CRP3370	Pollen Ole e I
TRINITY_GG_106269_c0_g1	CRP3375	Pollen Ole e I
TRINITY_GG_130591_c13_g1	CRP3375	Pollen Ole e I
TRINITY_GG_130591_c13_g2	CRP3375	Pollen Ole e I
TRINITY_GG_33040_c0_g1	CRP3375	Pollen Ole e I
TRINITY_GG_3917_c1_g1	CRP3375	Pollen Ole e I
TRINITY_GG_48006_c0_g1	CRP3375	Pollen Ole e I
TRINITY_GG_48006_c0_g3	CRP3375	Pollen Ole e I
TRINITY_GG_56460_c0_g1	CRP3375	Pollen Ole e I
TRINITY_GG_77361_c1_g1	CRP3375	Pollen Ole e I
TRINITY_GG_13133_c1_g1	CRP3380	Pollen Ole e I
TRINITY_GG_93150_c0_g1	CRP3380	Pollen Ole e I
TRINITY_GG_93150_c0_g2	CRP3380	Pollen Ole e I
TRINITY_GG_106603_c2_g1	CRP3390	Pollen Ole e I
TRINITY_GG_29191_c4_g1	CRP3390	Pollen Ole e I
TRINITY_GG_78340_c0_g2	CRP3390	Pollen Ole e I
TRINITY_GG_7761_c0_g1	CRP3400	Pollen Ole e I
TRINITY_GG_84383_c0_g1	CRP3400	Pollen Ole e I
TRINITY_GG_31663_c22_g1	CRP3410	Pollen Ole e I
TRINITY_GG_56221_c0_g1	CRP3420	Pollen Ole e I
TRINITY_GG_56221_c0_g2	CRP3420	Pollen Ole e I
TRINITY_GG_102795_c0_g1	CRP3430	Pollen Ole e I

Appendix

Transcript ID	CRP Class	CRP Description
TRINITY_GG_22826_c1_g1	CRP3430	Pollen Ole e I
TRINITY_GG_12478_c0_g1	CRP3440	Pollen Ole e I
TRINITY_GG_86962_c1_g1	CRP3440	Pollen Ole e I
TRINITY_GG_127687_c1_g1	CRP3460	Pollen Ole e I
TRINITY_GG_33736_c1_g1	CRP3460	Pollen Ole e I
TRINITY_GG_67368_c0_g1	CRP3460	Pollen Ole e I
TRINITY_GG_92504_c0_g1	CRP3460	Pollen Ole e I
TRINITY_GG_104814_c1_g1	CRP3470	Pollen Ole e I
TRINITY_GG_116142_c2_g1	CRP3470	Pollen Ole e I
TRINITY_GG_53805_c1_g1	CRP3470	Pollen Ole e I
TRINITY_GG_54117_c1_g1	CRP3470	Pollen Ole e I
TRINITY_GG_57839_c1_g1	CRP3470	Pollen Ole e I
TRINITY_GG_94075_c0_g1	CRP3480	Pollen Ole e I
TRINITY_GG_22095_c1_g1	CRP3500	Pollen Ole e I
TRINITY_GG_85304_c1_g1	CRP3510	Pollen Ole e I
TRINITY_GG_140737_c6_g1	CRP3600	LTP/2S Albumin/ECA 1
TRINITY_GG_143255_c6_g1	CRP3600	LTP/2S Albumin/ECA 1
TRINITY_GG_143255_c6_g2	CRP3600	LTP/2S Albumin/ECA 1
TRINITY_GG_84764_c0_g1	CRP3600	LTP/2S Albumin/ECA 1
TRINITY_GG_124100_c0_g1	CRP3610	LTP/2S Albumin/ECA 1
TRINITY_GG_139263_c1_g1	CRP3610	LTP/2S Albumin/ECA 1
TRINITY_GG_139263_c1_g2	CRP3610	LTP/2S Albumin/ECA 1
TRINITY_GG_66126_c0_g1	CRP3610	LTP/2S Albumin/ECA 1
TRINITY_GG_77780_c0_g1	CRP3610	LTP/2S Albumin/ECA 1
TRINITY_GG_82652_c0_g1	CRP3610	LTP/2S Albumin/ECA 1
TRINITY_GG_124114_c0_g1	CRP3620	LTP/2S Albumin/ECA 1
TRINITY_GG_140741_c0_g1	CRP3620	LTP/2S Albumin/ECA 1
TRINITY_GG_82642_c0_g1	CRP3620	LTP/2S Albumin/ECA 1
TRINITY_GG_84727_c0_g1	CRP3620	LTP/2S Albumin/ECA 1
TRINITY_GG_66136_c0_g1	CRP3640	LTP/2S Albumin/ECA 1
TRINITY_GG_109205_c0_g1	CRP3660	LTP/2S Albumin/ECA 1
TRINITY_GG_127545_c0_g1	CRP3660	LTP/2S Albumin/ECA 1
TRINITY_GG_139263_c4_g1	CRP3660	LTP/2S Albumin/ECA 1
TRINITY_GG_27988_c0_g1	CRP3660	LTP/2S Albumin/ECA 1
TRINITY_GG_19444_c0_g1	CRP3700	LTP/2S Albumin/ECA 1
TRINITY_GG_55782_c0_g1	CRP3700	LTP/2S Albumin/ECA 1
TRINITY_GG_56290_c2_g1	CRP3700	LTP/2S Albumin/ECA 1
TRINITY_GG_104506_c0_g1	CRP3710	LTP/2S Albumin/ECA 1
TRINITY_GG_119364_c0_g1	CRP3710	LTP/2S Albumin/ECA 1
TRINITY_GG_73481_c0_g1	CRP3710	LTP/2S Albumin/ECA 1
TRINITY_GG_102600_c0_g1	CRP3740	LTP/2S Albumin/ECA 1
TRINITY_GG_145620_c0_g1	CRP3740	LTP/2S Albumin/ECA 1
TRINITY_GG_95625_c0_g1	CRP3740	LTP/2S Albumin/ECA 1
TRINITY_GG_56852_c0_g1	CRP3800	LTP/2S Albumin/ECA 1
TRINITY_GG_94402_c0_g1	CRP3860	LTP/2S Albumin/ECA 1
TRINITY_GG_119884_c0_g1	CRP3885	LTP/2S Albumin/ECA 1
TRINITY_GG_78364_c0_g1	CRP3890	LTP/2S Albumin/ECA 1
TRINITY_GG_124111_c0_g5	CRP3920	LTP/2S Albumin/ECA 1
TRINITY_GG_112090_c1_g1	CRP3925	LTP/2S Albumin/ECA 1
TRINITY_GG_53673_c0_g1	CRP3925	LTP/2S Albumin/ECA 1
TRINITY_GG_54281_c3_g1	CRP3925	LTP/2S Albumin/ECA 1
TRINITY_GG_5930_c0_g1	CRP3925	LTP/2S Albumin/ECA 1
TRINITY_GG_63328_c0_g1	CRP3925	LTP/2S Albumin/ECA 1
TRINITY_GG_53501_c0_g1	CRP3940	LTP/2S Albumin/ECA 1
TRINITY_GG_103103_c0_g1	CRP3990	LTP/2S Albumin/ECA 1

Transcript ID	CRP Class	CRP Description
TRINITY_GG_103103_c0_g2	CRP3990	LTP/2S Albumin/ECA 1
TRINITY_GG_103103_c0_g3	CRP3990	LTP/2S Albumin/ECA 1
TRINITY_GG_108169_c0_g1	CRP3990	LTP/2S Albumin/ECA 1
TRINITY_GG_35045_c0_g3	CRP3990	LTP/2S Albumin/ECA 1
TRINITY_GG_87294_c1_g1	CRP3990	LTP/2S Albumin/ECA 1
TRINITY_GG_35045_c0_g1	CRP4010	LTP/2S Albumin/ECA 1
TRINITY_GG_43565_c0_g1	CRP4040	LTP/2S Albumin/ECA 1
TRINITY_GG_55197_c0_g1	CRP4040	LTP/2S Albumin/ECA 1
TRINITY_GG_55197_c0_g2	CRP4040	LTP/2S Albumin/ECA 1
TRINITY_GG_128222_c0_g1	CRP4050	LTP/2S Albumin/ECA 1
TRINITY_GG_67488_c0_g1	CRP4050	LTP/2S Albumin/ECA 1
TRINITY_GG_10180_c0_g1	CRP4060	LTP/2S Albumin/ECA 1
TRINITY_GG_104321_c3_g2	CRP4080	LTP/2S Albumin/ECA 1
TRINITY_GG_104321_c3_g3	CRP4080	LTP/2S Albumin/ECA 1
TRINITY_GG_142543_c2_g1	CRP4080	LTP/2S Albumin/ECA 1
TRINITY_GG_3359_c0_g1	CRP4080	LTP/2S Albumin/ECA 1
TRINITY_GG_68768_c0_g2	CRP4080	LTP/2S Albumin/ECA 1
TRINITY_GG_18367_c5_g1	CRP4090	LTP/2S Albumin/ECA 1
TRINITY_GG_136753_c22_g2	CRP4120	LTP/2S Albumin/ECA 1
TRINITY_GG_454_c0_g1	CRP4120	LTP/2S Albumin/ECA 1
TRINITY_GG_81987_c0_g1	CRP4120	LTP/2S Albumin/ECA 1
TRINITY_GG_81987_c0_g2	CRP4120	LTP/2S Albumin/ECA 1
TRINITY_GG_92570_c0_g1	CRP4140	LTP/2S Albumin/ECA 1
TRINITY_GG_142145_c0_g2	CRP4170	LTP/2S Albumin/ECA 1
TRINITY_GG_77818_c3_g1	CRP4170	LTP/2S Albumin/ECA 1
TRINITY_GG_99800_c0_g2	CRP4170	LTP/2S Albumin/ECA 1
TRINITY_GG_32142_c0_g1	CRP4180	LTP/2S Albumin/ECA 1
TRINITY_GG_50890_c1_g1	CRP4180	LTP/2S Albumin/ECA 1
TRINITY_GG_124418_c0_g1	CRP4190	LTP/2S Albumin/ECA 1
TRINITY_GG_132322_c0_g1	CRP4190	LTP/2S Albumin/ECA 1
TRINITY_GG_99009_c3_g1	CRP4190	LTP/2S Albumin/ECA 1
TRINITY_GG_114999_c0_g1	CRP4200	LTP/2S Albumin/ECA 1
TRINITY_GG_101078_c0_g1	CRP4210	LTP/2S Albumin/ECA 1
TRINITY_GG_104321_c1_g1	CRP4210	LTP/2S Albumin/ECA 1
TRINITY_GG_128226_c24_g1	CRP4210	LTP/2S Albumin/ECA 1
TRINITY_GG_35280_c1_g1	CRP4210	LTP/2S Albumin/ECA 1
TRINITY_GG_81414_c0_g1	CRP4210	LTP/2S Albumin/ECA 1
TRINITY_GG_137489_c0_g1	CRP4220	LTP/2S Albumin/ECA 1
TRINITY_GG_78744_c0_g1	CRP4220	LTP/2S Albumin/ECA 1
TRINITY_GG_78744_c0_g2	CRP4220	LTP/2S Albumin/ECA 1
TRINITY_GG_137995_c0_g1	CRP4240	LTP/2S Albumin/ECA 1
TRINITY_GG_57345_c0_g2	CRP4240	LTP/2S Albumin/ECA 1
TRINITY_GG_59140_c1_g2	CRP4240	LTP/2S Albumin/ECA 1
TRINITY_GG_95482_c1_g1	CRP4240	LTP/2S Albumin/ECA 1
TRINITY_GG_145389_c0_g1	CRP4290	LTP/2S Albumin/ECA 1
TRINITY_GG_113221_c0_g1	CRP4310	LTP/2S Albumin/ECA 1
TRINITY_GG_118899_c9_g1	CRP4310	LTP/2S Albumin/ECA 1
TRINITY_GG_122136_c2_g1	CRP4310	LTP/2S Albumin/ECA 1
TRINITY_GG_46248_c0_g1	CRP4310	LTP/2S Albumin/ECA 1
TRINITY_GG_33122_c1_g1	CRP4340	LTP/2S Albumin/ECA 1
TRINITY_GG_68768_c0_g1	CRP4340	LTP/2S Albumin/ECA 1
TRINITY_GG_53126_c0_g1	CRP4350	LTP/2S Albumin/ECA 1
TRINITY_GG_35044_c0_g1	CRP4380	LTP/2S Albumin/ECA 1
TRINITY_GG_88151_c1_g1	CRP4380	LTP/2S Albumin/ECA 1
TRINITY_GG_100111_c0_g1	CRP4410	LTP/2S Albumin/ECA 1

Appendix

Transcript ID	CRP Class	CRP Description
TRINITY_GG_41909_c0_g1	CRP4450	LTP/2S Albumin/ECA 1
TRINITY_GG_64907_c0_g2	CRP4450	LTP/2S Albumin/ECA 1
TRINITY_GG_136753_c50_g1	CRP4490	LTP/2S Albumin/ECA 1
TRINITY_GG_48536_c1_g1	CRP4490	LTP/2S Albumin/ECA 1
TRINITY_GG_53671_c0_g1	CRP4490	LTP/2S Albumin/ECA 1
TRINITY_GG_54133_c1_g1	CRP4490	LTP/2S Albumin/ECA 1
TRINITY_GG_40524_c0_g1	CRP4500	LTP/2S Albumin/ECA 1
TRINITY_GG_40524_c0_g2	CRP4500	LTP/2S Albumin/ECA 1
TRINITY_GG_40525_c0_g1	CRP4510	LTP/2S Albumin/ECA 1
TRINITY_GG_92570_c0_g2	CRP4510	LTP/2S Albumin/ECA 1
TRINITY_GG_38478_c0_g1	CRP4520	LTP/2S Albumin/ECA 1
TRINITY_GG_20922_c0_g1	CRP4530	LTP/2S Albumin/ECA 1
TRINITY_GG_31668_c0_g1	CRP4530	LTP/2S Albumin/ECA 1
TRINITY_GG_44807_c0_g1	CRP4540	LTP/2S Albumin/ECA 1
TRINITY_GG_52680_c1_g1	CRP4550	LTP/2S Albumin/ECA 1
TRINITY_GG_69704_c0_g1	CRP4550	LTP/2S Albumin/ECA 1
TRINITY_GG_69704_c0_g2	CRP4550	LTP/2S Albumin/ECA 1
TRINITY_GG_69704_c0_g3	CRP4550	LTP/2S Albumin/ECA 1
TRINITY_GG_92587_c0_g1	CRP4550	LTP/2S Albumin/ECA 1
TRINITY_GG_113_c0_g1	CRP4570	LTP/2S Albumin/ECA 1
TRINITY_GG_121898_c1_g1	CRP4570	LTP/2S Albumin/ECA 1
TRINITY_GG_136753_c22_g1	CRP4570	LTP/2S Albumin/ECA 1
TRINITY_GG_32142_c3_g1	CRP4570	LTP/2S Albumin/ECA 1
TRINITY_GG_34123_c2_g1	CRP4570	LTP/2S Albumin/ECA 1
TRINITY_GG_46718_c1_g1	CRP4570	LTP/2S Albumin/ECA 1
TRINITY_GG_46926_c0_g1	CRP4570	LTP/2S Albumin/ECA 1
TRINITY_GG_54279_c0_g1	CRP4570	LTP/2S Albumin/ECA 1
TRINITY_GG_97219_c0_g1	CRP4570	LTP/2S Albumin/ECA 1
TRINITY_GG_97219_c1_g1	CRP4570	LTP/2S Albumin/ECA 1
TRINITY_GG_13429_c0_g1	CRP4580	LTP/2S Albumin/ECA 1
TRINITY_GG_112001_c0_g1	CRP4620	LTP/2S Albumin/ECA 1
TRINITY_GG_112001_c0_g2	CRP4620	LTP/2S Albumin/ECA 1
TRINITY_GG_136437_c0_g1	CRP4625	LTP/2S Albumin/ECA 1
TRINITY_GG_39070_c0_g1	CRP4625	LTP/2S Albumin/ECA 1
TRINITY_GG_61136_c0_g1	CRP4625	LTP/2S Albumin/ECA 1
TRINITY_GG_104321_c0_g2	CRP4630	LTP/2S Albumin/ECA 1
TRINITY_GG_140274_c0_g1	CRP4630	LTP/2S Albumin/ECA 1
TRINITY_GG_142579_c1_g1	CRP4630	LTP/2S Albumin/ECA 1
TRINITY_GG_15094_c0_g1	CRP4630	LTP/2S Albumin/ECA 1
TRINITY_GG_34120_c0_g1	CRP4630	LTP/2S Albumin/ECA 1
TRINITY_GG_34120_c0_g2	CRP4630	LTP/2S Albumin/ECA 1
TRINITY_GG_53670_c0_g1	CRP4630	LTP/2S Albumin/ECA 1
TRINITY_GG_86148_c1_g1	CRP4630	LTP/2S Albumin/ECA 1
TRINITY_GG_97219_c0_g2	CRP4630	LTP/2S Albumin/ECA 1
TRINITY_GG_17433_c0_g1	CRP4640	LTP/2S Albumin/ECA 1
TRINITY_GG_2479_c0_g1	CRP4640	LTP/2S Albumin/ECA 1
TRINITY_GG_31986_c0_g1	CRP4640	LTP/2S Albumin/ECA 1
TRINITY_GG_36534_c0_g1	CRP4640	LTP/2S Albumin/ECA 1
TRINITY_GG_133986_c2_g2	CRP4650	LTP/2S Albumin/ECA 1
TRINITY_GG_1946_c0_g2	CRP4650	LTP/2S Albumin/ECA 1
TRINITY_GG_1946_c0_g3	CRP4650	LTP/2S Albumin/ECA 1
TRINITY_GG_84227_c0_g1	CRP4650	LTP/2S Albumin/ECA 1
TRINITY_GG_89237_c2_g1	CRP4650	LTP/2S Albumin/ECA 1
TRINITY_GG_54281_c2_g1	CRP4660	LTP/2S Albumin/ECA 1
TRINITY_GG_57413_c0_g1	CRP4660	LTP/2S Albumin/ECA 1

Transcript ID	CRP Class	CRP Description
TRINITY_GG_92577_c0_g1	CRP4660	LTP/2S Albumin/ECA 1
TRINITY_GG_104363_c0_g1	CRP4670	LTP/2S Albumin/ECA 1
TRINITY_GG_137673_c0_g1	CRP4670	LTP/2S Albumin/ECA 1
TRINITY_GG_137673_c0_g2	CRP4670	LTP/2S Albumin/ECA 1
TRINITY_GG_15094_c0_g2	CRP4670	LTP/2S Albumin/ECA 1
TRINITY_GG_35261_c0_g1	CRP4670	LTP/2S Albumin/ECA 1
TRINITY_GG_57_c1_g1	CRP4680	LTP/2S Albumin/ECA 1
TRINITY_GG_9121_c0_g1	CRP4680	LTP/2S Albumin/ECA 1
TRINITY_GG_118185_c0_g1	CRP4690	LTP/2S Albumin/ECA 1
TRINITY_GG_34321_c11_g1	CRP4690	LTP/2S Albumin/ECA 1
TRINITY_GG_71764_c2_g1	CRP4690	LTP/2S Albumin/ECA 1
TRINITY_GG_102377_c2_g1	CRP4710	LTP/2S Albumin/ECA 1
TRINITY_GG_32627_c0_g1	CRP4710	LTP/2S Albumin/ECA 1
TRINITY_GG_32627_c0_g2	CRP4710	LTP/2S Albumin/ECA 1
TRINITY_GG_99800_c0_g1	CRP4710	LTP/2S Albumin/ECA 1
TRINITY_GG_115915_c0_g1	CRP4720	LTP/2S Albumin/ECA 1
TRINITY_GG_75394_c1_g1	CRP4720	LTP/2S Albumin/ECA 1
TRINITY_GG_1063_c0_g1	CRP4750	LTP/2S Albumin/ECA 1
TRINITY_GG_35152_c1_g1	CRP4750	LTP/2S Albumin/ECA 1
TRINITY_GG_47501_c0_g1	CRP4750	LTP/2S Albumin/ECA 1
TRINITY_GG_97982_c2_g1	CRP4750	LTP/2S Albumin/ECA 1
TRINITY_GG_101589_c1_g2	CRP4780	LTP/2S Albumin/ECA 1
TRINITY_GG_101589_c4_g1	CRP4780	LTP/2S Albumin/ECA 1
TRINITY_GG_102776_c0_g1	CRP4780	LTP/2S Albumin/ECA 1
TRINITY_GG_10704_c0_g1	CRP4780	LTP/2S Albumin/ECA 1
TRINITY_GG_10704_c0_g2	CRP4780	LTP/2S Albumin/ECA 1
TRINITY_GG_10704_c0_g4	CRP4780	LTP/2S Albumin/ECA 1
TRINITY_GG_12571_c0_g1	CRP4780	LTP/2S Albumin/ECA 1
TRINITY_GG_126947_c5_g1	CRP4780	LTP/2S Albumin/ECA 1
TRINITY_GG_128872_c3_g1	CRP4780	LTP/2S Albumin/ECA 1
TRINITY_GG_135275_c0_g1	CRP4780	LTP/2S Albumin/ECA 1
TRINITY_GG_38700_c0_g1	CRP4780	LTP/2S Albumin/ECA 1
TRINITY_GG_38700_c3_g1	CRP4780	LTP/2S Albumin/ECA 1
TRINITY_GG_5464_c0_g1	CRP4780	LTP/2S Albumin/ECA 1
TRINITY_GG_5857_c0_g1	CRP4780	LTP/2S Albumin/ECA 1
TRINITY_GG_5857_c0_g2	CRP4780	LTP/2S Albumin/ECA 1
TRINITY_GG_62384_c0_g1	CRP4780	LTP/2S Albumin/ECA 1
TRINITY_GG_62384_c0_g2	CRP4780	LTP/2S Albumin/ECA 1
TRINITY_GG_104631_c0_g1	CRP4810	LTP/2S Albumin/ECA 1
TRINITY_GG_111575_c0_g1	CRP4810	LTP/2S Albumin/ECA 1
TRINITY_GG_114221_c0_g2	CRP4810	LTP/2S Albumin/ECA 1
TRINITY_GG_114221_c0_g3	CRP4810	LTP/2S Albumin/ECA 1
TRINITY_GG_121310_c0_g1	CRP4810	LTP/2S Albumin/ECA 1
TRINITY_GG_128206_c0_g1	CRP4810	LTP/2S Albumin/ECA 1
TRINITY_GG_13533_c0_g1	CRP4810	LTP/2S Albumin/ECA 1
TRINITY_GG_140011_c0_g1	CRP4810	LTP/2S Albumin/ECA 1
TRINITY_GG_140703_c0_g1	CRP4810	LTP/2S Albumin/ECA 1
TRINITY_GG_57504_c0_g1	CRP4810	LTP/2S Albumin/ECA 1
TRINITY_GG_57504_c0_g2	CRP4810	LTP/2S Albumin/ECA 1
TRINITY_GG_70412_c0_g1	CRP4810	LTP/2S Albumin/ECA 1
TRINITY_GG_72383_c0_g1	CRP4810	LTP/2S Albumin/ECA 1
TRINITY_GG_72383_c0_g2	CRP4810	LTP/2S Albumin/ECA 1
TRINITY_GG_79034_c0_g1	CRP4810	LTP/2S Albumin/ECA 1
TRINITY_GG_92372_c1_g1	CRP4810	LTP/2S Albumin/ECA 1
TRINITY_GG_92372_c1_g2	CRP4810	LTP/2S Albumin/ECA 1

Appendix

Transcript ID	CRP Class	CRP Description
TRINITY_GG_92372_c1_g3	CRP4810	LTP/2S Albumin/ECA 1
TRINITY_GG_92372_c1_g4	CRP4810	LTP/2S Albumin/ECA 1
TRINITY_GG_92372_c1_g5	CRP4810	LTP/2S Albumin/ECA 1
TRINITY_GG_93507_c0_g1	CRP4810	LTP/2S Albumin/ECA 1
TRINITY_GG_94367_c0_g1	CRP4810	LTP/2S Albumin/ECA 1
TRINITY_GG_9828_c0_g1	CRP4810	LTP/2S Albumin/ECA 1
TRINITY_GG_111092_c1_g1	CRP4820	LTP/2S Albumin/ECA 1
TRINITY_GG_131905_c1_g1	CRP4820	LTP/2S Albumin/ECA 1
TRINITY_GG_135331_c0_g1	CRP4820	LTP/2S Albumin/ECA 1
TRINITY_GG_140018_c0_g1	CRP4820	LTP/2S Albumin/ECA 1
TRINITY_GG_141073_c0_g1	CRP4820	LTP/2S Albumin/ECA 1
TRINITY_GG_48528_c0_g1	CRP4820	LTP/2S Albumin/ECA 1
TRINITY_GG_48528_c0_g2	CRP4820	LTP/2S Albumin/ECA 1
TRINITY_GG_48528_c0_g3	CRP4820	LTP/2S Albumin/ECA 1
TRINITY_GG_50839_c0_g1	CRP4820	LTP/2S Albumin/ECA 1
TRINITY_GG_70400_c1_g1	CRP4820	LTP/2S Albumin/ECA 1
TRINITY_GG_70422_c0_g1	CRP4820	LTP/2S Albumin/ECA 1
TRINITY_GG_70753_c0_g1	CRP4820	LTP/2S Albumin/ECA 1
TRINITY_GG_73861_c0_g1	CRP4820	LTP/2S Albumin/ECA 1
TRINITY_GG_81163_c0_g1	CRP4820	LTP/2S Albumin/ECA 1
TRINITY_GG_81185_c0_g1	CRP4820	LTP/2S Albumin/ECA 1
TRINITY_GG_81186_c0_g1	CRP4820	LTP/2S Albumin/ECA 1
TRINITY_GG_89103_c1_g1	CRP4820	LTP/2S Albumin/ECA 1
TRINITY_GG_89109_c0_g1	CRP4820	LTP/2S Albumin/ECA 1
TRINITY_GG_118259_c0_g1	CRP4900	LTP/2S Albumin/ECA 1
TRINITY_GG_118259_c0_g2	CRP4900	LTP/2S Albumin/ECA 1
TRINITY_GG_136853_c0_g1	CRP4900	LTP/2S Albumin/ECA 1
TRINITY_GG_137671_c0_g1	CRP4900	LTP/2S Albumin/ECA 1
TRINITY_GG_4824_c0_g1	CRP4900	LTP/2S Albumin/ECA 1
TRINITY_GG_12361_c2_g1	CRP4920	LTP/2S Albumin/ECA 1
TRINITY_GG_142145_c0_g1	CRP4920	LTP/2S Albumin/ECA 1
TRINITY_GG_9121_c1_g1	CRP4920	LTP/2S Albumin/ECA 1
TRINITY_GG_104964_c0_g1	CRP4948	LTP/2S Albumin/ECA 1
TRINITY_GG_40071_c0_g1	CRP4948	LTP/2S Albumin/ECA 1
TRINITY_GG_47744_c0_g1	CRP4950	LTP/2S Albumin/ECA 1
TRINITY_GG_104955_c0_g1	CRP4962	LTP/2S Albumin/ECA 1
TRINITY_GG_35045_c0_g2	CRP4970	LTP/2S Albumin/ECA 1
TRINITY_GG_40069_c0_g1	CRP5030	LTP/2S Albumin/ECA 1
TRINITY_GG_143337_c1_g1	CRP5330	Maternally-expressed gene (MEG)/Ae1
TRINITY_GG_4055_c0_g1	CRP5330	Maternally-expressed gene (MEG)/Ae1
TRINITY_GG_60044_c0_g1	CRP5330	Maternally-expressed gene (MEG)/Ae1
TRINITY_GG_60044_c0_g3	CRP5330	Maternally-expressed gene (MEG)/Ae1
TRINITY_GG_60044_c0_g4	CRP5330	Maternally-expressed gene (MEG)/Ae1
TRINITY_GG_60044_c0_g5	CRP5330	Maternally-expressed gene (MEG)/Ae1
TRINITY_GG_7062_c2_g2	CRP5330	Maternally-expressed gene (MEG)/Ae1
TRINITY_GG_87132_c0_g1	CRP5330	Maternally-expressed gene (MEG)/Ae1
TRINITY_GG_87132_c0_g2	CRP5330	Maternally-expressed gene (MEG)/Ae1
TRINITY_GG_87132_c0_g3	CRP5330	Maternally-expressed gene (MEG)/Ae1
TRINITY_GG_48471_c0_g1	CRP5440	Maternally-expressed gene (MEG)/Ae1
TRINITY_GG_48473_c0_g1	CRP5440	Maternally-expressed gene (MEG)/Ae1
TRINITY_GG_128967_c1_g1	CRP5545	Protease inhibitor II
TRINITY_GG_128967_c1_g10	CRP5545	Protease inhibitor II
TRINITY_GG_128967_c1_g3	CRP5545	Protease inhibitor II
TRINITY_GG_128967_c1_g4	CRP5545	Protease inhibitor II
TRINITY_GG_128967_c1_g7	CRP5545	Protease inhibitor II

Transcript ID	CRP Class	CRP Description
TRINITY_GG_128967_c1_g8	CRP5545	Protease inhibitor II
TRINITY_GG_129612_c1_g1	CRP5545	Protease inhibitor II
TRINITY_GG_129612_c1_g2	CRP5545	Protease inhibitor II
TRINITY_GG_129612_c1_g3	CRP5545	Protease inhibitor II
TRINITY_GG_129612_c1_g4	CRP5545	Protease inhibitor II
TRINITY_GG_129612_c3_g1	CRP5545	Protease inhibitor II
TRINITY_GG_64700_c0_g1	CRP5545	Protease inhibitor II
TRINITY_GG_64700_c0_g2	CRP5545	Protease inhibitor II
TRINITY_GG_7964_c1_g1	CRP5545	Protease inhibitor II
TRINITY_GG_102906_c0_g1	CRP5550	Protease inhibitor II
TRINITY_GG_102906_c0_g2	CRP5550	Protease inhibitor II
TRINITY_GG_118489_c0_g1	CRP5550	Protease inhibitor II
TRINITY_GG_118512_c1_g1	CRP5550	Protease inhibitor II
TRINITY_GG_20266_c0_g1	CRP5550	Protease inhibitor II
TRINITY_GG_20437_c5_g1	CRP5550	Protease inhibitor II
TRINITY_GG_55046_c0_g1	CRP5550	Protease inhibitor II
TRINITY_GG_55046_c0_g2	CRP5550	Protease inhibitor II
TRINITY_GG_9684_c0_g1	CRP5550	Protease inhibitor II
TRINITY_GG_128967_c1_g11	CRP5560	Protease inhibitor II
TRINITY_GG_128967_c1_g6	CRP5560	Protease inhibitor II
TRINITY_GG_128967_c1_g9	CRP5560	Protease inhibitor II
TRINITY_GG_33405_c0_g1	CRP5610	Hevein
TRINITY_GG_7229_c0_g1	CRP5610	Hevein
TRINITY_GG_86948_c0_g2	CRP5610	Hevein
TRINITY_GG_81648_c0_g1	CRP5620	Hevein
TRINITY_GG_120993_c0_g1	CRP5660	Hevein
TRINITY_GG_121017_c0_g1	CRP5660	Hevein
TRINITY_GG_144679_c0_g1	CRP5660	Hevein
TRINITY_GG_18144_c0_g2	CRP5660	Hevein
TRINITY_GG_68172_c1_g1	CRP5660	Hevein
TRINITY_GG_74648_c0_g1	CRP5660	Hevein
TRINITY_GG_83833_c0_g1	CRP5660	Hevein
TRINITY_GG_121013_c0_g1	CRP5710	Hevein
TRINITY_GG_7229_c0_g2	CRP5710	Hevein
TRINITY_GG_18144_c1_g1	CRP5725	Hevein
TRINITY_GG_106565_c2_g1	CRP5740	Hevein
TRINITY_GG_127052_c0_g1	CRP5740	Hevein
TRINITY_GG_144679_c0_g2	CRP5740	Hevein
TRINITY_GG_27713_c0_g1	CRP5740	Hevein
TRINITY_GG_38575_c0_g1	CRP5740	Hevein
TRINITY_GG_52095_c0_g1	CRP5740	Hevein
TRINITY_GG_68172_c0_g1	CRP5740	Hevein
TRINITY_GG_74648_c0_g2	CRP5740	Hevein
TRINITY_GG_83831_c0_g1	CRP5740	Hevein
TRINITY_GG_86948_c0_g1	CRP5740	Hevein
TRINITY_GG_15140_c9_g1	CRP5770	Hevein
TRINITY_GG_20239_c3_g1	CRP5770	Hevein
TRINITY_GG_28551_c0_g1	CRP5770	Hevein
TRINITY_GG_33405_c1_g1	CRP5770	Hevein
TRINITY_GG_1014_c0_g3	CRP5780	Hevein
TRINITY_GG_23404_c18_g1	CRP5780	Hevein
TRINITY_GG_59481_c0_g1	CRP5780	Hevein
TRINITY_GG_107818_c0_g1	CRP5800	Hevein
TRINITY_GG_112354_c0_g1	CRP5800	Hevein
TRINITY_GG_18144_c0_g1	CRP5800	Hevein

Appendix

Transcript ID	CRP Class	CRP Description
TRINITY_GG_74648_c1_g1	CRP5800	Hevein
TRINITY_GG_81643_c0_g1	CRP5800	Hevein
TRINITY_GG_132302_c1_g1	CRP5820	Hevein
TRINITY_GG_125076_c0_g1	CRP5940	Kazal type inhibitor
TRINITY_GG_12937_c0_g2	CRP5940	Kazal type inhibitor
TRINITY_GG_133758_c0_g1	CRP5940	Kazal type inhibitor
TRINITY_GG_15605_c0_g1	CRP5940	Kazal type inhibitor
TRINITY_GG_21773_c0_g1	CRP5940	Kazal type inhibitor
TRINITY_GG_21773_c0_g2	CRP5940	Kazal type inhibitor
TRINITY_GG_6229_c1_g1	CRP5940	Kazal type inhibitor
TRINITY_GG_6229_c1_g2	CRP5940	Kazal type inhibitor
TRINITY_GG_90668_c0_g1	CRP5940	Kazal type inhibitor
TRINITY_GG_90668_c0_g2	CRP5940	Kazal type inhibitor
TRINITY_GG_35592_c0_g1	CRP6010	Kunitz type inhibitor
TRINITY_GG_8804_c3_g1	CRP6020	Kunitz type inhibitor
TRINITY_GG_138914_c0_g1	CRP6025	Kunitz type inhibitor
TRINITY_GG_39915_c0_g1	CRP6025	Kunitz type inhibitor
TRINITY_GG_135818_c0_g1	CRP6030	Kunitz type inhibitor
TRINITY_GG_117357_c0_g1	CRP6035	Kunitz type inhibitor
TRINITY_GG_41500_c0_g1	CRP6035	Kunitz type inhibitor
TRINITY_GG_89777_c0_g1	CRP6035	Kunitz type inhibitor
TRINITY_GG_105559_c0_g1	CRP6040	Kunitz type inhibitor
TRINITY_GG_52459_c0_g1	CRP6040	Kunitz type inhibitor
TRINITY_GG_6378_c0_g1	CRP6040	Kunitz type inhibitor
TRINITY_GG_8805_c2_g1	CRP6070	Kunitz type inhibitor
TRINITY_GG_135804_c0_g1	CRP6090	Kunitz type inhibitor
TRINITY_GG_8805_c2_g2	CRP6090	Kunitz type inhibitor
TRINITY_GG_135810_c0_g1	CRP6110	Kunitz type inhibitor
TRINITY_GG_53389_c0_g1	CRP6110	Kunitz type inhibitor
TRINITY_GG_8816_c0_g1	CRP6110	Kunitz type inhibitor
TRINITY_GG_8816_c0_g2	CRP6110	Kunitz type inhibitor
TRINITY_GG_13672_c0_g1	CRP6140	Kunitz type inhibitor
TRINITY_GG_1857_c0_g1	CRP6140	Kunitz type inhibitor
TRINITY_GG_39625_c0_g1	CRP6155	Kunitz type inhibitor
TRINITY_GG_8814_c0_g1	CRP6155	Kunitz type inhibitor
TRINITY_GG_8804_c2_g1	CRP6160	Kunitz type inhibitor
TRINITY_GG_8804_c4_g1	CRP6160	Kunitz type inhibitor
TRINITY_GG_8804_c1_g1	CRP6170	Kunitz type inhibitor
TRINITY_GG_135822_c0_g1	CRP6180	Kunitz type inhibitor
TRINITY_GG_135825_c0_g1	CRP6180	Kunitz type inhibitor
TRINITY_GG_8804_c0_g1	CRP6180	Kunitz type inhibitor
TRINITY_GG_118340_c3_g1	CRP6200	no-name
TRINITY_GG_118340_c3_g2	CRP6200	no-name
TRINITY_GG_124670_c0_g1	CRP6200	no-name
TRINITY_GG_126102_c1_g1	CRP6200	no-name
TRINITY_GG_30692_c0_g1	CRP6200	no-name
TRINITY_GG_84398_c0_g1	CRP6200	no-name
TRINITY_GG_106856_c2_g1	CRP6250	no-name
TRINITY_GG_122915_c2_g1	CRP6250	no-name
TRINITY_GG_122915_c2_g2	CRP6250	no-name
TRINITY_GG_45336_c0_g1	CRP6250	no-name
TRINITY_GG_126999_c0_g1	CRP6260	no-name
TRINITY_GG_20786_c2_g1	CRP6260	no-name
TRINITY_GG_40371_c2_g1	CRP6260	no-name
TRINITY_GG_106417_c0_g2	CRP6280	no-name

Transcript ID	CRP Class	CRP Description
TRINITY_GG_106417_c0_g3	CRP6280	no-name
TRINITY_GG_114206_c0_g1	CRP6280	no-name
TRINITY_GG_115378_c0_g1	CRP6280	no-name
TRINITY_GG_115378_c0_g2	CRP6280	no-name
TRINITY_GG_124914_c0_g1	CRP6280	no-name
TRINITY_GG_124914_c0_g2	CRP6280	no-name
TRINITY_GG_131507_c0_g1	CRP6280	no-name
TRINITY_GG_131507_c0_g2	CRP6280	no-name
TRINITY_GG_135012_c0_g1	CRP6280	no-name
TRINITY_GG_135012_c0_g2	CRP6280	no-name
TRINITY_GG_136464_c0_g1	CRP6280	no-name
TRINITY_GG_139906_c0_g1	CRP6280	no-name
TRINITY_GG_19332_c0_g1	CRP6280	no-name
TRINITY_GG_27057_c0_g1	CRP6280	no-name
TRINITY_GG_27057_c0_g2	CRP6280	no-name
TRINITY_GG_27057_c0_g3	CRP6280	no-name
TRINITY_GG_30402_c0_g1	CRP6280	no-name
TRINITY_GG_30402_c0_g2	CRP6280	no-name
TRINITY_GG_32974_c0_g1	CRP6280	no-name
TRINITY_GG_32974_c0_g2	CRP6280	no-name
TRINITY_GG_35281_c0_g1	CRP6280	no-name
TRINITY_GG_36812_c0_g2	CRP6280	no-name
TRINITY_GG_44950_c0_g2	CRP6280	no-name
TRINITY_GG_48870_c0_g2	CRP6280	no-name
TRINITY_GG_49353_c0_g1	CRP6280	no-name
TRINITY_GG_49353_c0_g2	CRP6280	no-name
TRINITY_GG_506_c0_g1	CRP6280	no-name
TRINITY_GG_506_c0_g3	CRP6280	no-name
TRINITY_GG_57036_c0_g1	CRP6280	no-name
TRINITY_GG_61447_c0_g2	CRP6280	no-name
TRINITY_GG_6689_c0_g1	CRP6280	no-name
TRINITY_GG_72592_c0_g1	CRP6280	no-name
TRINITY_GG_86548_c0_g2	CRP6280	no-name
TRINITY_GG_94175_c0_g1	CRP6280	no-name
TRINITY_GG_94175_c0_g2	CRP6280	no-name
TRINITY_GG_94175_c0_g3	CRP6280	no-name
TRINITY_GG_94175_c0_g4	CRP6280	no-name
TRINITY_GG_94928_c0_g1	CRP6280	no-name
TRINITY_GG_111185_c0_g1	CRP63000	no-name
TRINITY_GG_112834_c0_g1	CRP63000	no-name
TRINITY_GG_115886_c26_g1	CRP63000	no-name
TRINITY_GG_120842_c0_g1	CRP63000	no-name
TRINITY_GG_124569_c0_g1	CRP63000	no-name
TRINITY_GG_124569_c0_g2	CRP63000	no-name
TRINITY_GG_1275_c0_g1	CRP63000	no-name
TRINITY_GG_15732_c0_g1	CRP63000	no-name
TRINITY_GG_24531_c0_g1	CRP63000	no-name
TRINITY_GG_41984_c0_g1	CRP63000	no-name
TRINITY_GG_41985_c0_g1	CRP63000	no-name
TRINITY_GG_41985_c0_g2	CRP63000	no-name
TRINITY_GG_44466_c0_g1	CRP63000	no-name
TRINITY_GG_5692_c1_g1	CRP63000	no-name
TRINITY_GG_58109_c4_g1	CRP63000	no-name
TRINITY_GG_58109_c7_g1	CRP63000	no-name
TRINITY_GG_61424_c0_g1	CRP63000	no-name

Appendix

Transcript ID	CRP Class	CRP Description
TRINITY_GG_71803_c0_g1	CRP63000	no-name
TRINITY_GG_73162_c0_g1	CRP63000	no-name
TRINITY_GG_73168_c1_g1	CRP63000	no-name
TRINITY_GG_93966_c0_g1	CRP63000	no-name
TRINITY_GG_111401_c0_g1	CRP63010	no-name
TRINITY_GG_111401_c0_g2	CRP63010	no-name
TRINITY_GG_129867_c0_g1	CRP63010	no-name
TRINITY_GG_129867_c2_g1	CRP63010	no-name
TRINITY_GG_137675_c0_g1	CRP63010	no-name
TRINITY_GG_137675_c1_g1	CRP63010	no-name
TRINITY_GG_19686_c1_g1	CRP63010	no-name
TRINITY_GG_3357_c1_g2	CRP63010	no-name
TRINITY_GG_3357_c1_g3	CRP63010	no-name
TRINITY_GG_49205_c1_g1	CRP63010	no-name
TRINITY_GG_89666_c0_g2	CRP63010	no-name
TRINITY_GG_9548_c0_g1	CRP63010	no-name
TRINITY_GG_104988_c1_g1	CRP63020	no-name
TRINITY_GG_105351_c0_g1	CRP63020	no-name
TRINITY_GG_105754_c1_g1	CRP63020	no-name
TRINITY_GG_109414_c0_g1	CRP63020	no-name
TRINITY_GG_111649_c0_g1	CRP63020	no-name
TRINITY_GG_111918_c0_g2	CRP63020	no-name
TRINITY_GG_1140_c0_g1	CRP63020	no-name
TRINITY_GG_118055_c13_g1	CRP63020	no-name
TRINITY_GG_118110_c0_g1	CRP63020	no-name
TRINITY_GG_118110_c0_g2	CRP63020	no-name
TRINITY_GG_12019_c1_g1	CRP63020	no-name
TRINITY_GG_121452_c1_g1	CRP63020	no-name
TRINITY_GG_121463_c0_g1	CRP63020	no-name
TRINITY_GG_122987_c0_g1	CRP63020	no-name
TRINITY_GG_124187_c0_g1	CRP63020	no-name
TRINITY_GG_124599_c1_g1	CRP63020	no-name
TRINITY_GG_125243_c2_g1	CRP63020	no-name
TRINITY_GG_125248_c0_g1	CRP63020	no-name
TRINITY_GG_132228_c0_g1	CRP63020	no-name
TRINITY_GG_132618_c1_g1	CRP63020	no-name
TRINITY_GG_132618_c1_g3	CRP63020	no-name
TRINITY_GG_133334_c0_g1	CRP63020	no-name
TRINITY_GG_134517_c0_g1	CRP63020	no-name
TRINITY_GG_134827_c1_g1	CRP63020	no-name
TRINITY_GG_138122_c0_g1	CRP63020	no-name
TRINITY_GG_139372_c1_g1	CRP63020	no-name
TRINITY_GG_140672_c0_g1	CRP63020	no-name
TRINITY_GG_143_c2_g1	CRP63020	no-name
TRINITY_GG_14764_c1_g1	CRP63020	no-name
TRINITY_GG_15765_c0_g1	CRP63020	no-name
TRINITY_GG_15765_c0_g2	CRP63020	no-name
TRINITY_GG_18804_c0_g1	CRP63020	no-name
TRINITY_GG_18804_c0_g2	CRP63020	no-name
TRINITY_GG_19954_c0_g1	CRP63020	no-name
TRINITY_GG_19954_c0_g2	CRP63020	no-name
TRINITY_GG_20299_c0_g1	CRP63020	no-name
TRINITY_GG_20837_c0_g1	CRP63020	no-name
TRINITY_GG_25548_c0_g1	CRP63020	no-name
TRINITY_GG_27286_c0_g1	CRP63020	no-name

Transcript ID	CRP Class	CRP Description
TRINITY_GG_28486_c3_g1	CRP63020	no-name
TRINITY_GG_30953_c0_g1	CRP63020	no-name
TRINITY_GG_30953_c0_g2	CRP63020	no-name
TRINITY_GG_31203_c0_g1	CRP63020	no-name
TRINITY_GG_31203_c0_g2	CRP63020	no-name
TRINITY_GG_32523_c1_g1	CRP63020	no-name
TRINITY_GG_32523_c1_g2	CRP63020	no-name
TRINITY_GG_3321_c0_g2	CRP63020	no-name
TRINITY_GG_33325_c2_g1	CRP63020	no-name
TRINITY_GG_33376_c0_g1	CRP63020	no-name
TRINITY_GG_35401_c0_g1	CRP63020	no-name
TRINITY_GG_35599_c1_g1	CRP63020	no-name
TRINITY_GG_37229_c2_g1	CRP63020	no-name
TRINITY_GG_38002_c5_g2	CRP63020	no-name
TRINITY_GG_38646_c0_g1	CRP63020	no-name
TRINITY_GG_38646_c0_g2	CRP63020	no-name
TRINITY_GG_38760_c1_g1	CRP63020	no-name
TRINITY_GG_41608_c8_g1	CRP63020	no-name
TRINITY_GG_41994_c0_g1	CRP63020	no-name
TRINITY_GG_41994_c0_g2	CRP63020	no-name
TRINITY_GG_41994_c0_g3	CRP63020	no-name
TRINITY_GG_42261_c0_g1	CRP63020	no-name
TRINITY_GG_42428_c1_g2	CRP63020	no-name
TRINITY_GG_44568_c1_g1	CRP63020	no-name
TRINITY_GG_47128_c0_g1	CRP63020	no-name
TRINITY_GG_47379_c0_g1	CRP63020	no-name
TRINITY_GG_47379_c0_g3	CRP63020	no-name
TRINITY_GG_47379_c0_g4	CRP63020	no-name
TRINITY_GG_47934_c31_g1	CRP63020	no-name
TRINITY_GG_49106_c0_g1	CRP63020	no-name
TRINITY_GG_49420_c0_g1	CRP63020	no-name
TRINITY_GG_50932_c1_g1	CRP63020	no-name
TRINITY_GG_5173_c1_g1	CRP63020	no-name
TRINITY_GG_52373_c0_g1	CRP63020	no-name
TRINITY_GG_53452_c0_g1	CRP63020	no-name
TRINITY_GG_54614_c0_g1	CRP63020	no-name
TRINITY_GG_54614_c0_g2	CRP63020	no-name
TRINITY_GG_54614_c0_g3	CRP63020	no-name
TRINITY_GG_54891_c1_g1	CRP63020	no-name
TRINITY_GG_55241_c1_g1	CRP63020	no-name
TRINITY_GG_55241_c1_g2	CRP63020	no-name
TRINITY_GG_56517_c9_g1	CRP63020	no-name
TRINITY_GG_58920_c0_g1	CRP63020	no-name
TRINITY_GG_6665_c22_g1	CRP63020	no-name
TRINITY_GG_66736_c0_g1	CRP63020	no-name
TRINITY_GG_67575_c1_g1	CRP63020	no-name
TRINITY_GG_67810_c1_g1	CRP63020	no-name
TRINITY_GG_70255_c0_g2	CRP63020	no-name
TRINITY_GG_73456_c1_g1	CRP63020	no-name
TRINITY_GG_73499_c0_g2	CRP63020	no-name
TRINITY_GG_73499_c0_g3	CRP63020	no-name
TRINITY_GG_74979_c0_g1	CRP63020	no-name
TRINITY_GG_75554_c0_g1	CRP63020	no-name
TRINITY_GG_77620_c0_g2	CRP63020	no-name
TRINITY_GG_78153_c1_g1	CRP63020	no-name

Appendix

Transcript ID	CRP Class	CRP Description
TRINITY_GG_78498_c1_g1	CRP63020	no-name
TRINITY_GG_78498_c1_g2	CRP63020	no-name
TRINITY_GG_80498_c2_g1	CRP63020	no-name
TRINITY_GG_80564_c0_g1	CRP63020	no-name
TRINITY_GG_85122_c0_g1	CRP63020	no-name
TRINITY_GG_86015_c1_g1	CRP63020	no-name
TRINITY_GG_88867_c0_g1	CRP63020	no-name
TRINITY_GG_89173_c0_g2	CRP63020	no-name
TRINITY_GG_95864_c0_g1	CRP63020	no-name
TRINITY_GG_95864_c0_g2	CRP63020	no-name
TRINITY_GG_97152_c0_g1	CRP63020	no-name
TRINITY_GG_97857_c0_g1	CRP63020	no-name
TRINITY_GG_98048_c0_g1	CRP63020	no-name
TRINITY_GG_99691_c0_g1	CRP63020	no-name
TRINITY_GG_99892_c1_g1	CRP63020	no-name
TRINITY_GG_102585_c0_g1	CRP63030	no-name
TRINITY_GG_11013_c0_g1	CRP63030	no-name
TRINITY_GG_11018_c0_g1	CRP63030	no-name
TRINITY_GG_11026_c0_g1	CRP63030	no-name
TRINITY_GG_112620_c0_g1	CRP63030	no-name
TRINITY_GG_113427_c0_g1	CRP63030	no-name
TRINITY_GG_113429_c0_g1	CRP63030	no-name
TRINITY_GG_113436_c0_g1	CRP63030	no-name
TRINITY_GG_113439_c0_g1	CRP63030	no-name
TRINITY_GG_117970_c0_g1	CRP63030	no-name
TRINITY_GG_117972_c0_g1	CRP63030	no-name
TRINITY_GG_117982_c0_g1	CRP63030	no-name
TRINITY_GG_117982_c0_g2	CRP63030	no-name
TRINITY_GG_117992_c2_g1	CRP63030	no-name
TRINITY_GG_118014_c0_g1	CRP63030	no-name
TRINITY_GG_123227_c0_g1	CRP63030	no-name
TRINITY_GG_123237_c0_g1	CRP63030	no-name
TRINITY_GG_123238_c0_g1	CRP63030	no-name
TRINITY_GG_134328_c1_g1	CRP63030	no-name
TRINITY_GG_136975_c0_g1	CRP63030	no-name
TRINITY_GG_136978_c0_g1	CRP63030	no-name
TRINITY_GG_140317_c0_g1	CRP63030	no-name
TRINITY_GG_141375_c0_g1	CRP63030	no-name
TRINITY_GG_144570_c0_g1	CRP63030	no-name
TRINITY_GG_14618_c0_g1	CRP63030	no-name
TRINITY_GG_15527_c0_g1	CRP63030	no-name
TRINITY_GG_16055_c0_g1	CRP63030	no-name
TRINITY_GG_16058_c0_g2	CRP63030	no-name
TRINITY_GG_1624_c0_g1	CRP63030	no-name
TRINITY_GG_19548_c0_g1	CRP63030	no-name
TRINITY_GG_21906_c0_g1	CRP63030	no-name
TRINITY_GG_22007_c0_g1	CRP63030	no-name
TRINITY_GG_31306_c0_g1	CRP63030	no-name
TRINITY_GG_36093_c0_g1	CRP63030	no-name
TRINITY_GG_37505_c0_g1	CRP63030	no-name
TRINITY_GG_40585_c0_g1	CRP63030	no-name
TRINITY_GG_41342_c0_g1	CRP63030	no-name
TRINITY_GG_43257_c0_g1	CRP63030	no-name
TRINITY_GG_43258_c0_g2	CRP63030	no-name
TRINITY_GG_46506_c0_g1	CRP63030	no-name

Transcript ID	CRP Class	CRP Description
TRINITY_GG_49599_c0_g1	CRP63030	no-name
TRINITY_GG_51191_c0_g1	CRP63030	no-name
TRINITY_GG_51430_c0_g1	CRP63030	no-name
TRINITY_GG_55508_c5_g1	CRP63030	no-name
TRINITY_GG_5736_c0_g1	CRP63030	no-name
TRINITY_GG_62599_c0_g1	CRP63030	no-name
TRINITY_GG_71422_c0_g1	CRP63030	no-name
TRINITY_GG_71422_c0_g2	CRP63030	no-name
TRINITY_GG_7336_c0_g1	CRP63030	no-name
TRINITY_GG_7337_c0_g2	CRP63030	no-name
TRINITY_GG_7339_c0_g1	CRP63030	no-name
TRINITY_GG_75486_c0_g1	CRP63030	no-name
TRINITY_GG_77843_c0_g1	CRP63030	no-name
TRINITY_GG_78339_c0_g1	CRP63030	no-name
TRINITY_GG_80175_c0_g1	CRP63030	no-name
TRINITY_GG_80195_c0_g1	CRP63030	no-name
TRINITY_GG_80195_c0_g2	CRP63030	no-name
TRINITY_GG_81939_c0_g2	CRP63030	no-name
TRINITY_GG_84183_c0_g1	CRP63030	no-name
TRINITY_GG_8674_c5_g1	CRP63030	no-name
TRINITY_GG_90348_c0_g1	CRP63030	no-name
TRINITY_GG_96719_c0_g1	CRP63030	no-name
TRINITY_GG_96823_c1_g1	CRP63030	no-name

5.8 List of Figures

5.9 List of Tables

6. References

Alandete-Saez, M., M. Ron and S. McCormick (2008). "GEX3, expressed in the male gametophyte and in the egg cell of Arabidopsis thaliana, is essential for micropylar pollen tube guidance and plays a role during early embryogenesis." Mol Plant **1**(4): 586-598.

Almasia, N. I., A. A. Bazzini, H. E. Hopp and C. Vazquez-Rovere (2008). "Overexpression of snakin-1 gene enhances resistance to Rhizoctonia solani and Erwinia carotovora in transgenic potato plants." Mol Plant Pathol **9**(3): 329-338.

Amien, S., I. Kliwer, M. L. Marton, T. Debener, D. Geiger, D. Becker and T. Dresselhaus (2010). "Defensin-like ZmES4 mediates pollen tube burst in maize via opening of the potassium channel KZM1." PLoS Biol **8**(6): e1000388.

Andersen, N. H., B. Cao, A. Rodriguez-Romero and B. Arreguin (1993). "Hevein: NMR assignment and assessment of solution-state folding for the agglutinin-toxin motif." Biochemistry **32**(6): 1407-1422.

Ankenbrand, M. J., L. Weber, D. Becker, F. Förster and F. Bemm (2016). "TBro: visualization and management of de novo transcriptomes." Database (Oxford) **2016**.

Ariizumi, T. and K. Toriyama (2011). "Genetic Regulation of Sporopollenin Synthesis and Pollen Exine Development." Annual Review of Plant Biology **62**(1): 437-460.

Asano, T., A. Miwa, K. Maeda, M. Kimura and T. Nishiuchi (2013). "The secreted antifungal protein thionin 2.4 in Arabidopsis thaliana suppresses the toxicity of a fungal fruit body lectin from Fusarium graminearum." PLoS Pathog **9**(8): e1003581.

Bajon, C., C. Horlow, J. C. Motamayor, A. Sauvanet and D. Robert (1999). "Megasporogenesis in Arabidopsis thaliana L.: an ultrastructural study." Sexual Plant Reproduction **12**(2): 99-109.

Beale, K. M., A. R. Leydon and M. A. Johnson (2012). "Gamete fusion is required to block multiple pollen tubes from entering an Arabidopsis ovule." Curr Biol **22**(12): 1090-1094.

Bedinger, P. (1992). "The remarkable biology of pollen." Plant Cell **4**(8): 879-887.

Bednarska, E. (1991). "Calcium uptake from the stigma by germinating pollen in Primula officinalis L. and Ruscus aculeatus L." Sexual Plant Reproduction **4**(1): 36-38.

Berger, F., Y. Hamamura, M. Ingouff and T. Higashiyama (2008). "Double fertilization - caught in the act." Trends Plant Sci **13**(8): 437-443.

Berger, F. and D. Twell (2011). "Germline specification and function in plants." Annu Rev Plant Biol **62**: 461-484.

Berrocal-Lobo, M., A. Segura, M. Moreno, G. Lopez, F. Garcia-Olmedo and A. Molina (2002). "Snakin-2, an antimicrobial peptide from potato whose gene is locally induced by wounding and responds to pathogen infection." Plant Physiol **128**(3): 951-961.

Blein, J. P., P. Coutos-Thevenot, D. Marion and M. Ponchet (2002). "From elicitins to lipid-transfer proteins: a new insight in cell signalling involved in plant defence mechanisms." Trends Plant Sci **7**(7): 293-296.

Boavida, L. C., F. Borges, J. D. Becker and J. A. Feijo (2011). "Whole genome analysis of gene expression reveals coordinated activation of signaling and metabolic pathways during pollen-pistil interactions in Arabidopsis." Plant Physiol **155**(4): 2066-2080.

Boex-Fontvieille, E., S. Rustgi, S. Reinbothe and C. Reinbothe (2015). "A Kunitz-type protease inhibitor regulates programmed cell death during flower development in Arabidopsis thaliana." J Exp Bot **66**(20): 6119-6135.

Boisson-Dernier, A., D. S. Lituiev, A. Nestorova, C. M. Franck, S. Thirugnanarajah and U. Grossniklaus (2013). "ANXUR receptor-like kinases coordinate cell wall integrity with growth at the pollen tube tip via NADPH oxidases." PLoS Biol **11**(11): e1001719.

Boisson-Dernier, A., S. Roy, K. Kritsas, M. A. Grobei, M. Jaciubek, J. I. Schroeder and U. Grossniklaus (2009). "Disruption of the pollen-expressed FERONIA homologs ANXUR1 and ANXUR2 triggers pollen tube discharge." Development **136**(19): 3279-3288.

Bokvaj, P., S. Hafidh and D. Honys (2015). "Transcriptome profiling of male gametophyte development in Nicotiana tabacum." Genom Data **3**: 106-111.

Boman, H. G. (2003). "Antibacterial peptides: basic facts and emerging concepts." J Intern Med **254**(3): 197-215.

Bonferroni, C. E. (1936). "Teoria statistica delle classi e calcolo delle probabilit\`{a}." Pubblicazioni del R Istituto Superiore di Scienze Economiche e Commerciali di Firenze **8**: 3-62.

Borg, M., L. Brownfield and D. Twell (2009). "Male gametophyte development: a molecular perspective." J Exp Bot **60**(5): 1465-1478.

Brett, C. T. and K. W. Waldron (1996). Physiology and Biochemistry of Plant Cell Walls, Springer Netherlands.

Brewbaker, J. L. and B. H. Kwack (1963). "The Essential Role of Calcium Ion in Pollen Germination and Pollen Tube Growth." American Journal of Botany **50**(9): 859-865.

Broekaert, W. F., B. P. A. Cammue, M. F. C. De Bolle, K. Thevissen, G. W. De Samblanx, R. W. Osborn and K. Nielson (1997). "Antimicrobial Peptides from Plants." Critical Reviews in Plant Sciences **16**(3): 297-323.

Broekaert, W. F., W. Marien, F. R. Terras, M. F. De Bolle, P. Proost, J. Van Damme, L. Dillen, M. Claeys, S. B. Rees, J. Vanderleyden and et al. (1992). "Antimicrobial peptides from Amaranthus caudatus seeds with sequence homology to the cysteine/glycine-rich domain of chitin-binding proteins." Biochemistry **31**(17): 4308-4314.

Bulet, P., R. Stocklin and L. Menin (2004). "Anti-microbial peptides: from invertebrates to vertebrates." Immunol Rev **198**: 169-184.

Cao, J. and F. Shi (2012). "Evolution of the RALF Gene Family in Plants: Gene Duplication and Selection Patterns." Evol Bioinform Online **8**: 271-292.

Capron, A., M. Gourgues, L. S. Neiva, J. E. Faure, F. Berger, G. Pagnussat, A. Krishnan, C. Alvarez-Mejia, J. P. Vielle-Calzada, Y. R. Lee, B. Liu and V. Sundaresan (2008). "Maternal control of male-gamete delivery in Arabidopsis involves a putative GPI-anchored protein encoded by the LORELEI gene." Plant Cell **20**(11): 3038-3049.

Carvalho Ade, O. and V. M. Gomes (2007). "Role of plant lipid transfer proteins in plant cell physiology-a concise review." Peptides **28**(5): 1144-1153.

Carvalho Ade, O. and V. M. Gomes (2011). "Plant defensins and defensin-like peptides - biological activities and biotechnological applications." Curr Pharm Des **17**(38): 4270-4293.

Chae, K., C. A. Kieslich, D. Morikis, S.-C. Kim and E. M. Lord (2009). "A gain-of-function mutation of Arabidopsis lipid transfer protein 5 disturbs pollen tube tip growth and fertilization." The Plant cell **21**(12): 3902-3914.

Chae, K., K. Zhang, L. Zhang, D. Morikis, S. T. Kim, J. C. Mollet, N. de la Rosa, K. Tan and E. M. Lord (2007). "Two SCA (stigma/style cysteine-rich adhesin) isoforms show structural differences that correlate with their levels of in vitro pollen tube adhesion activity." J Biol Chem **282**(46): 33845-33858.

Chakraborty, S., H. Pan, Q. Tang, C. Woolard and G. Xu (2018). "The Extracellular Domain of Pollen Receptor Kinase 3 is structurally similar to the SERK family of co-receptors." Sci Rep **8**(1): 2796.

Chang, F., Y. Gu, H. Ma and Z. Yang (2013). "AtPRK2 promotes ROP1 activation via RopGEFs in the control of polarized pollen tube growth." Mol Plant **6**(4): 1187-1201.

Chang, F., A. Yan, L.-N. Zhao, W.-H. Wu and Z. Yang (2007). "A Putative Calcium-Permeable Cyclic Nucleotide-Gated Channel, CNGC18, Regulates Polarized Pollen Tube Growth." Journal of Integrative Plant Biology **49**(8): 1261-1270.

Chapman, L. A. and D. R. Goring (2010). "Pollen-pistil interactions regulating successful fertilization in the Brassicaceae." J Exp Bot **61**(7): 1987-1999.

Chapman, L. A. and D. R. Goring (2011). "Misregulation of phosphoinositides in Arabidopsis thaliana decreases pollen hydration and maternal fertility." Sex Plant Reprod **24**(4): 319-326.

Chaturvedi, P., T. Ischebeck, V. Egelhofer, I. Lichtscheidl and W. Weckwerth (2013). "Cell-specific analysis of the tomato pollen proteome from pollen mother cell to mature pollen provides evidence for developmental priming." J Proteome Res **12**(11): 4892-4903.

Chen, C. Y., E. I. Wong, L. Vidali, A. Estavillo, P. K. Hepler, H. M. Wu and A. Y. Cheung (2002). "The regulation of actin organization by actin-depolymerizing factor in elongating pollen tubes." Plant Cell **14**(9): 2175-2190.

Chen, X.-Y. and J.-Y. Kim (2009). "Callose synthesis in higher plants." Plant Signaling & Behavior **4**(6): 489-492.

Chen, Y. H., H. J. Li, D. Q. Shi, L. Yuan, J. Liu, R. Sreenivasan, R. Baskar, U. Grossniklaus and W. C. Yang (2007). "The central cell plays a critical role in pollen tube guidance in Arabidopsis." Plant Cell **19**(11): 3563-3577.

Cheng, S. H., M. R. Willmann, H. C. Chen and J. Sheen (2002). "Calcium signaling through protein kinases. The Arabidopsis calcium-dependent protein kinase gene family." Plant Physiol **129**(2): 469-485.

Cheung, A. Y., S. Niroomand, Y. Zou and H.-M. Wu (2010). "A transmembrane formin nucleates subapical actin assembly and controls tip-focused growth in pollen tubes." Proceedings of the National Academy of Sciences of the United States of America **107**(37): 16390-16395.

Cheung, A. Y., H. Wang and H. M. Wu (1995). "A floral transmitting tissue-specific glycoprotein attracts pollen tubes and stimulates their growth." Cell **82**.

Cheung, A. Y. and H. M. Wu (2008). "Structural and signaling networks for the polar cell growth machinery in pollen tubes." Annu Rev Plant Biol **59**: 547-572.

Christensen, C. A., S. Subramanian and G. N. Drews (1998). "Identification of gametophytic mutations affecting female gametophyte development in Arabidopsis." Dev Biol **202**(1): 136-151.

Coimbra, S., J. Almeida, V. Junqueira, M. L. Costa and L. G. Pereira (2007). "Arabinogalactan proteins as molecular markers in Arabidopsis thaliana sexual reproduction." J Exp Bot **58**(15-16): 4027-4035.

Combier, J. P., H. Kuster, E. P. Journet, N. Hohnjec, P. Gamas and A. Niebel (2008). "Evidence for the involvement in nodulation of the two small putative regulatory peptide-encoding genes MtRALFL1 and MtDVL1." Mol Plant Microbe Interact **21**(8): 1118-1127.

Covey, P. A., C. C. Subbaiah, R. L. Parsons, G. Pearce, F. T. Lay, M. A. Anderson, C. A. Ryan and P. A. Bedinger (2010). "A pollen-specific RALF from tomato that regulates pollen tube elongation." Plant Physiol **153**(2): 703-715.

Craddock, C., I. Lavagi and Z. Yang (2012). "New insights into Rho signaling from plant ROP/Rac GTPases." Trends Cell Biol **22**(9): 492-501.

Crawford, B. C., G. Ditta and M. F. Yanofsky (2007). "The NTT gene is required for transmitting-tract development in carpels of Arabidopsis thaliana." Curr Biol **17**(13): 1101-1108.

Crawford, B. C. and M. F. Yanofsky (2011). "HALF FILLED promotes reproductive tract development and fertilization efficiency in Arabidopsis thaliana." Development **138**(14): 2999-3009.

Dai, X. R., X. Q. Gao, G. H. Chen, L. L. Tang, H. Wang and X. S. Zhang (2014). "ABNORMAL POLLEN TUBE GUIDANCE1, an Endoplasmic Reticulum-Localized Mannosyltransferase Homolog of GLYCOSYLPHOSPHATIDYLINOSITOL10 in Yeast and PHOSPHATIDYLINOSITOL GLYCAN ANCHOR BIOSYNTHESIS B in Human, Is Required for Arabidopsis Pollen Tube Micropylar Guidance and Embryo Development." Plant Physiol **165**(4): 1544-1556.

De Coninck, B., B. P. A. Cammue and K. Thevissen (2013). "Modes of antifungal action and in planta functions of plant defensins and defensin-like peptides." Fungal Biology Reviews **26**(4): 109-120.

de Graaf, B. H. J., A. Y. Cheung, T. Andreyeva, K. Levasseur, M. Kieliszewski and H.-m. Wu (2005). "Rab11 GTPase-Regulated Membrane Trafficking Is Crucial for Tip-Focused Pollen Tube Growth in Tobacco." The Plant Cell **17**(9): 2564-2579.

de Nettancourt, D. (2001). Incompatibility and Incongruity in Wild and Cultivated Plants.

de Souza Cândido, E., M. H. e Silva Cardoso, D. A. Sousa, J. C. Viana, N. G. de Oliveira-Júnior, V. Miranda and O. L. Franco (2014). "The use of versatile plant antimicrobial peptides in agribusiness and human health." Peptides **55**: 65-78.

De Storme, N. and D. Geelen (2013). "Cytokinesis in plant male meiosis." Plant Signaling & Behavior **8**(3): e23394.

Denninger, P., A. Bleckmann, A. Lausser, F. Vogler, T. Ott, D. W. Ehrhardt, W. B. Frommer, S. Sprunck, T. Dresselhaus and G. Grossmann (2014). "Male-female communication triggers calcium signatures during fertilization in Arabidopsis." Nat Commun **5**: 4645.

Dickinson, H. (1995). "Dry stigmas, water and self-incompatibility in Brassica." Sexual Plant Reproduction **8**(1): 1-10.

Dobritsa, A. A., Z. Lei, S.-i. Nishikawa, E. Urbanczyk-Wochniak, D. V. Huhman, D. Preuss and L. W. Sumner (2010). "LAP5 and LAP6 Encode Anther-Specific Proteins with Similarity to Chalcone Synthase Essential for Pollen Exine Development in Arabidopsis." Plant Physiology **153**(3): 937-955.

Dobritsa, A. A., J. Shrestha, M. Morant, F. Pinot, M. Matsuno, R. Swanson, B. L. Møller and D. Preuss (2009). "CYP704B1 Is a Long-Chain Fatty Acid ω-Hydroxylase Essential for Sporopollenin Synthesis in Pollen of Arabidopsis." Plant Physiology **151**(2): 574-589.

Douliez, J. P., T. Michon, K. Elmorjani and D. Marion (2000). "Mini Review: Structure, Biological and Technological Functions of Lipid Transfer Proteins and Indolines, the Major Lipid Binding Proteins from Cereal Kernels." Journal of Cereal Science **32**(1): 1-20.

Dresselhaus, T. and S. Coimbra (2016). "Plant Reproduction: AMOR Enables Males to Respond to Female Signals." Curr Biol **26**(8): R321-323.

Dresselhaus, T. and N. Franklin-Tong (2013). "Male-female crosstalk during pollen germination, tube growth and guidance, and double fertilization." Mol Plant **6**(4): 1018-1036.

Dresselhaus, T., S. Sprunck and G. M. Wessel (2016). "Fertilization Mechanisms in Flowering Plants." Curr Biol **26**(3): R125-139.

Du, S., L. J. Qu and J. Xiao (2018). "Crystal structures of the extracellular domains of the CrRLK1L receptor-like kinases ANXUR1 and ANXUR2." Protein Sci **27**(4): 886-892.

Duan, Q., D. Kita, E. A. Johnson, M. Aggarwal, L. Gates, H. M. Wu and A. Y. Cheung (2014). "Reactive oxygen species mediate pollen tube rupture to release sperm for fertilization in Arabidopsis." Nat Commun **5**: 3129.

Dubovskii, P. V., A. A. Vassilevski, A. A. Slavokhotova, T. I. Odintsova, E. V. Grishin, T. A. Egorov and A. S. Arseniev (2011). "Solution structure of a defense peptide from wheat with a 10-cysteine motif." Biochem Biophys Res Commun **411**(1): 14-18.

Edlund, A. F., R. Swanson and D. Preuss (2004). "Pollen and Stigma Structure and Function: The Role of Diversity in Pollination." The Plant Cell **16**(suppl 1): S84.

Emms, D. M. and S. Kelly (2015). "OrthoFinder: solving fundamental biases in whole genome comparisons dramatically improves orthogroup inference accuracy." Genome Biology **16**(1): 157.

Epple, P., K. Apel and H. Bohlmann (1997). "Overexpression of an endogenous thionin enhances resistance of Arabidopsis against Fusarium oxysporum." Plant Cell **9**(4): 509-520.

Erbar, C. (2003). "Pollen Tube Transmitting Tissue: Place of Competition of Male Gametophytes." International Journal of Plant Sciences **164**(S5): S265-S277.

Escobar-Restrepo, J. M., N. Huck, S. Kessler, V. Gagliardini, J. Gheyselinck, W. C. Yang and U. Grossniklaus (2007). "The FERONIA receptor-like kinase mediates male-female interactions during pollen tube reception." Science **317**(5838): 656-660.

Faure, J.-E., N. Rotman, P. Fortuné and C. Dumas (2002). "Fertilization in Arabidopsis thaliana wild type: Developmental stages and time course." The Plant Journal **30**(4): 481-488.

Fellenberg, C. and T. Vogt (2015). "Evolutionarily conserved phenylpropanoid pattern on angiosperm pollen." Trends in Plant Science **20**(4): 212-218.

Feng, W., D. Kita, A. Peaucelle, H. N. Cartwright, V. Doan, Q. Duan, M. C. Liu, J. Maman, L. Steinhorst, I. Schmitz-Thom, R. Yvon, J. Kudla, H. M. Wu, A. Y. Cheung and J. R. Dinneny (2018). "The FERONIA Receptor Kinase Maintains Cell-Wall Integrity during Salt Stress through Ca(2+) Signaling." Curr Biol **28**(5): 666-675 e665.

Feng, Y. J., Q. F. Liu, M. Y. Chen, D. Liang and P. Zhang (2016). "Parallel tagged amplicon sequencing of relatively long PCR products using the Illumina HiSeq platform and transcriptome assembly." Mol Ecol Resour **16**(1): 91-102.

Fiebig, A., R. Kimport and D. Preuss (2004). "Comparisons of pollen coat genes across Brassicaceae species reveal rapid evolution by repeat expansion and diversification." Proc Natl Acad Sci U S A **101**(9): 3286-3291.

Firon, N., M. Nepi and E. Pacini (2012). "Water status and associated processes mark critical stages in pollen development and functioning." Ann Bot **109**(7): 1201-1214.

Franklin-Tong, V. (1999). "Signaling and the modulation of pollen tube growth." Plant Cell **11**(4): 727-738.

Frietsch, S., Y. F. Wang, C. Sladek, L. R. Poulsen, S. M. Romanowsky, J. I. Schroeder and J. F. Harper (2007). "A cyclic nucleotide-gated channel is essential for polarized tip growth of pollen." Proc Natl Acad Sci U S A **104**(36): 14531-14536.

Fu, Y., G. Wu and Z. Yang (2001). "Rop GTPase-dependent dynamics of tip-localized F-actin controls tip growth in pollen tubes." J Cell Biol **152**(5): 1019-1032.

Furness, C. A. and P. J. Rudall (2001). "Pollen and anther characters in monocot systematics." Grana **40**(1-2): 17-25.

Furness, C. A. and P. J. Rudall (2004). "Pollen aperture evolution – a crucial factor for eudicot success?" Trends in Plant Science **9**(3): 154-158.

Ganapathi, T., S. Penna, P. S. Rao and V. Bapat (2004). Tobacco (Nicotiana tabacum L.) - A model system for tissue culture interventions and genetic engineering.

García, A. N., N. D. Ayub, A. R. Fox, M. C. Gómez, M. J. Diéguez, E. M. Pagano, C. A. Berini, J. P. Muschietti and G. Soto (2014). "Alfalfa snakin-1 prevents fungal colonization and probably coevolved with rhizobia." BMC Plant Biology **14**(1): 248.

Garcia-Olmedo, F., A. Molina, J. M. Alamillo and P. Rodriguez-Palenzuela (1998). "Plant defense peptides." Biopolymers **47**(6): 479-491.

Gaspar, Y. M., J. A. McKenna, B. S. McGinness, J. Hinch, S. Poon, A. A. Connelly, M. A. Anderson and R. L. Heath (2014). "Field resistance to Fusarium oxysporum and Verticillium dahliae in transgenic cotton expressing the plant defensin NaD1." J Exp Bot **65**(6): 1541-1550.

Ge, Z., T. Bergonci, Y. Zhao, Y. Zou, S. Du, M. C. Liu, X. Luo, H. Ruan, L. E. Garcia-Valencia, S. Zhong, S. Hou, Q. Huang, L. Lai, D. S. Moura, H. Gu, J. Dong, H. M. Wu, T. Dresselhaus, J. Xiao, A. Y. Cheung and L. J. Qu (2017). "Arabidopsis pollen tube integrity and sperm release are regulated by RALF-mediated signaling." Science **358**(6370): 1596-1600.

Gifford, E. M. and A. S. Foster (1989). Morphology and Evolution of Vascular Plants, W. H. Freeman.

Giulietti, A., L. Overbergh, D. Valckx, B. Decallonne, R. Bouillon and C. Mathieu (2001). "An overview of real-time quantitative PCR: applications to quantify cytokine gene expression." Methods **25**(4): 386-401.

Grabherr, M. G., B. J. Haas, M. Yassour, J. Z. Levin, D. A. Thompson, I. Amit, X. Adiconis, L. Fan, R. Raychowdhury, Q. Zeng, Z. Chen, E. Mauceli, N. Hacohen, A. Gnirke, N. Rhind, F. di Palma, B. W. Birren, C. Nusbaum, K. Lindblad-Toh, N. Friedman and A. Regev (2011). "Full-length transcriptome assembly from RNA-Seq data without a reference genome." Nature biotechnology **29**(7): 644-652.

Gremski, K., G. Ditta and M. F. Yanofsky (2007). "The HECATE genes regulate female reproductive tract development in Arabidopsis thaliana." Development **134**(20): 3593-3601.

Grobei, M. A., E. Qeli, E. Brunner, H. Rehrauer, R. Zhang, B. Roschitzki, K. Basler, C. H. Ahrens and U. Grossniklaus (2009). "Deterministic protein inference for shotgun proteomics data provides new insights into Arabidopsis pollen development and function." Genome Res **19**(10): 1786-1800.

Gu, Y., Y. Fu, P. Dowd, S. Li, V. Vernoud, S. Gilroy and Z. Yang (2005). "A Rho family GTPase controls actin dynamics and tip growth via two counteracting downstream pathways in pollen tubes." J Cell Biol **169**(1): 127-138.

Guan, Y., J. Guo, H. Li and Z. Yang (2013). "Signaling in Pollen Tube Growth: Crosstalk, Feedback, and Missing Links." Molecular Plant **6**(4): 1053-1064.

Guan, Y., J. Lu, J. Xu, B. McClure and S. Zhang (2014). "Two Mitogen-Activated Protein Kinases, MPK3 and MPK6, Are Required for Funicular Guidance of Pollen Tubes in Arabidopsis." Plant Physiol **165**(2): 528-533.

Haag, A. F., B. Kerscher, S. Dall'Angelo, M. Sani, R. Longhi, M. Baloban, H. M. Wilson, P. Mergaert, M. Zanda and G. P. Ferguson (2012). "Role of cysteine residues and disulfide bonds in the activity of a legume root nodule-specific, cysteine-rich peptide." J Biol Chem **287**(14): 10791-10798.

Hafidh, S., J. Fila and D. Honys (2016). "Male gametophyte development and function in angiosperms: a general concept." Plant Reprod **29**(1-2): 31-51.

Hafidh, S., D. Potesil, J. Fila, V. Capkova, Z. Zdrahal and D. Honys (2016). "Quantitative proteomics of the tobacco pollen tube secretome identifies novel pollen tube guidance proteins important for fertilization." Genome Biol **17**(1): 81.

Hamamura, Y., M. Nishimaki, H. Takeuchi, A. Geitmann, D. Kurihara and T. Higashiyama (2014). "Live imaging of calcium spikes during double fertilization in Arabidopsis." Nat Commun **5**: 4722.

Haruta, M. and C. P. Constabel (2003). "Rapid Alkalinization Factors in Poplar Cell Cultures. Peptide Isolation, cDNA Cloning, and Differential Expression in Leaves and Methyl Jasmonate-Treated Cells." Plant Physiology **131**(2): 814-823.

Hashimoto, K. and J. Kudla (2011). "Calcium decoding mechanisms in plants." Biochimie **93**(12): 2054-2059.

Heberle, H., G. V. Meirelles, F. R. da Silva, G. P. Telles and R. Minghim (2015). "InteractiVenn: a web-based tool for the analysis of sets through Venn diagrams." BMC Bioinformatics **16**: 169.

Heslop-Harrison, Y. and J. Heslop-Harrison (1992). "Germination of Monocolpate Angiosperm Pollen: Evolution of the Actin Cytoskeleton and Wall during Hydration, Activation and Tube Emergence." Annals of Botany **69**(5): 385-394.

Higashiyama, T. (2002). "The synergid cell: attractor and acceptor of the pollen tube for double fertilization." J Plant Res **115**(1118): 149-160.

Higashiyama, T. (2010). "Peptide signaling in pollen-pistil interactions." Plant Cell Physiol **51**(2): 177-189.

Higashiyama, T. and Y. Hamamura (2008). "Gametophytic pollen tube guidance." Sexual Plant Reproduction **21**(1): 17-26.

Higashiyama, T., R. Inatsugi, S. Sakamoto, N. Sasaki, T. Mori, H. Kuroiwa, T. Nakada, H. Nozaki, T. Kuroiwa and A. Nakano (2006). "Species preferentiality of the pollen tube attractant derived from the synergid cell of Torenia fournieri." Plant Physiol **142**(2): 481-491.

Higashiyama, T., H. Kuroiwa, S. Kawano and T. Kuroiwa (1998). "Guidance in vitro of the pollen tube to the naked embryo sac of torenia fournieri." The Plant Cell **10**(12): 2019-2032.

Higashiyama, T. and H. Takeuchi (2015). "The mechanism and key molecules involved in pollen tube guidance." Annu Rev Plant Biol **66**: 393-413.

Higashiyama, T., S. Yabe, N. Sasaki, Y. Nishimura, S. Miyagishima, H. Kuroiwa and T. Kuroiwa (2001). "Pollen tube attraction by the synergid cell." Science **293**(5534): 1480-1483.

Higashiyama, T. and W. C. Yang (2017). "Gametophytic Pollen Tube Guidance: Attractant Peptides, Gametic Controls, and Receptors." Plant Physiol **173**(1): 112-121.

Hiscock, S. J. and D. A. Tabah (2003). "The different mechanisms of sporophytic self-incompatibility." Philos Trans R Soc Lond B Biol Sci **358**(1434): 1037-1045.

Holdaway-Clarke, T. L., J. A. Feijo, G. R. Hackett, J. G. Kunkel and P. K. Hepler (1997). "Pollen Tube Growth and the Intracellular Cytosolic Calcium Gradient Oscillate in Phase while Extracellular Calcium Influx Is Delayed." The Plant Cell **9**(11): 1999-2010.

Holdaway-Clarke, T. L. and P. K. Hepler (2003). "Control of pollen tube growth: role of ion gradients and fluxes." New Phytologist **159**(3): 539-563.

Holmes-Davis, R., C. K. Tanaka, W. H. Vensel, W. J. Hurkman and S. McCormick (2005). "Proteome mapping of mature pollen of Arabidopsis thaliana." Proteomics **5**(18): 4864-4884.

Honys, D. and D. Twell (2004). "Transcriptome analysis of haploid male gametophyte development in Arabidopsis." Genome Biol **5**(11): R85.

Hou, Y., X. Guo, P. Cyprys, Y. Zhang, A. Bleckmann, L. Cai, Q. Huang, Y. Luo, H. Gu, T. Dresselhaus, J. Dong and L. J. Qu (2016). "Maternal ENODLs Are Required for Pollen Tube Reception in Arabidopsis." Curr Biol **26**(17): 2343-2350.

Hsieh, K. and A. H. Huang (2005). "Lipid-rich tapetosomes in Brassica tapetum are composed of oleosin-coated oil droplets and vesicles, both assembled in and then detached from the endoplasmic reticulum." Plant J **43**(6): 889-899.

Huang, B.-Q. and S. D. Russell (1992). "Female Germ Unit: Organization, Isolation, and Function." International Review of Cytology **140**: 233-293.

Huang, Q., T. Dresselhaus, H. Gu and L. J. Qu (2015). "Active role of small peptides in Arabidopsis reproduction: Expression evidence." J Integr Plant Biol **57**(6): 518-521.

Huang, W. J., H. K. Liu, S. McCormick and W. H. Tang (2014). "Tomato Pistil Factor STIG1 Promotes in Vivo Pollen Tube Growth by Binding to Phosphatidylinositol 3-Phosphate and the Extracellular Domain of the Pollen Receptor Kinase LePRK2." Plant Cell **26**(6): 2505-2523.

Huck, N., J. M. Moore, M. Federer and U. Grossniklaus (2003). "The Arabidopsis mutant feronia disrupts the female gametophytic control of pollen tube reception." Development **130**.

Hwang, J.-U., Y. Gu, Y.-J. Lee and Z. Yang (2005). "Oscillatory ROP GTPase Activation Leads the Oscillatory Polarized Growth of Pollen Tubes." Molecular Biology of the Cell **16**(11): 5385-5399.

Hwang, J. U., V. Vernoud, A. Szumlanski, E. Nielsen and Z. Yang (2008). "A tip-localized RhoGAP controls cell polarity by globally inhibiting Rho GTPase at the cell apex." Curr Biol **18**(24): 1907-1916.

Hwang, J. U., G. Wu, A. Yan, Y. J. Lee, C. S. Grierson and Z. Yang (2010). "Pollen-tube tip growth requires a balance of lateral propagation and global inhibition of Rho-family GTPase activity." J Cell Sci **123**(Pt 3): 340-350.

Illumina, I. (2015).

Ingram, G. and J. Gutierrez-Marcos (2015). "Peptide signalling during angiosperm seed development." J Exp Bot **66**(17): 5151-5159.

Ischebeck, T., L. Valledor, D. Lyon, S. Gingl, M. Nagler, M. Meijón, V. Egelhofer and W. Weckwerth (2014). "Comprehensive Cell-specific Protein Analysis in Early and Late Pollen Development from Diploid Microsporocytes to Pollen Tube Growth." Mol Cell Proteomics **13**(1): 295-310.

Iwano, M., Q. A. Ngo, T. Entani, H. Shiba, T. Nagai, A. Miyawaki, A. Isogai, U. Grossniklaus and S. Takayama (2012). "Cytoplasmic Ca2+ changes dynamically during the interaction of the pollen tube with synergid cells." Development **139**(22): 4202-4209.

Iwano, M., H. Shiba, T. Miwa, F. S. Che, S. Takayama, T. Nagai, A. Miyawaki and A. Isogai (2004). "Ca2+ dynamics in a pollen grain and papilla cell during pollination of Arabidopsis." Plant Physiol **136**(3): 3562-3571.

J B Nasrallah, a. T Nishio and M. E. Nasrallah (1991). "The Self-Incompatibility Genes of Brassica: Expression and Use in Genetic Ablation of Floral Tissues." Annual Review of Plant Physiology and Plant Molecular Biology **42**(1): 393-422.

Jaffe, L. A., M. H. Weisenseel and L. F. Jaffe (1975). "Calcium accumulations within the growing tips of pollen tubes." J Cell Biol **67**(2PT.1): 488-492.

Ji, H., G. Gheysen, C. Ullah, R. Verbeek, C. Shang, D. De Vleesschauwer, M. Hofte and T. Kyndt (2015). "The role of thionins in rice defence against root pathogens." Mol Plant Pathol **16**(8): 870-881.

Jones-Rhoades, M. W., J. O. Borevitz and D. Preuss (2007). "Genome-wide expression profiling of the Arabidopsis female gametophyte identifies families of small, secreted proteins." PLoS Genet **3**(10): 1848-1861.

Kader, J. C. (1996). "LIPID-TRANSFER PROTEINS IN PLANTS." Annu Rev Plant Physiol Plant Mol Biol **47**: 627-654.

Kägi, C., N. Baumann, N. Nielsen, Y.-D. Stierhof and R. Groß-Hardt (2010). "The gametic central cell of Arabidopsis determines the lifespan of adjacent accessory cells." Proceedings of the National Academy of Sciences of the United States of America **107**(51): 22350-22355.

Kanaoka, M. M. and T. Higashiyama (2015). "Peptide signaling in pollen tube guidance." Curr Opin Plant Biol **28**: 127-136.

Kanaoka, M. M., N. Kawano, Y. Matsubara, D. Susaki, S. Okuda, N. Sasaki and T. Higashiyama (2011). "Identification and characterization of TcCRP1, a pollen tube attractant from Torenia concolor." Ann Bot **108**(4): 739-747.

Kandasamy, M. K. and U. Kristen (1987). "Developmental Aspects of Ultrastructure, Histochemistry and Receptivity of the Stigma of Nicotiana sylvestris." Annals of Botany **60**(4): 427-437.

Kasahara, R. D., D. Maruyama, Y. Hamamura, T. Sakakibara, D. Twell and T. Higashiyama (2012). "Fertilization recovery after defective sperm cell release in Arabidopsis." Curr Biol **22**(12): 1084-1089.

Kasahara, R. D., M. F. Portereiko, L. Sandaklie-Nikolova, D. S. Rabiger and G. N. Drews (2005). "MYB98 is required for pollen tube guidance and synergid cell differentiation in Arabidopsis." Plant Cell **17**.

Kearse, M., R. Moir, A. Wilson, S. Stones-Havas, M. Cheung, S. Sturrock, S. Buxton, A. Cooper, S. Markowitz, C. Duran, T. Thierer, B. Ashton, P. Meintjes and A. Drummond (2012). "Geneious Basic: an integrated and extendable desktop software platform for the organization and analysis of sequence data." Bioinformatics **28**(12): 1647-1649.

Kessler, S. A., H. Lindner, D. S. Jones and U. Grossniklaus (2015). "Functional analysis of related CrRLK1L receptor-like kinases in pollen tube reception." EMBO Rep **16**(1): 107-115.

Koike, M., T. Okamoto, S. Tsuda and R. Imai (2002). "A novel plant defensin-like gene of winter wheat is specifically induced during cold acclimation." Biochem Biophys Res Commun **298**(1): 46-53.

Koornneef, M. and D. Meinke (2010). "The development of Arabidopsis as a model plant." Plant J **61**(6): 909-921.

Kost, B., E. Lemichez, P. Spielhofer, Y. Hong, K. Tolias, C. Carpenter and N. H. Chua (1999). "Rac homologues and compartmentalized phosphatidylinositol 4, 5-bisphosphate act in a common pathway to regulate polar pollen tube growth." J Cell Biol **145**(2): 317-330.

Lee, O. S., B. Lee, N. Park, J. C. Koo, Y. H. Kim, D. T. Prasad, C. Karigar, H. J. Chun, B. R. Jeong, D. H. Kim, J. Nam, J. G. Yun, S. S. Kwak, M. J. Cho and D. J. Yun (2003). "Pn-AMPs, the hevein-like proteins from Pharbitis nil confers disease resistance against phytopathogenic fungi in tomato, Lycopersicum esculentum." Phytochemistry **62**(7): 1073-1079.

Lee, Y. J. and Z. Yang (2008). "Tip growth: signaling in the apical dome." Curr Opin Plant Biol **11**(6): 662-671.

Lennon, K. A., S. Roy, P. K. Hepler and E. M. Lord (1998). "The structure of the transmitting tissue of Arabidopsis thaliana (L.) and the path of pollen tube growth." Sexual Plant Reproduction **11**(1): 49-59.

Leshem, Y., C. Johnson and V. Sundaresan (2013). "Pollen tube entry into the synergid cell of Arabidopsis is observed at a site distinct from the filiform apparatus." Plant Reprod **26**(2): 93-99.

Leydon, A. R., K. M. Beale, K. Woroniecka, E. Castner, J. Chen, C. Horgan, R. Palanivelu and M. A. Johnson (2013). "Three MYB transcription factors control pollen tube differentiation required for sperm release." Curr Biol **23**(13): 1209-1214.

Li, C., F. L. Yeh, A. Y. Cheung, Q. Duan, D. Kita, M. C. Liu, J. Maman, E. J. Luu, B. W. Wu, L. Gates, M. Jalal, A. Kwong, H. Carpenter and H. M. Wu (2015). "Glycosylphosphatidylinositol-anchored proteins as chaperones and co-receptors for FERONIA receptor kinase signaling in Arabidopsis." Elife **4**.

Li, H., Y. Lin, R. M. Heath, M. X. Zhu and Z. Yang (1999). "Control of pollen tube tip growth by a Rop GTPase-dependent pathway that leads to tip-localized calcium influx." The Plant Cell **11**(9): 1731-1742.

Li, H. J., Y. Xue, D. J. Jia, T. Wang, D. Q. Hi, J. Liu, F. Cui, Q. Xie, D. Ye and W. C. Yang (2011). "POD1 regulates pollen tube guidance in response to micropylar female signaling and acts in early embryo patterning in Arabidopsis." Plant Cell **23**(9): 3288-3302.

Li, H. J., S. S. Zhu, M. X. Zhang, T. Wang, L. Liang, Y. Xue, D. Q. Shi, J. Liu and W. C. Yang (2015). "Arabidopsis CBP1 Is a Novel Regulator of Transcription Initiation in Central Cell-Mediated Pollen Tube Guidance." Plant Cell **27**(10): 2880-2893.

Li, S., F. R. Ge, M. Xu, X. Y. Zhao, G. Q. Huang, L. Z. Zhou, J. G. Wang, A. Kombrink, S. McCormick, X. S. Zhang and Y. Zhang (2013). "Arabidopsis COBRA-LIKE 10, a GPI-anchored protein, mediates directional growth of pollen tubes." Plant J **74**(3): 486-497.

Li, Y. L., X. R. Dai, X. Yue, X. Q. Gao and X. S. Zhang (2014). "Identification of small secreted peptides (SSPs) in maize and expression analysis of partial SSP genes in reproductive tissues." Planta **240**(4): 713-728.

Ling, Y., T. Chen, Y. Jing, L. Fan, Y. Wan and J. Lin (2013). "γ-Aminobutyric acid (GABA) homeostasis regulates pollen germination and polarized growth in Picea wilsonii." Planta **238**(5): 831-843.

Ling, Y., C. Zhang, T. Chen, H. Hao, P. Liu, R. A. Bressan, P. M. Hasegawa, J. B. Jin and J. Lin (2012). "Mutation in SUMO E3 ligase, SIZ1, disrupts the mature female gametophyte in Arabidopsis." PLoS One **7**(1): e29470.

Liu, F., X. Zhang, C. Lu, X. Zeng, Y. Li, D. Fu and G. Wu (2015). "Non-specific lipid transfer proteins in plants: presenting new advances and an integrated functional analysis." J Exp Bot **66**(19): 5663-5681.

Liu, J., S. Zhong, X. Guo, L. Hao, X. Wei, Q. Huang, Y. Hou, J. Shi, C. Wang, H. Gu and L. J. Qu (2013). "Membrane-bound RLCKs LIP1 and LIP2 are essential male factors controlling male-female attraction in Arabidopsis." Curr Biol **23**(11): 993-998.

Liu, X., C. A. Castro, Y. Wang, J. A. Noble, N. D. Ponvert, M. G. Bundy, C. R. Hoel, E. D. Shpak and R. Palanivelu (2016). "The Role of LORELEI in Pollen Tube Reception at the Interface of the Synergid Cell and Pollen Tube Requires the Modified Eight-Cysteine Motif and the Receptor-Like Kinase FERONIA." Plant Cell.

Lord, E. M. and S. D. Russell (2002). "The mechanisms of pollination and fertilization in plants." Annu Rev Cell Dev Biol **18**: 81-105.

Love, M. I., W. Huber and S. Anders (2014). "Moderated estimation of fold change and dispersion for RNA-seq data with DESeq2." Genome Biol **15**(12): 550.

Lu, P., M. Chai, J. Yang, G. Ning, G. Wang and H. Ma (2014). "The Arabidopsis CALLOSE DEFECTIVE MICROSPORE1 Gene Is Required for Male Fertility through Regulating Callose Metabolism during Microsporogenesis." Plant Physiology **164**(4): 1893-1904.

Lush, W. M., F. Grieser and M. Wolters-Arts (1998). "Directional Guidance of Nicotiana alata Pollen Tubes in Vitro and on the Stigma." Plant Physiology **118**(3): 733-741.

Luu, D.-T., E. Passelègue, C. Dumas and P. Heizmann (1998). "Pollen-stigma capture is not species discriminant within the Brassicaceae family." Comptes Rendus de l'Académie des Sciences - Series III - Sciences de la Vie **321**(9): 747-755.

Luu, D. T., D. Marty-Mazars, M. Trick, C. Dumas and P. Heizmann (1999). "Pollen-stigma adhesion in Brassica spp involves SLG and SLR1 glycoproteins." Plant Cell **11**(2): 251-262.

Maheshwari, P. (1950). An introduction to the embryology of angiosperms. New York, McGraw-Hill.

Mang, H., B. Feng, Z. Hu, A. Boisson-Dernier, C. M. Franck, X. Meng, Y. Huang, J. Zhou, G. Xu, T. Wang, L. Shan and P. He (2017). "Differential Regulation of Two-Tiered

Plant Immunity and Sexual Reproduction by ANXUR Receptor-Like Kinases." Plant Cell **29**(12): 3140-3156.

Mansfield, S. G., L. G. Briarty and S. Erni (1991). "Early embryogenesis in Arabidopsis thaliana. I. The mature embryo sac." Canadian Journal of Botany **69**(3): 447-460.

Marshall, E., L. M. Costa and J. Gutierrez-Marcos (2011). "Cysteine-rich peptides (CRPs) mediate diverse aspects of cell-cell communication in plant reproduction and development." J Exp Bot **62**(5): 1677-1686.

Marton, M. L., S. Cordts, J. Broadhvest and T. Dresselhaus (2005). "Micropylar pollen tube guidance by egg apparatus 1 of maize." Science **307**.

Marton, M. L., A. Fastner, S. Uebler and T. Dresselhaus (2012). "Overcoming hybridization barriers by the secretion of the maize pollen tube attractant ZmEA1 from Arabidopsis ovules." Curr Biol **22**(13): 1194-1198.

Maruyama, D., Y. Hamamura, H. Takeuchi, D. Susaki, M. Nishimaki, D. Kurihara, R. D. Kasahara and T. Higashiyama (2013). "Independent control by each female gamete prevents the attraction of multiple pollen tubes." Dev Cell **25**(3): 317-323.

Maruyama, D., R. Volz, H. Takeuchi, T. Mori, T. Igawa, D. Kurihara, T. Kawashima, M. Ueda, M. Ito, M. Umeda, S. Nishikawa, R. Gross-Hardt and T. Higashiyama (2015). "Rapid Elimination of the Persistent Synergid through a Cell Fusion Mechanism." Cell **161**(4): 907-918.

Mayfield, J. A., A. Fiebig, S. E. Johnstone and D. Preuss (2001). "Gene families from the Arabidopsis thaliana pollen coat proteome." Science **292**(5526): 2482-2485.

Mayfield, J. A. and D. Preuss (2000). "Rapid initiation of Arabidopsis pollination requires the oleosin-domain protein GRP17." Nat Cell Biol **2**(2): 128-130.

McCue, A. D., M. Cresti, J. A. Feijo and R. K. Slotkin (2011). "Cytoplasmic connection of sperm cells to the pollen vegetative cell nucleus: potential roles of the male germ unit revisited." J Exp Bot **62**(5): 1621-1631.

Mee Do, H., S. Chul Lee, H. Won Jung, K. Hoon Sohn and B. Kook Hwang (2004). "Differential expression and in situ localization of a pepper defensin (CADEF1) gene in response to pathogen infection, abiotic elicitors and environmental stresses in Capsicum annuum." Plant Science **166**(5): 1297-1305.

Messerli, M. A., R. Creton, L. F. Jaffe and K. R. Robinson (2000). "Periodic increases in elongation rate precede increases in cytosolic Ca2+ during pollen tube growth." Dev Biol **222**(1): 84-98.

Michard, E., P. T. Lima, F. Borges, A. C. Silva, M. T. Portes, J. E. Carvalho, M. Gilliham, L. H. Liu, G. Obermeyer and J. A. Feijo (2011). "Glutamate receptor-like genes form Ca2+ channels in pollen tubes and are regulated by pistil D-serine." Science **332**(6028): 434-437.

Mingossi, F. B., J. L. Matos, A. P. Rizzato, A. H. Medeiros, M. C. Falco, M. C. Silva-Filho and D. S. Moura (2010). "SacRALF1, a peptide signal from the grass sugarcane (Saccharum spp.), is potentially involved in the regulation of tissue expansion." Plant Mol Biol **73**(3): 271-281.

Miyawaki, K. N. and Z. Yang (2014). "Extracellular signals and receptor-like kinases regulating ROP GTPases in plants." Front Plant Sci **5**: 449.

Miyazaki, S., T. Murata, N. Sakurai-Ozato, M. Kubo, T. Demura, H. Fukuda and M. Hasebe (2009). "ANXUR1 and 2, sister genes to FERONIA/SIRENE, are male factors for coordinated fertilization." Curr Biol **19**(15): 1327-1331.

Moeder, W. and K. Yoshioka (2017). "CNGCs break through-A rice cyclic nucleotide-gated channel paves the way for pollen tube growth." PLoS Genet **13**(11): e1007066.

Mollet, J. C., S. Y. Park, E. A. Nothnagel and E. M. Lord (2000). "A lily stylar pectin is necessary for pollen tube adhesion to an in vitro stylar matrix." Plant Cell **12**(9): 1737-1750.

Mullis, K. B., H. A. Erlich, N. Arnheim, G. T. Horn, R. K. Saiki and S. J. Scharf (1987). Process for amplifying, detecting, and/or-cloning nucleic acid sequences, Google Patents.

Muramoto, N., T. Tanaka, T. Shimamura, N. Mitsukawa, E. Hori, K. Koda, M. Otani, M. Hirai, K. Nakamura and T. Imaeda (2012). "Transgenic sweet potato expressing thionin from barley gives resistance to black rot disease caused by Ceratocystis fimbriata in leaves and storage roots." Plant Cell Rep **31**(6): 987-997.

Murgia, M., B.-Q. Huang, S. C. Tucker and M. E. Musgrave (1993). "Embryo Sac Lacking Antipodal Cells in Arabidopsis thaliana (Brassicaceae)." American Journal of Botany **80**(7): 824-838.

Murphy, E. and I. De Smet (2014). "Understanding the RALF family: a tale of many species." Trends in Plant Science **19**(10): 664-671.

Mygind, P. H., R. L. Fischer, K. M. Schnorr, M. T. Hansen, C. P. Sonksen, S. Ludvigsen, D. Raventos, S. Buskov, B. Christensen, L. De Maria, O. Taboureau, D. Yaver, S. G. Elvig-Jorgensen, M. V. Sorensen, B. E. Christensen, S. Kjaerulff, N. Frimodt-Moller, R. I. Lehrer, M. Zasloff and H. H. Kristensen (2005). "Plectasin is a peptide antibiotic with therapeutic potential from a saprophytic fungus." Nature **437**(7061): 975-980.

Nagahara, S., H. Takeuchi and T. Higashiyama (2015). "Generation of a homozygous fertilization-defective gcs1 mutant by heat-inducible removal of a rescue gene." Plant Reprod **28**(1): 33-46.

Nahirnak, V., N. I. Almasia, H. E. Hopp and C. Vazquez-Rovere (2012). "Snakin/GASA proteins: involvement in hormone crosstalk and redox homeostasis." Plant Signal Behav **7**(8): 1004-1008.

Nasrallah, J. B. (2002). "Recognition and Rejection of Self in Plant Reproduction." Science **296**(5566): 305.

Nawrot, R., J. Barylski, G. Nowicki, J. Broniarczyk, W. Buchwald and A. Goździcka-Józefiak (2014). "Plant antimicrobial peptides." Folia Microbiologica **59**(3): 181-196.

Ngo, Q. A., H. Vogler, D. S. Lituiev, A. Nestorova and U. Grossniklaus (2014). "A calcium dialog mediated by the FERONIA signal transduction pathway controls plant sperm delivery." Dev Cell **29**(4): 491-500.

Noir, S., A. Bräutigam, T. Colby, J. Schmidt and R. Panstruga (2005). "A reference map of the Arabidopsis thaliana mature pollen proteome." Biochemical and Biophysical Research Communications **337**(4): 1257-1266.

Nour-Eldin, H. H., B. G. Hansen, M. H. H. Nørholm, J. K. Jensen and B. A. Halkier (2006). "Advancing uracil-excision based cloning towards an ideal technique for cloning PCR fragments." Nucleic Acids Res **34**(18): e122.

Okuda, S., T. Suzuki, M. M. Kanaoka, H. Mori, N. Sasaki and T. Higashiyama (2013). "Acquisition of LURE-binding activity at the pollen tube tip of Torenia fournieri." Mol Plant **6**(4): 1074-1090.

Okuda, S., H. Tsutsui, K. Shiina, S. Sprunck, H. Takeuchi, R. Yui, R. D. Kasahara, Y. Hamamura, A. Mizukami, D. Susaki, N. Kawano, T. Sakakibara, S. Namiki, K. Itoh, K. Otsuka, M. Matsuzaki, H. Nozaki, T. Kuroiwa, A. Nakano, M. M. Kanaoka, T. Dresselhaus, N. Sasaki and T. Higashiyama (2009). "Defensin-like polypeptide LUREs are pollen tube attractants secreted from synergid cells." Nature **458**(7236): 357-361.

Onelli, E., M. Scali, M. Caccianiga, N. Stroppa, P. Morandini, G. Pavesi and A. Moscatelli (2018). "Microtubules play a role in trafficking prevacuolar compartments to vacuoles in tobacco pollen tubes." Open biology **8**(10): 180078.

Palanivelu, R., L. Brass, A. F. Edlund and D. Preuss (2003). "Pollen tube growth and guidance is regulated by POP2, an Arabidopsis gene that controls GABA levels." Cell **114**(1): 47-59.

Palanivelu, R. and D. Preuss (2006). "Distinct short-range ovule signals attract or repel Arabidopsis thaliana pollen tubes in vitro." BMC Plant Biology **6**(1): 7.

Palanivelu, R. and T. Tsukamoto (2012). "Pathfinding in angiosperm reproduction: pollen tube guidance by pistils ensures successful double fertilization." Wiley Interdiscip Rev Dev Biol **1**(1): 96-113.

Pan, Y., X. Chai, Q. Gao, L. Zhou, S. Zhang, L. Li and S. Luan (2019). "Dynamic Interactions of Plant CNGC Subunits and Calmodulins Drive Oscillatory Ca(2+) Channel Activities." Dev Cell.

Park, S. Y., G. Y. Jauh, J. C. Mollet, K. J. Eckard, E. A. Nothnagel, L. L. Walling and E. M. Lord (2000). "A lipid transfer-like protein is necessary for lily pollen tube adhesion to an in vitro stylar matrix." Plant Cell **12**(1): 151-164.

Patro, R., G. Duggal, M. I. Love, R. A. Irizarry and C. Kingsford (2016). "Salmon provides accurate, fast, and bias-aware transcript expression estimates using dual-phase inference." bioRxiv: 021592.

Pearce, G., D. S. Moura, J. Stratmann and C. A. Ryan, Jr. (2001). "RALF, a 5-kDa ubiquitous polypeptide in plants, arrests root growth and development." Proc Natl Acad Sci U S A **98**(22): 12843-12847.

Pearson, K. (1901). "{On lines and planes of closest fit to systems of points in space}." Philosophical Magazine **2**(6): 559-572.

Peng, X., S. Li and H. Wang (2018). "Time bomb for pollen tubes: peptide RALF-mediated signaling." Mol Plant.

Pereira, A. M., A. L. Lopes and S. Coimbra (2016). "Arabinogalactan Proteins as Interactors along the Crosstalk between the Pollen Tube and the Female Tissues." Front Plant Sci **7**: 1895.

Pereira, A. M., L. G. Pereira and S. Coimbra (2015). "Arabinogalactan proteins: rising attention from plant biologists." Plant Reprod **28**(1): 1-15.

Pii, Y., B. Molesini, S. Masiero and T. Pandolfini (2012). "The non-specific lipid transfer protein N5 of Medicago truncatula is implicated in epidermal stages of rhizobium-host interaction." BMC Plant Biol **12**: 233.

Polowick, P. L. and V. K. Sawhney (1993). "Differentiation of the Tapetum During Microsporogenesis in Tomato (Lycopersicon esculentum Mill.), with Special Reference to the Tapetal Cell Wall." Annals of Botany **72**(6): 595-605.

Porto, W. F. and O. L. Franco (2013). "Theoretical structural insights into the snakin/GASA family." Peptides **44**: 163-167.

Preuss, D., B. Lemieux, G. Yen and R. W. Davis (1993). "A conditional sterile mutation eliminates surface components from Arabidopsis pollen and disrupts cell signaling during fertilization." Genes Dev **7**(6): 974-985.

Punwani, J. A. and G. N. Drews (2008). "Development and function of the synergid cell." Sexual Plant Reproduction **21**(1): 7-15.

Qin, Y., A. R. Leydon, A. Manziello, R. Pandey, D. Mount, S. Denic, B. Vasic, M. A. Johnson and R. Palanivelu (2009). "Penetration of the stigma and style elicits a novel transcriptome in pollen tubes, pointing to genes critical for growth in a pistil." PLoS Genet **5**(8): e1000621.

Qin, Y., R. J. Wysocki, A. Somogyi, Y. Feinstein, J. Y. Franco, T. Tsukamoto, D. Dunatunga, C. Levy, S. Smith, R. Simpson, D. Gang, M. A. Johnson and R. Palanivelu (2011). "Sulfinylated azadecalins act as functional mimics of a pollen germination stimulant in Arabidopsis pistils." Plant J **68**(5): 800-815.

Qin, Y. and Z. Yang (2011). "Rapid tip growth: insights from pollen tubes." Semin Cell Dev Biol **22**(8): 816-824.

Qu, L. J., L. Li, Z. Lan and T. Dresselhaus (2015). "Peptide signalling during the pollen tube journey and double fertilization." J Exp Bot **66**(17): 5139-5150.

Quail, M. A., M. Smith, P. Coupland, T. D. Otto, S. R. Harris, T. R. Connor, A. Bertoni, H. P. Swerdlow and Y. Gu (2012). "A tale of three next generation sequencing platforms: comparison of Ion Torrent, Pacific Biosciences and Illumina MiSeq sequencers." BMC Genomics **13**: 341-341.

Quilichini, T. D., E. Grienenberger and C. J. Douglas (2015). "The biosynthesis, composition and assembly of the outer pollen wall: A tough case to crack." Phytochemistry **113**(Supplement C): 170-182.

R, R. S., D. V. V, A. K. Nikonorova, R. A. Komakhin, V. K. V, A. E. T, V. G. E and V. B. A (2012). "Transformation of tobacco and Arabidopsis plants with Stellaria media genes encoding novel hevein-like peptides increases their resistance to fungal pathogens." Transgenic Res **21**(2): 313-325.

R., H. P. W., Y. Sung - Hyun, M. Antonio, L. Gemma, M. Martin and B. M. A. (2014). "Plant Antimicrobial Peptides Snakin - 1 and Snakin - 2: Chemical Synthesis and Insights into the Disulfide Connectivity." Chemistry – A European Journal **20**(17): 5102-5110.

Ramesh, S. A., S. D. Tyerman, B. Xu, J. Bose, S. Kaur, V. Conn, P. Domingos, S. Ullah, S. Wege, S. Shabala, J. A. Feijó, P. R. Ryan and M. Gilliham (2015). "GABA signalling modulates plant growth by directly regulating the activity of plant-specific anion transporters." Nature Communications **6**: 7879.

Rhee, S. Y. and C. R. Somerville (1998). "Tetrad pollen formation in quartet mutants of Arabidopsis thaliana is associated with persistence of pectic polysaccharides of the pollen mother cell wall." The Plant Journal **15**(1): 79-88.

Richter, J., M. Ploderer, G. Mongelard, L. Gutierrez and M. T. Hauser (2017). "Role of CrRLK1L Cell Wall Sensors HERCULES1 and 2, THESEUS1, and FERONIA in Growth Adaptation Triggered by Heavy Metals and Trace Elements." Front Plant Sci **8**: 1554.

Rong, W., L. Qi, J. Wang, L. Du, H. Xu, A. Wang and Z. Zhang (2013). "Expression of a potato antimicrobial peptide SN1 increases resistance to take-all pathogen Gaeumannomyces graminis var. tritici in transgenic wheat." Funct Integr Genomics **13**(3): 403-409.

Russell, S. D. and D. S. Jones (2015). "The male germline of angiosperms: repertoire of an inconspicuous but important cell lineage." Frontiers in Plant Science **6**(173).

Russell, S. D., G. W. Strout, A. K. Stramski, T. W. Mislan, R. A. Thompson and L. M. Schoemann (1996). "Microgametogenesis in Plumbago zeylanica (Plumbaginaceae). 1. Descriptive Cytology and Three-Dimensional Organization." American Journal of Botany **83**(11): 1435-1453.

Samuel, M. A., Y. T. Chong, K. E. Haasen, M. G. Aldea-Brydges, S. L. Stone and D. R. Goring (2009). "Cellular pathways regulating responses to compatible and self-incompatible pollen in Brassica and Arabidopsis stigmas intersect at Exo70A1, a putative component of the exocyst complex." Plant Cell **21**(9): 2655-2671.

Sanger, F., S. Nicklen and A. R. Coulson (1977). "DNA sequencing with chain-terminating inhibitors." Proc Natl Acad Sci U S A **74**(12): 5463-5467.

Sato, R. and M. Maeshima (2019). "The ER-localized aquaporin SIP2;1 is involved in pollen germination and pollen tube elongation in Arabidopsis thaliana." Plant Molecular Biology.

Schindelin, J., I. Arganda-Carreras, E. Frise, V. Kaynig, M. Longair, T. Pietzsch, S. Preibisch, C. Rueden, S. Saalfeld, B. Schmid, J. Y. Tinevez, D. J. White, V. Hartenstein, K. Eliceiri, P. Tomancak and A. Cardona (2012). "Fiji: an open-source platform for biological-image analysis." Nat Methods **9**(7): 676-682.

Schneitz, K., M. Hülskamp and R. E. Pruitt (1995). "Wild-type ovule development in Arabidopsis thaliana: a light microscope study of cleared whole-mount tissue." The Plant Journal **7**(5): 731-749.

Schopfer, C. R., M. E. Nasrallah and J. B. Nasrallah (1999). "The male determinant of self-incompatibility in Brassica." Science **286**(5445): 1697-1700.

Scott, R. J., M. Spielman and H. G. Dickinson (2004). "Stamen Structure and Function." The Plant Cell **16**(suppl 1): S46-S60.

Sehgal, N. and S. Singh (2018). "Progress on deciphering the molecular aspects of cell-to-cell communication in Brassica self-incompatibility response." 3 Biotech **8**(8): 347.

Sheoran, I. S., K. A. Sproule, D. J. H. Olson, A. R. S. Ross and V. K. Sawhney (2006). "Proteome profile and functional classification of proteins in Arabidopsis thaliana (Landsberg erecta) mature pollen." Sexual Plant Reproduction **19**(4): 185-196.

Shimizu, K. K. and K. Okada (2000). "Attractive and repulsive interactions between female and male gametophytes in Arabidopsis pollen tube guidance." Development **127**.

Shirasawa-Seo, N., S. Nakamura, N. Ukai, R. Honkura, T. Iwai and Y. Ohashi (2002). "Ectopic Expression of an Oat Thionin Gene in Carnation Plants Confers Enhanced Resistance to Bacterial Wilt Disease." Plant Biotechnology **19**(5): 311-317.

Sierro, N., J. N. D. Battey, S. Ouadi, N. Bakaher, L. Bovet, A. Willig, S. Goepfert, M. C. Peitsch and N. V. Ivanov (2014). "The tobacco genome sequence and its comparison with those of tomato and potato." Nature communications **5**: 3833-3833.

Silverstein, K. A., W. A. Moskal, Jr., H. C. Wu, B. A. Underwood, M. A. Graham, C. D. Town and K. A. VandenBosch (2007). "Small cysteine-rich peptides resembling antimicrobial peptides have been under-predicted in plants." Plant J **51**(2): 262-280.

Smith, A. G., C. A. Eberle, N. G. Moss, N. O. Anderson, B. M. Clasen and A. D. Hegeman (2013). "The transmitting tissue of Nicotiana tabacum is not essential to pollen tube growth, and its ablation can reverse prezygotic interspecific barriers." Plant Reprod **26**(4): 339-350.

Smith, D. K., J. F. Harper and I. S. Wallace (2018). "A potential role for protein O-fucosylation during pollen-pistil interactions." Plant Signaling & Behavior **13**(5): e1467687.

Sogo, A. and H. Tobe (2006). "Mode of Pollen-Tube Growth in Pistils of Myrica rubra (Myricaceae): A Comparison with Related Families." Annals of Botany **97**(1): 71-77.

Sprunck, S. and R. Gross-Hardt (2011). "Nuclear behavior, cell polarity, and cell specification in the female gametophyte." Sex Plant Reprod **24**(2): 123-136.

Stec, B. (2006). "Plant thionins--the structural perspective." Cell Mol Life Sci **63**(12): 1370-1385.

Steinhorst, L. and J. Kudla (2013). "Calcium - a central regulator of pollen germination and tube growth." Biochim Biophys Acta **1833**(7): 1573-1581.

Strable, J. and M. J. Scanlon (2009). "Maize (Zea mays): a model organism for basic and applied research in plant biology." Cold Spring Harb Protoc **2009**(10): pdb emo132.

Student, W. S. G. (1908). "The Probable error of a Mean." Biometrika **6**(1): 25.

Suarez, C., A. Zienkiewicz, A. J. Castro, K. Zienkiewicz, A. Majewska-Sawka and M. I. Rodriguez-Garcia (2013). "Cellular localization and levels of pectins and arabinogalactan proteins in olive (Olea europaea L.) pistil tissues during development: implications for pollen-pistil interaction." Planta **237**(1): 305-319.

Sundaresan, V. and M. Alandete-Saez (2010). "Pattern formation in miniature: the female gametophyte of flowering plants." Development **137**(2): 179-189.

Swanson, R., A. F. Edlund and D. Preuss (2004). "Species Specificity in Pollen-Pistil Interactions." Annual Review of Genetics **38**(1): 793-818.

Takayama, S., H. Shiba, M. Iwano, K. Asano, M. Hara, F. S. Che, M. Watanabe, K. Hinata and A. Isogai (2000). "Isolation and characterization of pollen coat proteins of Brassica campestris that interact with S locus-related glycoprotein 1 involved in pollen-stigma adhesion." Proc Natl Acad Sci U S A **97**(7): 3765-3770.

Takeuchi, H. and T. Higashiyama (2012). "A species-specific cluster of defensin-like genes encodes diffusible pollen tube attractants in Arabidopsis." PLoS Biol **10**(12): e1001449.

Takeuchi, H. and T. Higashiyama (2016). "Tip-localized receptors control pollen tube growth and LURE sensing in Arabidopsis." Nature **531**(7593): 245-248.

Tang, W., D. Kelley, I. Ezcurra, R. Cotter and S. McCormick (2004). "LeSTIG1, an extracellular binding partner for the pollen receptor kinases LePRK1 and LePRK2, promotes pollen tube growth in vitro." Plant J **39**(3): 343-353.

Tavormina, P., B. De Coninck, N. Nikonorova, I. De Smet and B. P. Cammue (2015). "The Plant Peptidome: An Expanding Repertoire of Structural Features and Biological Functions." Plant Cell **27**(8): 2095-2118.

Tesfaye, M., K. A. T. Silverstein, S. Nallu, L. Wang, C. J. Botanga, S. K. Gomez, L. M. Costa, M. J. Harrison, D. A. Samac, J. Glazebrook, F. Katagiri, J. F. Gutierrez-Marcos and K. A. VandenBosch (2013). "Spatio-Temporal Expression Patterns of Arabidopsis thaliana and Medicago truncatula Defensin-Like Genes." PLOS ONE **8**(3): e58992.

Theis, T. and U. Stahl (2004). "Antifungal proteins: targets, mechanisms and prospective applications." Cell Mol Life Sci **61**(4): 437-455.

Ting, J. T., S. S. Wu, C. Ratnayake and A. H. Huang (1998). "Constituents of the tapetosomes and elaioplasts in Brassica campestris tapetum and their degradation and retention during microsporogenesis." Plant J **16**(5): 541-551.

Tirlapur, U. K., J. L. Van Went and M. Cresti (1993). "Visualization of Membrane Calcium and Calmodulin in Embryo Sacs in situ and Isolated from Petunia hybvida L. and Nicotiana tabacum L." Annals of Botany **71**(2): 161-167.

Toujani, W., J. Munoz-Bertomeu, M. Flores-Tornero, S. Rosa-Tellez, A. D. Anoman, S. Alseekh, A. R. Fernie and R. Ros (2013). "Functional characterization of the plastidial 3-phosphoglycerate dehydrogenase family in Arabidopsis." Plant Physiol **163**(3): 1164-1178.

Tousheh, M., M. Miroliaei, A. Asghar Rastegari, K. Ghaedi, A. Esmaeili and A. Matkowski (2013). "Computational evaluation on the binding affinity of non-specific lipid-transfer protein-2 with fatty acids." Comput Biol Med **43**(11): 1732-1738.

Tsukamoto, T., Y. Qin, Y. Huang, D. Dunatunga and R. Palanivelu (2010). "A role for LORELEI, a putative glycosylphosphatidylinositol-anchored protein, in Arabidopsis thaliana double fertilization and early seed development." Plant J **62**(4): 571-588.

Uebler, S., T. Dresselhaus and M. Márton (2013). "Species-specific interaction of EA1 with the maize pollen tube apex." Plant Signaling & Behavior **8**(10): e25682.

van der Weerden, N. L., M. R. Bleackley and M. A. Anderson (2013). "Properties and mechanisms of action of naturally occurring antifungal peptides." Cell Mol Life Sci **70**(19): 3545-3570.

van Loon, L. C., M. Rep and C. M. Pieterse (2006). "Significance of inducible defense-related proteins in infected plants." Annu Rev Phytopathol **44**: 135-162.

Vernoud, V., A. C. Horton, Z. Yang and E. Nielsen (2003). "Analysis of the small GTPase gene superfamily of Arabidopsis." Plant Physiol **131**(3): 1191-1208.

von Besser, K., A. C. Frank, M. A. Johnson and D. Preuss (2006). "Arabidopsis HAP2 (GCS1) is a sperm-specific gene required for pollen tube guidance and fertilization." Development **133**(23): 4761-4769.

Vriens, K., B. P. Cammue and K. Thevissen (2014). "Antifungal plant defensins: mechanisms of action and production." Molecules **19**(8): 12280-12303.

Wang, J.-G., C. Feng, H.-H. Liu, Q.-N. Feng, S. Li and Y. Zhang (2017). "AP1G mediates vacuolar acidification during synergid-controlled pollen tube reception." Proceedings of the National Academy of Sciences **114**(24): E4877-E4883.

Wang, N. J., C. C. Lee, C. S. Cheng, W. C. Lo, Y. F. Yang, M. N. Chen and P. C. Lyu (2012). "Construction and analysis of a plant non-specific lipid transfer protein database (nsLTPDB)." BMC Genomics **13 Suppl 1**: S9.

Wang, T., L. Liang, Y. Xue, P. F. Jia, W. Chen, M. X. Zhang, Y. C. Wang, H. J. Li and W. C. Yang (2016). "A receptor heteromer mediates the male perception of female attractants in plants." Nature **531**(7593): 241-244.

Webb, M. C. and B. E. S. Gunning (1994). "Embryo sac development in Arabidopsis thaliana II. The cytoskeleton during megagametogenesis." Sexual Plant Reproduction **7**(3): 153-163.

Wei, L. Q., W. Y. Xu, Z. Y. Deng, Z. Su, Y. Xue and T. Wang (2010). "Genome-scale analysis and comparison of gene expression profiles in developing and germinated pollen in Oryza sativa." BMC Genomics **11**: 338-338.

Weiler, E. and L. Nover (2008). Allgemeine und molekulare Botanik, Georg Thieme Verlag.

Wengier, D., I. Valsecchi, M. L. Cabanas, W. H. Tang, S. McCormick and J. Muschietti (2003). "The receptor kinases LePRK1 and LePRK2 associate in pollen and when expressed in yeast, but dissociate in the presence of style extract." Proc Natl Acad Sci U S A **100**(11): 6860-6865.

Weterings, K. and S. D. Russell (2004). "Experimental analysis of the fertilization process." Plant Cell **16 Suppl**.

Willemse, M. T. M. and J. L. van Went (1984). The Female Gametophyte. Embryology of Angiosperms. B. M. Johri. Berlin, Heidelberg, Springer Berlin Heidelberg**:** 159-196.

Wolters-Arts, M., W. M. Lush and C. Mariani (1998). "Lipids are required for directional pollen-tube growth." Nature **392**(6678): 818-821.

Woriedh, M., R. Merkl and T. Dresselhaus (2015). "Maize EMBRYO SAC family peptides interact differentially with pollen tubes and fungal cells." J Exp Bot **66**(17): 5205-5216.

Woriedh, M., S. Wolf, M. L. Marton, A. Hinze, M. Gahrtz, D. Becker and T. Dresselhaus (2013). "External application of gametophyte-specific ZmPMEI1 induces pollen tube burst in maize." Plant Reprod **26**(3): 255-266.

Worrall, D., D. L. Hird, R. Hodge, W. Paul, J. Draper and R. Scott (1992). "Premature dissolution of the microsporocyte callose wall causes male sterility in transgenic tobacco." The Plant Cell **4**(7): 759-771.

Wu, H. M., H. Wang and A. Y. Cheung (1995). "A pollen tube growth stimulatory glycoprotein is deglycosylated by pollen tubes and displays a glycosylation gradient in the flower." Cell **82**(3): 395-403.

Wu, H. M., E. Wong, J. Ogdahl and A. Y. Cheung (2000). "A pollen tube growth-promoting arabinogalactan protein from nicotiana alata is similar to the tobacco TTS protein." Plant J **22**(2): 165-176.

Wu, J., E. L. Kurten, G. Monshausen, G. M. Hummel, S. Gilroy and I. T. Baldwin (2007). "NaRALF, a peptide signal essential for the regulation of root hair tip apoplastic pH in Nicotiana attenuata, is required for root hair development and plant growth in native soils." Plant J **52**(5): 877-890.

Xiang, Y., R. H. Huang, X. Z. Liu, Y. Zhang and D. C. Wang (2004). "Crystal structure of a novel antifungal protein distinct with five disulfide bridges from Eucommia ulmoides Oliver at an atomic resolution." J Struct Biol **148**(1): 86-97.

Yadegari, R. and G. N. Drews (2004). "Female Gametophyte Development." The Plant Cell **16**(suppl 1): S133.

Yan, A., G. Xu and Z.-B. Yang (2009). "Calcium participates in feedback regulation of the oscillating ROP1 Rho GTPase in pollen tubes." Proceedings of the National Academy of Sciences **106**(51): 22002-22007.

Yang, Z. (1998). "Signaling tip growth in plants." Curr Opin Plant Biol **1**(6): 525-530.

Yang, Z. and I. Lavagi (2012). "Spatial control of plasma membrane domains: ROP GTPase-based symmetry breaking." Curr Opin Plant Biol **15**(6): 601-607.

Ye, J., Y. Zheng, A. Yan, N. Chen, Z. Wang, S. Huang and Z. Yang (2009). "Arabidopsis Formin3 Directs the Formation of Actin Cables and Polarized Growth in Pollen Tubes." The Plant Cell **21**(12): 3868-3884.

Yu, G. H., J. Zou, J. Feng, X. B. Peng, J. Y. Wu, Y. L. Wu, R. Palanivelu and M. X. Sun (2014). "Exogenous gamma-aminobutyric acid (GABA) affects pollen tube growth via modulating putative Ca2+-permeable membrane channels and is coupled to negative regulation on glutamate decarboxylase." J Exp Bot **65**(12): 3235-3248.

Zhang, J., H. Yang, L. Zhu and H. Tong (1995). "Ultracytochemical localization of calcium in the stigma, style and micropyle of sunflower." Acta Botanica Sinica **37**(9): 691-696.

Zhang, J. S., H. Y. Yang, L. Zhu and H. Tong (1997). Ultracytochemical localization of calcium in the pollen tube track of cotton gynoecium.

Zhao, X. Y., Q. Wang, S. Li, F. R. Ge, L. Z. Zhou, S. McCormick and Y. Zhang (2013). "The juxtamembrane and carboxy-terminal domains of Arabidopsis PRK2 are critical for ROP-induced growth in pollen tubes." J Exp Bot **64**(18): 5599-5610.

Zheng, R. H., S. Su, H. Xiao and H. Q. Tian (2019). "Calcium: A Critical Factor in Pollen Germination and Tube Elongation." Int J Mol Sci **20**(2).

Zheng, Y. Y., X. J. Lin, H. M. Liang, F. F. Wang and L. Y. Chen (2018). "The Long Journey of Pollen Tube in the Pistil." Int J Mol Sci **19**(11).

Zheng, Z. L. and Z. Yang (2000). "The Rrop GTPase switch turns on polar growth in pollen." Trends Plant Sci **5**(7): 298-303.

Zhou, L., Y. Fu and Z. Yang (2009). "A genome-wide functional characterization of Arabidopsis regulatory calcium sensors in pollen tubes." J Integr Plant Biol **51**(8): 751-761.

Zhu, L., L. C. Chu, Y. Liang, X. Q. Zhang, L. Q. Chen and Ye (2018). "The Arabidopsis CrRLK1L Protein Kinases BUPS1 and BUPS2 are Required for Normal Growth of Pollen Tubes in the Pistil." Plant J.

Zinkl, G. M., B. I. Zwiebel, D. G. Grier and D. Preuss (1999). "Pollen-stigma adhesion in Arabidopsis: a species-specific interaction mediated by lipophilic molecules in the pollen exine." Development **126**(23): 5431-5440.

7. Affidavit

Eidesstattliche Erklärungen nach §7 Abs. 2 Satz 3, 4, 5

der Promotionsordnung der Fakultät für Biologie

Eidesstattliche Erklärung

Hiermit erkläre ich an Eides statt, die Dissertation: „Molekulare Charakterisierung Defensin-ähnlicher Proteine beim Befruchtungsvorgang in *Nicotiana tabacum*“, eigenständig, d. h. insbesondere selbständig und ohne Hilfe eines kommerziellen Promotionsberaters, angefertigt und keine anderen, als die von mir angegebenen Quellen und Hilfsmittel verwendet zu haben.

Ich erkläre außerdem, dass die Dissertation weder in gleicher noch in ähnlicher Form bereits in einem anderen Prüfungsverfahren vorgelegen hat.

Weiterhin erkläre ich, dass bei allen Abbildungen und Texten bei denen die Verwertungsrechte (Copyright) nicht bei mir liegen, diese von den Rechtsinhabern eingeholt wurden und die Textstellen bzw. Abbildungen entsprechend den rechtlichen Vorgaben gekennzeichnet sind sowie bei Abbildungen, die dem Internet entnommen wurden, der entsprechende Hypertextlink angegeben wurde.

Affidavit

I hereby declare that my thesis entitled: „Molecular characterization of defensin-like proteins in the fertilization process of *Nicotiana tabacum*" is the result of my own work. I did not receive any help or support from commercial consultants. All sources and / or materials applied are listed and specified in the thesis.

Furthermore I verify that the thesis has not been submitted as part of another examination process neither in identical nor in similar form.

Besides I declare that if I do not hold the copyright for figures and paragraphs, I obtained it from the rights holder and that paragraphs and figures have been marked according to law or for figures taken from the internet the hyperlink has been added accordingly.

Würzburg, den_____

_____

Katharina von Meyer